แอลคาลอยด์บิสเตตราไฮโดรไอโซควิโนลีน ที่มีฤทธิ์เป็นพิษต่อเซลล์จากฟองน้ำทะเล *Xestospongia* sp. ของไทย

นางสุรัตนา อำนวยผล

วิทยานิพนธ์นี้เป็นส่วนหนึ่งของการศึกษาตามหลักสูตรปริญญาวิทยาศาสตรดุษฎีบัณฑิต
สาขาวิชาเภสัชเคมีและผลิตภัณฑ์ธรรมชาติ
คณะเภสัชศาสตร์ จุฬาลงกรณ์มหาวิทยาลัย
ปีการศึกษา ๒๕๔๗

ISBN 974-17-5920-7

CYTOTOXIC BISTETRAHYDROISOQUINOLINE ALKALOIDS FROM THE THAI MARINE SPONGE, *XESTOSPONGIA* SP.

Mrs. Surattana Amnuoypol

A Dissertation Submitted in Partial Fulfillment of the Requirements
for the Degree of Doctor of Philosophy in Pharmaceutical Chemistry and Natural Products
Faculty of Pharmaceutical Sciences
Chulalongkorn University
Academic Year 2004

ISBN 974-17-5920-7

Thesis Title	Cytotoxic bistetrahydroisoquinoline alkaloids from the Thai marine sponge, *Xestospongia* sp.
By	Mrs. Surattana Amnuoypol
Field of Study	Pharmaceutical Chemistry and Natural Products
Thesis Advisor	Khanit Suwanborirux, Ph.D.

Accepted by the Faculty of Pharmaceutical Sciences, Chulalongkorn University in Partial Fulfillment of the Requirements for the Doctor's Degree

……Dean of the Faculty of Pharmaceutical Sciences

(Associate Professor Boonyong Tantisira, Ph.D.)

THESIS COMMITTEE

……Chairman

(Associate Professor Sumphan Wongseripipatana, Ph.D.)

…… Thesis Advisor

(Khanit Suwanborirux, Ph.D.)

…… Member

(Professor Akinori Kubo, Ph.D.)

……. Member

(Professor Somsak Ruchirawat, Ph.D.)

…… Member

(Associate Professor Sunibhond Pummangura, Ph.D.)

…….. Member

(Assistant Professor Chamnan Patarapanich, Ph.D.)

นางสุรัตนา อำนวยผล: แอลคาลอยด์บิสเตตราไฮโดรไอโซควิโนลีน ที่มีฤทธิ์เป็นพิษต่อเซลล์จากฟองน้ำทะเล *Xestospongia* sp. ของไทย (CYTOTOXIC BISTETRA HYDROISOQUINOLINE ALKALOIDS FROM THE THAI MARINE SPONGE, *XESTOSPONGIA* SP.) อ. ที่ปรึกษา: อ. ดร. คณิต สุวรรณบริรักษ์, ๒๐๓ หน้า. ISBN 974-17-5920-7

รายงานการแยกสารแอลคาลอยด์กลุ่ม bistetrahydroisoquinoline ซึ่งประกอบด้วยสารหลัก renieramycin M และอนุพันธุ์ในกลุ่มเดียวกันที่มีปริมาณน้อยอีก ๕ สาร ได้แก่ renieramycins N O Q R และ S จากฟองน้ำทะเล *Xestospongia* sp. ของไทย ที่ได้ทำการเติม potassium cyanide ก่อนการสกัด ได้ทำการพิสูจน์สูตรโครงสร้าง และสเตอริโอเคมีของสารที่แยกได้นี้ โดยใช้ข้อมูลทาง สเปกโทรสโคปี การแทนที่หมู่ฟังก์ชัน carbinolamine ด้วย cyanoamine สามารถเพิ่มความเสถียรของสาร renieramycinsได้ ดังนั้นกลยุทธ์การเติม potassium cyanide ก่อนการสกัดนี้ เป็นตัวอย่างแรกในการเตรียมสาร renieramycins ให้มีปริมาณมากพอ เพื่อการนำไปศึกษาคุณสมบัติทางเคมีและชีวภาพของสารต่อไป นอกจากนี้ได้สังเคราะห์อนุพันธ์ใหม่ของสารกลุ่ม renieramycins เพิ่มเติมอีก ๑๐ สาร จากสาร renieramycin M ด้วยปฏิกิริยาทางเคมี ได้แก่ ปฏิกิริยา allylic oxidation โดยใช้ selenium dioxide ในตัวทำละลายแอลกอฮอล์ชนิดต่างๆ ปฏิกิริยา reductive deangelation และ ปฏิกิริยา reductive acetylation และยังได้ทำการเปลี่ยนสาร renieramycin M ไปเป็น renieramycins ที่เคยค้นพบแล้ว ได้แก่ renieramycins E และ J และ jorumycin นอกจากนี้ได้ศึกษาปฏิกิริยา oxidative degradation ของ renieramycin E และ jorumycin ที่เกิดเป็นสารกลุ่ม simple isoquinolinequinone alkaloids และได้เสนอกลไกของการสลายตัวนี้ไว้ด้วย

ได้ทำการทดสอบฤทธิ์ความเป็นพิษต่อเซลล์ และศึกษาหาความสัมพันธ์ระหว่างสูตรโครงสร้างและฤทธิ์ทางชีวภาพของสารที่แยกได้และสารกึ่งสังเคราะห์ของ renieramycins ต่อ carcinoma cell lines หลายชนิด พบว่า หมู่แทนที่ cyano และ hydroxyl ที่คาร์บอนตำแหน่ง ที่ ๒๑ มีความจำเป็นต่อการออกฤทธิ์ความเป็นพิษต่อเซลล์ นอกจากนี้ สารที่ไม่มีหมู่แทนที่ angeloyl มีฤทธิ์ความเป็นพิษต่อเซลล์สูงกว่าสารต้นแบบ ส่วนสารที่มีหมู่แทนที่ที่ประกอบด้วย ออกซิเจน ที่คาร์บอนตำแหน่งที่ ๑๔ มีฤทธิ์ความเป็นพิษต่อเซลล์ต่ำมาก และอนุพันธ์ *O*-acetyl hydroquinone มีฤทธิ์ความเป็นพิษต่อเซลล์ใกล้เคียงกับสารต้นแบบที่เป็นquinone

การค้นพบครั้งนี้ ส่งผลกระทบที่สำคัญยิ่งต่อวงการวิทยาศาสตร์ของไทย โดยเป็นการเปิดโอกาสให้เกิดความร่วมมือในการวิจัยด้านต่างๆ เพื่อพัฒนาสารในกลุ่ม renieramycins เป็นสารต้านมะเร็งชนิดแรก ที่ได้จากทรัพยากรธรรมชาติในทะเลไทย

สาขาวิชา เภสัชเคมีและผลิตภัณฑ์ธรรมชาติ ลายมือชื่อนิสิต.....

ปีการศึกษา ๒๕๔๗ ลายมือชื่ออาจารย์ที่ปรึกษา.....

4476974333 : MAJOR PHARMACEUTICAL CHEMISTRY AND NATURAL PRODUCTS

KEY WORD: ISOQUINOLINE/ CYTOTOXIC ACTIVITY/ RENIERAMYCINS

SURATTANA AMNUOYPOL: CYTOTOXIC BISTETRAHYDROISOQUINOLINE ALKALOIDS FROM THE THAI MARINE SPONGE, *XESTOSPONGIA* SP.:

THESIS ADVISOR: KHANIT SUWANBORIRUX, Ph.D., 203 pp. ISBN 974-17-5920-7

A group of bistetrahydroisoquinoline alkaloids, including renieramycin M as a major component, together with five minor derivatives, renieramycins N, O, Q, R, and S, were isolated from the Thai sponge, *Xestospongia* sp., pretreated with potassium cyanide. Their structures and relative stereochemistries were elucidated on the basis of spectroscopic data. Replacement of the carbinolamine by the cyanoamine dramatically increased the stability of renieramycins. Therefore, the KCN-pretreated strategy is the first example to provide an important solution to increase large-scale supply of renieramycins for further chemical and biological investigations.

Ten new additional renieramycins were obtained by several chemical transformations of renieramycin M, including allylic oxidation by selenium dioxide in alcoholic solvents, reductive deangelation and reductive acetylation. The transformations of renieramycin M into known renieramycins including renieramycins E and J and jorumycin were achieved. The oxidative degradations of renieramycin E and jorumycin to generate simple isoquinolinequinone alkaloids were also demonstrated and the degradation mechanism was proposed.

The cytotoxicity and structure-activity relationship (SAR) of the isolated and semisynthetic renieramycins against carcinoma cell lines revealed that the cyano or hydroxyl groups at C-21 position was essential for the activity. Moreover, the deangeloyl compounds displayed higher potent cytotoxicity than the parent compounds. In addition, the presence of the oxygen containing functionality at C-14 caused less cytotoxic activity. The *O*-acetyl hydroquinone derivatives displayed equipotent cytotoxicity to the parent quinone compounds.

The important impact of this discovery is the opening for new biomedical research collaborations to develop renieramycins as first anticancer agent from Thai marine natural resources.

Field of Study Pharmaceutical Chemistry and Natural Products Student's signature……

Academic Year 2004 Advisor's signature……...

ACKNOWLEDGEMENTS

I would like to express my appreciation to my thesis advisor, Dr. Khanit Suwanborirux, for his valuable advice, continual guidance, kindness, and understanding throughout this research study.

I would like to acknowledge Professor Akinori Kubo and Associate Professor Naoki Saito, of Meiji Pharmaceutical University, Japan for supporting my research in Japan and I am indebted for their helpful discussions and suggestions.

It is my great pleasure to acknowledge Assistant Professor Chamnan Patarapanich for his valuable guidance and suggestion.

I would like to thank all of my thesis committee, for their valuable suggestion, discussion and correctitude.

I would like to thank the Pharmaceutical Research Instrument Center, Faculty of Pharmaceutical Sciences for providing 300 MHz NMR spectrometer and other scientific equipments, the Analysis Center, Meiji Pharmaceutical University, for recording 500 MHz NMR and mass spectra, and the National Center for Genetic Engineering and Biotechnology (BIOTEC), Thailand and Dr. Nobuo Shimma, Chugai Pharmaceutical Company Research Center, Japan for cytotoxicity assays.

The Bioactive Marine Natural Product Chemistry Research Unit (BMNCU), was supported by a grant for Center of Excellence from Chulalongkorn University. This research was partially supported by a grant (No. BT-38-06-NPI-09-09) from BIOTEC, the Ministry of Science, Technology and Environment of Thailand and a Grant-in-Aid for Scientific Research (B) (No. 14370725) from the Ministry of Education, Culture, Sports, Science and Technology (MEXT), Japan. I am grateful to the Japan Society for the Promotion of Science (JSPS) and the National Research Cooperation of Thailand (NRCT) for supporting the collaboration between Thai and Japanese researchers in this work. Financial supports for this work were also provided by the Graduate School of Chulalongkorn University.

I would like to thank Associate Professor Sumphan Wongseripipatana, Head of the Department of Pharmacognosy and all staffs for their supports during my study. Finally, I would like to express my appreciation to my family for their patient, encouragement and support throughout my study.

CONTENTS

LIST OF FIGURES

LIST OF SCHEMES

LIST OF TABLES

ABBREVIATIONS

%	=	percent or part per hundred
^{o}C	=	degree Celsius
δ	=	chemical shift
ε	=	molar absorptivity
µg	=	microgram
µl	=	microliter
λ_{max}	=	wave length at maximum absorption
ν_{max}	=	wave number at maximum absorption
$[\alpha]_D^{25}$	=	specific rotation at 25 ^{o}C and sodium D line (589 nm)
A375	=	malignant melanoma cell line
A549	=	lung carcinoma cell line
$AgNO_3$	=	silver nitrate
B16	=	melanoma cell line
br s	=	broad singlet
c	=	concentration
^{13}C NMR	=	carbon-13 nuclear magnetic resonance
Cbz	=	benzyloxycarbonyl
$CDCl_3$	=	deuterated chloroform
$CHCl_3$	=	chloroform
cm	=	centimeter
d	=	doublet
DBU	=	1,8-diazabicyclo[5.4.0]undec-7-ene
dd	=	doublet of doublets
ddd	=	doublet of doublets of doublets
DDQ	=	2,3-dichloro-5,6-dicyano-1,4-benzoquinone
DEPT	=	distortionless enhancement by polarization transfer
DLD1	=	human colon carcinoma cell line
DMAP	=	4-N,N-dimethylaminopyridine
DMSO	=	dimethylsulfoxide
DMTS	=	dimethylthexylsilyl
dq	=	doublet of quartets

dt	=	doublet of triplets
DTT	=	dithiothreitol
DU145	=	human prostrate cancer cell line
ED_{50}	=	50% effective dose
ESI	=	elctrospray ionization
EtOAc	=	ethyl acetate
EtOH	=	ethyl alcohol or ethanol
Fmoc	=	9-fluorenylmethoxycarbonyl
g	=	gram
HCT-116	=	human colon cancer cell line
^{1}H-^{1}H COSY	=	^{1}H-^{1}H correlation spectroscopy
HMBC	=	^{1}H-detected heteronuclear multiple bond correlation
HMQC	=	^{1}H-detected heteronuclear multiple quantum coherence
^{1}H NMR	=	proton nuclear magnetic resonance
HT 29	=	colon cancer cell line
Hz	=	hertz
IC_{50}	=	50% inhibition concentration
IC_{90}	=	90% inhibition concentration
ID_{50}	=	50% inhibition dose
IR	=	infrared
J	=	coupling constant
KB	=	human epidermoid carcinoma cells of the nasopharynx
KBr	=	potassium bromide
Kg	=	kilogram
L, l	=	liter
L1210	=	leukemia cell line
m	=	multiplet
M	=	molar
M^+	=	molecular ion
MEL-28	=	melanoma cell line
MeOH	=	methyl alcohol or methanol
mg	=	milligram
MHz	=	megahertz
MIC	=	minimum inhibition concentration

min	=	minute
ml	=	milliliter
m/z	=	mass to charge
NCI-H 460	=	human lung carcinoma cell line
nm	=	nanometer
nM	=	nanomolar
NMR	=	nuclear magnetic resonance
No.	=	number
P 388	=	murine leukemia cells
PC-3	=	prostate carcinoma
Pd/C	=	palladium on activated charcoal
$Pd(OH)_2/C$	=	palladium hydroxide on activated charcoal
ppm	=	part per million
p-TsOH	=	*p*-toluenesulfonic acid
pyridine-d_5	=	deuterated pyridine
q	=	quartet
QG 56	=	human lung carcinoma cell line
s	=	singlet
sp.	=	species
SeO_2	=	selenium oxide
t	=	triplet
TFA	=	trifluoroacetic acid
TLC	=	thin layer chromatography
UV	=	ultraviolet

CHAPTER I

INTRODUCTION

During the past two decades, renieramycins were isolated from marine sponges, belonging to genera *Reniera* (Frincke and Faulkner, 1982; He and Faulkner, 1989), *Xestospongia* (Davidson, 1992), *Haliclona* (Parameswaran *et al.*, 1998), *Cribrochalina* (Pettit *et al.*, 2000) and *Neopetrosia* (Oku *et al.*, 2003). Another related compound, jorumycin (**2**), was reported from the nudibranch, *Jorunna funebris* (Fontana *et al.*, 2000). The previously isolated renieramycins A-I (**1a**-**1i**) and P (**1p**) are summarized in Figure 1. The ring systems of these natural products including their relative stereochemistries were identical with those of saframycins (Arai and Kubo, 1983; Tomson, 1987; Kubo and Saito, 1992; Ozturk, 2000), which exhibited strong cytotoxicity toward cultured cells and antitumor activity against several experimental tumors. One of the most intriguing problems, however, is that the marine natural products are isolated only in very minute quantities. Therefore, it is difficult to provide a consistent supply of renieramycins for drug development from marine sources as well as by total synthesis, and it cannot be determined whether they have antitumor activities similar to those of saframycins and ecteinascidins (Wright *et al.*,1990; Rinehart *et al.*, 1990a; Sakai *et al.*,1992; 1996).

As part of the search for new metabolites *via* the isolation and characterization of biologically active compounds from Thai marine animals, the blue sponge, *Xestospongia* sp. was collected in the vicinity of Si Chang Island, in the Gulf of Thailand in December 1992. Extraction and isolation were performed on wet animal using the standard procedure and resulted in the isolation of three monomeric isoquinolinequinones; 1,6-dimethyl-7-methoxy-5,8-dihydroisoquinoline-5,8-dione (**3**, 10 mg, 0.018% yield of the methanol extract), renierone (**4**, 30 mg, 0.053% yield), and *N*-formyl-1,2-dihydrorenierone (**5**, 35 mg, 0.061% yield). The more polar fraction was purified to yield dimeric isoquinoline quinones; renieramycins J (**1j**, 2 mg, 0.004% yield), K (**1k**, 7 mg, 0.012% yield), and L (**1l**, 30 mg, 0.053% yield) along with two known monomeric isoquinolinequinones; mimosamycin (**6**, 35 mg,

0.061% yield) and the *N*-ethylenemethyl ketone derivative of renierone (**7**, 5 mg, 0.009% yield) (Suwanborirux *et al.*, 2003).

One interesting feature in the structures of renieramycins J-L is that they are the first example of alkylated analogues of renieramycins at C-21 position. Furthermore, it is difficult to rule out the possibility that renieramycins J-L are artifacts resulting from solvent exchange during separation with acetone.

From these above described problems, the *Xestospongia* sponge has been chosen to be reinvestigated for the chemical constituents.

The main objectives of this thesis are to

1. isolate isoquinolinequinone alkaloids from the Thai marine sponge, *Xestospongia* sp. and increase the quantity of these marine natural alkaloids, especially the dimeric compounds, for further chemical and biological studies.
2. elucidate the structures of the isolated isoquinolinequinone alkaloids.
3. transform the isolated renieramycins for new renieramycin derivatives.
4. evaluate cytotoxic activity of the isolated and the transformed products of renieramycins.

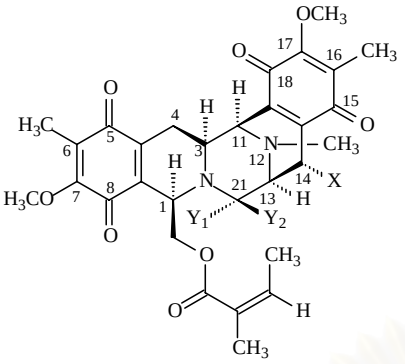

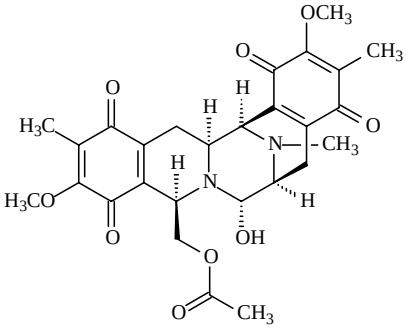

Jorumycin (**2**)

Renieramycins A (**1a**) : X = OH, $Y_1 = Y_2 = H$

B (**1b**) : X = OCH_2CH_3, $Y_1 = Y_2 = H$

C (**1c**) : X = OH, Y_1 , Y_2 = O

D (**1d**) : X = OCH_2CH_3, Y_1 , Y_2 = O

E (**1e**) : X = H, Y_1 = OH, $Y_2 = H$

F (**1f**) : X = OCH_3, Y_1 = OH, $Y_2 = H$

G (**1g**) : X = H, $Y_1 = Y_2 = H$

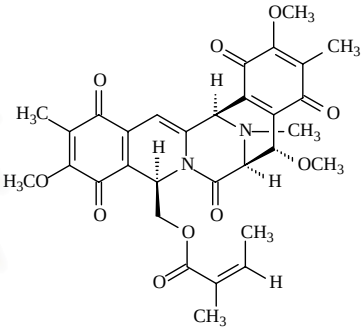

Renieramycin I (**1i**)

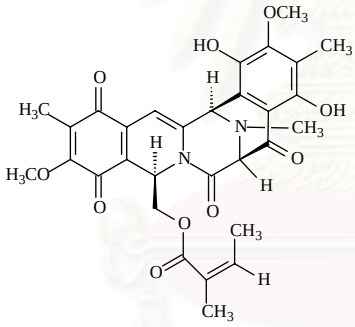

Renieramycin H (**1h**)

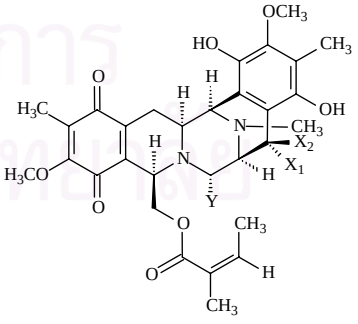

Renieramycins J (**1j**) : X = H,

K (**1k**): X = OCH_3

Renieramycin L (**1l**) : X_1, X_2 = O; Y = CH_2COCH_3

P (**1p**) : X_1 = OH, X_2 = H; Y = OH

Figure 1 Structures of renieramycins.

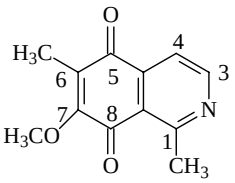

1,6-dimethyl-7-methoxy-5,8-dihydroisoquinoline-5,8-dione (**3**)

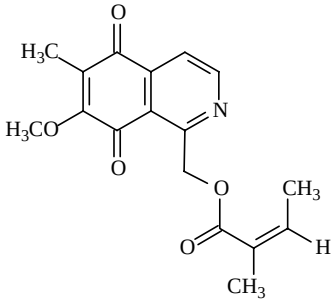

renierone (**4**)

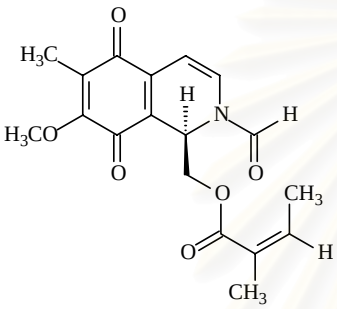

N-formyl-1,2-dihydrorenierone (**5**)

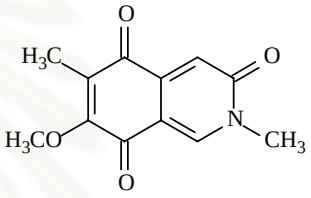

mimosamycin (**6**)

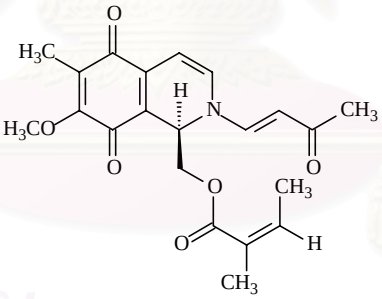

N-ethylenemethyl ketone derivative of renierone (**7**)

Figure 2 Structures of the monomeric isoquinolinequinones.

CHAPTER II

LITERATURE REVIEW

1. THE GENUS *XESTOSPONGIA*

Taxa and Description

Sponge identifications are primarily based on morphology. Major characters are shape, size, colour, texture, mucus production, surface ornamentation, organic and inorganic skeletons (spongin fiber and spicule), skeletal structure, larvae and reproductive strategy.

According to "Sponguide" version August 2000 by Dr. John A. Hooper from Queensland Museum, Australia, all the sponges are classified in phylum Porifera which contains 4 classes (one completely extinct), 5 subclasses, 28 orders, 232 families and 977 valid genera. Two subphyla are now recognized : Cellularia including classes Demospongiae and Calcarea, and subphylum Symplasia including class Hexactinellida. Class Demospongiae contains about 95 % of living species which genus *Xestospongia* belongs to. The taxa of this genus is given by Hooper (2000) as follows.

Phylum Porifera
Subphylum Cellularia
Class Demospongiae
Order Haplosclerida
Family Petrosiidae van Soest, 1980
Genus *Xestospongia* de Laubenfels, 1932
(Syn. *Neopetrosia* de Laubenfels, 1949,
Prianos Gray, 1867)

The bluish sponge sample was collected from Si Chang Island in 1992 and identified as *Reniera* sp. at that time. *Reniera* also belongs to class Demospongiae, order Haplosclerida, but in family Chalinidae Gray, 1867 as genus *Reniera* Nardo,

1847. There were many reports of the isolation of renieramycin isoquinoline alkaloids from sponges in order Haplosclerida but different families, such as; genus *Haliclona* Grant, 1835 from family Chalinidae, genus *Cribrochalina* Schmidt, 1870 from family Niphatidae van Soest, 1980.

Hooper (2000) described the characters of sponges belonging to genus *Xestospongia* as following :

Xestospongia de Laubenfels, 1932

Ectosomal skeleton indistinct; choanosomal skeleton confused isotropic reticulation of multispicular tracts, generally lacking spongin and sometimes with single spicule scattered throughout mesohyl between major spicule tracts, stony texture; oxeote spicules in one size category only (Hooper, 2000).

The bluish sponge was collected in December 1992 and later was identified by Hooper as *Xestospongia* sp. #2133 (sample code QMG 306998, family Petrosiidae). The voucher specimens have been deposited at Queensland Museum, Australia and at Department of Pharmacognosy, Faculty of Pharmaceutical Sciences, Chulalongkorn University, Bangkok, Thailand. This sponge exhibits thick, encrusted, lobate growth. Its texture is rough, although it is brittle and easily crumbles. It is light bluish-gray when alive, and pinkish in ethanol. Osculal are numerous and of moderate size, and are found on apices of surface lobes, with a slightly raised lip. The surface has prominent bulbous surface lobes with some that are nearly digitate in size. The surface is translucent, membranous, optically smooth, macroscopically bulbous, microscopically even, with choanosomal drainage canals that are slightly visible below the surface. Ectosomal skeleton membranes have no specialized speculation or structure. Choanosomal skeleton with isotropic reticulation of paucispicular tracts of oxeas forms tight oval meshes. Many free oxeas are scattered between tracts. Small to moderately sized subdermal cavities are observed throughout skeleton. There are no visible fibers, and only small amounts of collagen in the mesohyl. The oxeas are robust, straight or slightly curved at center, sharply pointed, hastate (190-210 x 12-18 micrometers). This species is probably a new one.

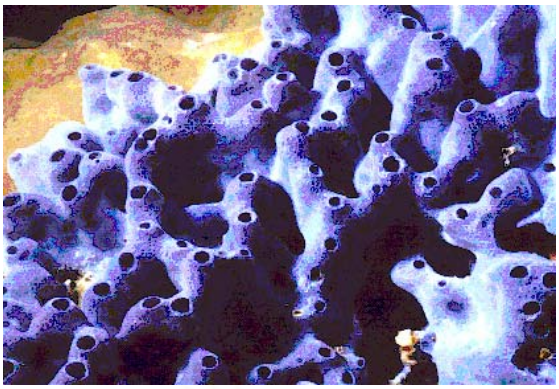

Figure 3 Picture of *Xestospongia* sp. collected from Si Chang Island

2. ISOQUINOLINEQUINONE ANTITUMOR ANTIBIOTICS

Several naturally occurring isoquinolinequinones have been isolated from Actinomycetes, marine organisms such as sponges, tunicates and nudibranchs. The isoquinolinequinones include potent cytotoxic agents that display antitumor and antimicrobial activities.

These natural products are classified by their chemical structures into 4 groups

2.1 saframycin type compounds

2.2 monomeric or simple isoquinolinequinones

2.3 naphthyridinomycin type compounds

2.4 quinocarcin type compounds

The structures of these groups of natural isoquinolinequinones are shown in Figure 4.

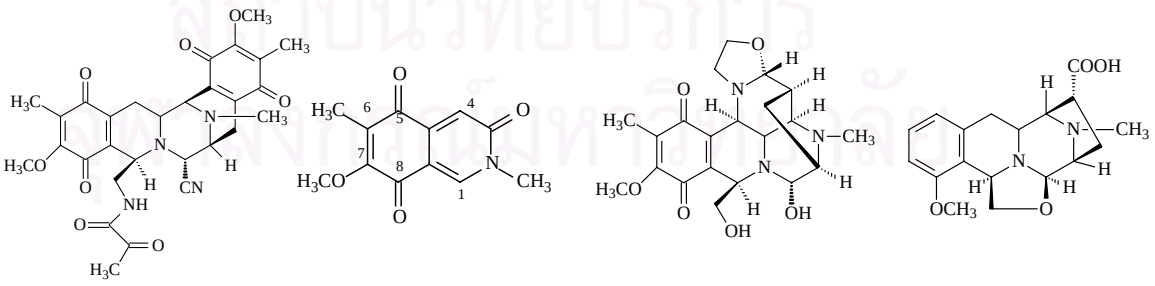

saframycin A mimosamycin naphthyridinomycin quinocarcin

Figure 4 Structures of isoquinolinequinone antitumor antibiotics.

Naphthyridinomycin was isolated from *Streptomyces lusitanus* AYB-1026 in 1974 as an unstable red crystalline solid. This compound has potent antibiotic activity against both Gram-(-) and Gram-(+) bacteria. Naphthyridinomycin inhibits DNA synthesis and the alkylation to DNA was suggested to be the mechanism of this action (Scott and Williams, 2002).

Quinocarcin was isolated from *Streptomyces melanovinaceus* nov. sp. in 1983, it has moderate activity against Gram-(+) bacteria. Quinocarcin citrate has shown potent antitumor activity against several tumor cell lines including St-4 gastric carcinoma, Co-3 human colon carcinoma, MX-1 human mammary carcinoma, M5075 sarcoma, B16 melanoma, and P388 leukemia (Scott and Williams, 2002).

In this thesis, the saframycin type compounds and monomeric or simple isoquinolinequinones will be reviewed, covering on chemical structures , biosynthetic, synthetic, and biological activities studies (Arai and Kubo, 1983; Kubo and Saito, 1992; Ozturk, 2000; Scott and William, 2002).

2.1 Saframycin type compounds

Saframycins, ecteinascidins and renieramycins are included in the saframycin type compounds. Saframycins and renieramycins are bistetrahydro isoquinolines in which two tetrahydroisoquinolines are condensed to form pentacyclic isoquinoline compounds, (rings A to E from left to right, respectively).

Most saframycins and renieramycins are classified into two groups, the bisquinones and the quinone-hydroquinone, depending on whether ring E is quinone or hydroquinone. The members of the bisquinones are saframycins A, B, C, G, H, and S and renieramycins A to G, while saframycins D, E, F and renieramycin H are the member of the quinone-hydroquinone with hydroquinone at ring E. The ring systems and their relative stereochemistries of these two groups are identical. The main difference between the two groups is the side chain, saframycins contain a pyruvamide whereas renieramycins contain an angelate ester.

Ecteinascidins are bistetrahydroisoquinoline alkaoids in which two units, units A and B of tetrahydroisoquinoline are also condensed to form pentacyclic ring and the side chain is a ten membered sulfide-containing lactone ring attached with unit C of a tetrahydroisoquinoline or β-carboline or a chain of carbon.

The basic structures of saframycins, renieramycins and ecteinascidins are shown below.

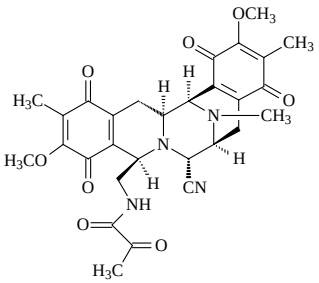

saframycin A

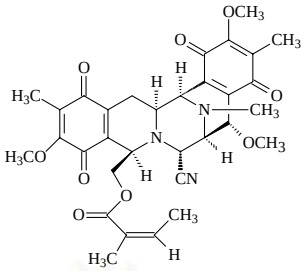

renieramycin R

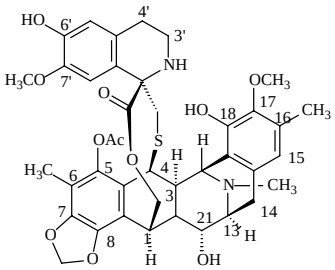

ecteinascidin 743

Figure 5 Structures of selected saframycin type compounds.

2.1.1. Saframycins

Structures of some saframycins are shown in Figure 6.

Isolation and structure determination

Saframycins A, B, C, D and E were isolated from growing-cell system of *Streptomyces lavendulae* No. 314 (Arai *et al*., 1977). During studies of the optimization of saframycin A production, led to the discovery of saframycin S (Arai *et al*., 1980a). In order to increase the production of this highly active antibiotic, sodium cyanide was added to the broth to remarkably increase in the amount of saframycin A. The incorporation of cyanide to form the nitrile moiety of saframycin A was proved by the addition of $Na^{14}CN$ to the broth (Arai *et al.*, 1980a; Ozturk, 2000). Treatment of saframycin A with acid caused hydrolysis of the nitrile functionality and produced saframycin S. Furthermore, treatment of saframycin S with NaCN in neutral or acidic solution formed saframycin A. The interconversion of saframycin S and saframycin A is shown in Scheme 1 (Lown, Joshua and Chen, 1981).

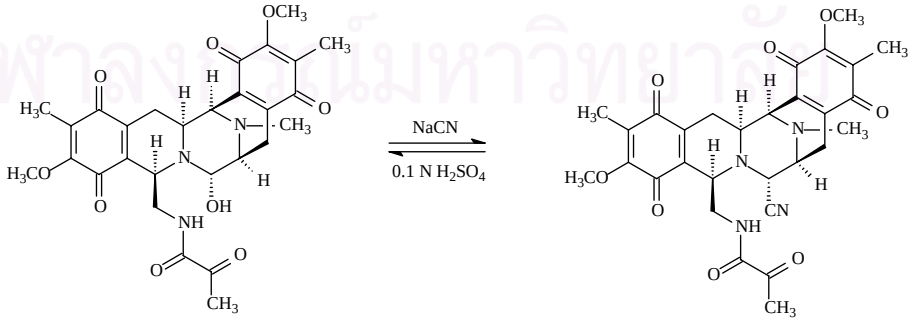

Saframycin S Saframycin A

Scheme 1 Interconversion of saframycin S and saframycin A

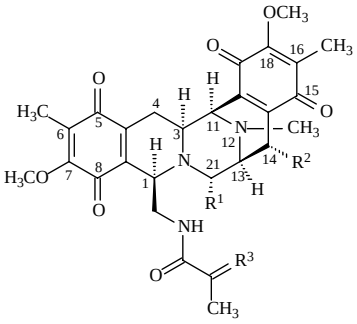

Saframycin A $R^1 = CN, R^2 = H, R^3 = O$
B $R^1 = H, \quad R^2 = H, R^3 = O$
C $R^1 = H, \quad R^2 = OCH_3, R^3 = O$
G $R^1 = CN, R^2 = OH, R^3 = O$
H $R^1 = CN, R^2 = H, R^3 = OH, CH_2COCH_3$
S $R^1 = OH, R^2 = H, R^3 = O$

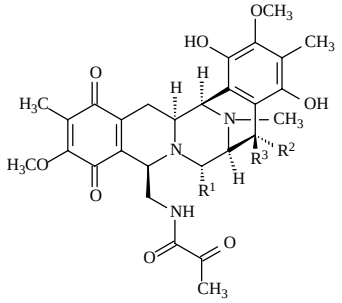

Saframycin D $R^1 = H, R^2, R^3 = O$
E $R^1 = R^3 = H, R^2 = OH$
F $R^1 = CN, R^2, R^3 = O$

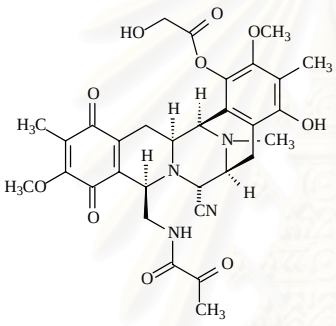

Saframycin R

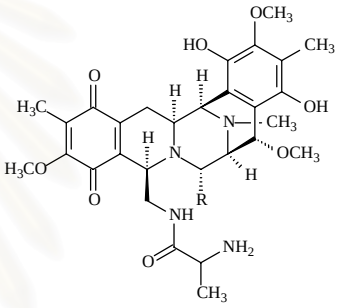

Saframycin Mx1 R = OH
Mx2 R = H

Figure 6 Structures of saframycins

Later the directed biosynthesis employing resting cells of this bacterium could produce saframycins F, G, H, R and Y3. In the search for more biologically active saframycins, six new saframycins were produced by directed biosynthesis employing *S. lavendulae* No. 314 (Yazawa *et al.*, 1986). The supplementation of different amino acids such as alanine, glycine, alanylglycine, 2-amino-n-butyric acid, and glycylglycine yielded saframycins Y3 and the dimer Y2b, saframycins Yd-1, Ad-1, and dimer Y2b-d and saframycin Yd-2.

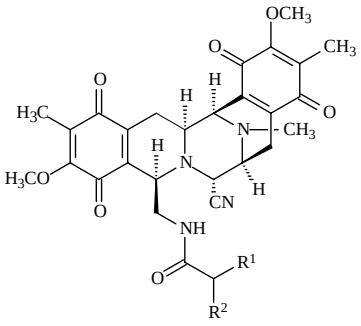

Saframycin Y3 $R^1 = NH_2$, $R^2 = CH_3$
Yd-1 $R^1 = NH_2$, $R^2 = CH_2CH_3$
Yd-2 $R^1 = NH_2$, $R^2 = H$

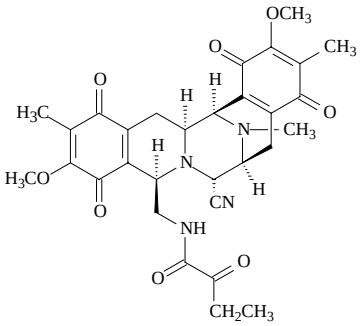

Saframycin Ad-1

Saframycin Y2b $R^1 = CH_3$

$R^2 =$

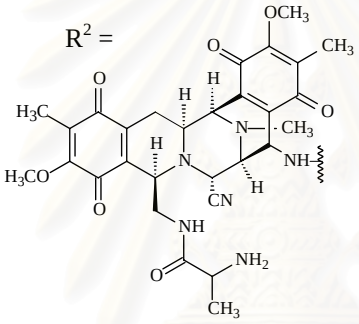

Saframycin Y2b-d $R^1 = CH_3$

$R^2 =$

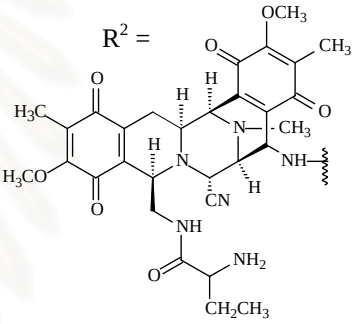

Figure 7 Saframycins obtained from directed biosynthesis.

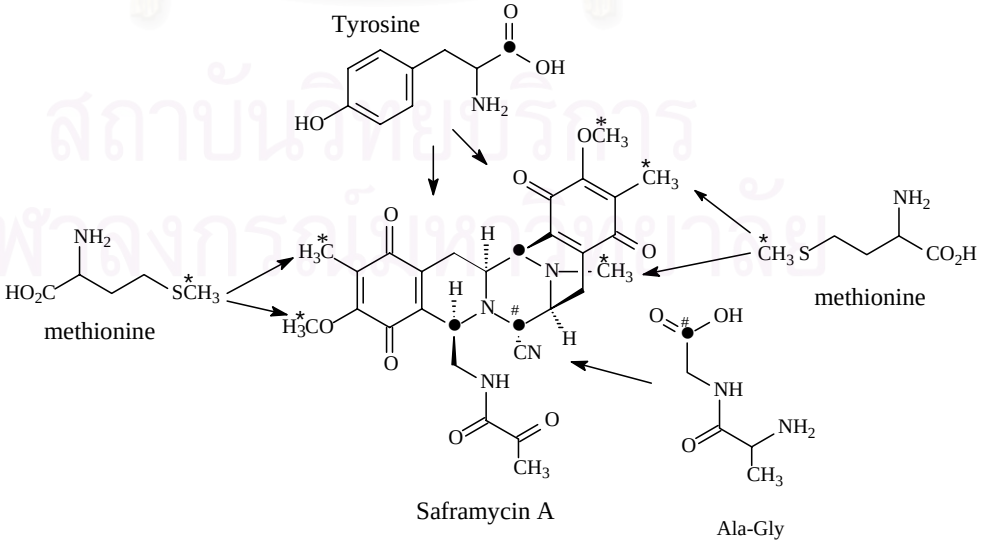

Figure 8 Primary biosynthetic precursors of saframycin A.

Biosynthesis

Mikami *et al*. showed that saframycin A was biosynthesized by the condensation of two ^{13}C-labeled tyrosine moieties (Mikami *et al.,* 1985) (Figure 8), and glycine (Gly) and alanine (Ala) were incorporated into saframycin A (Arai *et al.,* 1985). The dipeptide Ala-^{13}C-Gly was synthesized and incorporated into the pyruvamide side chain. The five methyl groups of saframycin A were found to be derived from *S*-adenosylmethionine (SAM) formed *in vivo* by addition of labeled methionine. Studies were also conducted by Pospiech *et al*. to determine that two multifunctional nonribosomal peptide synthetases and an *O*-methyltransferase are involved in the biosynthesis of this natural product (Pospiech *et al*., 1995; Pospiech, Bietenhader, and Schupp, 1996).

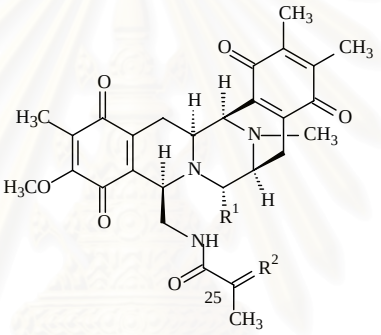

Saframycin	$AR_1 = AH_2$	R^1 = CN, R^2 = H, OH
	AH_1	R^1 = H, R^2 = OH, H
	AR_3	R^1 = H, R^2 = H, OH
	AH_1Ac	R^1 = CN, R^2 = OAc, H
	AH_2Ac	R^1 = CN, R^2 = H, OAc

Figure 9 Saframycin analogs obtained *via* bioconversion and semisynthesis.

The first series of saframycin analogs was obtained by microbial bioconversions of natural (-)- *Rhodococcus amidophilus* IFM 144 yielded three products, saframycins AR_1, AR_2 (saframycin B), and AR_3 (Scott and William, 2002). In this study saframycin A was also treated with sodium borohydride to reduce the carbonyl at C-25 to afford a mixture of diastereomeric alcohols, AH_1 and AH_2 (same as AR_1). The reduced diastereomers were then converted to their acetates forming AH_1Ac and AH_2Ac (Kishi *et al.,* 1984).

Total syntheses of the saframycins

The total synthesis of (±)-saframycin B, which was reported by Fukuyama and Sachleben in 1982, constitutes the first total synthesis of a member of the saframycin family. Starting with two different aromatic aldehydes, cyclization was accomplished using formic acid to form tetracycle, reduction of the lactam carbonyl yielded the key Pictet-Spengler precursor and the pentacycle was formed. Coupling with pyruvyl chloride and oxidation afforded (±)-saframycin B in 37% yield. Kubo *et al*. also reported the synthesis of (±)-saframycin B (Kubo *et al*., 1987a,b). Two-step condensation of the aromatic aldehydes with diketopierazine following by partial reduction with lithium aluminium tri-*tert*-butoxyhydride afforded the tricyclic intermediate. Pictet-Spengler cyclization of the intermediate afforded the pentacyclic intermediate which was further acylated with pyruvyl chloride and oxidized to finally yield (±)-saframycin B in 41% yield.

In 1990, Fukuyama *et al*. reported the first synthesis of (±)-saframycin A. Condensation of aromatic aldehyde with diketopiperazine were the precursors with Cbz-carbamate as a protecting group of the amide, followed by the second aldol condensation, reduction with sodium borohydride and treatment with formic acid afforded the tricyclic intermediate. Pictet-Spengler cyclization of the intermediate finally yielded the pentacyclic core. The final steps involving amide formation with pyruvyl chloride and oxidation of the hydroquinones to quinones afforded saframycin A (Fukuyama *et al*., 1990).

Myers and Plowright reported the synthesis of a series of bishydroquinone saframycin A analogs that were synthesized from the pentacyclic intermediate **8** *via* the removal of the Fmoc group followed by coupling of several acids to the primary amine (Myers and Plowright, 2001, Scheme 2). These analogs were evaluated for antiproliferative activity.

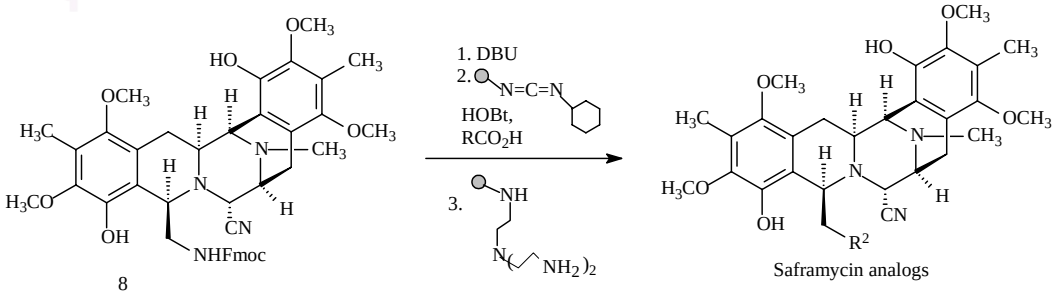

Scheme 2 Myers' synthesis of bishydroquinone saframycin A analogs.

Biological activity

All of the saframycins have been found to display antitumor and antimicrobial activities. Saframycins A and S displayed the most potent antitumor activity as shown in Table 2 (Scott and William, 2002), these saframycins have either a nitrile or a hydroxyl at C-21 which allows the formation of an electrophilic iminium species that alkylates DNA in the minor groove. The ID_{50} activities against L1210 leukemia of several saframycins are listed in Table 2 (Kishi *et al.*, 1984). Saframycins A, S, AH_1, and AH_2 containing either a nitrile or a hydroxyl group at C-21 possessed the highest activities. Saframycins G, H, F, AH_1Ac, and AH_2Ac containing a leaving group at C-21 also have sterically demanding side chains that apparently block the incipient iminium species from alkylating DNA. Saframycins B, C, D, and AR_3 which lack a leaving group at C-21 had much lower activities. Saframycin S showed very potent *in vivo* activity against Ehrlich ascites tumors.

In a study to examine side chain effects on biological activity, it was found that the acyl derivatives had lower activity while the alkyl derivatives had similar activities to the natural product. Also, as the side chain became bulkier, the activity decreased (Kaneda *et al.*, 1986; 1987).

Table 1 Antimicrobial activity of saframycins A and S

Tested organism	**Saframycin A, MIC (µg/mL)**	**Saframycin S, MIC (µg/mL)**
Staphylococcus aureus FDA 209P	0.1	0.025
Streptococcus faecalis	12.4	3.12
Bacillus subtilis PCI 219	0.1	0.025
Corynebacterium diphtheriae	0.003	0.004
Sarcina lutea	0.05	0.025

Table 2 Antitumor activity of saframycins and analogs against L1210 leukemia

Compound	**ID_{50} (nM)**	**Compound**	**ID_{50} (nM)**
Saframycin A	5.6	Saframycin AH_1Ac	25.0
Saframycin S	5.3	Saframycin AH_2Ac	27.0
Saframycin $AR_1(AH_2)$	6.1	Saframycin B	800.0
Saframycin AH_1	8.0	Saframycin C	3,900.0
Saframycin G	30.0	Saframycin D	4,800.0
Saframycin H	33.0	Saframycin AR_3	650.0
Saframycin F	590.0		

The bishydroquinone saframycin A analogs synthesized by Myers and Plowright were investigated (Myers and Plowright, 2001), these analogues showed very potent activity against A375 melanoma and A549 lung carcinoma tumor cell lines with some analogs having a 20-fold increase in activity over saframycin A (Table 3).

Table 3 Antiproliferative activities of bishydroquinone saframycin analogs.

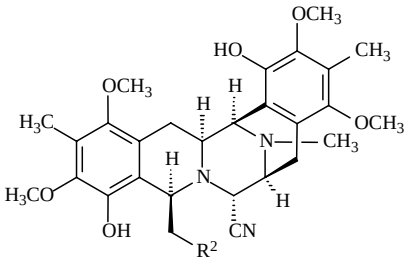

Saframycin analogs

IC_{50}(nM)			IC_{50}(nM)		
R^2=	A375	A549	R^2=	A375	A549
Saframycin A	**5.3**	**133**	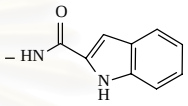	**2.7**	**31**
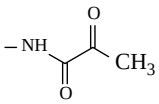	**4.5**	**160**	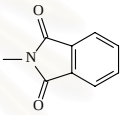	**1.7**	**9.2**
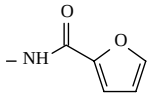	**13**	**290**	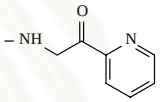	**3.3**	**40**
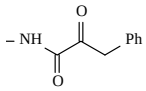	**2.4**	**39**	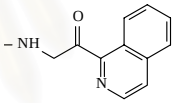	**2.5**	**32**
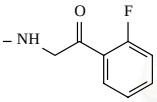	**2.5**	**37**	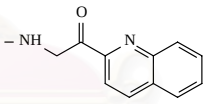	**1.3**	**4.4**
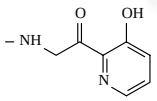	**1.4**	**14**	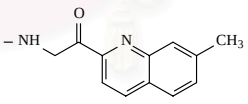	**1.4**	**4.6**
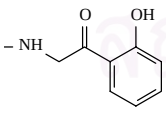	**1.2**	**11**	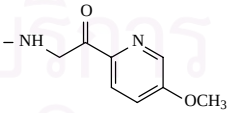	**2.0**	**3.5**
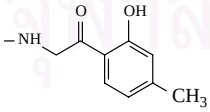	**1.2**	**6.5**	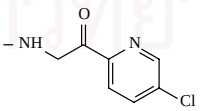	**1.5**	**4.1**
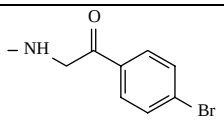	**1.7**	**25**	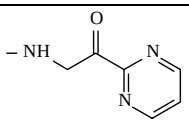	**1.2**	**4.7**
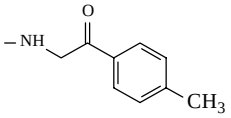	**1.9**	**37**	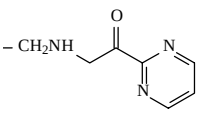	**3.6**	**78**

2.1.2 Renieramycins

The chemical structures of renieramycins from sponges are closely related to naturally occurring tetrahydroisoquinoline families from different sources such as bacteria actinomycetes and marine tunicates (Arai and Kubo, 1983; Ozturk, 2000; Scott and William, 2002). The structures of renieramycins are shown in Figures 1 and 10.

Isolation and structure determination

In 1982, Frincke and Faulkner isolated four new natural products from the sponge *Reniera* sp. collected near Isla Grande, Mexico, and were named renieramycins A-D (**1a-1d**). Seven years later, He and Faulkner (1989) isolated renieramycins E (**1e),** and F **(1f**); from the sponge *Reniera* sp. collected in Palau, both compounds proved to be unstable. These compounds possess identical stereochemical and similar dimeric structures to those of the saframycins. Renieramycin G (**1g**) was isolated in 1992 by Davidson from the Fijian sponge *Xestospongia caycedoi,* and two different renieramycins with the unique benzylic olefin, renieramycins H and I, were isolated in 1998 by Parameswaran *et al*. from the Indian sponge *Haliclona cribricutis.* The originally assigned structures for renieramycins H and I were **9** and **10,** respectively. Recently, the structure of renieramycin H has been revised to that of **1h** (Saito *et al.,* 2001), which was also isolated from an Australian sponge, *Cribrochalina* sp. and given the name cribrostatin 4 (Pettit *et al.,* 2000). The structure of cribrostatin 4 was determined by X-ray crystal analysis. Renieramycin P (**1p**) was recently isolated from a southern Japan collection sponge, *Neopetrosia* sp. by the Fusetani's group (Oku *et al.,* 2003). In 2000, Fontana *et al*. isolated jorumycin (**2**) from a nudibranch mollusc, *Jorunna funebris* feeding on the *Reniera* sponge. The structure of jorumycin is most similar to that of **1e** with exception of the acetate group on the alcohol versus the angelate ester on the renieramycins.

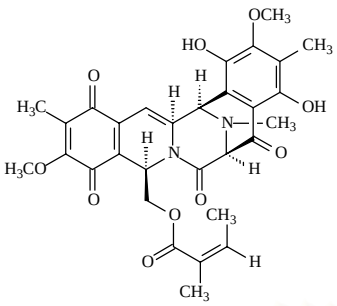

renieramycin H **(1h)**

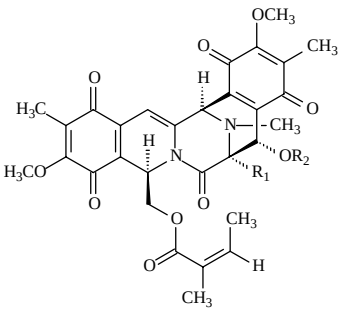

9 : R_1=OH, R_2=H
10 : R_1=H, R_2=CH_3

Figure 10 Structures of renieramycin H and the originally assigned structures for renieramycins H and I

Total synthesis of renieramycin A

To date there has been only one total synthesis of renieramycins. In 1990, Fukuyama, Linton and Tun reported the total synthesis of (±)-renieramycin A. This synthesis used a similar strategy to saframycin A synthesis (Fukuyama *et al.,* 1990; Myers and Kung, 1999; Myers *et al.,* 1999a; 1999b). The main difference was that a different starting phenol was used in the E-ring to allow the necessary benzylic oxidation at C-15. The phenol was protected as the corresponding 3-hydroxypropyl ether, which was further protected as the dimethylthexylsilyl (DMTS) ether.

The protected aldehyde **12** was synthesized in 10 steps from the aldehyde **11**. Aldol condensation with the diketopiperazine **13** followed by hydrogenation and carbamate formation yielded the diketopiperazine **14**. The second Aldol condensation followed by reduction of the amide with sodium borohydride yielded the carbinolamine, which was treated with formic acid to cyclize ring D. Sodium hydroxide in methanol removed the DMTS group to provide **15**. High-pressure hydrogenation of the benzylic olefin along with removal of the Cbz and benzyl groups of **15** yielded a single tricyclic diastereomer. The bridgehead amine was then reprotected as a base-labile carbamate. Protection of the phenols followed by Swern oxidation to remove the hydroxy ether yielded **16**. Selective oxidation of the benzylic position with DDQ installed the necessary C-15 hydroxyl group. Following methylation of the phenol, the carbamate was removed using DBU and the methyl

group was installed *via* a reductive amination to yield **17**. Reduction of the amide followed by benzyl group removal resulted in **18**. The final two steps to (±)-renieramycin A were a Pictet-Spengler cyclization using glycoaldehyde angelate and DDQ oxidation of the hydroquinones to quinones, which was accomplished in 48% yield.

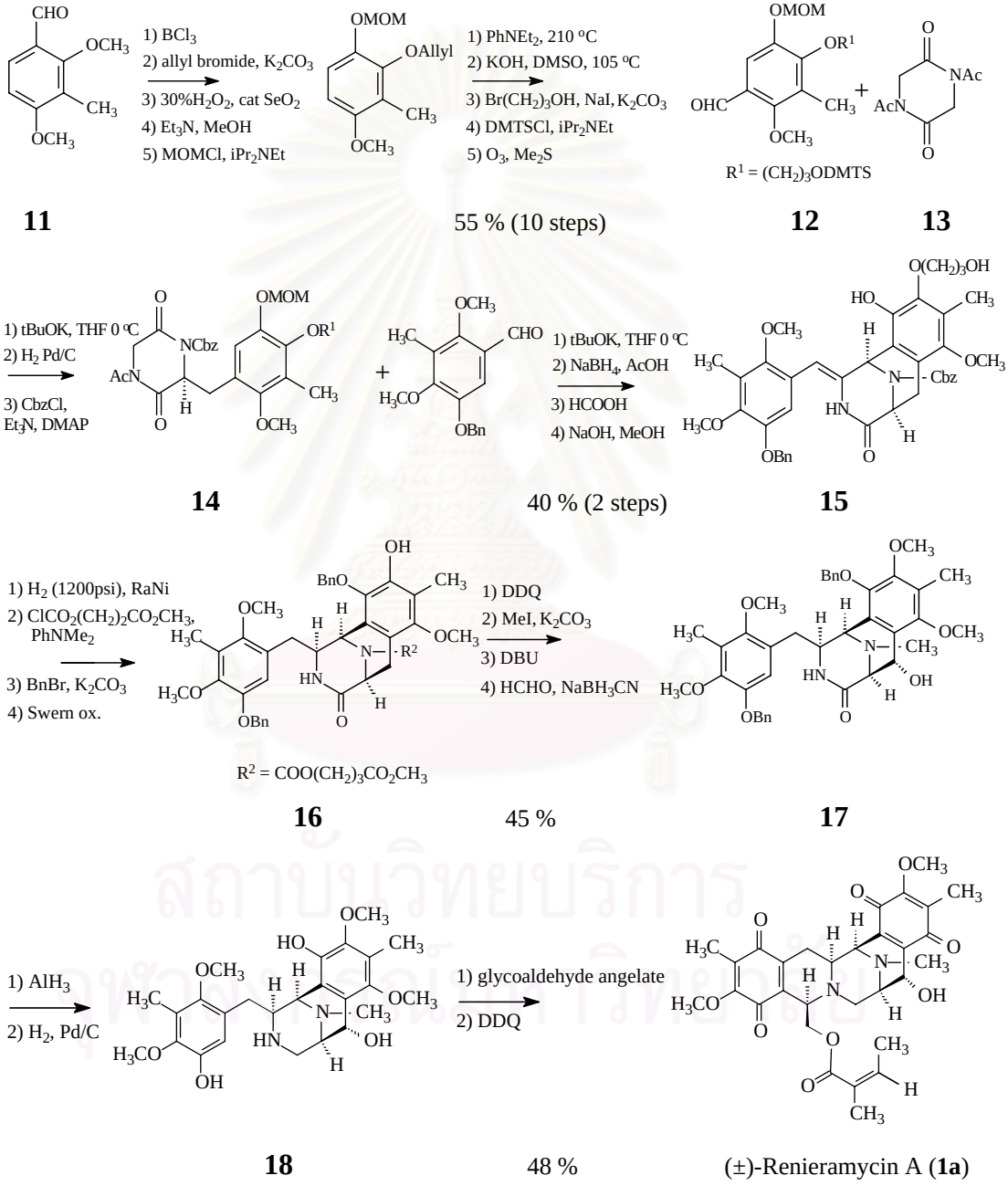

Scheme 3 Fukuyama's synthesis of renieramycin A (**1a**)

Biological activity

There has been scant data reported in the literature on the biological activity of renieramycins. Reineramycins A-D (Frincke and Faulkner, 1982), H, and I (Parameswaran *et al.*, 1998) have moderate antimicrobial activities, while renieramycin G has shown moderate activity against KB and LoVo cell lines with MIC of 0.5 and 1.0 μg/mL, respectively (Davidson, 1992). The cytotoxicities of renieramycin P against 3Y1, HeLa and P388 cells with IC_{50} of 5.3, 12.3, and 0.53 nM, respectively (Oku *et al.*, 2003).

2.1.3 Ecteinascidins

Ecteinascidins are tetrahydroisoquinoline alkaloids which compose of three units, in which units A and B of tetrahydroisoquinoline are condensed to form a pentacyclic ring and unit C attached to unit B by a ten membered sulfide-containing lactone ring. Ecteinascidins are either the bis- or tris-tetrahydroisoquinoline units and can be divided into three groups based on the unit C.

1. Ecteinascidins with three tetrahydroisoquinoline units (A-C)

These ecteinascidins compose of three tetrahydroisoquinolines (see basic structure in Figure 11). The members of this group are Ets 729, 743, 745, and 770 (the number indicates the molecular weight of each compound) (Rinehart *et al*., 1990b).

2. Ecteinascidins with two tetrahydroisoquinoline units (A, B) and one tetrahydro-β-carboline unit (C). The members of this group are Ets 722, and 736.

3. Ecteinascidins with two tetrahydroisoquinoline units (A, B) and a chain of carbons (unit C). The members of this group are Ets 594, 597, 583, and 596.

Isolation and structure determination

The isolation of the ecteinascidins (Ets) was first reported from *Ecteinascidia turbinata* including Ets 729, 743, 745, 759A, 759B, and 770 (Rinehart *et al*., 1990b). The structures of Ets 729 and 743 with the correct relative stereochemistry were reported by the Rinehart and Wright groups (Wright *et al.*, 1990), simultaneously. In 1992, Rinehart *et al.* published the isolation of Ets 722, 736, and 734 N_{12}-oxide (Sakai *et al.*, 1992). Four putative biosynthetic precursors

(Ets 594, 597, 583, and 596) were also isolated (Sakai *et al.*, 1996). The structures of some ecteinascidins are shown in Figure 11.

In 2002, Suwanborirux *et al.* isolated Ets 770 and 786 from the KCN-pretreated Thai tunicate, *Ecteinascidia thurstoni* Herdman. Ets 770 and 786 are 21-cyano derivatives of Et 743 and Et 759B, respectively. The authors stated that natural product containing an α−carbinolamine (hydroxylamine) functionality such as Et 743 was relatively unstable during extraction. Et 743 should be stabilized by converting to Et 770 in which the cyanide was directly incorporated to form the more stable aminonitrile functionality (Suwanborirux *et al.*, 2002).

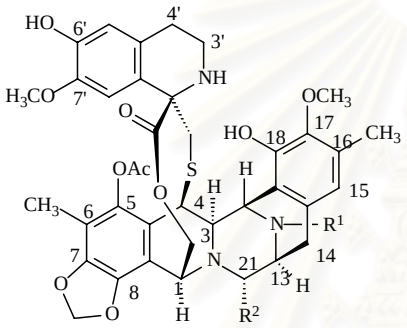

Et 743 $R^1 = CH_3$, $R^2 = OH$
Et 729 $R^1 = H$, $R^2 = OH$
Et 745 $R^1 = CH_3$, $R^2 = H$
Et 759B $R^1 = CH_3$, $R^2 = OH$, S-oxide
Et 770 $R^1 = CH_3$, $R^2 = CN$
Et 786 $R^1 = CH_3$, $R^2 = CN$, S-oxide

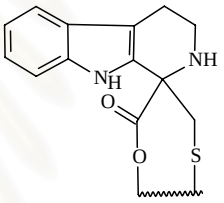

Et 736 $R^1 = CH_3$, $R^2 = OH$
Et 722 $R^1 = H$, $R^2 = OH$

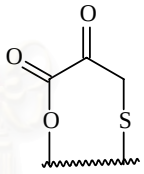

ET 594 $R^1 = CH_3$, $R^2 = OH$

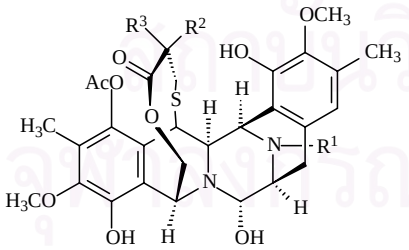

Et 597 $R^1 = CH_3$, $R^2 = NH_2$, $R^3 = H$
Et 583 $R^1 = H$, $R^2 = NH_2$, $R^3 = H$
Et 596 $R^1 = CH_3$, R^2, $R^3 = O$

Figure 11 Structures of ecteinascidins

Biosynthesis

In 1995 Kerr and Miranda showed that ^{14}C-labelled tyrosine and 35S-cysteine were incorporated into ecteinascidin 743 in a cell-free extract from *Ecteinascidia turbinata.* This report also showed that labelled serine was not incorporated. Later, Kerr *et al.* synthesized three radiolabeled diketopiperazines (**19-21**) and used as the precursors for biosynthetic study (Jeedigunta, Krenisky, and Kerr, 2000). Using the same cell-free extract as above, the tyrosine-containing diketopiperazine **20** and the DOPA-containing diketopiperazine **21** were incorporated into Et 743. The conversion of **20** to **21** indicated that tyrosine was first condensed to form **20** which then was oxidized to yield **21** in the biosynthetic route to Et 743.

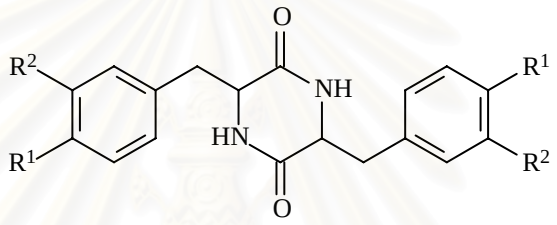

19 : $R^1 = R^2 = H$
20 : R^1 =OH, $R^2 = H$
21 : $R^1 = R^2 = OH$

Figure 12 Biosynthetic precursors to ecteinascidin 743.

Corey *et al*. reported the synthesis and biological activity of potent analogs of Et 743 (Martinez *et al*., 1999). In this study, a compound named phthalascidin (Pt 650) was synthesized, which was surprisingly found to have comparable biological activity to that of Et 743. The synthesis provided phthalascidin in six steps and 72% overall yield. Several other ecteinascidin analogs were also prepared as described in Scheme 4.

These analogs were formed by the conversion of alcohol to amine followed by amide or succinimide formation affording **22**-**29**. In 2000, shorter syntheses of phthalascidin (**22**)were reported (Martinez and Corey, 2000; Cuevas *et al*., 2000).

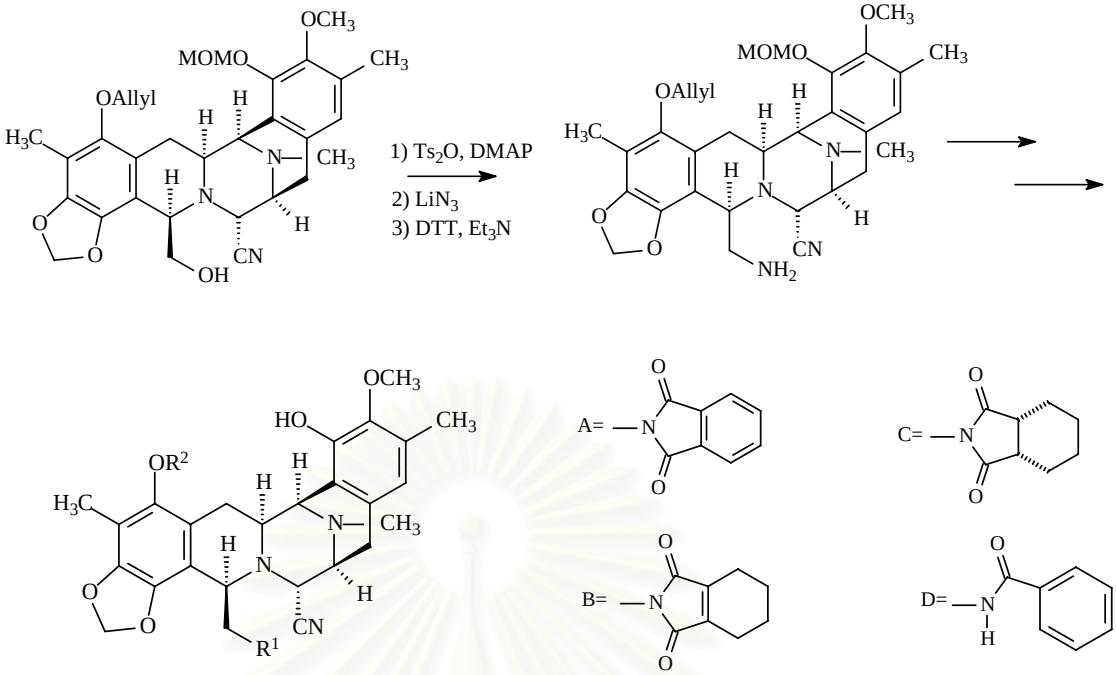

Pt 650; R^1 = A, R^2 = $COCH_3$
22; R^1 = D, R^2 = $COCH_3$
23; R^1 = C, R^2 = $COCH_3$
24; R^1 = B, R^2 = $COCH_3$
25; R^1 = A, R^2 = $COCH_2OCH_3$
26; R^1 = A, R^2 = SO_2CH_3
27; R^1 = A, R^2 = COC_2H_5
28; R^1 = A, R^2 = CH_3
29; R^1 = A, R^2 = C_2H_5

Scheme 4 Phthalascidin analogs

Biological activity

The ecteinascidins have the most potent biological activities by a significant margin relative to that of the tetrahydroisoquinoline antitumor antibiotics. Et743 was more potent than saframycin A against B16 melanoma (Rinehart, 2000). Et 729 exhibited higher *in vivo* activity against P 388 leukemia than Et 743 and Et 745 (Table 4) (Rinehart *et al*., 1990a). Ets 722 and 736 were found to have high *in vitro* activities against L1210 with IC_{90} of 2.5 and 5.0 ng/mL, respectively (Sakai *et al*., 1992). Et 722 was also highly active *in vivo* against a variety of cell lines (Table 5).

The *in vitro* activities of Et 743 against several common tumor cell lines were exceedingly high (Table 6). Et 743 showed tumor growth reduction of breast, melanoma, nonsmall cell lung cancer and ovarian cancer (Rinehart, 2000). Et 743 has

been under investigated in clinical trial phases I and II and currently has been approved as a new drug, named Yondelis (Pharma Mar Company).

Table 4 Activities of Ets 729, 743, and 745 against P388 Leukemia

compound	dose(μg/kg)	T/C
Ecteinascidin 729	3.8	214
Ecteinascidin 743	15	167
Ecteinascidin 745	250	111

T/C : is the increased lifespan of mice treated with the drug versus the control group.

Table 5 Activity of Et 722 against several tumor cell lines

tumor type	dose(μg/kg)	T/C
P388 leukemia	25	>265.0
B16 melanoma	50	200.0

T/C : is the increased lifespan of mice treated with the drug versus the control group.

Table 6 Activity of Et 743 against several tumor cell lines

Tumor type	IC_{50} (nM)
P388 leukemia	0.34
L1210 leukemia	0.66
A549 lung cancer	0.26
HT29 colon cancer	0.46
MEL-28 melanoma	0.50

The biological activity of several pthalascidin analogues were found to be similar to that of Et 743 (Table 7) (Martinez *et al.*, 1999). This was an important

observation due to the fact that the phthalascidins are structurally less complex than the ecteinascidins and are also much easier to synthesize than the natural products.

Table 7 Activities of pthalascidin analogs versus various tumor cell lines

Compound	A-549 (nM)	A375 (nM)	PC-3 (nM)
Pt650	0.95	0.17	0.55
22	3.2	0.35	0.64
23	1.5	0.27	1.1
24	1.2	0.35	0.75
25	1.6	0.31	0.90
26	1.7	0.29	0.86
27	2.1	0.51	2.9
28	3.1	0.55	3.1
29	3.0	0.97	2.4
Et-743	1.0	0.15	0.70

The mechanism of action

The mechanism of action of the ecteinascidins has been studied by several groups. Et 743 inhibited RNA, DNA, and protein synthesis (Rinehart, 2000). Et 743 has a similar structure to that of saframycin S, indicating that DNA alkylation should indeed be possible. The alkylation took place in the minor groove, and the alkylated DNA substrate exhibited a bend or widening of the minor groove (Zewail-Foote and Hurley, 1999). The C-subunit, which is perpendicular to the rest of the molecule, makes the ecteinascidins unique from the saframycins. It has been postulated that this bend in DNA disrupts DNA-protein binding and may be, in part, the source of the enhanced biological activities of the ecteinascidins. It has been demonstrated that the ecteinascidins alkylate DNA at the N-2 residue of guanine in glycine rich regions (Zewail-Foote and Hurley, 2001).

In 1998, Hurley *et al*. showed by NMR studies that the N-12 of Et 743 was protonated in the Et 743-DNA covalent adduct (Moore *et al.*, 1998), which facilitates expulsion of the hydroxyl group in the form of water to form the iminium species. The exocyclic nitrogen of guanine is then envisioned to attack this electrophilic species resulting in covalent adduct formation. Et 743 induced an accumulation of cells in the S and G2-M cell cycle phases after 14 h. After 24 h there was an accumulation in the G2-M phase. This profile was consistent with other DNA alkylating agents (Takebayashi *et al.*, 2001a).

It was reported by Pommier *et al*. that Et 743 halted the DNA excision repair (NER) system in cells (Takebayashi *et al.*, 2001b). It was postulated that the Et 743 DNA covalent adduct trapped an intermediate in NER processing which would not allow the DNA to be fully repaired.

2.2 Monomeric or simple isoquinolinequinones

The compounds in this class are simple isoquinolinequinones, the prototype is mimosamycin (**6**). Substituted groups on the nucleus are varied and depended on biological sources of each compound. The pyruvamide, angelate ester, and other alkanoate ester groups are substituted groups of isoquinolinequinones from the *Streptomyces*, the *Reniera*, and the *Xestospongia*, respectively.

Mimosamycin was firstly isolated from the filtrate of the microorganism *Streptomyces lavendulae* No. 314 in 1976. Later, isolation of mimosamycin from various sources, such as *Reniera* sponge in 1982, blue sponges of the genus *Xestospongia* in 1987, *Cribrochalina* in 1992, and the bright-blue sponge *Petrosia* sp. in 1993 (Faulkner *et al.*, 1982; McKee and Ireland, 1987; Pettit *et al.*, 1992; Venkateswarlu *et al.*, 1993, respectively). In 1994, Kobayashi *et al.*, isolated other mimosamycin derivatives; 4-amino mimosamycin (**30**) and 7-amino-7-demethoxy mimosamycin (**31**) from the blue sponge *Petrosia* sp., collected off the east coast of India.

The chemical structures of monomeric isoquinolinequinones are shown in Figure 13.

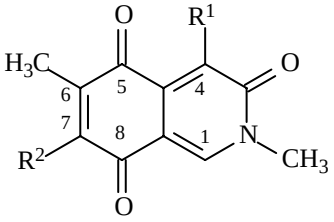

mimosamycin (**6**); $R^1 = H$, $R^2 = OCH_3$
4-amino-mimosamycin (**30**); $R^1 = NH_2$, $R^2 = OCH_3$
7-amino-7-demethoxy mimosamycin (**31**); $R^1 = H$, $R^2 = NH_2$

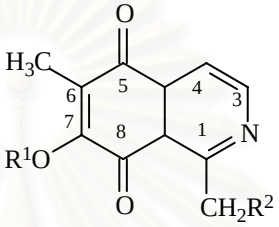

renierone (**4**); $R^1 = CH_3$, R^2 = angelate ester
O-demethylrenierone (**32**); $R^1 = H$, R^2 = angelate ester
renierol (**33**); $R^1 = CH_3$, $R^2 = OH$
renierol acetate (**34**); $R^1 = CH_3$, $R^2 = OCOCH_3$
renierol propionate (**35**); $R^1 = CH_3$, $R^2 = OCOCH_2CH_3$

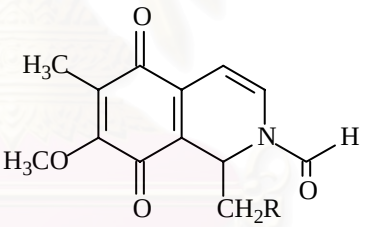

N-formyl-1,2-dihydrorenierone (**5**); R = angelate ester
N-formyl-1,2-dihydrorenierol acetate (**36**); R = $OCOCH_3$
N-formyl-1,2-dihydrorenierol propionate (**37**); R = $OCOCH_2CH_3$

Figure 13 Chemical structures of monomeric isoquinolinequinones.

In 1979, Faulkner *et al.* reported the isolation of renierone (**4**) from a bright-blue sponge, *Reniera* sp., collected near Isla Grande, Mexico (McIntyre *et al.*,1979). Further studies on *Reniera* sp. resulted in the isolation of more renierone-related metabolites; *O*-demethyl renierone (**32**), N-formyl-1, 2-dihydrorenierone (**5**), 1, 6-dimethyl-7-methoxy-5,8-dihydroisoquinoline-5,8-dione (**3**), 2,5-dimethyl-6-methoxy-4,7-dihydro isoindole-4,7-dione (Frincke and Faulkner, 1982). In 1992, **32** and its dimer were isolated from *Haliclona* sp. sponge, collected from Gujarat coast, India

(Parameswaran *et al.*, 1992), **4** and **32** were also isolated from the blue marine sponge, *Cribrochalina* sp. collected in Republic of the Maldives (Pettit *et al.*, 1992).

Renierol (**33**) was isolated from the hard blue sponge *Xestospongia caycedoi* collected at Fiji (McKee and Ireland, 1987). Later, isolation of renierol derivatives; renierol acetate (**34**), renierol propionate (**35**), N-formyl-1,2-dihydrorenierol acetate (**36**), and N-formyl-1,2-dihydrorenierol propionate (**37**) also reported. (Kubo, Kitahara, and Nakahara, 1989).

Biological activity

Mimosamycin (**6**) was mainly active against *Mycobacterium tuberculosis* and inactive on the murine tumors (Ozturk, 2000), it also showed aldose reductase inhibitory effect (34.6 %). **6** was found to have significant activiy against the P388 leukemia cell line (ED_{50} 0.73 µg/ml) (Pettit *et al.*, 1992). 7-Amino-7-demethoxy mimosamycin (**31**) showed a cAMP phosphodiesterase inhibitory effect (26.3 %) (Kobayashi *et al.*, 1994).

Renierone (**4**) showed strong antimicrobial activity against *Staphylococcus aureus, Bacillus subtilis,* and *Candida albicans* (McIntyre *et al.*,1979). **4** and N-formyl-1,2-dihydrorenierone (**5**) were reported to inhibit cell division in the fertilized sea urchin egg assay (Frincke and Faulkner, 1982). 1, 6-Dimethyl-7-methoxy-5,8-dihydroisoquinoline-5,8-dione (**3**) inhibited human immunodeficiency virus (HIV) reverse transcriptase and avian myeloblastosis virus (AMV) reverse transcriptase (Inouye *et al.*, 1987; Ozturk, 2000; Take *et al.*,1987).

Renierol (**33**), renierol acetate (**34**), renierol propionate (**35**), N-formyl-1,2-dihydrorenierol acetate (**36**), and N-formyl-1,2-dihydrorenierol propionate (**37**) were active against *Staphylococcus aureus* (McKee and Ireland, 1987; Kubo *et al.*, 1989) and the latter four compounds were active against *Bacillus subtilis,* and renierol showed mild cytotoxicity against the L1210 cell line with IC_{50} 3.0 µg/ml (McKee and Ireland, 1987).

CHAPTER III

EXPERIMENTAL

1. Source of animal material

The sponge sample was identified as *Xestospongia* sp. #2133 (Family Petrosiidae) by Dr. John N. A. Hooper and the voucher specimens have been deposited at Queensland Museum (serial no. QMG 306998), Australia and in Department of Pharmacognosy, Faculty of Pharmaceutical Sciences, Chulalongkorn University. The sponge was collected by scuba divers in the vicinity of Si Chang Island at the depth of 3 – 5 meters in December 2002 and frozen until used.

2. General techniques

2.1. Thin-layer chromatography (TLC)

Technique	:	One dimension, ascending
Adsorbent	:	Silica gel GF_{254} (E. Merck)
Layer thickness	:	250 μm
Distance	:	8 cm
Temperature	:	Room temperature (25-32 °C)
Detection	:	1. Ultraviolet light at wavelengths of 254 and 365 nm. 2. Visual detection in iodine vapor

2.2. Preparative thin-layer chromatography (p-TLC)

Technique	:	One dimension, ascending
Adsorbent	:	Silica gel GF_{254} (E. Merck)
Layer thickness	:	250 μm
Distance	:	20 cm
Temperature	:	Room temperature (25 °C)
Detection	:	Ultraviolet light at wavelengths of 254 and 365 nm

2.3 Flash column chromatography

Adsorbent	:	Silica gel (No. 1.09385), particle size 0.040-0.063 mm (230-400 mesh ASTM) (E. Merck)

Packing method : The adsorbent was suspended in the eluant. The slurry of the adsorbent was poured into the column and then allowed to settle for 1 hour.

Sample loading : The sample was dissolved in a small volume of benzene and loaded on top of the column

Detection : Fractions were detected by TLC technique as described in the section 2.1.

3. Physical constants and spectroscopy

3.1. Proton and carbon nuclear magnetic resonance (^{1}H and ^{13}C - NMR) spectroscopy

^{1}H and ^{13}C NMR, DEPT 90 and 135, ^{1}H,^{1}H-COSY, HMQC, HMBC and NOESY spectra were obtained on a JEOL-JNM-LA 500 FT-NMR spectrometer at 500 and 125.65 MHz, respectively, and on a Bruker Avance DPX-300 FT-NMR spectrometer, operating at 300 MHz and 75 MHz, respectively. Solvents for NMR spectra were deuterated pyridine (pyridine-d_5) and deuterated chloroform ($CDCl_3$). Chemical shifts were reported in ppm scale using the chemical shift of the solvent as the reference signal and TMS as internal standard. Proton-detected heteronuclear correlations were measured using HMQC (optimized for $^{n}J_{HC}$ = 145 Hz) and HMBC (optimized for $^{n}J_{HC}$ = 4 and 8 Hz) pulse sequences.

3.2. Ultraviolet (UV) absorption spectroscopy

UV spectra were determined in methanol with a Milton Roy Spectronic 3000 Array spectrophotometer.

3.3. Circular Dichroism spectroscopy(CD)

CD was obtained using a JASCO J-720 WI spectropolarimeter.

3.4. Infrared (IR) absorption spectroscopy

IR spectra were obtained on a Perkin Elmer 2000 FT-IR 1760X and on a Hitachi 260-10 spectrophotometer.

3.5. Mass spectrometry

Mass spectra were recorded on JMS-DX 302 and JMS-700 instrument with a direct inlet system operating at 70 eV.

3.6. Elemental analyses

Elemental analyses were conducted on a Perkin-Elmer model 240B and a Yanaco MT-6 CHN CORDER elemental analysers.

3.7. Optical rotation

Optical rotations were measured on a Horiba-SEPA.

3.8. Melting points

All melting points were determined using a Yanagimoto micromelting point apparatus and were uncorrected.

The measurement of physical constants and spectroscopic properties were performed at the Pharmaceutical Research Instrument Center, Faculty of Pharmaceutical Sciences, Chulalongkorn University, Thailand and at Meiji Pharmaceutical University, Japan.

4. Chemicals

Acetic anhydride	Merck
Acetone	Labscan
Acetonitrile	Labscan
Dichloromethane	Labscan
4-Dimethyl aminopyridine (DMAP)	Fluka
Molecular sieve type 4^{o}A	Fluka
Ethyl acetate	Merck
Ethyl alcohol	Labscan
1.0 M Lithium aluminium hydride in THF	Fluka
Methyl alcohol	Labscan
10% Palladium on activated charcoal	Merck
20% Palladium hydroxide on activated charcoal	Kawaken
Pyridine	Merck
Selenium dioxide	Wako
Silver nitrate	Wako
Sodium sulfate, anhydrous	Merck
Sulfuric acid concentrated	Merck
Tetrahydrofuran	Labscan

Triethanolamine Fluka

5. Solvents

All solvents used were either analytical or laboratory grade and were redistilled prior to use.

For chemical reactions, ethyl acetate, ethyl alcohol, and methyl alcohol were dried with molecular sieve type 4^{o}A. Tetrahydrofuran was refluxed and distilled from sodium. Reactions were monitored by TLC on silica gel plates, spots were visualized under UV light at wavelengths 254 and 365 nm. and in iodine vapor.

6. Cytotoxic assay

A single-cell suspension of HCT116 cells (2 x 10^3 cells/well) was added to the serially diluted tested compounds in a microplate. The cell were then cultured for 4 days. The degree of cell growth was measured with a cell counting kit (DOJINDO, Osaka, Japan). IC_{50} was expressed as the concentration at which cell growth was inhibited by 50 % compared with the control.

7. Extraction and isolation of *Xestospongia* sp.

7.1. Extraction of *Xestospongia* sp.

The *Xestospongia* sp. sponge (8.4 kg. wet weight) was homogenized, and adjusted to pH 7 with phosphate buffer solution. Then, 10 % potassium cyanide solution (60 ml) was added dropwise to the homogenized solution (9 L), and the mixture was stirred for 5 hours. Thereafter, the mixture was macerated with methanol (5 L x 3), the extract was filtered, and the filtrate was concentrated under reduced pressure. The aqueous methanolic solution (800 ml) was partitioned with ethyl acetate (500 ml x 4), and concentrated to give the ethyl acetate extract (16.2 g, 0.2 % yield based on the sponge wet weight).

The ethyl acetate extract was subjected to triturate with methanol to give the orange precipitate of renieramycin M (**1m**, 681 mg). The mother-liquor was concentrated *in vacuo* to give the methanol extract (F001, 13.9 g), which was further chromatographed on a silica gel flash column with hexane:ethyl acetate as a mobile solvent, beginning from 5:1, 4:1, 3:1, 7:3, 2:1, 1:1, 1:2, 100 % ethyl acetate, 5%

methanol in ethyl acetate, 10% methanol in ethyl acetate, and methanol. Eleven combined fractions, F002 to F012 were examined by TLC (silica gel plate, hexane:ethyl acetate 1:1) (see Scheme 5).

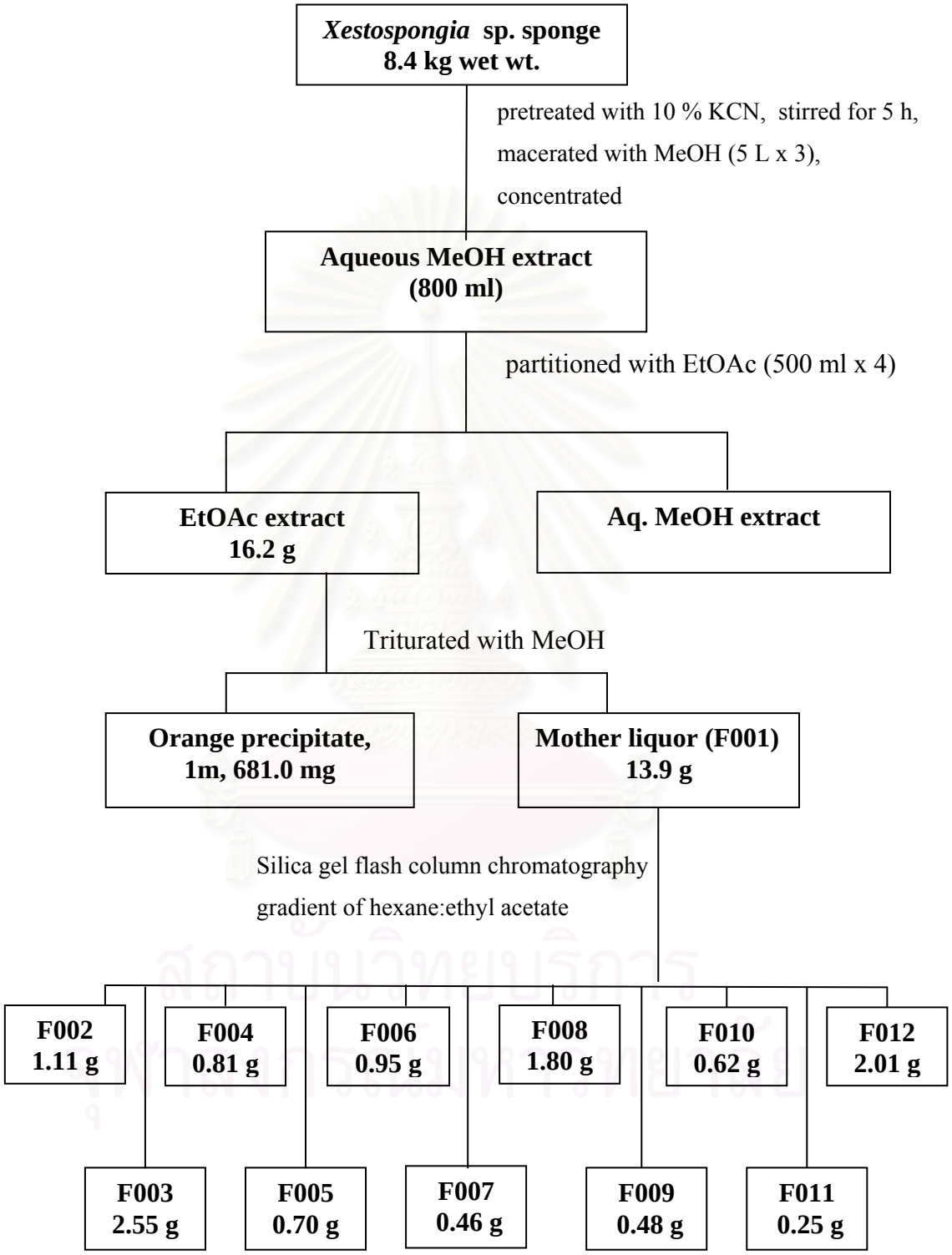

Scheme 5 Extraction and isolation of *Xestospongia* sp. sponge

7.2. Isolation of renieramycins M, N, O, Q, R, and S

From F006 and F007 (1.41 g), renieramycin M (812 mg) was crystallized and the mother liquor was combined and concentrated *in vacuo* to obtain 580 mg of crude mother liquor which was chromatographed by flash silica gel columns with hexane/ethyl acetate as mobile solvents, beginning from 8:1, 6:1, 5:1, 4:1, 3:1, 7:3, 2:1, 1:1, 1:2, 100 % ethyl acetate, 5% methanol in ethyl acetate, 10% methanol in ethyl acetate, and methanol. Five combined fractions were examined by TLC (silica gel plate, hexane:ethyl acetate 1:1), the first fraction contained renieramycin R (**1r**) (65.0 mg), the second contained renieramycin R and renieramycin M (80.5 mg), the third contained renieramycin M (110.0 mg), the fourth contained renieramycin M and renieramycin O (**1o**) (150.0 mg), and the last fraction, F017 (150.7 mg). The second and fourth fractions (F014 and F016) were further chromatographed by using the

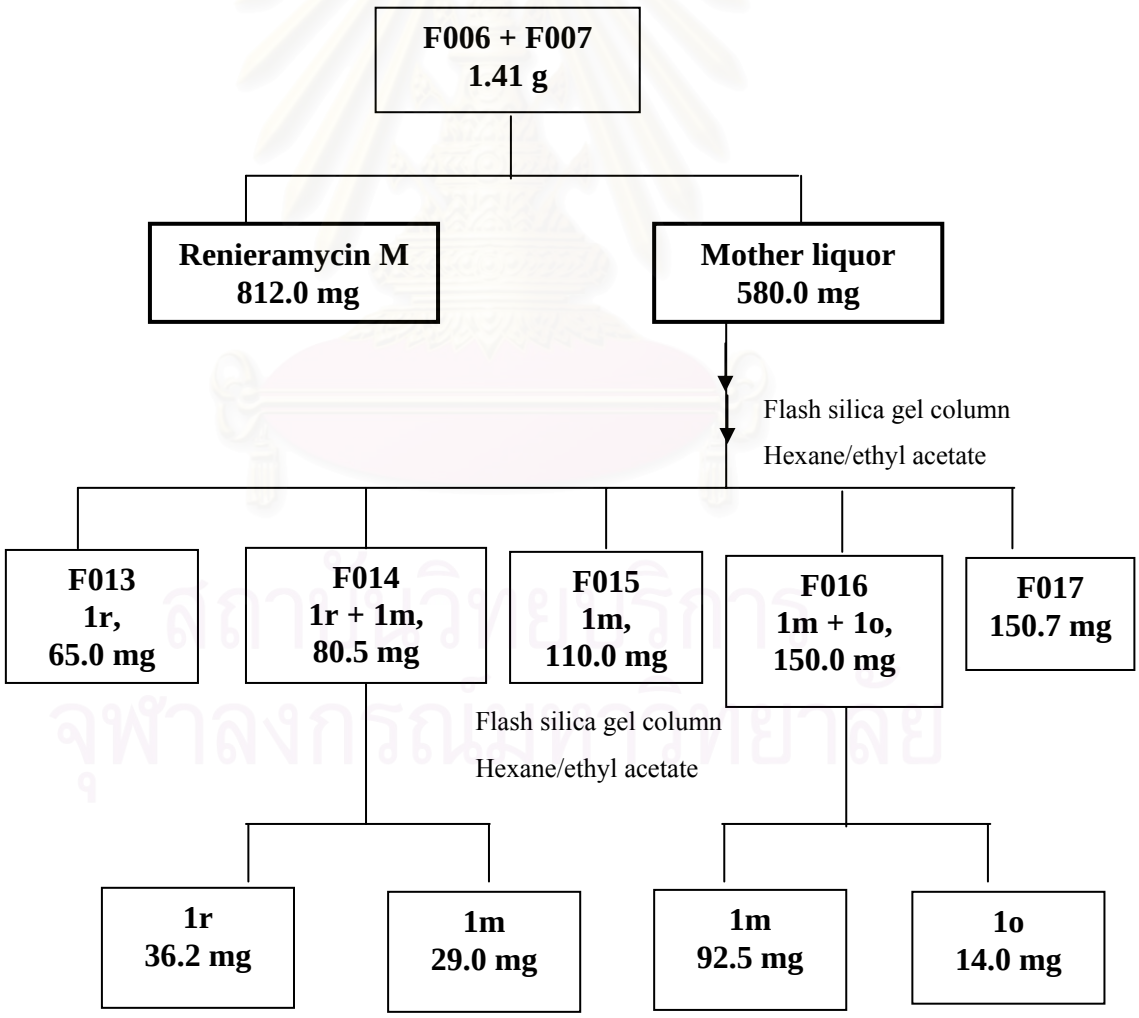

Scheme 6 Isolation of renieramycins M, O, and R from F006-F007

same solvent system to obtain renieramycins R , M and O (36.2 , 121.5 and 14.0 mg, respectively) (see Scheme 6).

From F008 (1.8 g), renieramycin N (**1n**, 122 mg) was crystallized and the mother liquor was concentrated *in vacuo* to give a residue (1.65 g), that was subjected to flash silica gel column chromatography using hexane : ethyl acetate gradiently, to give six fractions, F018-F023. The first fraction, F018 contained renieramycin M (47.0 mg), F019 contained renieramycin M and renieramycin Q (**1q**) (75.5 mg), F020 contained renieramycin M and renieramycin O (58.0 mg), F021 contained renieramycin O and renieramycin N (105.0 mg), F022 contained renieramycin S (**1s**) and renieramycin N (118.0 mg), and the last fraction, F023 (1.15 g).

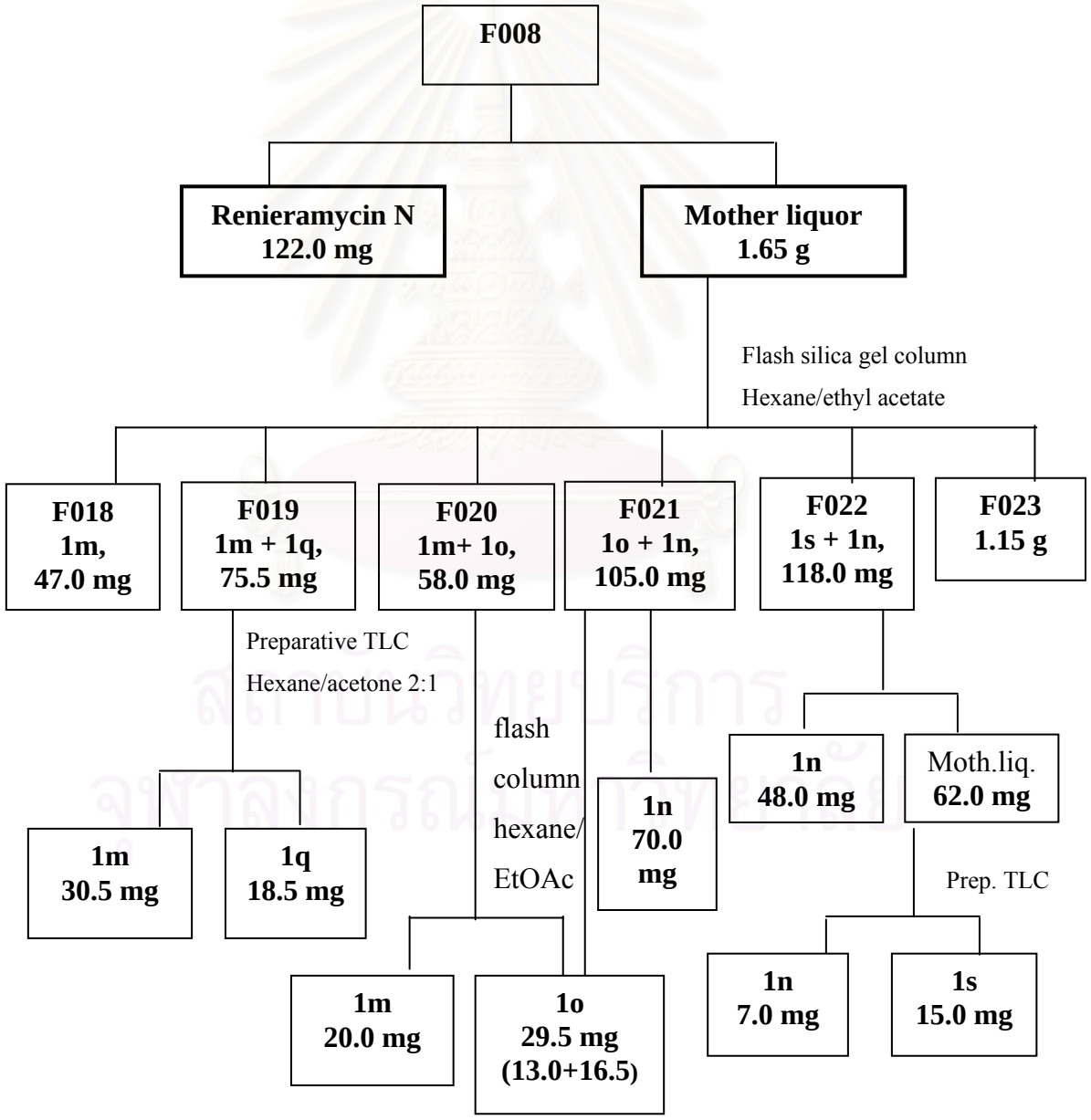

Scheme 7. Isolation of renieramycins M, N, O, Q, and S from F008

The second fraction, F019, was further chromatographed by using preparative silica gel thin-layer chromatography with hexane:acetone 2:1 as the solvent system to obtain renieramycins M and Q (30.5 and 18.5 mg, respectively). F020 and F021 were further chromatographed by using hexane:ethyl acetate gradiently to obtain renieramycins M, O and N (20.0, 29.5 and 70.0 mg, respectively). Renieramycin N (48.0 mg) was also crystallized from F022 and the mother liquor was concentrated (62.0 mg) and chromatographed by using preparative silica gel thin-layer chromatography with hexane:ethyl acetate 1:1 as the solvent system to obtain renieramycins N and S (7.0 and 15.0 mg, respectively) (see Scheme 7).

In conclusion, renieramycins M, N, O, Q, R, and S were isolated in the amount of 1.822 g., 247.0, 43.5, 18.5, 101.2, and 15.0 mg, respectively, or in the yields of 11.25, 1.52, 0.27, 0.11, 0.62, and 0.09 % based on the ethyl acetate extract, respectively.

The TLC chromatogram of the isolated renieramycins on silica gel plate/hexane:ethyl acetate 1:1 is shown in Figure 16.

8. **Physical and spectral data of isolated compounds**

8.1 Renieramycin M

Renieramycin M was obtained as dark yellow prisms from ethyl acetate, soluble in chloroform (1.822 g, 11.25 % based on the ethyl acetate extract).

Melting point	: 194.5-197 ^{o}C
$[\alpha]^{20}_{D}$	: -49.5 (c 1.0, $CHCl_3$)
UV	: λ_{max} nm (ε), in methanol; Figure 17
	269 (21275)
CD	: $\Delta\varepsilon$ nm (c 68 μM, methanol, 22 ^{o}C); Figure 18
	-5.2 (359), -1.9 (305), -8.7 (282), 0 (270), +9.5 (258), 0 (243), -2.2 (232), 0 (223), +10.5 (211)
EIMS	: m/z (% intensity); Figure 19
	575 (M^+, 3), 464 (4), 462 (3), 260 (11), 221 (22), 220 (100), 219 (16), 218 (25), 204 (11), 83 (11), 55 (14).
Elemental analysis	: C 64.52%, H 5.84%, N 7.11%, calculated for $C_{31}H_{33}N_3O_8$, C 64.68%, H 5.78%, N 7.30%.

IR : ν_{max} cm^{-1}, KBr; Figure 20
3270, 2940, 2320w, 1705, 1690, 1650, 1640, 1605.

^{1}H-NMR : δ ppm, 500 MHz, in $CDCl_3$; Figure 21 , Table 8

^{13}C-NMR : δ ppm, 125 MHz, in $CDCl_3$; Figure 23 , Table 8

8.2 Renieramycin N

Renieramycin N was obtained as pale yellow prisms from ethanol, soluble in chloroform (247 mg, 1.52 % based on the ethyl acetate extract).

Melting point : 162.5-164 ^{o}C

$[\alpha]^{20}_{D}$: -24.7 (c 0.015, methanol)

UV : λ_{max} nm (ε), in methanol; Figure 29
272 (11963)

CD : Δε nm (c 45 μM, methanol, 22 ^{o}C); Figure 30
0 (398), -1.0 (355), 0 (310), +0.5 (300), 0 (287), -1.7 (266), 0 (248), +11.8 (222), +25.2 (206).

EIMS : m/z (% intensity); Figure 31
593 (M^{+}, 0.1), 455 (4), 315 (10), 245 (50), 244 (17), 243 (100), 204 (12), 100 (18), 83 (25), 82 (15), 57 (12), 55 (42), 45 (19), 43 (66).

Elemental analysis : C 61.00%, H 6.07%, N 6.68%, calculated for $C_{31}H_{35}N_3O_9$ - H_2O, C 60.88%, H 6.10%, N 6.87%.

IR : ν_{max} cm^{-1}, KBr; Figure 32
3700-3070, 2230w, 1740, 1720, 1655, 1630.

^{1}H-NMR : δ ppm, 500 MHz, in pyridine-d_5 ; Figure 33, Table 11

^{13}C-NMR : δ ppm, 125 MHz, in pyridine-d_5 ; Figure 35, Table 12

8.3 Renieramycin O

Renieramycin O was obtained as pale yellow amorphous solid from ethyl acetate, soluble in chloroform (43.5 mg, 0.27 % based on the ethyl acetate extract).

$[\alpha]^{20}_{D}$: –134.4 (c 0.7, $CHCl_3$)

UV : λ_{max} nm (ε), in methanol; Figure 39
268 (20508)

CD : Δε nm (*c* 88 μM, methanol, 22 ^{o}C); Figure 40
0 (380), -0.5 (352), 0 (310), -1.9 (278), -0.4 (246), 0 (241), +7.1 (213)

EIMS : m/z (% intensity); Figure 41
591 (M^+, 3), 577 (7), 575 (6), 566 (7), 476 (9), 464 (5), 462 (8), 460 (8), 315 (7), 260 (14), 243 (43), 236 (18), 235 (25), 221 (24), 220 (100), 219 (23), 218 (50), 205 (11), 204 (24), 83 (14), 55 (11)

HR-EIMS m/z 591.2222 $[M]^+$ (calcd for $C_{31}H_{33}N_3O_9$, 591.2217).

IR : ν_{max} cm^{-1}, $CHCl_3$; Figure 42
3270, 2940, 2320w, 1705, 1690, 1650, 1640, 1605.

^{1}H-NMR : δ ppm, 270 MHz, in $CDCl_3$; Figure 43, Table 9

^{13}C-NMR : δ ppm, 67.5 MHz, in $CDCl_3$; Figure 45, Table 10

8.4 Renieramycin Q

Renieramycin Q was obtained as pale yellow amorphous solid from ethyl acetate, soluble in chloroform (18.5 mg, 0.11 % based on the ethyl acetate extract).

$[\alpha]^{18}_D$: –69.8 (c 0.1, $CHCl_3$)

UV : λ_{max} nm (ε), in methanol; Figure 49
273 (15169), 372 (4964)

CD : Δε nm (c 92 μM, methanol, 22 ^{o}C); Figure 50
+3.3 (378), -4.0 (291), +2.5 (261), -1.6 (244), +8.2 (220)

ESIMS : m/z (% intensity); Figure 51
591 (M^+, 1), 480 (4), 478 (7), 476 (6), 451 (8), 359 (13), 315 (25), 236 (100), 235 (74), 220 (19) 217 (15), 204 (27), 83 (25), 55 (19).

HR-EIMS : *m/z* 591.2222 $[M]^+$ (calcd for $C_{31}H_{33}N_3O_9$, 591.2217).

IR : ν_{max} cm^{-1}, ($CHCl_3$); Figure 52
3510, 2940, 2220w, 1710, 1680, 1660, 1640, 1620

^{1}H-NMR : δ ppm, 500 MHz, in $CDCl_3$; Figure 53, Table 11

^{13}C-NMR : δ ppm, 125 MHz, in $CDCl_3$; Figure 55, Table 12

8.5 Renieramycin R

Renieramycin R was obtained as pale yellow amorphous solid, soluble in chloroform (101.2 mg, 0.62 % based on the ethyl acetate extract).

$[\alpha]^{18}_{D}$	: –17.6 (c 0.1, $CHCl_3$)
UV	: λ_{max} nm (ε), in methanol; Figure 60
	267 (18990)
CD	: Δε nm (c 88 μM, methanol, 22 ^{o}C); Figure 61
	–0.7 (346), -0.2 (315), -2.7 (275), +10.7 (214)
ESIMS	: m/z (% intensity); Figure 62
	605 (M^+, 3), 577 (5), 462 (6), 460 (7), 290 (8), 275 (8), 260 (8), 243 (30), 221 (19), 220 (100), 219 (23), 218 (63), 205 (10), 204 (12), 83 (9), 55 (7).
HREIMS	: *m/z* 605.2375 $[M]^+$ (calcd for $C_{32}H_{35}N_3O_9$, 605.2373).
IR	: ν_{max} cm^{-1}, $CHCl_3$; Figure 63
	2930, 2830, 2220w, 1715, 1660, 1650, 1620
^{1}H-NMR	: δ ppm, 500 MHz, in $CDCl_3$; Figure 64, Table 9
^{13}C-NMR	: δ ppm, 125 MHz, in $CDCl_3$; Figure 66, Table 10

8.5 Renieramycin S

Renieramycin S was obtained as pale yellow needles from ethyl acetate-ether, soluble in chloroform (15.0 mg, 0.09 % based on the ethyl acetate extract).

Melting point	: 179-180 ^{o}C
$[\alpha]^{20}_{D}$	: –38.8 (c 1.0, $CHCl_3$)
CD	: Δε nm (c 92 μM, methanol, 22 ^{o}C); Figure 73
	–2.8 (359), -1.8 (309), -7.8 (282), +7.6 (261), -3.2 (230), +1.6 (212), -2.0 (202)
EIMS	: m/z (% intensity); Figure 74
	561 (M^+, 5), 449 (20), 448 (74), 446 (13), 423 (10), 260 (29), 230 (16), 229 (100), 221 (28), 220 (71), 219 (11), 218 (21), 205 (14), 204 (11), 203 (21), 100 (77), 85 (19), 83 (25), 55 (41), 54 (10), 53 (10)
HR-FABMS	: *m/z* 561.2112 $[M]^+$ (calcd for $C_{30}H_{31}N_3O_8$, 561.2111).

IR : ν_{max} cm^{-1}, KBr; Figure 75
3280, 2950, 2220w, 1720, 1660, 1645, 1630

^{1}H-NMR : δ ppm, 300 MHz, in $CDCl_3$; Figure 76, Table 9

^{13}C-NMR : δ ppm, 75 MHz, in $CDCl_3$; Figure 78, Table 10

9. Chemical transformation of renieramycin M

9.1 Modification of renieramycin M at carbon 14 :

Allylic oxidation with selenium oxide in alcoholic solvents.

9.1.1. Chemical transformation of renieramycin M to renieramycin R

A solution of renieramycin M (58.7 mg, 0.10 mmol) and selenium oxide (116.3 mg, 1.05 mmol) in methanol (10 ml) was heated at 80 ^{o}C for 160 h. The reaction mixture was diluted with water (20 ml), made alkaline with 5% $NaHCO_3$, and extracted with chloroform (20 ml x 3). The combined extract was washed with water (20 ml), dried, and concentrated *in vacuo* to give a residue (65.0 mg). The purification of the residue by silica gel flash column chromatography (hexane:ethyl acetate, 2:1) afforded renieramycin R, **1r** (21.7 mg, 35.1%) as a yellow solid. **1r** gave spectral data (^{1}H NMR and ^{13}C NMR, IR) that were in complete agreement with those of the isolated derivative described above.

9.1.2. Chemical transformation of renieramycin M to renieramycin R'

A solution of renieramycin M (**1m**, 58.7 mg, 0.10 mmol) and selenium oxide (116.3 mg, 1.05 mmol) in ethanol (10 ml) was refluxed at 90 ^{o}C for 160 h. The reaction mixture was diluted with water (20 ml), made alkaline with 5% $NaHCO_3$, and extracted with chloroform (20 ml x 3). The combined extract was washed with water (20 ml), dried, and concentrated *in vacuo* to give a residue (66.5 mg). The purification of the residue by silica gel flash column chromatography (hexane:ethyl acetate, 2:1) afforded renieramycin R', **1r'** (21.9 mg, 35.3%).

$[\alpha]^{18}_{D}$: –17.6 (c 0.1, $CHCl_3$)

UV : λ_{max} nm (ε), in methanol; Figure 83
268 (20148)

ESIMS : m/z (% intensity); Figure 84

619 (M^+, 6), 577 (1), 462 (1), 460 (1), 304 (2), 275 (8), 264 (4), 243 (10), 221 (9), 220 (54), 219 (27), 218 (100), 205 (5), 204 (7), 83 (6), 55 (5).

HREIMS : *m/z* 619.2528 $[M]^+$ (calcd for $C_{33}H_{37}N_3O_9$, 619.2528).

^{1}H-NMR : δ ppm, 500 MHz, in $CDCl_3$; Figure 85, Table 13

^{13}C-NMR : δ ppm, 125 MHz, in $CDCl_3$; Figure 87, Table 14

9.2 Modification of renieramycin M at carbon 21

9.2.1. Chemical transformation of renieramycin M to renieramycin E

Renieramycin M (**1m**, 5.8 mg, 0.01 mmol) was dissolved in a mixture of acetonitrile and water [3:2 (v/v), 2.5 ml], and silver nitrate (35 mg, 0.2 mmol, 20 equiv) was added to this solution. The mixture was stirred at 40 ^{o}C for 24 h. A mixture of saturated sodium chloride solution and saturated aqueous sodium bicarbonate solution [1:1 (v/v), 20 ml] was added, and the mixture was extracted with dichloromethane (3 x 20 ml). The combined extract was dried and filtered through a pad of cellulose powder. The filtrate was concentrated to give renieramycin E, **1e** (3.0 mg, 53%) as a yellow solid, which gave spectral data (^{1}H NMR, ^{13}C NMR, IR, HR-FABMS) that were in complete agreement with those of the authentic standard;

CD : Δε nm (c 92 μM, methanol, 22^{o}C); Figure 94
–3.1 (350), -1.4 (306), 0.02 (271), -0.06 (238), -2.7 (230), +0.07 (221)

HR-FABMS *m/z* 549.2247 $[M + H - H_2O]^+$ (calcd for $C_{30}H_{34}N_2O_9$, 566.2348 +1.0008 – 18.0106 = 549.2250); Figure 95.

IR : ν_{max} cm^{-1}, $CHCl_3$; Figure 96
3390, 1700, 1655, 1615 cm^{-1};

^{1}H-NMR : δ ppm, 500 MHz, in $CDCl_3$; Figure 97, Table 13

^{13}C-NMR : δ ppm, 125 MHz, in $CDCl_3$; Figure 99, Table 14

9.2.2. Chemical transformation of renieramycin M to renieramycin J

Silver nitrate (144.1 mg, 0.80 mmol) was added to a stirred solution of **1m** (24.4 mg, 0.04 mmol) in acetone (4 ml) at 25 ^{o}C, and the mixture was stirred at 50 ^{o}C for 1 h. After the solvent was removed, the residue was diluted with water (20 ml) and extracted with chloroform (20 ml x 3). The combined extract was washed with brine (20 ml), dried, and concentrated *in vacuo* to give a solid (31.3 mg) The purification of the residue by silica gel column chromatography (hexane:ethyl acetate, 2:1) afforded renieramycin J, **1j** (17.9 mg, 69.6%) as a yellow amorphous powder.

$[\alpha]_D^{20}$	:–708.8 (c 0.1, $CHCl_3$);
CD	: Δε nm (*c* 83.5 μM, methanol, 24^{o}C); Figure 104 –2.9 (367), -0.4(316), -0.9 (303), -7.6 (284), +6.3 (259), -3.4 (230), +8.1 (209);
EI-MS	: m/z (% intensity); Figure 105 606 (M^+, 35), 493 (50), 388 (12), 290 (43), 272(63), 220 (100);
HR-EIMS	*m/z* 606.2580 $[M]^+$ (calcd for $C_{33}H_{38}N_2O_9$, 606.2567).
^{1}H NMR	: δ ppm, 500 MHz, in $CDCl_3$, Figure 106, Table 13
^{13}C NMR	: δ ppm, 125 MHz, in $CDCl_3$, Figure 108, Table 14

9.3. Modification of Renieramycin M at carbon 22

9.3.1 Reductive deangelation

7-Cyano-6,7,9,14,14a,15-hexahydro-9-(hydroxymethyl)-2,11-dimethoxy-3,12,16-trimethyl (6S,7S,9R,14aS,15R) 6,15-imino-4H-isoquino[3,2-b][3]benzazocine-1,4,10,13(9H)-tetrone **(deangeloyl renieramycin M)**

9.3.1.1. *Direct transformation of renieramycin M* ***(1m)*** *into deangeloyl renieramycin M with $LiAlH_4$:*

A stirred solution of **1m** (57.5 mg, 0.1 mmol) in dry THF (4 ml) was cooled with ice water. A 1.0 M THF solution of lithium aluminium hydride (0.6 ml, 0.6 mmol) was added dropwise over 10 min, and stirring was continued at 0 ^{o}C for 1 h. After quenching by the addition of brine (30 ml), the reaction mixture was extracted

with chloroform (30 ml x 3). The combined extract was washed with brine (30 ml), dried, and concentrated *in vacuo* to give a residue (48.7 mg). The purification of the residue by silica gel column chromatography (hexane:ethyl acetate, 3:1) afforded the alcohol, deangeloyl renieramycin M, **38** (13.2 mg, 26.8%) and **1m** (8.6 mg, 15.0% recovery).

9.3.1.2. *Direct transformation of **1m** into **38** with AlH_3*:

A stirred solution of **1m** (23.7 mg, 0.05 mmol) in dry THF (2 ml) was cooled with ice water. A THF solution of aluminium hydride (0.5 M, 0.6 ml, 0.3 mmol) was added dropwise over 10 min, and stirring was continued at 0 ^{o}C for 1 h. After quenching by the addition of brine (30 ml), the reaction mixture was extracted with chloroform (30 ml x 3). The combined extract was washed with brine (30 ml), dried, and concentrated *in vacuo* to give a residue (28.1 mg). The purification of the residue by silica gel column chromatography (hexane:ethyl acetate, 3:1) afforded the alcohol, **38** (6.4 mg, 26.0%) as a yellow amorphous powder.

9.3.1.3. *Two-step transformation of **1m** into **38** via bishydroquinone **1m (39)**: Procedure A*:

A solution of renieramycin M (**1m**, 86.3 mg, 0.15 mmol) in ethyl acetate (8 ml) was hydrogenated over 20% $Pd(OH)_2/C$ (43.2 mg) at 1 atm for 3 h. The catalyst was removed by filtration and washed with ethyl acetate (200 ml). The combined filtrates were concentrated *in vacuo* to give the leuco compound, **39** (115.8 mg) as a colorless amorphous powder, which was used in the next step without further purification. A stirred solution of **39** in dry THF (6 ml) was cooled with ice water. A 0.5 M THF solution of aluminium hydride (2.4 ml, 1.2 mmol) was added dropwise over 10 min at –20 ^{o}C, and stirring was continued at -20 ^{o}C for 4 h. After quenching by the addition of water (0.1 ml) and chloroform (10 ml), stirring was continued at room temperature overnight. The reaction mixture was diluted with brine (30 ml) and extracted with chloroform (30 ml x 3). The combined extract was washed with brine (30 ml), dried, and concentrated *in vacuo* to give a residue (87.6 mg) that was subjected to chromatography on a silica gel (2.5 g) column with hexane:ethyl acetate (3:1) as the eluent to give the alcohol, **38** (39.4 mg, 53.3%) and **1m** (17.7 mg, 20.5% recovery). Further elution with ethyl acetate gave the decyano deangeloyl renieramycin M, **40** (9.9 mg, 14.1%) as a yellow amorphous powder.

Procedure B:

A solution of renieramycin M (**1m**, 16.0 mg, 0.028 mmol) in ethyl acetate (3 ml) was hydrogenated over 20% $Pd(OH)_2/C$ (8.0 mg) at 1 atm for 3 h. The catalyst was removed by filtration and washed with ethyl acetate (50 ml). The combined filtrates were concentrated *in vacuo* to give the bishydroquinone **1m**, **39** (19.2 mg) as a colorless amorphous powder, which was used in the next step without further purification. A stirred solution of **39** in dry THF (1.5 ml) was cooled with ice water. A 1.0 M THF solution of lithium aluminium hydride (0.2 ml, 0.2 mmol) was added dropwise over 10 min at –20 ^oC, and stirring was continued at –20 ^oC for 4 h. After quenching by the addition of water (0.1 ml) and chloroform (10 ml), stirring was continued at room temperature overnight. The reaction mixture was diluted with brine (30 ml) and extracted with chloroform (30 ml x 3). The combined extract was washed with brine (30 ml), dried, and concentrated *in vacuo* to give a residue (19.2 mg) that was subjected to chromatography on a silica gel (1.5 g) column with hexane:ethyl acetate (3:1) as the eluent to give the alcohol, **38** (4.7 mg, 34.3%) and **1m** (3.4 mg, 21.3% recovery).

deangeloyl renieramycin M (38):

$[\alpha]_D^{25}$: –270.6 (c 1.0, $CHCl_3$);

FAB-MS (Magic bullet) : m/z (% intensity); Figure 114

494 ($[M + H]^+$, 8), 309 (20), 220 (15), 155 (59), 154 (17), 152 (13), 137 (10), 135 (24), 121 (13), 118 (100), 102 (42), 101 (14), 89 (15), 87 (12), 85 (77), 69 (12), 55 (14);

HR-FABMS : *m/z* 494.1910 $[M + H]^+$ (calcd for $C_{26}H_{28}N_3O_7$, 494.1927);

^1H NMR : δ ppm, 500 MHz, in $CDCl_3$, Figure 115, Table 15

^{13}C NMR : δ ppm, 125 MHz, in $CDCl_3$Figure 117, Table 16

6,7,9,14,14a,15-Hexahydro-9-(hydroxymethyl)-2,11-dimethoxy-3,12,16-trimethyl (6S,9R,14aS,15R)6,15-imino-4H-isoquino[3,2-b][3]benzazocine-1,4,10,13(9H)-tetrone **(decyano deangeloyl renieramycin M, 40)**:

$[\alpha]_D^{25}$: –109.8 (c 0.2, $CHCl_3$);

FAB-MS : (*m*-nitrobenzyl alcohol) : m/z (% intensity); Figure 120

469 ($[M + H]^+$, 6), 437 (3), 391 (3), 307 (17), 289 (12),

220 (30), 218 (20), 154 (100), 136 (72);

HR-FABMS : *m/z* 469.1970 $[M + H]^+$ (calcd for $C_{25}H_{29}N_2O_7$, 469.1975);

^1H NMR : δ ppm, 270 MHz, in $CDCl_3$, Figure 121, Table 15

^{13}C NMR : δ ppm, 67.5 MHz, in $CDCl_3$Figure 122, Table 16

9.4. Modification of deangeloyl renieramycin M

9.4.1. Acetylation

9-[Acetoxymethyl]-7-cyano-6,7,9,14,14a,15-hexahydro-2,11-dimethoxy-3,12,16-trimethyl(6S,7S,9R,14aS,15R)6,15-imino-4H-isoquino[3,2-b][3]benzazocine-1,4,10,13(9H)-tetrone **(21-cyanojorumycin, 41)**

Acetyl chloride (9.4 μl, 0.13 mmol) was added to a solution of **38** (16.4 mg, 0.033 mmol), triethylamine (9.2 μl, 0.0066 mmol), and 4-dimethylaminopyridine (8.1 mg, 0.0066 mmol) in dichloromethane (4 ml) at 0 ^oC, and the reaction mixture was stirred at 25^oC for 1 h. The reaction mixture was diluted with water (20 ml) and extracted with dichloromethane (20 ml x 3). The combined extract was washed with brine (20 ml), dried, and concentrated *in vacuo* to give a residue (18.7 mg). The purification of the residue by flash silica gel column chromatography (hexane:ethyl acetate 5:1) afforded the acetate, 21-cyanojorumycin, **41** (12.9 mg, 72.9%) as an amorphous powder.

21-cyanojorumycin, 41

$[\alpha]_D^{25}$: –94.5 (c 0.2, $CHCl_3$);

EIMS : m/z (% intensity); Figure 123
535 (M^+, 7), 260 (8), 243 (6), 221 (19), 220 (100), 218 (24), 204 (12);

HR-EIMS : *m/z* 535.1953 $[M]^+$ (calcd for $C_{28}H_{29}N_3O_8$, 535.1955);

^1H NMR : δ ppm, 500 MHz, in $CDCl_3$, Figure 124, Table 15

^{13}C NMR : δ ppm, 125 MHz, in $CDCl_3$, Figure 126, Table 16

9.4.2. **Chemcal transformation of 21-cyanojorumycin to jorumycin *9-[(Acetoxy)methyl]-6,7,9,14,14a,15-hexahydro-7-hydroxy-2,11-dimethoxy-3,12,16-trimethyl(6S,7S,9R,14aS,15R)6,15-imino-4H-isoquino[3,2-b][3]benzazocine-1,4,10,13(5H)-tetrone* (jorumycin, 2)**

21-cyanojorumycin (**41**, 28.5 mg, 0.053 mmol) was dissolved in a mixture of acetonitrile and water [3:2 (v/v), 5 ml], and silver nitrate (225.1 mg, 1.33 mmol) was added. After stirring at 40°C for 2 h, the reaction mixture was filtered and then washed with chloroform (50 ml), and the combined filtrates were concentrated. The residue was diluted with water (20 ml) and extracted with chloroform (20 ml x 3). The combined extract was washed with brine (20 ml), dried, and concentrated *in vacuo* to give a residue (28.7 mg). The purification of the residue by flash silica gel column chromatography (hexane : ethyl acetate 2:1) afforded jorumycin, **2** (23.1 mg, 82.9%) as a pale yellow amorphous powder;

jorumycin, 2

$[\alpha]_D^{25}$	: –82.0 (c 0.31, $CHCl_3$);
EIMS	: m/z (% intensity); Figure 129
	526 (M^+, 3), 508 (2), 437 (3), 369 (26), 368 (26),313 (15),
	262 (13), 236 (16), 232 (12), 220 (100);
HR-FABMS	: *m/z* 509.1916 $[M + H – H_2O]^+$ (calcd for $C_{27}H_{29}N_2O_8$,
	526.2022 + 1.0008 – 18.0106 = 509.1924);
^{1}H NMR	: δ ppm, 500 MHz, in $CDCl_3$, Figure 130, Table 17
^{13}C NMR	: δ ppm, 125 MHz, in $CDCl_3$, Figure 132, Table 17

9.5 Reductive Acetylation of renieramycin M

A solution of renieramycin M (**1m**, 46.0 mg, 0.08 mmol) in ethyl acetate (8 ml) was hydrogenated over 20% $Pd(OH)_2/C$ (23.0 mg) at 1 atm for 3 h. The catalyst was removed by filtration and washed with ethyl acetate (100 ml). The combined filtrate was concentrated *in vacuo* to give the bishydroquinone 1m, **39** (58.6 mg) as a colorless amorphous solid.

Compound 39:

^{1}H NMR	: δ ppm, 270 MHz, in $CDCl_3$, Figure 135, Table 18

^{13}C NMR : δ ppm, 67.5 MHz, in $CDCl_3$, Figure 137, Table 19

This material was used in the next step without further purification. Acetic anhydride (1.2 ml) was added to a solution of crude **39** (58.6 mg) and 4-dimethylaminopyridine (2.0 mg) in pyridine (3.0 ml), and the reaction mixture was stirred for 3 h at room temperature. The reaction mixture was diluted with water (20 ml) and extracted with chloroform (20 ml x 3). The combined extract was washed with water (20 ml), dried, and concentrated *in vacuo* to give a residue (340 mg). The purification of the residue by silica gel column chromatography (hexane:ethyl acetate, 2:1) afforded the 5,8-di-*O*-acetyl hydroquinone renieramycin M, **42** (5.5 mg, 11.0%) as a pale yellow amorphous solid. Further elution with hexane:ethyl acetate (1:1) afforded 5,8,15,18-tetra-*O*-acetyl bishydroquinone renieramycin M, **43** as a solid, recrystallization of which from ethyl acetate:ether afforded pure **43** (44.5 mg, 74.4%) as colorless needles.

Compound 42:

$[\alpha]^{21}_D$ +33.1 (c 0.2, $CHCl_3$);

EIMS : m/z (% intensity); Figure 142
661 (M^+, 16), 549 (7), 548 (17), 506 (5), 304 (7), 260 (18), 221 (23), 220 (100), 219 (42), 218 (18), 204 (9), 100 (5), 55 (5);

HR-FABMS : *m/z* 661.2639 $[M]^+$ (calcd for $C_{35}H_{39}N_3O_{10}$, 661.2636);

^{1}H NMR : δ ppm, 270 MHz, in $CDCl_3$, Figure 143, Table 18

^{13}C NMR : δ ppm, 67.5 MHz, in $CDCl_3$, Figure 145, Table 19

Compound 43:

Melting point : 230-231°C;

$[\alpha]^{20}_D$: +3.7 (c 1.0, $CHCl_3$);

EIMS : m/z (% intensity); Figure 152
747 (M^+, 1), 635 (6), 634 (10), 344 (34), 305 (22), 304 (100), 262 (20), 220 (10);

Elemental analyses C 61.90%, H 5.95%, N 5.56%, calcd $C_{39}H_{45}N_3O_{12}$-1/2H_2O, C 61.90%, H 6.07%, N 5.46%;.

^{1}H NMR : δ ppm, 270 MHz, in $CDCl_3$, Figure 153, Table 20

^{13}C NMR : δ ppm, 67.5 MHz, in $CDCl_3$, Figure 155, Table 21

10. Transformation of renieramycin N (1n)

10.1. Oxidation

A solution of renieramycin N (**1n**, 23.7 mg, 0.04 mmol) in ethyl acetate (5 mL) and 5%$NaHCO_3$ (5 mL) was stirred in air at 25 ^oC overnight. After dilution with water (5 mL), the mixture was extracted with ethyl acetate (5 mL x 3). The combined extracts were washed with water (10 mL), dried, and concentrated *in vacuo*. The residue was purified by silica gel column chromatography (hexane : ethyl acetate = 3:1) to afford the corresponding quinone, renieramycin O (**1o**, 16.3 mg, 69%) as pale yellow amorphous powder.

Acetylation of renieramycin O (1o).

Acetic anhydride (0.2 ml) was added to a solution of renieramycin O (**1o**, 13.6 mg, 0.023 mmol) in pyridine (0.5 ml), and the reaction mixture was stirred for 1 h at room temperature. The reaction mixture was diluted with water (10 ml) and extracted with chloroform (10 ml x 3). The combined extracts were washed with water (10 ml), dried, and concentrated *in vacuo* to give a residue (16.2 mg), the purification of which by silica gel column chromatography (hexane:ethyl acetate, 3:1) afforded the 14-*O*-acetyl renieramycin O, **44 (**7.7 mg, 51.7%) as a pale yellow amorphous solid.

10.2. Acetylation

Acetic anhydride (0.4 ml) was added to a solution of renieramycin N (**1n**, 23.8 mg, 0.04 mmol) in pyridine (1.0 ml), and the reaction mixture was stirred for 3 h at room temperature. The reaction mixture was diluted with water (10 ml) and extracted with chloroform (10 ml x 3). The combined extracts were washed with water (10 ml), dried, and concentrated *in vacuo* to give a residue (32.6 mg), the purification of which by silica gel column chromatography (hexane:ethyl acetate, 2:1) afforded the 14,15,18-tri-*O*-triacetyl renieramycin N, **45 (**16.9 mg, 58.9%) as an amorphous solid and the 14-*O*-acetyl renieramycin O, **44** (1.6 mg, 6.2%).

Compound 44:

$[\alpha]^{18}_D$: –63.4 (c 0.22, $CHCl_3$);

EIMS : m/z (% intensity); Figure 139

634 ($[M + H]^+$, 13), 633 (M^+, 1), 607 (7), 309 (16), 220

(44), 219 (32), 218 (76), 155 (47), 154 (13),153 (12), 149 (10), 135 (37), 121 (15), 119 (100), 103 (54), 101 (24), 89 (18), 87 (16), 85 (84), 55 (14);

HR-FABMS : *m/z* 634.2399 $[M + H]^+$ (calcd for $C_{33}H_{36}N_3O_{10}$, 634.2401);

^{1}H NMR : δ ppm, 270 MHz, in $CDCl_3$, Figure 140, Table 18

^{13}C NMR : δ ppm, 67.5 MHz, in $CDCl_3$, Figure 141, Table 19

Compound 45:

$[\alpha]^{25}_D$: –42.7 (c 0.56, $CHCl_3$);

EIMS : m/z (% intensity); Figure 147

719 (M^+, 6), 609 (7), 608 (19), 579 (9), 403 (11), 402 (49), 359 (13), 317 (9), 305 (18), 304 (100), 262 (25), 220 (13), 218 (18), 100 (11), 35 (11);

HR-FABMS : *m/z* 719.2683 $[M]^+$ (calcd for $C_{37}H_{41}N_3O_{12}$, 719.2690);

^{1}H NMR : δ ppm, 500 MHz, in $CDCl_3$, Figure 148, Table 20

^{13}C NMR : δ ppm, 125 MHz, in $CDCl_3$, Figure 150, Table 21

10.3 Reductive acetylation

A solution of renieramycin N (1n, 32.2 mg, 0.0552 mmol) in 10% methanol in dichloromethane (8 ml) was hydrogenated over 10% Pd/C (22.0 mg) at 1 atm for 1 h. The catalyst was removed by filtration and washed with 10% methanol in chloroform (100 ml). The combined filtrates were concentrated *in vacuo* to give the bishydroquinone compound (39.0 mg) as a colorless amorphous solid.

This material was used in the next step without further purification. Acetic anhydride (0.8 ml) and 4-dimethylaminopyridine (1.5 mg) in pyridine (1.5 ml) was added to a solution, and the reaction mixture was stirred overnight for 23 h at room temperature. The reaction mixture was diluted with water (20 ml) and extracted with chloroform (20 ml x 3). The combined extracts were washed with water (20 ml), dried, and concentrated *in vacuo* to give a residue (49.0 mg), the purification of which by silica gel column chromatography (hexane:ethyl acetate, 2:1) afforded the 5,8,14,15,18-*O*-pentaacetyl bishydroquinone renieramycin M, **46 (**33.5 mg, 76.7%) as a pale yellow amorphous solid.

Compound 46:

EIMS	: m/z (% intensity); Figure158 806 ($[M + H]^+$, 25), 805 (M^+, 4), 780 (19), 779 (40), 692 (5), 679 (4), 608 (1), 607 (3), 579 (1), 403 (4), 402 (16), 362 (11), 359 (4), 317 (9), 305 (19), 304 (100), 262 (38), 220 (16), 218 (13), 100 (7), 91 (19), 85 (41);
HR-FABMS	: *m/z* 806.3154 $[M + H]^+$ (calcd for $C_{41}H_{48}N_3O_{14}$, 806.3136);
^{1}H NMR	: δ ppm, 300 MHz, in $CDCl_3$, Figure 159, Table 20
^{13}C NMR	: δ ppm, 75 MHz, in $CDCl_3$, Figure 161, Table 21

11. Oxidative degradation

11.1 Oxidative degradation of renieramycin E (1e)

Method A. Trifluoroacetic acid (28 µl, 0.36 mmol) was added to a stirred solution of **1e** (12.5 mg, 0.022 mmol) in chloroform (2 ml), and the mixture was heated under reflux for 3 h. The reaction mixture was diluted with water (10 ml), made alkaline with 5% $NaHCO_3$, and extracted with chloroform (10 ml x 3). The combined extracts were washed with water (10 ml), dried, and concentrated *in vacuo*. The residue (11.3 mg) was subjected to chromatography on preparative thin layer silica gel (Merck 5715, solvent ethyl acetate:hexane, 2:1) to give 1, 6-dimethyl-7-methoxy-5, 6-dihydroisoquinoline-5, 8-dione (**3**, 0.2 mg, 4.4%), renierone (**4**, 1.1 mg, 15.8%), N-formyl-1, 2-dihydrorenierone (**5**, 1.4 mg, 18.4%), and mimosamycin (**6**, 0.6 mg, 11.7%).

Method B. *p*-Toluenesulfonic acid (5.1 mg, 0.027 mmol) was added to a stirred solution of **1e** (15.5 mg, 0.027 mmol) and selenium oxide (30.4 mg, 0.27 mmol) in 1,4-dioxane (5 ml), and the mixture was stirred for 14 h at 80 ^oC. The reaction mixture was filtered and then washed with chloroform (50 ml). The combined filtrates were concentrated *in vacuo* and the residue was diluted with water (10 ml), made alkaline with 5% $NaHCO_3$, and extracted with chloroform (10 ml x 3). The combined extracts were washed with water (10 ml), dried, and concentrated *in vacuo* to give a residue (10.6 mg), the purification of which by silica gel column chromatography (ethyl acetate:hexane, 1:3) afforded **6** (2.8 mg, 43.9%). Further elution with ethyl acetate:hexane (1:2) gave **4** (4.0 mg, 46.4%). The pH was carefully

brought to approximately 6-7 with acetic acid and further extraction was carried out with chloroform (10 ml x 3). The combined extract was washed with brine (10 ml), dried, and concentrated *in vacuo* to give demethylrenierone (**32,** 1.8 mg, 21.8%) as pale yellow needles.

1,6-Dimethyl-7-methoxy-5,6-dihydroisoquinoline-5,8-dione (3):

Melting point : 189-190°C

EIMS : m/z (% intensity); Figure 163
217 (M^+, 100), 202 (13), 187 (17), 174 (18), 146 (7), 130 (10), 118 (11);

HR-EIMS : *m/z* 217.0748 $[M]^+$ (calcd for $C_{12}H_{11}NO_3$, 217.0739).

^{1}H NMR : δ ppm, 270 MHz, in $CDCl_3$, Figure 164, Table 24

(*Z*)-2-Methyl-2-butenoic acid (5,8-dihydro-7-methoxy-6-methyl-5,8-dioxo-1-isoquinolinyl)methyl ester (renierone, 4):

Melting point : 89-90°C (ethyl acetate/ether)

HR-EIMS : *m/z* 315.1113 $[M]^+$ (calcd for $C_{17}H_{17}NO_5$, 315.1107).

^{1}H NMR : δ ppm, 270 MHz, in $CDCl_3$, Figure 174, Table 23

^{13}C NMR : δ ppm, 67.5 MHz, in $CDCl_3$, Figure 176, Table 25

(*Z*)-2-Methyl-2-butenoic acid (2-formyl-1,2,5,8-tetrahydro-7-methoxy-6-methyl-5,8- dioxo-1-isoquinolinyl)methyl ester (*N*-Formyl-1,2-dihydrorenierone, 5):
dark red amorphous powder;

EIMS : m/z (% intensity); Figure 170
345 (M^+, 6), 315 (15), 232 (100), 204 (79), 117 (10), 83 (21);

HR-EIMS : *m/z* 345.1226 (calcd for $C_{18}H_{19}NO_6$, 345.1212).

^{1}H NMR : δ ppm, 270 MHz, in $CDCl_3$, major isomer and minor isomer, Figure 171, Table 23

7-Methoxy-2,6-dimethyl-3,5,8(2H)isoquinolinetrione (mimosamycin, 6):

Melting point : 223-224°C (dichloromethane-CH_3OH, yellow prisms)

EIMS : m/z (% intensity); Figure 165

233 (M^+, 100), 218 (33), 204 (10), 190 (16), 177 (12), 149 (11);

HR-EIMS : *m/z* 233.0682 $[M]^+$ (calcd for $C_{12}H_{11}NO_3$, 233.0688).

^{1}H NMR : δ ppm, 270 MHz, in $CDCl_3$, Figure 166, Table 24

^{13}C NMR : δ ppm, 67.5 MHz, in $CDCl_3$, Figure 168, Table 25

(*Z*)-2-Methyl-2-butenoic acid (5,8-dihydro-7-hydroxy-6-methyl-5,8-dioxo-1-isoquinolinyl)methyl ester (demethylrenierone, 32):

Melting point : 134.5-136^{o}C (dichloromethane/hexane)

EIMS : m/z (% intensity); Figure 172

301 (M^+, 100), 218 (14), 203 (10), 202 (19), 83 (44), 82 (74), 55 (33);

HR-EIMS : *m/z* 301.0943 $[M]^+$ (calcd for $C_{16}H_{15}NO_5$, 301.0950).

^{1}H NMR : δ ppm, 270 MHz, in $CDCl_3$, Figure 173, Table 23

11.2 Oxidative degradation of jorumycin (2)

p-Toluenesulfonic acid (16.7 mg, 1.09 mmol) was added to a stirred solution of **2** (23.1 mg, 0.044 mmol) and selenium oxide (58.6 mg, 0.53 mmol) in 1,4-dioxane (7 ml), and the mixture was stirred for 12 h at 80 ^{o}C. The reaction mixture was filtered and then washed with chloroform (50 ml). The combined filtrates were concentrated *in vacuo*, and the residue was diluted with water (20 ml), made alkaline with 5% $NaHCO_3$, and extracted with chloroform (20 ml x 3). The combined extracts were washed with water (20 ml), dried, and concentrated *in vacuo* to give a residue (14.6 mg), the purification of which by silica gel column chromatography (ethyl acetate:hexane, 1:5) afforded **34** (4.5 mg, 37.2%). Further elution with ethyl acetate:hexane (1:2) gave **6** (2.1 mg, 20.5%).

Acetic acid (5,8-Dihydro-7-methoxy-6-methyl-5,8-dioxo-1-isoquinolinyl)methyl ester (renierol acetate, 34):

pale yellow amorphous powder;

HR-EIMS : *m/z* 275.0793 $[M]^+$ (calcd for $C_{14}H_{13}NO_5$, 275.0794).

^{1}H NMR : δ ppm, 500 MHz, in $CDCl_3$, Figure 178, Table 23

^{13}C NMR : δ ppm, 125 MHz, in $CDCl_3$, Figure 179, Table 25

CHAPTER IV

RESULTS AND DISCUSSION

1. Comparative study of the extraction methods

Due to the α–carbinolamine functionality in the structures, some renieramycins were relatively unstable during extraction and isolation processes causing minute yields. The addition of cyanide salt was successively used to significantly increase the production of saframycin A in the culture broth of *Streptomyces lavendulae* (Arai *et al.,* 1980a, b) and of ecteinascidins from the Thai tunicate *Ecteinascidia thurstoni* (Suwanborirux *et al.,* 2002). The renieramycins should also be stabilized by converting the labile α–carbinolamine group into the more stable α-cyanoamine group by addition of potassium cyanide to the homogenized sponge during extraction process.

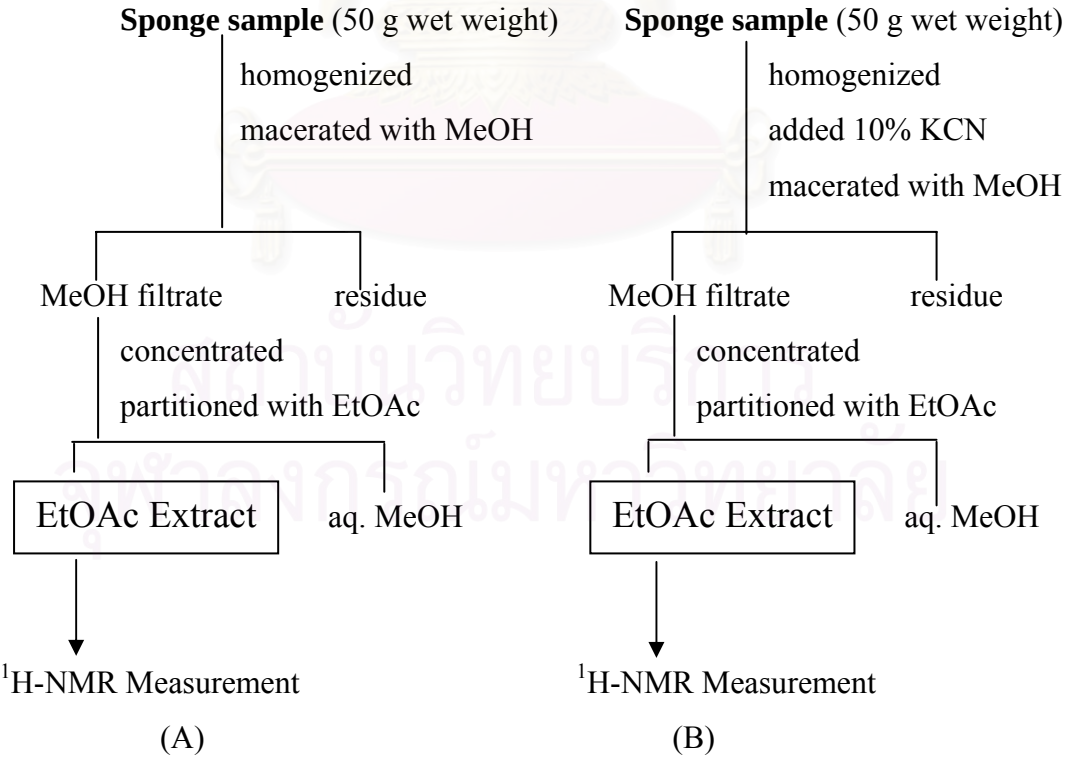

Scheme 8. Comparison of the conventional extraction method (A) with the modified KCN-pretreated method (B).

The Thai *Xestospongia* sp. sponge sample from Si Chang Island, Thailand, was used to comparatively study the conventional extraction method (A) with the modified KCN-pretreated method (B) to obtain the ethyl acetate extracts as shown in Scheme 8.

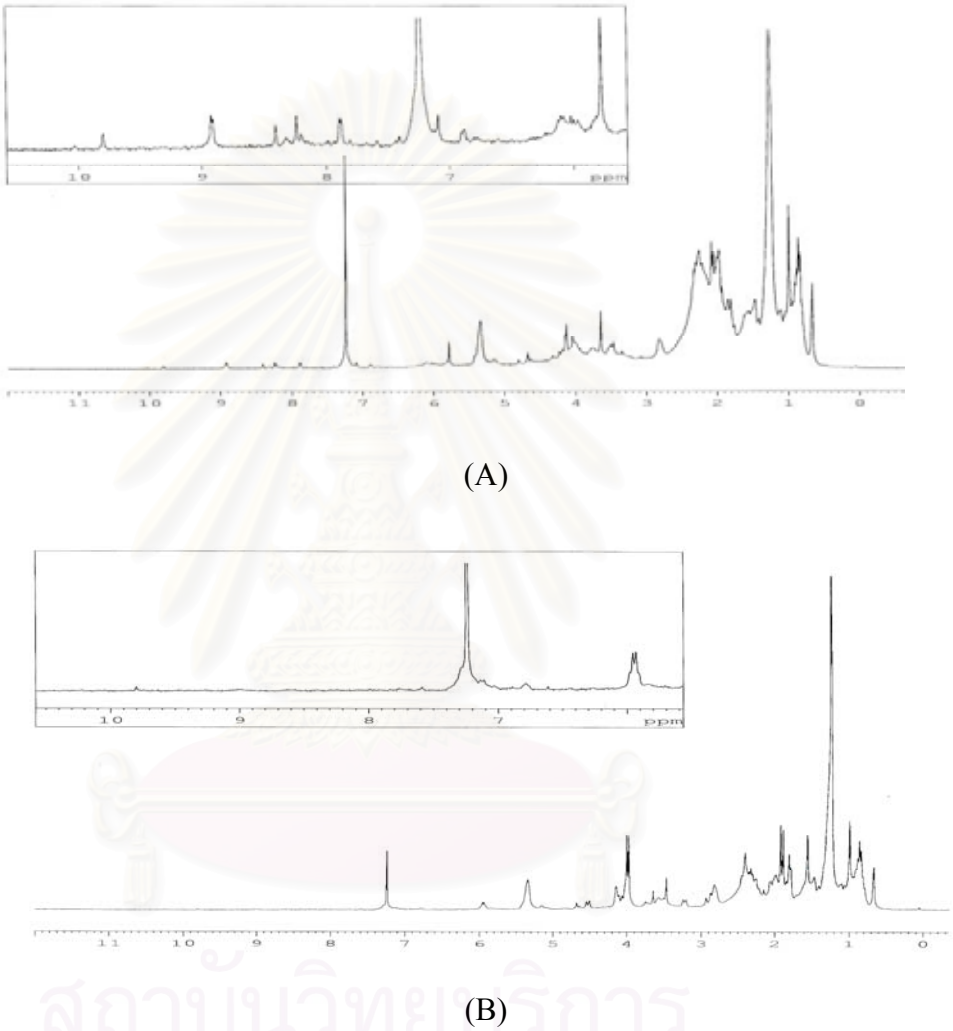

Figure 14. Comparison of the ^{1}H-NMR spectrum of the ethyl acetate extracts from the conventional extraction method (A) and the KCN-pretreated method (B).

The ^{1}H-NMR measurements of both ethyl acetate extracts were displayed in Figure 14. The ^{1}H-NMR spectrum of the extract from the conventional extraction method showed the aromatic proton signals of the monomeric isoquinoline compounds (δ 7.0 to 10.0 ppm), while that of the extract from the KCN-pretreated method clearly showed no signals at this region but the intense proton signal of the angelate olefinic proton at δ 5.9 ppm. The result demonstrated that only bistetra

hydroisoquinolines containing the angelate ester be the main components obtained by this KCN-pretreated method.

This KCN-pretreated strategy was then applied to extract renieramycins from the *Xestospongia* sponge (8.4 kg) collected in December 2002. The addition of potassium cyanide for consistency to the homogenized sponge resulted in about 14 % yield of all isolated renieramycins. It is important to note that we did not obtain monomeric isoquinolines as major components from the sponge that was pretreated with potassium cyanide. These monomerics usually coexisted as main components with renieramycins as minor components when the conventional extraction was used (Frincke and Faulkner, 1982; He and Faulkner, 1989; Davidson, 1992; Parameswaran *et al.,* 1988; Pettit *et al.,*1992; 2000; Fontana *et al.,*2000). We believe that these results provide support for the hypothesis that all the monomeric isoquinolines are degradation products and/or artifacts of isolation procedures.

Actually, the α-cyanoamine group is easily reconverted to the corresponding carbinolamine group in high yield with silver nitrate. Therefore, this strategy provides an answer to the question of how to increase the large-scale supply of the natural renieramycins for further chemical and biological investigations in order to develop this class of compounds as new anticancer agents from Thai *Xestospongia* sponge.

From the methanolic extraction of the blue sponge, *Xestospongia* sp. (8.4 kg wet weight) pretreated with potassium cyanide afforded the crude methanolic extract, which was subjected to partition with ethyl acetate to give the crude ethyl acetate extract (16.2 g) and was further triturated with methanol to give the precipitate of the new renieramycin M (**1m**, 681 mg). Silica gel chromatography of the residual filtrate gave an additional **1m** (1.141 g; 1.822 g in total, 11.25 % yield based on the ethyl acetate extract) as dark orange prisms and renieramycin N (**1n**, 247 mg, 1.52 % yield) as orange rods. The mother liquors of renieramycins M and N were further column and preparative thin layer chromatographed to give additional four renieramycin-type compounds as yellow amorphous solids, including renieramycins O (**1o**), Q (**1q**), R (**1r**), and S (**1s**) in 0.27, 0.11, 0.62, and 0.09 % yield, respectively.

2. Structure elucidation of the isolated compounds

The isolated renieramycins in this study are divided into two main groups; the bisquinone renieramycins and the quinone-hydroquinone renieramycins. The structures of the isolated renieramycins were elucidated predominantly by interpretation of NMR and mass spectral data and comparison with the previous spectral data of related saframycins and renieramycins. Assignments for all protons and carbons of the compounds were mainly accomplished by extensive 2D-NMR measurements including COSY, NOESY, HMQC, and HMBC techniques.

2.1 Structure elucidation of bisquinone renieramycins, renieramycins M, O, R, and S

Renieramycins M (**1m**, $C_{31}H_{33}N_3O_8$), O (**1o**, $C_{31}H_{33}N_3O_9$), R (**1r**, $C_{32}H_{35}N_3O_9$), and S (**1s**, $C_{30}H_{31}N_3O_8$) all share the same carbon skeleton consisting of two quinone rings in the structures. The IR absorption spectrum showed bands at 1650,1640 cm^{-1} (C=O stretching) implied the quinone characters and at 1705 cm^{-1} (C=O stretching) implied the α,β-unsaturated ester. In general, four quinone carbonyl carbons and an ester carbon signal appeared at δ ~ 180-188 ppm and at δ ~ 164-167 ppm in their ^{13}C NMR spectra, respectively. In addition, two olefinic methyl protons at δ ~ 1.5-1.8 ppm and one olefinic proton at δ ~ 5.9-6.0 ppm were characteristic of an angelate ester side chain. The signal of the cyano carbon resonated at δ ~ 116-117 ppm (21-CN) and additional α-cyanoamine-containing carbon (C-21) was upfield shifted to δ ~ 56-58 ppm compared to that of the corresponding carbinolamine carbon in **1e** and **1f** at δ ~ 83 ppm (He and Faulkner,1989). Two aryl methyl proton signals appeared closely at δ ~ 1.90-1.95 ppm while the aryl methoxyl protons at δ ~ 3.97-4.03 ppm and the N-methyl signal at δ ~ 2.2-2.5 ppm. It is noteworthy that the unusual upfield position of the 4-Hβ could be explained by the shielding effects; 4-Hβ should be placed in the strong shielding zone of the E ring and in close proximity to the lone pair of bridging central nitrogen atoms (Kubo and Saito, 1992). The characteristic 4-Hβ signal appeared as a ddd (doublet of doublets of doublets) resulting from the geminal coupling with 4-Hα (J ~ 17-18 Hz), the vicinal coupling with 3-H (J ~ 11 Hz), and the unique homoallylic coupling with 1-H (J ~ 2-3 Hz). Interestingly, the homoallylic coupling occurred only when ring A was a quinone ring

The NMR data of renieramycin M is illustrated in Table 8, and the ^{1}H and ^{13}C NMR data of renieramycins M, O, R, and S are summarized in Tables 9 and 10, respectively.

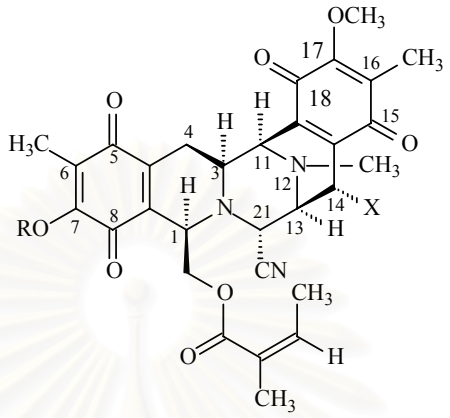

Renieramycin M; X = H, R = CH_3
O; X = OH, R = CH_3
R; X = OCH_3, R = CH_3
S; X = H, R = H

2.1.1 Structure elucidation of Renieramycin M

Renieramycin M was obtained as dark yellow prisms from ethyl acetate showing mp. 194.5-197 ^{o}C and $[\alpha]^{20}_{D}$ -49.5 (c 1.0, $CHCl_3$). This compound has the molecular formula $C_{31}H_{33}N_3O_8$ as deduced by elemental analysis and EI-MS (Figure 19) showing a molecular ion peak at m/z 575. The UV spectrum (Figure 17) exhibited the quinone absorption at λ_{max} 269 nm (ε 21,275).

The proton and carbon NMR assignments of renieramycin M were mainly achieved by comparison with those of the previous data of renieramycins (Frincke and Faulkner, 1982; He and Faulkner, 1989) and interpretation of $^{1}H,^{1}H$-COSY spectrum (Figure 22), HMQC spectrum (Figures 25 and 26), and long-range ^{1}H, ^{13}C connectivities from HMBC experiments (Figure 27).

The substituents of ring E were assigned as follows the methyl group was located at C-16 based upon HMBC correlations of 16-CH_3 proton to C-15, C-16 and C-17. A methoxy group was attached to C-17 based upon long-range correlation of the 17-OCH_3 protons to C-17, whereas C-18 was confirmed by the HMBC correlation between 11-H and C-18. The positions of C-11 and C-13 were determined by long-

range correlations of 13-H, 4-Hβ, and N-CH_3 to C-11; H-11, H-21, 14-Hα, 14-Hβ, and N-CH_3 to C-13; respectively.

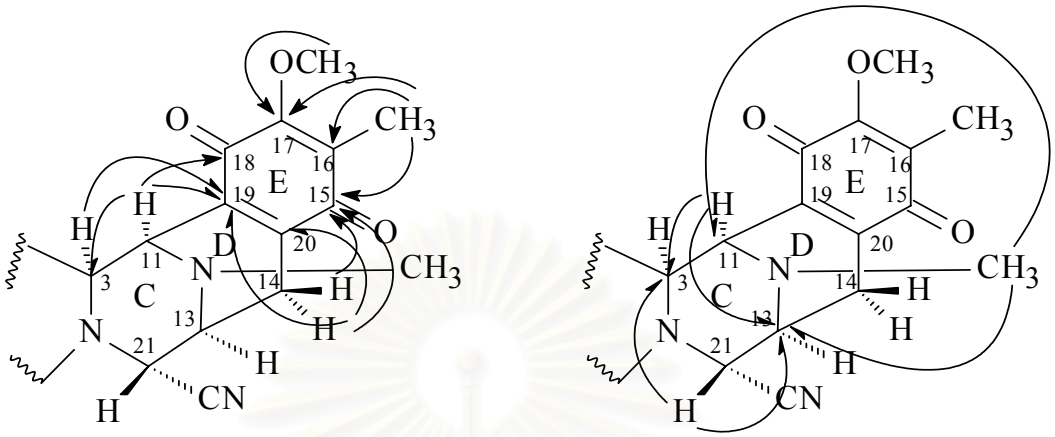

The ring C was formed by insertion of a nitrogen between C-1, C-3 and C-21 based on their chemical shifts and HMBC correlations between 21-H to C-1, C-3 and between 1-H, 14-Hα, and 14-Hβ to C-21 and 1-H to C-22. The 21-CN carbon (116.9 ppm) showed long-range correlation to 21-H.

The substituents on the ring A were confirmed nearly the same as on ring E; the 6-CH_3 proton has long-range correlations to C-5, C-6 and C-7. The methoxy group was attached to C-7 based upon long-range correlation of the 7-OCH_3 protons to C-7. There were the correlations between 22-H_2, 4-Hα, and 4-Hβ to C-9; 4-Hα and 4-Hβ to C-10; and 4-Hα to C-5. The angelate ester side chain was confirmed by the HMBC correlations as follows; the correlations between 22-H_2, 28-H_3 to C-24(carbonyl ester), and between 27-H_3, 28-H_3 to the olefinic carbons,C-25 and C-26.

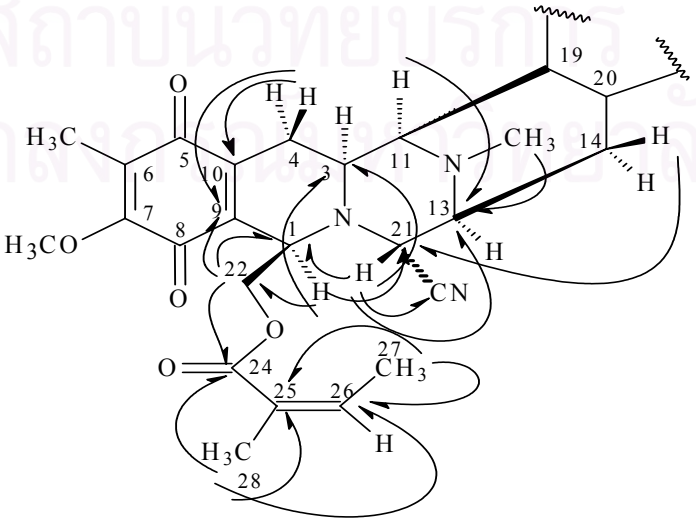

The relative stereochemistries at C-1, C-3, C-11, C-13, and C-21 of renieramycin M were deduced from NOESY experiments (Figure 28). The NOE correlations of 1-H/ 3-H/ 4-Hα/ 11-H/ 13-H / 14-Hα assured the α-orientation of those protons in the molecule. The NOE between 14-Hβ and 21-Hβ revealed the relative stereochemistry at C-21.

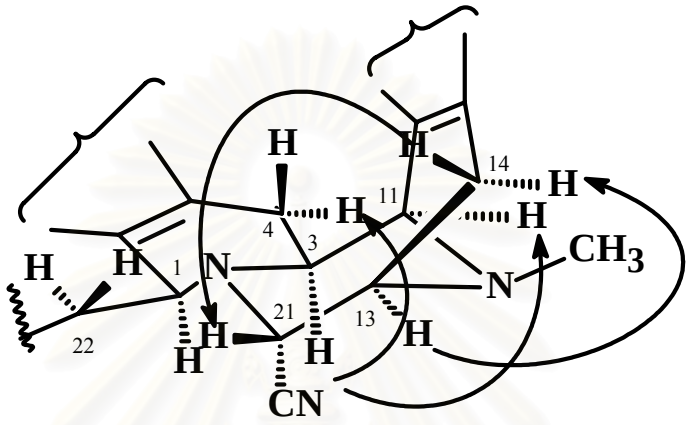

The proton and carbon NMR spectra of renieramycin M were the same as other bisquinone renieramycins, except that the C-14 of **1m** was a methylene carbon (δ ~ 21 ppm). The 14-Hβ signal appeared as a doublet at δ 2.31 ppm, showing only geminal coupling with 14-Hα (J = 21.1 Hz). The 14-Hα signal appeared as doublet of doublets showing additional coupling with 13-H at δ ~ 2.74 ppm (J = 7.6 Hz). The absence of coupling between the signals of 14-H and 13-H (δ 3.42 ppm) required a dihedral angle of 80-90^{o} and suggested a β orientation of 14-H.

The structure of renieramycin M is shown as follows.

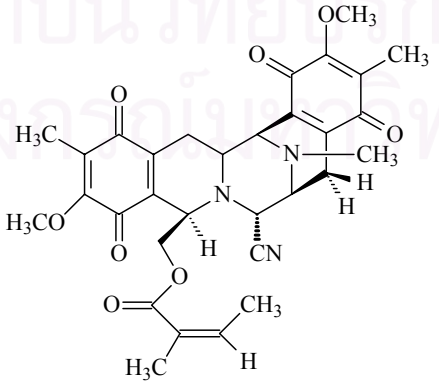

Renieramycin M (**1m**)

The mass spectra for all renieramycins are similar, the molecular ions are weak, a major fragment ion is due to the cleavage of the C3-C11 bond and C13-C21 bond of ring C, and the loss of the side chain at C1 position. The proposed mass fragmentation of renieramycin M is shown in Figure 15. The base peak is the fragment ion at m/z 220 due to the ring C cleavage.

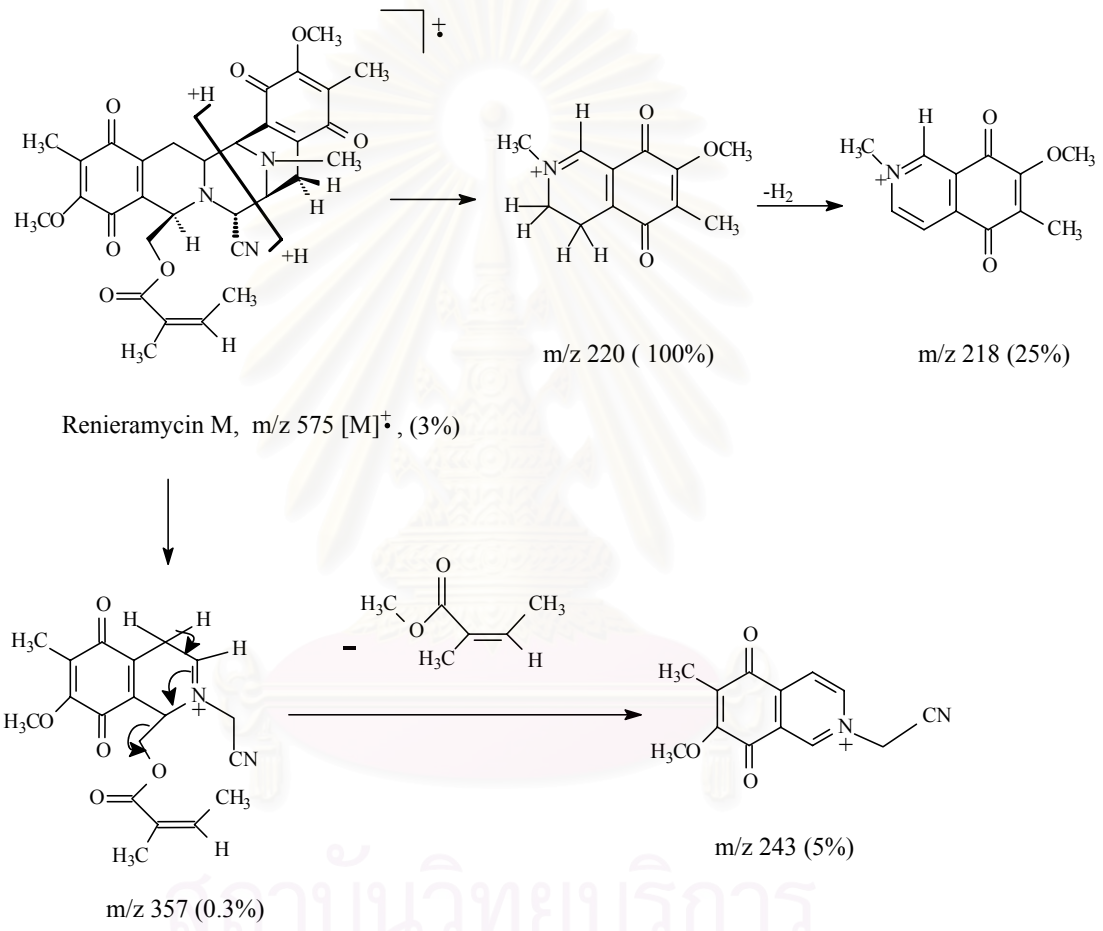

Figure 15 The proposed mass fragmentation of renieramycin M (**1m**)

Table 8 ^{1}H and ^{13}C NMR assignments, HMBC and NOESY correlations of renieramycin M in $CDCl_3$.

Atom no.	δ ^{13}C NMR	δ ^{1}H NMR (integral,multi., *J* in Hz)	HMBC Correlations from C no.	NOESY Correlations
1	56.3 CH	3.99 (1H, ddd, 3.1, 2.9)	21-H	22-H
3	54.1 CH	3.11 (1H, d, 11.3, 3.1, 2.8)	21-H, 1-H, 11-H, 4-Hα	11-H
4	25.4 CH_2	α 2.89 (1H, dd, 17.4, 2.8)	3-H, 11-H	
		β 1.36 (1H, ddd, 17.4, 11.3, 2.7)		
5	185.4 C		4-Hα, 6-CH_3	
6	128.6 C		6-CH_3	
7	155.8 C		6-CH_3, 7-OCH_3	
8	180.9 C			
9	135.7 C		22-H, 4-Hα, 4-Hβ	
10	141.3 C		4-Hα, 4-Hβ	
11	54.2 CH	4.01 (1H, dd, 3.1, 1.8)	13-H, 4-Hβ, N-CH_3	4-Hα, 3-H, N-CH_3
13	54.6 CH	3.40 (1H, ddd, 7.6, 2.5, 1.8)	11-H, 21-H, 14-Hα, 14-Hβ, N-CH_3	14-Hα, 14-Hβ
14	21.3CH_2	α 2.74 (1H, dd, 21.1, 7.6)		13-H
		β 2.31 (1H, d, 21.1)		21-H
15	185.9 C		14-Hα, 14-Hβ, 16-CH_3	
16	128.4 C		16-CH_3	
17	155.2 C		16-CH_3, 17-OCH_3	
18	182.5 C		11-H	
19	135.0 C		11-H, 3-H, 14-Hα, 14-Hβ,	
20	142.0 C		11-H, 13-H, 14-Hα, 14-Hβ,	
21	58.5 CH	4.07 (1H, d, 2.5)	1-H, 14-Hα, 14-Hβ,	13-H, 14-Hβ
22	62.0CH_2	4.10 (1H, dd, 11.6, 2.5)	1-H	22-H, 1-H
		4.53 (1H, dd, 11.6, 3.1)		
24	166.5 C		22-H, 28-H_3	
25	126.3 C		28-H_3, 27-H_3	
26	140.5CH	5.96 (1H, qq, 7.3, 1.5)	28-H_3, 27-H_3	28-H_3, 27-H_3
27	15.7CH_3	1.82 (3H, dq, 7.3, 1.3)		26-H, 28-H_3
28	20.4CH_3	1.58 (3H, dq, 1.5, 1.3)		26-H, 27-H_3
6-CH_3	8.5 CH_3	1.90 (3H, s)		
16-CH_3	8.7 CH_3	1.94 (3H, s)		
7-OCH_3	60.9CH_3	3.99 (3H, s)		
17-OCH_3	61.0 CH_3	4.02 (3H, s)		
NCH_3	41.5 CH_3		11-H, 13-H	11-H, 13-H, 14-Hα
CN	116.9 C	2.28 (3H, s)	21-H	

2.1.2 Structure elucidation of renieramycin O (**1o**)

Renieramycin O was obtained as a pale yellow amorphous solid from ethyl acetate, $[\alpha]^{20}_{D}$ −134.4 (c 0.7, $CHCl_3$). This compound has the molecular formula $C_{31}H_{33}N_3O_9$ as deduced by HREI-MS showing a molecular ion peak at m/z 591.2222. The molecular formula of renieramycin O (**1o**) revealed that **1o** was an oxygenated analog of **1m**. The UV absorption (Figure 39) exhibited at λ_{max} 268 nm (ε 20,508) and IR absorption spectrum (Figure 42) showed bands at 1650,1640 cm^{-1} (C=O stretching) implied the quinone characters of **1o**.

The proton and carbon assignments of renieramycin O in the ^1H NMR spectrum (Figure 43) and the ^{13}C NMR spectrum (Figure 45) were achieved by interpretation of the data obtained from ^1H, ^1H-COSY spectrum (Figure 44), HMQC (Figures 47), and HMBC (Figure 48) experiments and by comparison with those of **1m**. The ^1H and ^{13}C NMR spectra of **1o** were almost identical to those of **1m**. However, the methylene protons of C-14 (δ 2.76 ppm, 14-Hα and 2.31 ppm, 14-Hβ) and the methylene carbon of C-14 (δ 21.3 ppm) in the ^1H and ^{13}C NMR spectra of **1m** were absent in those of **1o**, respectively. Instead, the new methine proton signal at δ 4.37 ppm (14-H) together with the D_2O exchangeable OH signal at δ 3.52 ppm in the ^1H NMR spectrum of **1o** and the corresponding methine carbon signal at δ 62.0 ppm (C-14) were present in the ^{13}C-NMR spectrum. This information imply the placement of a hydroxyl group at C-14 position. The absence of coupling between the signals of 14-H and 13-H (δ 3.42 ppm) required a dihedral angle of 80-90° and suggested a β orientation of 14-H and an α orientation of 14-OH. Thus, the structure of **1o** was considered to be 14α–hydroxy renieramycin M. The ^1H and ^{13}C NMR data of the isolated bisquinone renieramycins are summarized in Tables 9 and 10.

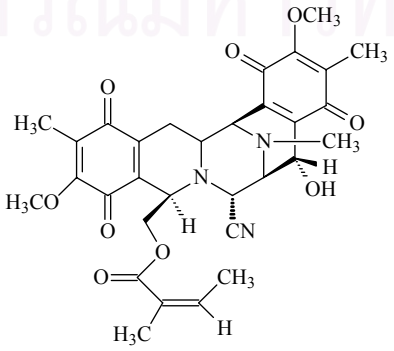

Renieramycin O (**1o**)

2.1.3 Structure elucidation of renieramycin R (**1r**)

Renieramycin R (**1r**) was obtained as a pale yellow amorphous solid, $[\alpha]^{18}_{D}$ –17.6 (c 0.1, $CHCl_3$). This compound has the molecular formula $C_{32}H_{35}N_3O_9$ as deduced by HREI-MS showing a molecular ion peak at m/z 605.2375. The 30 and 14 higher mass units different from **1m** and **1o**, respectively, implied that **1r** was a methoxyl analog of **1m**. The UV spectrum (Figure 60) exhibited : λ_{max} at 267 nm (ε 18,990).

Its structure was determined by comparison of spectral data with those of **1m** and **1o.** The ^{1}H NMR spectrum of renieramycin R (**1r**) displayed a methoxyl signal at δ 3.54 ppm and a down field methine proton as a singlet at δ 3.84 ppm (14-H) is indicative of the placement of the methoxyl group at C-14 in **1m**. Similar to **1o**, the 14-H showed no coupling with the 13-H. These data, in addition to the almost identical chemical shifts and coupling constants of the remaining signals to those of **1m** and **1o** as well as characteristic carbon signals including C-14 (δ 70.0 ppm) and methoxyl carbon (δ 59.5 ppm), enabled the structure of **1r** to be determined as 14α-methoxyrenieramycin M or 14-*O*-methylrenieramycin O. The ^{1}H and ^{13}C NMR data of **1r** are summarized in Tables 9 and 10, respectively.

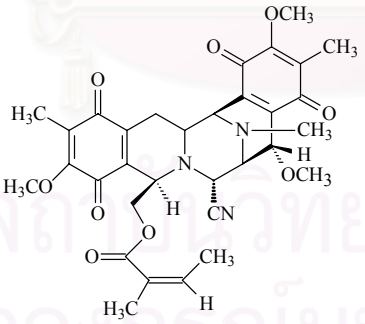

Renieramycin R (**1r)**

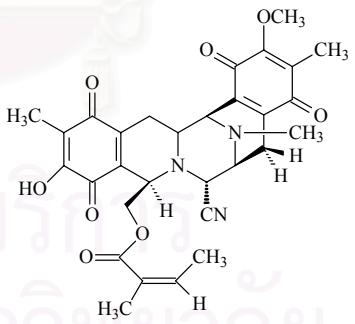

Renieramycin S (**1s**)

2.1.4 Structure elucidation of renieramycin S (**1s**)

Renieramycin S (**1s**) was obtained as a pale yellow needles from ethyl acetate-ether, mp. 179-180 ^{o}C; $[\alpha]^{20}_{D}$ –38.8 (c 1.0, $CHCl_3$). The HREI-MS data at m/z 561.2112 provided the molecular formula for **1s** as $C_{30}H_{31}N_3O_8$ The molecular weight of renieramycin S (**1s**) was 14 mass units less than that of **1m**.

Comparison of spectral data with those of **1m** and the fact that **1m** was obtained after treating **1s** with CH_2N_2 led to the conclusion that **1s** was lacking one of the methyl group of the vinylogous ester at one quinone ring of **1m**. Therefore, there are two possibilities of the remaining methyl ester substituent at either C-7 or C-17. Thus, all protons and carbons of 1s were assigned after extensive NMR measurements using COSY, NOESY, HMQC, and HMBC techniques as summarized in Tables 9 and 10. The position of the methyl ester at C-17 was secured by selected H-C long range correlations in the HMBC spectrum (Figure 81) of **1s** including; 14-Hα, 14-Hβ, 16-CH_3 to C-15; 16-CH_3 to C-16; 16-CH_3, 17-OCH_3 to C-17; 4-Hα, 6-CH_3 to C-5; and 6-CH_3 to C-7 as shown below. Thus, the structure of **1s** was established to be 7-demethylrenieramycin M. The selected H-C long range correlations in the HMBC spectrum of renieramycin S (**1s**) was shown below.

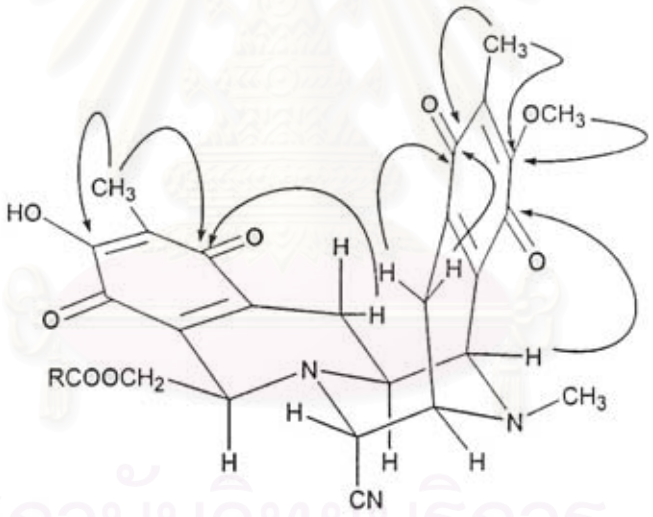

Table 9 ^{1}H-NMR spectral data of renieramycins M, O, R, and S (in $CDCl_3$)

proton	1m	1o	1r	1s
1-H	3.99 (1H, ddd, 3.1, 2.9)	3.98 (1H, m)	4.01 (1H, dt, 3.4, 2.5)	4.03 (1H, ddd, 3.1, 2.9)
3-H	3.11 (1H, d, 11.3, 3.1, 2.8)	3.05 (1H, ddd, 11.6, 3.3, 2.3)	3.02 (1H, ddd, 11.6, 3.1, 2.8)	3.12 (1H, d, 11.3, 3.1, 2.2)
4-H β	β 1.36 (1H, ddd, 17.4, 11.3, 2.7)	1.20 (1H, ddd, 17.2, 11.6, 2.6)	1.26 (1H, ddd, 17.1, 11.6, 2.5)	1.40 (1H, ddd, 17.7, 11.3, 2.8
4-H α	α 2.89 (1H, dd, 17.4, 2.8)	2.87 (1H, dd, 17.2, 2.3)	2.86 (1H, dd, 17.1, 2.8)	2.92 (1H, dd, 17.7, 2.2)
11-H	4.01 (1H, dd, 3.1, 1.8)	4.02 (1H, dd, 3.3, 1.3)	4.08 (1H, dd, 3.1, 1.0)	3.99 (dd, 1H, 3.1, 1.0)
13-H	3.40 (1H, ddd, 7.6, 2.5, 1.8)	3.42 (1H, br s)	3.44 (1H, br d, 2.4)	3.38 (1H, ddd, 7.7, 2.5, 1.0)
14-H β	2.31 (1H, d, 21.1)	4.37 (1H, s)	3.84 (1H, s)	2.31 (1H, d, 21.1)
14-H α	α 2.74 (1H, dd, 21.1, 7.6)	-	-	2.74 (1H, dd, 21.1, 7.7)
21-H	4.07 (1H, d, 2.5)	4.14 (1H, d, 2.6)	4.17 (1H, d, 2.4)	4.09 (1H, d, 2.5)
22-Ha	4.10 (1H, dd, 11.6, 2.5)	4.09 (1H, dd, 11.6, 2.6)	4.13 (1H, dd, 11.6, 3.4)	4.04 (1H, dd, 11.9, 2.9)
22-Hb	4.53 (1H, dd, 11.6, 3.1)	4.53 (1H, dd, 11.6, 3.4)	4.34 (1H, dd, 11.6, 3.4)	4.65 (1H, dd, 11.9, 3.1)
6-CH_3	1.90 (3H, s)	1.92 (3H, s)	1.92 (3H, s)	1.90 (3H, s)
16-CH_3	1.94 (3H, s)	1.94 (3H, s)	1.92 (3H, s)	1.94 (3H, s)
7-OCH_3	3.99 (3H, s)	4.02(3H, s)	3.97 (3H, s)	-
17-OCH_3	4.02 (3H, s)	4.03 (3H, s)	4.01 (3H, s)	3.98 (3H, s)
N- CH_3	2.28 (3H, s)	2.46 (3H, s)	2.48 (3H, s)	2.27 (3H, s)
14-OH		3.52 (3H, br s, OH)		
14-OCH_3			3.54 (3H, s)	
26-H	5.96 (1H, qq, 7.3, 1.5)	5.98 (1H, qq, 7.3, 1.7)	5.97 (1H, qq, 7.3, 1.5)	5.96 (1H, qq, 7.4, 1.5)
27- H_3	1.82 (3H, dq, 7.3, 1.3)	1.82 (3H, dq, 7.3, 1.3)	1.83 (3H, dq, 7.3, 1.6)	1.82 (3H, dq, 7.4, 1.4)
28- H_3	1.58 (3H, dq, 1.5, 1.3)	1.57 (3H, dq, 1.7, 1.3)	1.59 (3H, dq, 1.6, 1.5)	1.57 (3H, dq, 1.5, 1.4)

Table 10 ^{13}C-NMR spectral data of renieramycins M, O, R, and S (in $CDCl_3$)

carbon	1m	1o	1r	1s
1	56.3 CH	56.4 CH	56.3 CH	56.0 CH
3	54.1 CH	53.4 CH	53.4 CH	54.2 CH
4	25.4 CH_2	25.3 CH_2	25.1 CH_2	26.0 CH_2
5	185.4 C	185.4 C	185.3 C	184.8 C
6	128.6 C	128.6 C	129.8 C	117.2 C
7	155.8 C	155.6 C	155.8 C	151.1 C
8	180.9 C	180.8 C	180.8 C	180.9 C
9	135.7 C	135.7 C	135.6 C	133.5 C
10	141.3 C	141.1 C	141.2 C	144.1 C
11	54.2 CH	55.0 CH	54.5 CH	54.2 CH
13	54.6 CH	62.4 CH	60.0 CH	54.5 CH
14	21.3CH_2	62.0 CH	70.0 CH	21.0 CH_2
15	185.9 C	187.8 C	185.1 C	185.8 C
16	128.4 C	128.4 C	128.3 C	128.6 C
17	155.2 C	155.8 C	154.9 C	155.2 C
18	182.5 C	182.8 C	182.9 C	182.5 C
19	135.0 C	135.3 C	135.2 C	135.0 C
20	142.0 C	141.0 C	140.8 C	142.1 C
21	58.5 CH	56.4 CH	56.5 CH	58.3 CH
22	62.0CH_2	62.1 CH_2	62.8 CH_2	61.4 CH_2
6-CH_3	8.5 CH_3	8.4 CH_3	8.7 CH_3	8.1 CH_3
16-CH_3	8.7 CH_3	8.7 CH_3	8.7 CH_3	8.5 CH_3
7-OCH_3	60.9CH_3	61.1 CH_3	61.0 CH_3	-
17-OCH_3	61.0 CH_3	61.1 CH_3	60.9 CH_3	60.9 CH_3
N- CH_3	41.5 CH_3	42.4 CH_3	42.7 CH_3	41.5 CH_3
21-CN	116.9 C	116.3 C	116.5 C	116.8 C
14-OCH_3	-	-	59.5 CH_3	-
24	166.5 C	166.5 C	166.7 C	166.5 C
25	126.3 C	126.2 C	126.3 C	126.2 C
26	140.5CH	140.6 CH	140.3 CH	140.8 CH
27	15.7CH_3	15.7 CH_3	15.7 CH_3	15.8 CH_3
28	20.4CH_3	20.3 CH_3	20.3 CH_3	20.4 CH_3

2.2 Structure elucidation of quinone-hydroquinone renieramycins, renieramycins N, and Q

Renieramycins N (**1n**, $C_{31}H_{35}N_3O_9$) and Q (**1q**, $C_{31}H_{33}N_3O_9$) have the common carbon skeleton containing one quinone ring, one hydroquinone ring and an angelate ester side chain. The extinction coefficients at maximum UV absorption for the quinone moiety of **1n** (ε = 11,963 at 269 nm) and **1q** (ε = 15,169 at 273 nm) were reduced to about one-half compared to those in the bisquinones, such as **1m** (ε = 21,275 at 269 nm). The ^{13}C NMR spectra of **1n** (Figure 35) and **1q** (Figure 55) are quite different from those of the bisquinone renieramycins by showing only two quinone carbonyl carbon signals at δ 183.6, 179.1 and at δ 185.7, 180.7 ppm, respectively. These data implied that one of the quinone ring in **1n** and **1q** might have been reduced to form a hydroquinone ring. In addition, a pair of the phenolic carbon signals at δ 145.2, 139.4 for **1n** and at δ 155.9, 139.3 ppm for **1q** supported the presence of the hydroquinone ring. In the ^{1}H-NMR spectra, the aryl methyl and methoxyl proton signals of ring A were the same as other quinones while those of ring E, the methyl proton signal shifted down field from δ 1.92 ppm (**1m**) to δ 2.40 (**1n**) and 2.09 ppm (**1q**), and the methoxyl proton signal shifted up field from δ about 3.9-4.0 ppm (**1m**) to δ 3.74 (**1n**) and 3.79 ppm (**1q**). The unique homoallylic coupling (~ 2 Hz) between 1-H and 4-Hβ confirmed that ring A of both compounds still remained as the quinone ring. The carbon signals at δ 117.8 and 115.9 ppm in the ^{13}C NMR spectra of **1n** and **1q**, respectively, assured the presence of 21-CN.

Ring E of the quinone-hydroquinone renieramycins is reduced to form the hydroquinone ring while ring A is oxidized to form the quinone ring. The hydrogen-bond formation between the oxygenated substituent at C-14 and the hydroxyl group at C-15 may cause the hydroquinone ring E resist to the oxidation process.

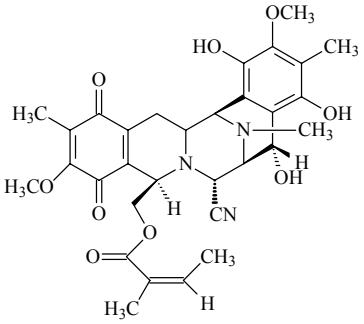

Renieramycin N (**1n**)

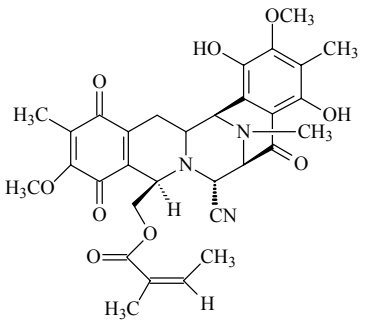

Renieramycin Q (**1q**)

2.2.1 Structure elucidation of renieramycin N (**1n**)

Renieramycin N was obtained as pale yellow prisms from ethanol, mp. 162.5-164 ^{o}C, $[\alpha]^{20}_{D}$ -24.7 (c 0.015, methanol). This compound has the molecular formula $C_{31}H_{35}N_3O_9$ as deduced by elemental analysis and EI-MS (Figure 31) showing a molecular ion peak at m/z 593. The molecular weight of renieramycin N (**1n**) was 18 mass units more than that of **1m** and revealed that **1n,** was an oxygenated hydroquinone analog of **1m**. In addition, the ^{1}H (Figure 33) and ^{13}C (Figure 35) NMR spectra of **1n**, the methine proton signal of 14-H appeared as a singlet and shifted down field to δ 5.18 and the corresponding methine carbon signal also shifted down field to δ 62.0 (C-14) indicated the presence of the 14α-hydroxy substitution of **1n**.

2.2.2 Structure elucidation of renieramycin Q

Renieramycin Q was obtained as a pale yellow amorphous solid from ethyl acetate, $[\alpha]^{18}_{D}$ –69.8 (c 0.1, $CHCl_3$), The molecular formula $C_{31}H_{33}N_3O_9$ for **1q** was deduced on the basis of HREI-MS showing a molecular ion peak at m/z 591.2222. The molecular weight of renieramycin Q (**1q**) was 2 mass units less than that of **1n**. From the ^{1}H (Figure 53) and ^{13}C (Figure 55) NMR spectra of **1q,** in stead of the 14-H methine proton and C-14 carbon signals as in **1n**, the characteristic ketone carbonyl resonance (δ 198.4 ppm) was observed for **1q**. These data revealed the peri-carbonyl function at C-14 in **1q**.

Table 11 ^{1}H-NMR spectral data of renieramycins N, and Q

proton	**1n** (pyridine-d_5)	**1q** ($CDCl_3$)
1-H	4.37 (1H, dt, 2.6, 2.0)	3.95 (1H, dt,3.4, 2.5)
3-H	3.44 (1H, ddd, 11.2, 2.6, 2.6)	3.23 (1H, ddd, 11.0, 3.1, 2.5)
4-H β	2.20 (1H, ddd, 17.8, 11.2, 2.6)	1.54 (1H, ddd, 17.7, 11.0, 2.5)
4-H α	3.60 (1H, dd, 17.8, 2.6)	3.03 (1H, dd,17.7, 2.5)
11-H	4.74 (1H, d, 2.0)	4.28 (1H, dd, 3.1, 0.5)
13-H	3.94 (1H, dd, 2.6, 2.0)	3.37 (1H, dd, 1.0, 0.5)
14-H β	5.18 (1H, s)	-
14-H α	-	-
21-H	4.94 (1H, d, 2.6)	4.31 (1H, d, 1.0)
22-Ha	4.51 (1H, dd, 11.6, 2.0)	4.02 (1H, dd, 11.6, 2.5)
22-Hb	4.58 (1H, dd, 11.6, 2.6)	4.09 (1H, dd, 11.6, 3.4)
6-CH_3	1.92 (3H, s)	1.85 (3H, s)
16-CH_3	2.40 (3H, s)	2.09 (3H, s)
7-OCH_3	3.94 (3H, s)	3.94 (3H, s)
17-OCH_3	3.74 (3H, s)	3.79 (3H, s)
N- CH_3	2.70 (3H, s)	2.38 (3H, s)
OH	10.68, 9.30, 7.60 (each 1H, br s, OH)	5.51(br s, 18-OH) 11.40(s, 15-OH)
Angelate		
26-H	5.70 (1H, qq, 7.3, 1.3)	5.81 (1H, qq, 7.3, 1.3)
27- H_3	1.74 (3H, dq, 7.3, 1.7)	1.68 (3H, dq, 7.3, 1.6)
28- H_3	1.44 (3H, dq, 1.7, 1.3)	1.54 (3H, dq, 1.6, 1.3)

Table 12 ^{13}C-NMR spectral data of renieramycins N, and Q

carbon	**1n** (pyridine-d_5)	**1q**($CDCl_3$)
1	54.4 CH	54.8 CH
3	53.1 CH	53.8 CH
4	22.9 CH_2	24.1 CH_2
5	183.6 C	185.7 C
6	124.9 C	128.0 C
7	153.8 C	156.0 C
8	179.1 C	180.7 s
9	133.9 C	135.6 C
10	140.3 C	141.4 C
11	54.6 CH	56.5 CH
13	63.1 CH	66.2 CH
14	62.0 CH	198.4 C
15	145.2 C	155.0 C
16	115.7 C	118.4 C
17	144.2 C	153.0 C
18	139.4 C	139.3 C
19	115.9 C	117.7 C
20	114.7 C	112.2 C
21	55.2 CH	56.0 CH
22	60.5 CH_2	62.0 CH_2
6-CH_3	6.3 CH_3	8.6 CH_3
16-CH_3	7.3 CH_3	8.8 CH_3
7-OCH_3	58.3 CH_3	61.1 CH_3
17-OCH_3	57.7 CH_3	61.0 CH_3
N- CH_3	40.8 CH_3	42.4 CH_3
21-CN	117.8 C	115.9 C
(Angelate)		
24	164.8 C	166.6 C
25	125.4 C	126.5 C
26	136.5 CH	139.6 CH
27	13.1 CH_3	15.4 CH_3
28	17.7 CH_3	19.8 CH_3

3. Chemical transformation of renieramycins

Since the isolated renieramycin M (**1m**) was available in sufficient quantity from natural source, we were enabled to prepare additional derivatives of this class of compounds which are necessary for the evaluation of antitumor activity and for the clarification of the mechanism of action. The chemical transformations of **1m** at carbons 14 and 21, the side chain at carbon 22, and the quinone to the hydroquinone were explored.

3.1 Chemical transformation of renieramycin M at carbon 14

In order to introduce the alkoxyl group at C-14, allylic oxidation by selenium oxide in alcoholic solvents was studied. Reflux of **1m** with selenium oxide (10 equiv.) in both methanol and ethanol provided **1r** and 14α-ethoxyrenieramycin M or renieramycin R' (**1r'**), each in 35% yield, respectively. These nucleophilic substitution occurred only in the α- position due to the steric hindrance of 14-Hβ and rings D and E.

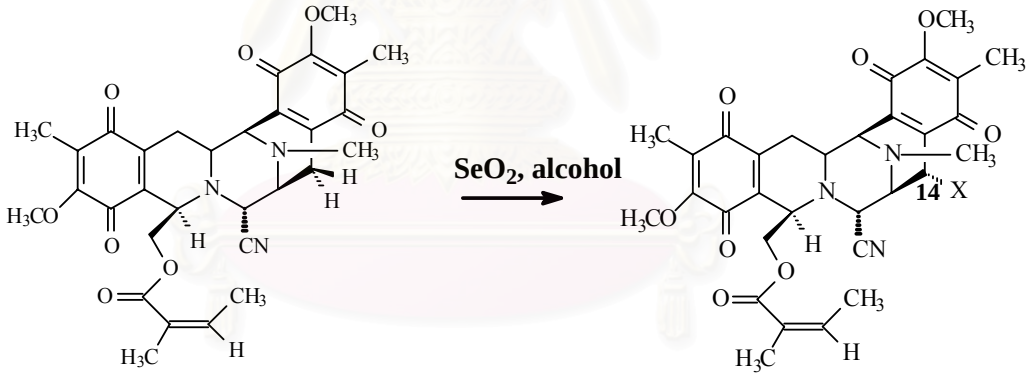

renieramycin M, (**1m**)

renieramycin R; (**1r**), X = OCH_3
renieramycin R'; (**1r'**), X = OCH_2CH_3

Scheme 9 Transformation of reniramycin M to reniramycins R and R'

The ^{1}H- and ^{13}C-NMR spectral data of the synthetic **1r** was identical with those of the isolated **1r** mentioned above. The molecular weight of **1r'** was 14 unit more than **1r**. The NMR spectral data of **1r'** were almost similar to those of **1r**, except the signals of the ethoxyl group as follows: methylene protons as a quartet at δ 3.76 and methyl protons as a triplet at δ 1.18 ppm in the ^{1}H-NMR spectrum of **1r'** and the methylene carbon and methyl carbon signals at δ 67.6 and 15.6 ppm in the ^{13}C -

NMR spectrum. The above data and the singlet proton of H-14 (δ 3.92 ppm) confirmed that **1r'** was 14α-ethoxyrenieramycin M.

3.2 Chemical transformation of renieramycin M at carbon 21

3.2.1 Chemical transformation of renieramycin M to renieramycin E

Renieramycin E (**1e)**, the same as saframycin S from *Streptomyces lavandulae* No. 134, were believed to be the unstable naturally occurring compounds. The modified extraction method by adding sodium or potassium cyanide before maceration with methanol solvent made these modified isoquinolinequinones, renieramycin M (**1m)** and saframycin A, more stable. In order to interconvert **1m** to **1e,** treatment of **1m** with excess silver nitrate in aqueous acetonitrile at 40 ^{o}C for 24 h gave the natural **1e** in 53% yield. The ^{1}H–NMR spectral data (Figure 97) of **1e** was identical with the isolated compound (He and Faulkner, 1989).

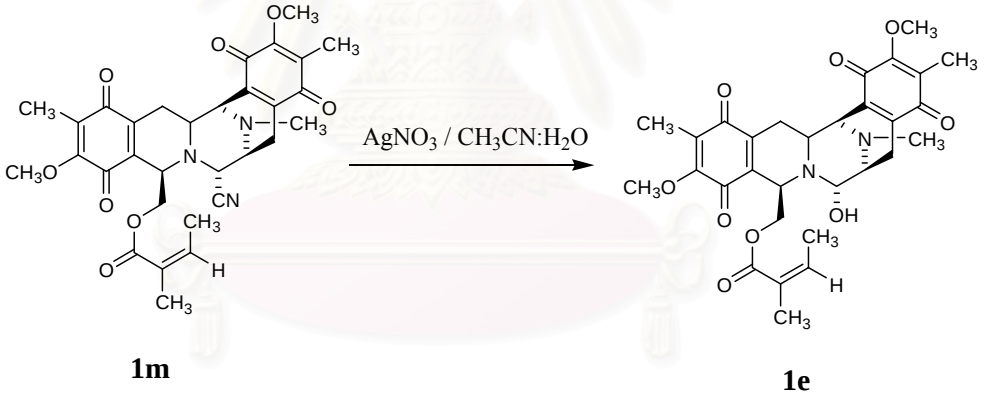

1m **1e**

Scheme 10 Transformation of renieramycin M (**1m**) to renieramycin E (**1e**)

3.2.2 Chemical transformation of renieramycin M to renieramycin J

In 1992, renieramycins J – L (**1j-1l)** were discovered in the first study of this Thai sponge, *Xestospongia* sp., and it was noted that these isolated products contained an acetone residue at C-21 (Suwanborirux *et al.,* 2003).

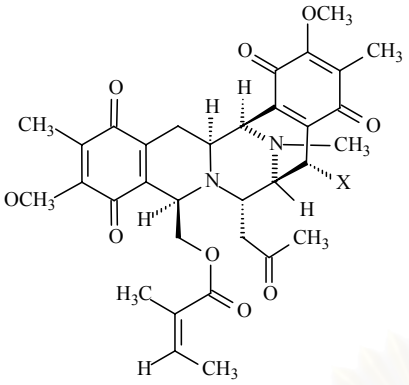

Renieramycins J (**1j**) : X = H,
K (**1k**): X = OCH_3

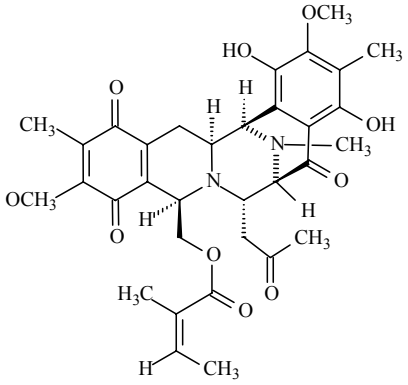

Renieramycin L (**1l**)

One possible pathway to generate these compounds is shown in Scheme 11 which involves partial reduction of type I compound (such as renieramycin G) to give type II compound (such as renieramycin E), into which an acetone nucleophile can be substituted at the C-21 position stereoselectively to give type IV compound (such as renieramycin J) *via* type III iminium intermediate.

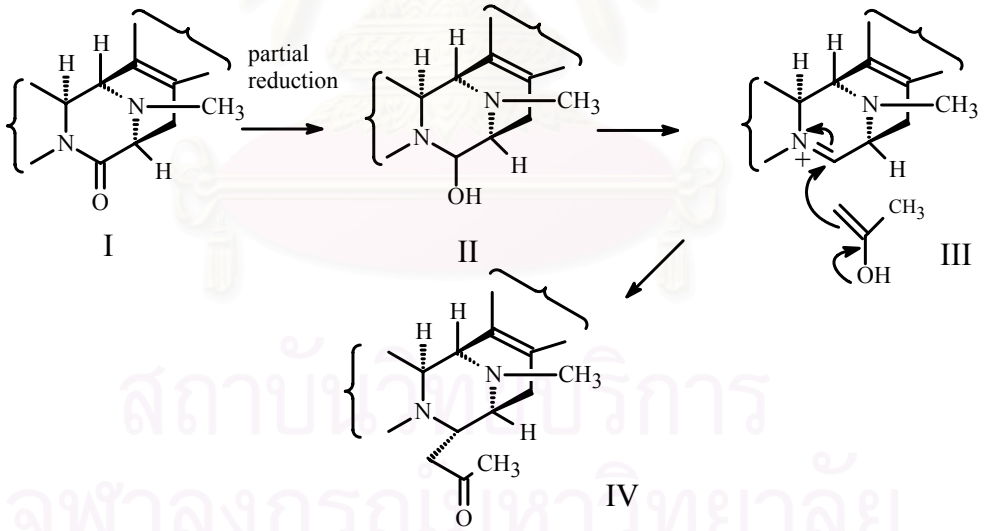

Scheme 11 Possible pathway to generate natural products that have an acetone residue at C-21

Koizumi *et al.* reported the preparation of the ABC ring model (VIII) of type IV compound from the lactam V *via* the α-aminonitrile intermediate VII reacting with silver nitrate in acetone at 60 ^{o}C as shown in Scheme 12 (Koizumi *et al.*, 2002).

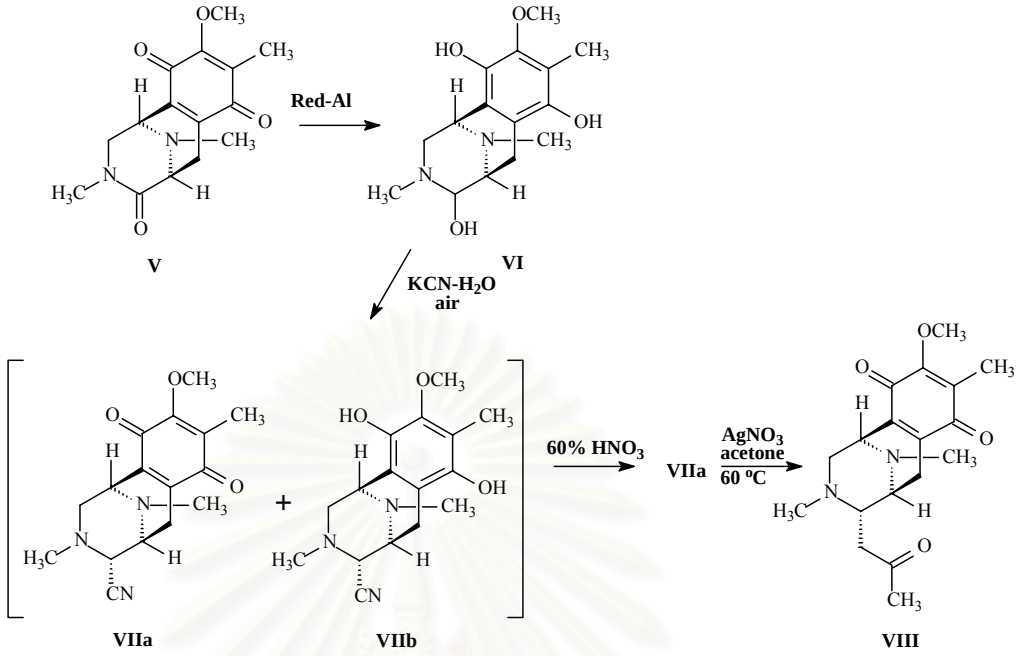

Scheme 12 Preparation of the ABC ring model of type IV compound from the lactam V *via* the aminonitrile VII.

Encouraged by this results of the model transformation, the procedure was successfully applied to the preparation of **1j** from **1m**. A two-step transformation of **1m** into **1j** *via* **1e** was unsuccessful because the intermediate **1e** was unstable. However, treatment of **1m** with silver nitrate in acetone at 50°C for 1 h gave **1j** in 69.6% yield, which gave all spectral data in full agreement with those of the isolated **1j** (Suwanborirux *et al.*, 2003).

The ^{1}H- (Figure 106) and ^{13}C-NMR (Figure 108) spectral data of renieramycin J were shown in Tables 13 and 14, respectively. Comparison of the ^{1}H NMR data of **1j** with those of **1e** revealed that the two molecules were almost identical except for signals at δ 2.10 (3H, s), δ 2.35 (1H, dd, J = 17.7, 1.7), and δ 3.41 (1H, dd, J = 17.7, 8.9 Hz) due to 2-propanone unit and the absence of hydroxyl signal in the spectra of renieramycin J. Furthermore, the 21-H signal at δ 3.50 of **1j** was shifted up field to the corresponding signal (δ 4.44) in **1e**. The ^{13}C NMR spectral data of **1j** revealed a signal at δ 59.3 for C-21 carbon, which was shifted up field compared to that of **1e** at δ 83.0, as well as additional signals for the 2-propanone unit [δ 39.0

(CH_2), δ 208.1 (CO), δ 30.6 (CH_3)]. From these data, the structure of renieramycin J was deduced to be **1j**.

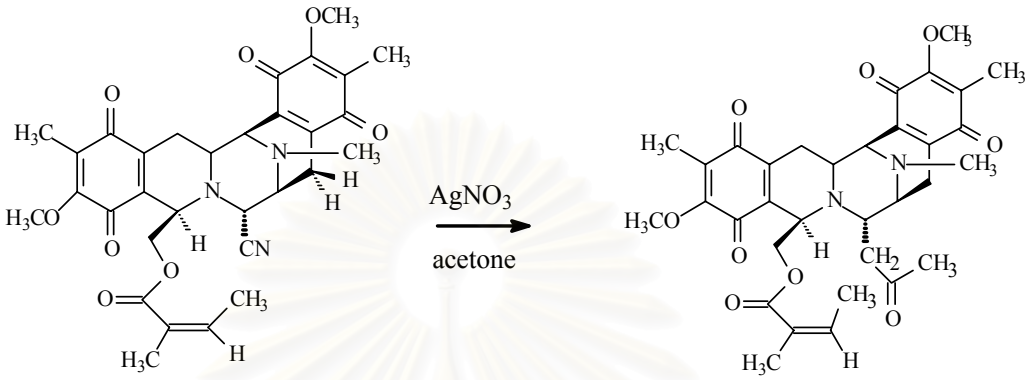

renieramycin M **(1m)** renieramycin J (**1j)**

Scheme 13 Chemical transformation of renieramycin M (**1m**)to renieramycin J (**1j**)

Table 13 ^{1}H-NMR spectral data for renieramycins R' (**1r'**), E (**1e**), and J (**1j**)

(in $CDCl_3$)

proton	1r'	1e	1j ($CDCl_3$)
1-H	3.99 (1H, br s)	4.44 (1H, m)	3.87 (1H, br s)
3-H	3.02 (1H, ddd, 11.6, 3.3, 2.8)	3.16 (1H, ddd, 11.0, 2.6, 2.6)	2.89 (1H, m)
4-H β	1.33 (1H, ddd, 17.4, 11.6, 2.5)	1.31 (1H, ddd, 16.2, 11.0, 2.0)	1.21 (1H, ddd, 16.2, 11.0, 2.0)
4-H α	2.86 (1H, dd, 17.4, 2.6)	2.75 (1H, dd, 16.2, 2.7)	2.75 (1H, dd, 16.2, 2.7)
11-H	4.08 (1H, dd, 3.5,1.0)	3.92 (1H, dd, 2.5, 1.0)	3.83 (1H, dd, 2.7, 1.1)
13-H	3.44 (1H, br d)	3.21 (1H, br d, 7.6)	2.90 (1H, br d, 7.3)
14-H β	3.92 (1H, s)	2.21 (1H, d, 20.9)	2.22 (1H, d, 20.9)
14-H α	-	2.66 (1H, dd, 20.9, 7.3)	2.73 (1H, dd, 20.9, 7.3)
21-H	4.16 (1H, d, 2.4)	4.44 (1H, m)	3.50 (1H, br dd, 8.9, 1.7)
22-Ha	4.12 (1H, dd, 11.6, 2.9)	4.15(1H, dd, 11.2, 3.1)	4.10 (1H, dd, 11.2, 3.1)
22-Hb	4.34 (1H, dd, 11.6, 2.7)	4.45(1H, dd, 11.2, 3.1)	4.16 (1H, dd, 11.2, 3.1)
6-CH_3	1.92 (3H, s)	1.91 (3H, s)	1.90 (3H, s)
16-CH_3	1.92 (3H, s)	1.91 (3H, s)	1.90 (3H, s)
7-OCH_3	4.01 (3H, s)	4.00 (3H, s)	4.00 (3H, s)
17-OCH_3	3.97 (3H, s)	3.98 (3H, s)	3.97 (3H, s)
N- CH_3	2.50 (3H, s)	2.25 (3H, s)	2.14 (3H, s)
OH	-	10.68, 9.30, 7.60	-
O$\underline{CH_2}$$CH_3$	3.76(2H, q, 7.3,)	-	-
$OCH_2\underline{CH_3}$	1.18(3H, t, 7.3,)	-	-
CO$\underline{CH_3}$	-	-	2.10 (3H, s)
$\underline{CH_2}$ $COCH_3$	-	-	2.35 (1H, dd, 17.7, 1.7), 3.41 (1H, dd, 17.7, 8.9)
26-H	5.97(1H, qq, 7.3, 1.5)	5.92(1H, qq, 7.3, 1.4)	5.91(1H, qq, 7.3, 1.4)
27- H_3	1.83(3H, dq, 7.3, 1.6)	1.80(3H, dq, 7.3, 1.7)	1.75(3H, dq, 7.3, 1.7)
28- H_3	1.59(3H, dq, 1.6, 1.5)	1.57(3H, dq, 1.7, 1.4)	1.59(3H, dq, 1.7, 1.4)

He and Faulkner, 1989

Table 14 ^{13}C-NMR Spectral Data for renieramycins R' (**1r'**), E (**1e**), and J (**1j**) (in $CDCl_3$)

carbon	1r'	1e	1j
1	56.3 CH	54.2 CH	54.0 CH
3	53.4 CH	51.0 CH	52.5 CH
4	25.1 CH_2	26.1 CH_2	26.1 CH_2
5	185.1 C	184.0 C	186.0 C
6	129.8 C	128.8 C	128.9 C
7	155.8 C	156.0 C	155.6 C
8	180.8 C	181.0 C	181.5 C
9	135.6 C	138.5 C	137.7 C
10	141.2 C	142.0 C	143.9 C
11	54.5 CH	53.5 CH	54.0 CH
13	60.0 CH	58.0 CH	55.6 CH
14	68.3 CH	20.9 CH_2	23.5 CH_2
15	185.3 C	186.0 C	186.7 C
16	128.3 C	128.2 C	127.9 C
17	154.9 C	158.0 C	156.4 C
18	182.9 C	182.5 C	183.5 C
19	135.2 C	133.0 C	137.7 C
20	141.0 s	141.8 C	141.7 C
21	56.4 CH	83.0 CH	59.3 CH
22	62.8 CH_2	63.6 CH_2	64.9 CH_2
6-CH_3	8.7 CH_3	8.7 CH_3	8.7 CH_3
16-CH_3	8.7 CH_3	8.7 CH_3	8.7 CH_3
7-OCH_3	60.9 CH_3	61.0 CH_3	60.7 CH_3
17-OCH_3	61.0 CH_3	61.0 CH_3	60.7 CH_3
N- CH_3	42.7 CH_3	41.8 CH_3	41.5 CH_3
21-CN	116.5 C	-	-
O$\underline{CH_2}$$CH_3$	67.6 CH_2	-	-
$OCH_2\underline{CH_3}$	15.6 CH_3	-	-
21-$CH_2\underline{CO}CH_3$	-	-	208.1 C
21-$\underline{CH_2}COCH_3$	-	-	39.0 CH_2
21-$CH_2CO\underline{CH_3}$	-	-	30.6 CH_3
24	166.7 C	166.5 C	167.2 C
25	126.3 C	126.5 C	127.2 C
26	140.3 CH	140.0 CH	139.5 CH
27	15.7 CH_3	15.8 CH_3	15.7 CH_3
28	20.3 CH_3	20.8 CH_3	20.5 CH_3

3.3 Chemical transformation of renieramycin M of the side chain at carbon 22

3.3.1 Chemical transformation of **1m** to deangeloyl renieramycin M (**38**)

In 2000, jorumycin (**2)** was discovered in very minute quantity from the mantle and mucus of the Indian nudibranch, *Jorunna funebris*. Compound **2** is the only natural renieramycin possessing an acetyl ester side chain, and its cytotoxicity against various human cancer cell lines has been evaluated. We then became interested in the analogs of renieramycins containing different ester side chain at carbon 22.

The crucial step of this transformation involves the removal of the angeloyl group of **1m**. It is well known that the angeloyl ester can be easily hydrolyzed with potassium cyanide in aqueous alcohol, and that the initial Michael-type addition of HCN saturates the angelates and the basic medium thereby generated causes the hydrolysis of the saturated esters (Roman *et al.,* 1985). However, treatment of **1m** with potassium cyanide in aqueous methanol gave an inseparable mixture of polymeric material since the vinylogous esters in quinone rings. Catalytic hydrogenation of the α, β-unsaturated ester residue in **1m** followed by alkaline hydrolysis also gave unsatisfactory results. Furthermore, numerous attempts at the hydrolysis of the ester side chain of **1m** under acidic conditions were unsuccessful. By contrast, direct transformation by reductive deangelation of **1m** with lithium aluminium hydride or with less bulky reagent, such as aluminium hydride in THF at 0 ^{o}C for 1 h gave the alcohol, deangeloyl renieramycin M (**38)** only 26% yield. Comparison with those of **1m**, the ^{1}H- (Figure 115) and ^{13}C-NMR (Figure 117) spectral data of **38** showed no signals of the angeloyl group. In addition, the methylene proton signals of C-22 shifted up field to 3.48 and 3.71 ppm when compared with the ones at δ 4.04 and 4.65 ppm in **1m**.

Accordingly, the two-step transformation was studied, beginning with hydrogenation of **1m** with 20% $Pd(OH)_2/C$ for 3 h gave the leuco compound, bishydroquinone renieramycin M (**39)**, which was subsequently treated with aluminium hydride in THF at –20 ^{o}C and oxidized in air to provide the quinone alcohol **38** in 53% overall yield along with the decyanated compound, **40** (14%). Alternatively, treatment of **39** with 1.0 M lithium aluminium hydride in dry THF at –20 ^{o}C for 4 h and further oxidation in air overnight afforded only the alcohol, **38** in

lower yield (34.3 %). Decyano deangeloyl renieramycin M (**40**) compared with **38,** **t**he disappearance of cyano carbon and the appearance of methylene carbon at δ 58.7 ppm in the ^{13}C-NMR spectrum (Figure 122) and the methylene protons at δ 3.03 and 2.80 ppm in the ^{1}H- NMR spectrum (Figure 121) confirmed the structure of **40**.

3.3.2 Transformation of deangeloyl renieramycin M (**38)** to jorumycin (**2**) *via* 21-cyanojorumycin (**41**)

The esterification reaction of **38** with acetyl chloride, triethylamine, and DMAP afforded the acetate, 21-cyanojorumycin, **41** in 73% yield. The esterification with acetic anhydride under basic condition gave the lower yield of **41**. The acetyl group in **41** appeared as the methyl carbon at δ 20.5 ppm and the ester carbonyl carbon signal at δ 169.9 ppm in the ^{13}C-NMR spectrum (Figure 126) and as the methyl protons at δ 1.76 ppm in the ^{1}H-NMR spectrum (Figure 124). The placement of the acetyl group at C-22 confirmed by the down field shift of the 22-H at 3.82 and 4.43 ppm. Compound **41** was easily transformed into **2** in 83% yield by treatment with silver nitrate in aqueous acetonitrile at 40^{o}C (see Scheme 14). **2** had identical spectral data to the previously reported data (Fontana *et al.*,2000) as shown in Table 17.

The cleavage of the deangeloyl ester of renieramycin M is the important step for introduction of new ester side chains of the renieramycins. The attempts to increase the yield of deangeloyl renieramycin M still have to be continued. The transformation of deangeloyl renieramycin M to jorumycin is the first modification of renieramycins for other new ester derivatives. The procedure using for the preparation of jorumycin should be applied for other esters from both aliphatic and aromatic acids.

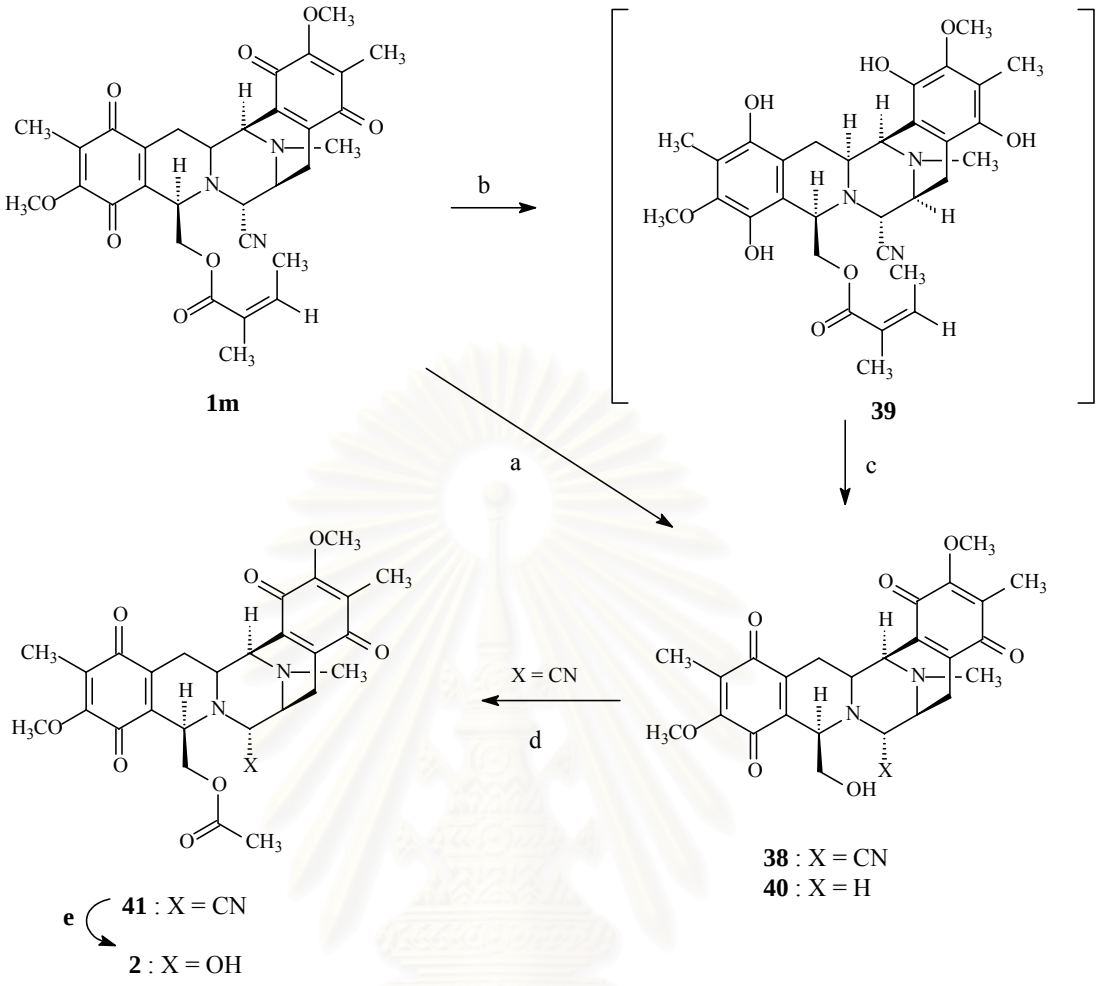

a: AlH_3, THF, 26% (38); b: H_2, 20% $Pd(OH)_2/C$, EtOAc; c: AlH_3, THF, 53% (38), 14% (40); d: AcCl, TEA, DMAP, CH_2Cl_2, 73%; e: $AgNO_3$, CH_3CN/H_2O, 83%

Scheme 14 Transformation of renieramycin M (**1m**) to jorumycin (**2**)

Table 15 ^{1}H-NMR spectral data for deangeloyl renieramycin M, decyano deangeloyl renieramycin M and cyanojorumycin (in $CDCl_3$)

proton	Deangeloyl RM (**38**)	Decyano deangeloyl RM (**40**)	Cyano jorumycin (**41**)
1-H	3.89 (1H, ddd, 3.7, 3.1, 2.4)	3.51 (1H, ddd, 3.7, 2.9, 1.0)	4.36 (1H, ddd, 3.6, 3.4, 2.7)
3-H	3.17 (1H, ddd, 11.6, 2.6, 2.4)	2.81 (1H, ddd, 11.7, 2.7, 2.4)	3.16 (1H, ddd, 11.2, 2.7, 2.1)
4-H β	1.42 (1H, ddd, 17.4, 11.6, 2.4)	1.41 (1H, ddd, 18.1, 11.7, 2.9)	1.29 (1H, ddd, 16.8, 11.2, 2.7)
4-H α	2.92 (1H, dd, 17.4, 2.4)	2.81 (1H, dd, 18.1, 2.4)	2.84 (1H, dd, 16.8, 2.1)
11-H	4.07 (1H, d, 2.6)	4.06 (1H, dd, 2.7, 0.5)	3.91 (1H, d, 2.7)
13-H	3.41 (1H, dd, 7.6, 2.4)	3.18 (1H, m)	3.18 (1H, dd, 7.9, 2.4)
14-H β	2.27 (1H, d, 21.1)	2.24 (1H, d, 21.0)	2.25 (1H, d, 21.1)
14-H α	2.82 (1H, dd, 21.1, 7.6)	2.80 (1H, dd, 21.0, 7.6)	2.66 (1H, dd, 21.1, 7.9)
21-H	4.15 (1H, d, 2.4)	β 3.03 (1H, dd, 11.0, 2.4) α 2.80 (1H, dd, 11.0, 2.4)	4.44 (1H, d, 2.4)
22-Ha	3.48 (1H, dd, 11.3, 3.7)	3.52 (1H, dd, 11.2, 1.0)	3.82 (1H, dd, 11.3, 3.6)
22-Hb	3.71 (1H, dd, 11.3, 3.1)	3.75 (1H, dd, 11.2, 3.7)	4.43 (1H, dd, 11.3, 3.4)
6-CH_3	1.93 (3H, s)	1.94 (3H, s)	1.92 (3H, s)
16-CH_3	1.93 (3H, s)	1.92 (3H, s)	1.96 (3H, s)
7-OCH_3	3.99 (3H, s)	4.01 (3H, s)	3.99 (3H, s)
17-OCH_3	4.02 (3H, s)	3.96 (3H, s)	4.01 (3H, s)
N- CH_3	2.32 (3H, s)	2.26 (3H, s)	2.27 (3H, s)
CO$\underline{CH_3}$	-	-	1.76(3H, s)

Table 16 ^{13}C-NMR spectral data for deangeloyl renieramycin M, decyano deangeloyl renieramycin M and cyanojorumycin (in $CDCl_3$)

carbon	Deangeloyl RM (38)	Decyano deangeloyl RM (40)	Cyano jorumycin (41)
1	58.0 CH	58.7 CH	55.8 CH
3	54.3 CH	54.8 CH	54.5 CH
4	25.4 CH_2	26.2 CH_2	25.3 CH_2
5	185.5 C	185.8 C	185.4 C
6	128.8 C	128.8 C	128.7 C
7	155.5 C	155.6 C	155.5 C
8	181.4 C	182.1 C	181.0 C
9	136.1 C	137.3 C	135.4 C
10	141.4 C	142.0 C	141.8 C
11	54.2 CH	52.2 CH	54.3 CH
13	54.5 CH	57.2 CH	54.6 CH
14	21.5 CH_2	22.7 CH_2	21.3 CH_2
15	186.3 C	185.9 C	186.1 C
16	128.6 C	128.6 C	128.7 C
17	155.4 C	155.5 C	155.2 C
18	182.3 C	182.6 C	182.5 C
19	135.6 C	136.3 C	134.9 C
20	141.7 C	142.8 C	142.2 C
21	59.1 CH	58.7 CH_2	59.7 CH
22	64.2 CH_2	61.5 CH_2	63.6 CH_2
6-CH_3	8.7 CH_3	8.7 CH_3	8.8 CH_3
16-CH_3	8.7 CH_3	8.7 CH_3	8.6 CH_3
7-OCH_3	61.0 CH_3	60.9 CH_3	61.0 CH_3
17-OCH_3	61.1 CH_3	61.0 CH_3	61.1 CH_3
N- CH_3	41.5 CH_3	41.1 CH_3	41.5 CH_3
21-CN	116.9 C	-	116.9 C
22-O$\underline{CO}$$CH_3$	-	-	169.9 C
22-OCO$\underline{CH_3}$	-	-	20.5 CH_3

Table 17 ^{1}H and ^{13}C NMR assignment for jorumycin (**2**) in $CDCl_3$

Atom no.	δ ^{13}C NMR	δ, multi., original	δ ^{1}H NMR (integral, multi., *J* in Hz)	HMBC Correlations from C no.	NOESY Correlations
1	52.7 CH	52.6 CH	4.36 (1H, ddd, 3.6, 3.4, 2.7)	22-H_2, 21-H, 3-H	22-H_2
3	51.1 CH	50.8 CH	3.16 (1H, ddd, 11.2, 2.7, 2.1)	1-H, 11-H, 21-H	4-Hα
4	25.6 CH_2	25.5 CH_2	α 2.84 (1H, dd, 16.8, 2.1) β 1.29(1H, ddd, 16.8, 11.2, 2.7)		3-H, 11-H
5	185.8 C	185.5 C		4-Hα, 6-CH_3	
6	128.3 C	128.4 C		6-CH_3	
7	155.7 C	155.7 C		6-CH_3, 7-OCH_3	
8	181.3 C	181.0 C			
9	137.3 C	141.7 C		22-H_2, 4-Hα, 4-Hβ	
10	141.8 C	141.9 C		3-H, 4-Hα, 4-Hβ	
11	54.2 CH	54.4 CH	3.91 (1H, d, 2.7)	4-Hβ, 13-H, NCH_3	4-Hα, 4-Hβ, 13-H, NCH_3
13	57.5 CH	57.7 CH	3.18 (1H,m)	11-H, NCH_3, 14-Hα, 14-Hβ	11-H,14-Hα, NCH_3
14	20.4 CH_2	20.6 CH_2	α 2.66 (1H, dd, 21.1, 7.9) β 2.25 (d, 1H, 21.1)		13-H
15	186.5 C	185.7 C		14-Hα, 14-Hβ, 16-CH_3	21-H
16	128.7 C	128.8 C		16-CH_3	
17	155.3 C	155.1 C		16-CH_3, 17-OCH_3	
18	182.6 C	181.3 C		11-H	
19	134.5 C	137.2 C		3-H, 11-H, 14-Hα, 14-Hβ	
20	141.9 C	141.9 C		11-H, 14-Hα, 14-Hβ	
21	83.0 CH	83.0 CH	4.44 (1H, br s)	1-H, 14-Hα, 14-Hβ	14-Hβ
22	64.3 CH_2	64.2 CH_2	4.43 (1H, dd, 11.3, 3.4) 3.82 (1H, dd, 11.3, 3.6)		1-H, 22-H 1-H, 22-H
CO	170.0 C	170.0 C	1.76 (3H, s)	CO$\underline{CH_3}$, 22-H_2	
CO$\underline{CH_3}$	20.5 C	20.7 C	1.94 (3H, s)		
6-CH_3	8.6 CH_3	8.7 CH_3	1.96 (3H, s)		
16-CH_3	8.7 CH_3	8.7 CH_3	3.99 (3H, s)		
7-OCH_3	61.0 CH_3	61.0 CH_3	4.01 (3H, s)		
17-OCH_3	61.0 CH_3	61.0 CH_3	2.27 (3H, s)		
NCH_3	41.4 CH_3	41.3 CH_3			11-H, 13-H

3.4 Chemical transformation of renieramycin M to hydroquinone renieramycin M

Martinez and Corey have recently reported that a structural analog of ecteinascidin 743, named phthalascidin, exhibited antitumor activity (Martinez and

Corey, 2000; Martinez *et al.,* 1999). In addition, Myers and co-workers have reported that a designed analog, QAD, which has been modified by replacement of the pyruvamide side chain of saframycin A with a quinaldic acid amide, and by transformation of its two quinone rings into hydroquinone methyl ethers which became a potent antitumor compound (Myers and Lanman, 2002). The preparation of hydroquinones were transformed from **1m**, **1n** and **1o.**

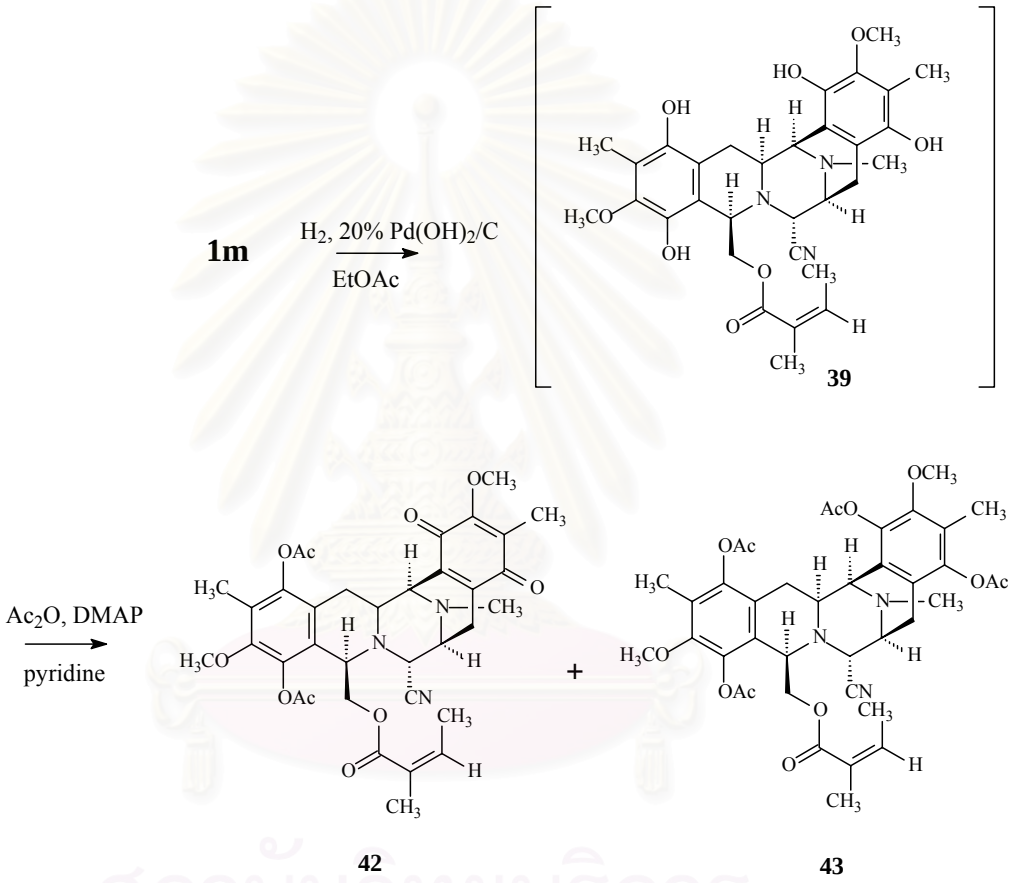

Scheme 15 Reductive acetylation of renieramycin M (**1m**)

Hydrogenation of **1m** with 20% $Pd(OH)_2/C$ in ethyl acetate for 3 h gave the leuco compound (**39**) in quantitative yield. Acetylation with acetic anhydride and DMAP in dry pyridine gave the 5,8-*O*-diacetylhydroquinone renieramycin M (**42**) and the 5,8,15,18-*O*-tetraacetylbishydroquinone renieramycin M (**43**) in 11% and 74% yields, respectively as shown in Scheme 15.

In the case of 5,8-*O*-diacetylhydroquinone renieramycin M (**42**), containing one quinone ring, one hydroquinone ring and an angelate ester side chain, only two

quinone carbonyl carbon signals at δ 186.1 and 182.8 ppm, two ester carbonyl signals at δ 168.2 and 168.3 ppm, and two methyl of acetyl were observed in the ^{13}C NMR spectrum (Figure 145). In addition, a pair of the phenolic carbon signals at δ 144.2, 139.0 ppm supported the hydroquinone ring. The aryl methyl and methoxyl proton signals of ring E in the ^{1}H NMR spectrum (Figure 143) were the same as other quinones while that of ring A, methyl signal shifted down field from δ 1.92 ppm to δ 2.10 and methoxyl signal shifted up field from δ about 3.9-4.0 ppm to δ 3.73. The absence of the unique homoallylic coupling (~ 2 Hz) between 1-H and 4-Hβ confirmed that ring A of this compound was reduced to a hydroquinone ring. The NMR data indicated that **42** was 5,8-*O*-diacetylhydroquinone renieramycin M.

The disappearance of the quinone carbonyl carbon signals of 5,8,15,18-*O*-tetraacetylbishydroquinone renieramycin M (**43**) and the appearance of four ester carbonyls, four methyl of acetyls and four phenolic carbon signals confirmed the bishydroquinone ring and four protecting acetyl groups in the ^{13}C NMR spectrum (Figure 155). The aryl methyl and methoxyl proton signals of both rings in the ^{1}H NMR spectrum (Figure 153) at 2.04, 2.06 ppm and 3.71, 3.74 ppm, respectively, indicated that both rings were hydroquinones.

3.5 Chemical transformation of renieramycin M to acetylated and hydroquinone renieramycin M

14,15,18-*O*-triacetyl renieramycin N (**45**; 59%) and 14-*O*-acetyl renieramycin O (**44,** 6%) were obtained by the reaction of **1n** with acetic anhydride in pyridine (Scheme 16). **44** was also obtained from **1o** which was easily prepared by oxidation of **1n** under basidic condition. The ^{1}H- and ^{13}C-NMR spectral data of the 14-*O*-acetylrenieramycin O, **44** were compared with those of **1o**, **44** had one more methyl of acetyl proton signal at δ 2.10 ppm in the ^{1}H-NMR spectrum (Figure 140) and an ester carbonyl carbon signal at δ 169.7 ppm, methyl of acetyl carbon signal at δ 20.7 ppm in the ^{13}C-NMR spectrum (Figure 141). The doublet C-14 carbon signal appeared at δ 61.4, the 14H-β proton signal shifted down field to 5.43 ppm. These data concluded that **44** was 14-*O*-acetyl renieramycin O.

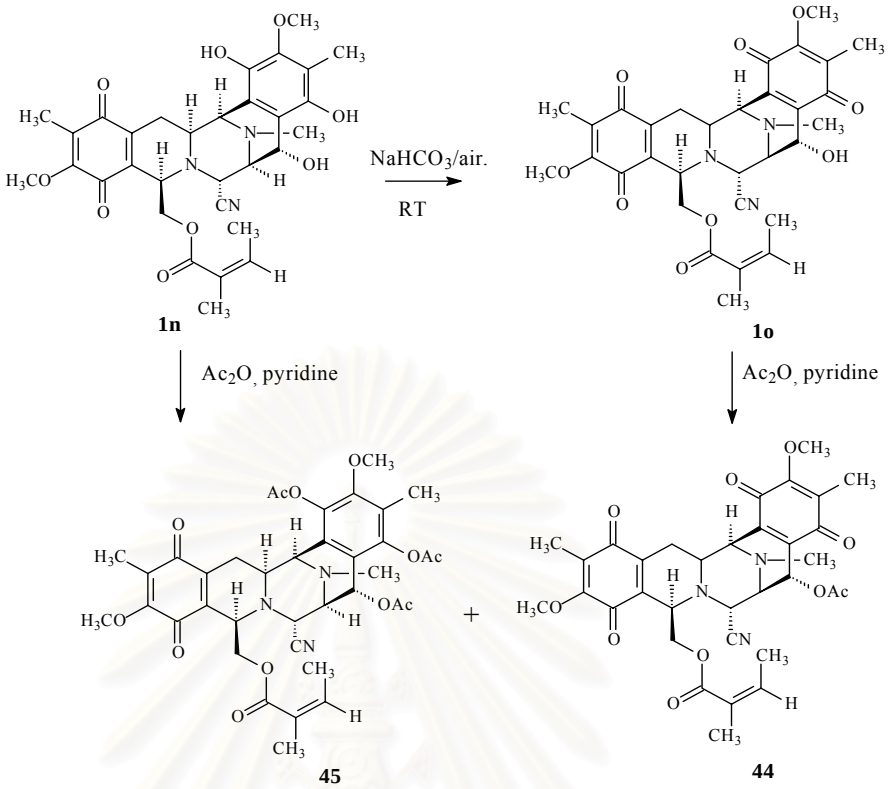

Scheme 16 Transformation of renieramycin N (**1n**) to the acetylated analogs.

Comparison NMR specral data of 14,15,18-*O*-triacetyl renieramycin N (**45**) with those of **1n**, **45** was a monoquinone with one quinone ring, either ring A or ring E, two quinone carbonyl carbon, three ester carbonyl, and three methyl of acetyl carbon signals were observed in the ^{13}C-NMR spectrum (Figure 150). The aryl methyl and methoxyl proton signals of ring A were the same as other quinones while those of ring E, methyl signal shifted down field to δ 2.04 and methoxyl signal shifted up field to δ 3.75 ppm in the ^{1}H-NMR spectrum (Figure 148). The presence of unique homoallylic coupling (~ 2 Hz) between 1-H and 4-Hβ confirmed that ring A of this compounds was still a quinone ring. The methine carbon of C-14 signal was shown at δ 63.1 ppm and the 14H-β proton signal shifted down field to 5.53 ppm, indicated that there was an acetoxyl substituted at C-14.

Hydrogenation of **1n** with 10% Pd/C in 10% methanol in dichloromethane for 1 h followed by acetylation with acetic anhydride and DMAP in dry pyridine gave the 5,8,14,15,18-*O*-pentaacetylbishydroquinone renieramycin M (**46**) in 76.7 % yields (Scheme 17).

The ^{1}H- and ^{13}C-NMR spectral data of the 5,8,14,15,18-*O*-pentaacetyl bishydroquinone renieramycin M **46** was compared with those of 5,8,15,18-*O*-tetra acetylbishydroquinone renieramycin M (**43**). There was no appearance of quinone carbonyl carbon signals but one more acetyl group. The methine carbon signal of C-14 was shown at δ 63.3 ppm in the ^{13}C-NMR spectrum (Figure 161) and the 14H-β proton signal shifted down field to 5.59 ppm in the ^{1}H-NMR spectrum (Figure 159) confirmed that **46** was 5,8,14,15,18-*O*-pentaacetylbishydroquinone renieramycin M.

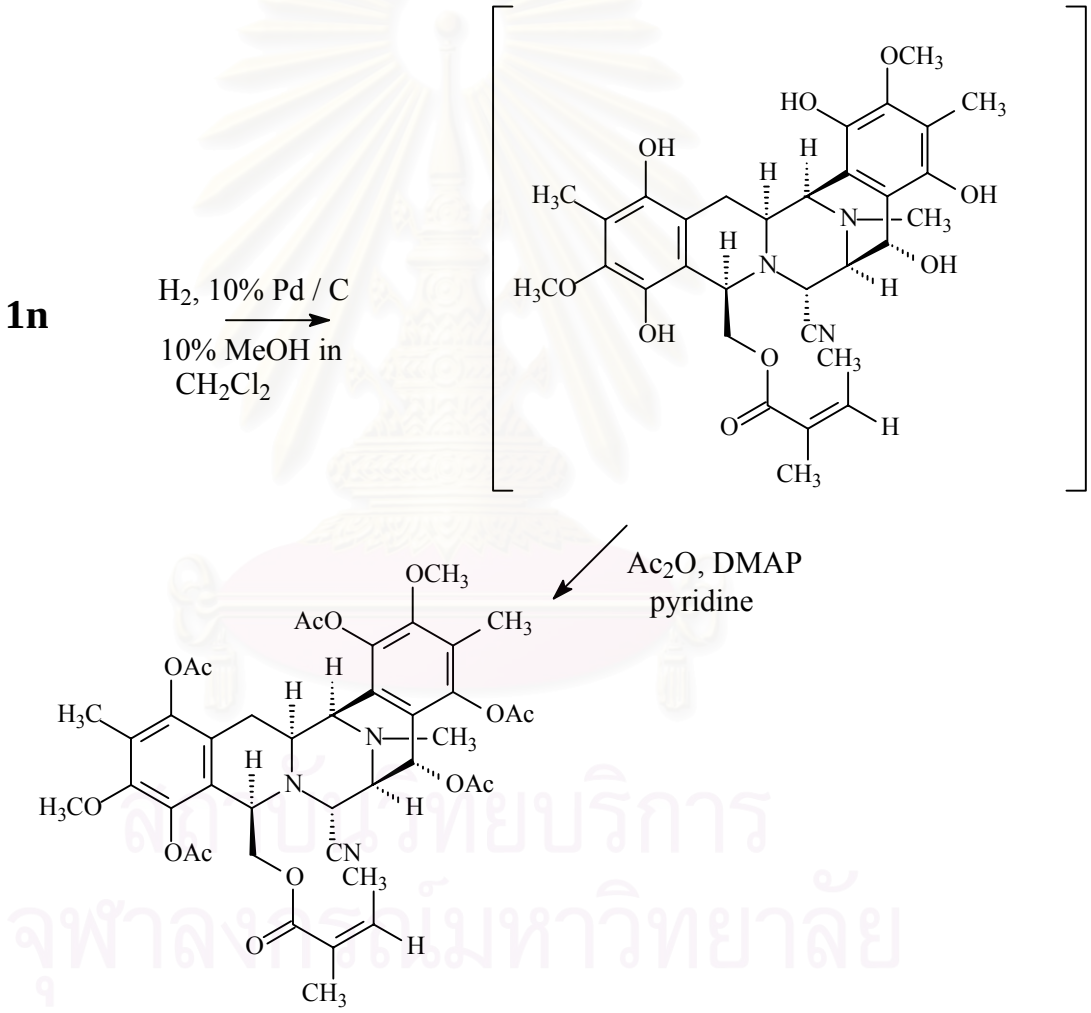

Scheme 17 Reductive acetylation of renieramycin N (**1n**)

Table 18 ^{1}H-NMR spectral data for Hydroquinone renieramycin acetates, **39**, **44** and **42** (in $CDCl_3$)

proton	Bishydroquinone renieramycin M (39)	14-*O*-acetyl renieramycin O (44)	5,8-*O*-diacetyl hydroquinone-quinone renieramycin M (42)
1-H	4.27 (1H, dd, 4.0, 3.0)	4.03 (1H, br s)	4.13 (1H, dd, 3.3, 3.0)
3-H	3.27 (1H, ddd, 11.9, 2.6, 2.5)	3.08 (1H, ddd, 11.6, 3.0, 2.6)	3.20 (1H, ddd, 12.3, 2.6, 2.3)
4-H β	1.89 (1H, dd, 15.5, 11.9)	1.26 (1H, ddd, 16.8, 11.6, 2.6)	1.66 (1H, dd, 15.5, 12.3)
4-H α	2.83 (1H, dd, 17.8, 7.9)	2.89 (1H, dd, 17.4, 2.8)	2.57 (1H, dd, 15.5, 2.6)
11-H	4.14 (1H, d, 2.1)	4.16 (1H, d, 3.0)	3.97 (1H, d, 2.3)
13-H	3.39 (1H, br d)	3.31 (1H, br d)	3.34 (1H, ddd, 7.9, 2.6, 1.3)
14-H β	2.42 (1H, d, 17.8)	5.43 (1H, s)	2.27 (1H, d, 20.8)
14-H α	3.04 (1H, dd, 15.5, 2.6)	-	2.76 (1H, dd, 20.8, 7.6)
21-H	4.14 (1H, d, 2.6)	4.37 (1H, d, 2.6)	4.01 (1H, d, 2.6)
22-Ha	3.96 (1H, dd, 10.9, 4.0)	4.21 (1H, dd, 11.6, 3.3)	3.73 (1H, dd, 11.2, 3.0)
22-Hb	4.56 (1H, dd, 10.9, 3.0)	4.30 (1H, dd, 11.6, 2.6)	4.34 (1H, dd, 11.2, 3.0)
6-CH_3	2.16 (3H, s)	1.93 (3H, s)	2.10 (3H, s)
16-CH_3	2.14 (3H, s)	1.92 (3H, s)	1.94 (3H, s)
7-OCH_3	3.73 (3H, s)	4.03 (3H, s)	3.73 (3H, s)
17-OCH_3	3.74 (3H, s)	4.01 (3H, s)	3.99 (3H, s)
N- CH_3	2.30 (3H, s)	2.46 (3H, s)	2.27 (3H, s)
OH	3.98 (br s, OH),	-	-
	4.33 (br s, OH)	-	-
	5.40 (2H, br s, OHx2)	-	-
$OCO\underline{CH_3}$	-	2.10 (3H, s)	2.36 (3H, s),
	-	-	2.35 (3H, s)
26-H	5.85 (1H, qq, 7.3, 1.7)	5.96 (1H, qq, 7.3, 1.5)	6.07 (1H, qq, 7.3, 1.7)
27- H_3	1.80 (3H, dq, 7.3, 1.3)	1.80 (3H, dq, 7.3, 1.7)	1.92 (3H, dq, 7.3, 1.3)
28- H_3	1.43 (3H, dq, 1.7, 1.3)	1.60 (3H, dq, 1.7, 1.5)	1.76 (3H, dq, 1.7, 1.3)

Table 19 ^{13}C-NMR spectral data for Hydroquinone renieramycin acetates, **39**, **44** and **42** (in $CDCl_3$)

carbon	Bishydroquinone renieramycin M (39)	14-O-acetylrenieramycin O (44)	5,8-O-diacetyl hydroquinone renieramycin M (42)
1	56.9 CH	56.3 CH	56.5 CH
3	56.7 CH	53.7 CH	55.4 CH
4	25.3 CH_2	25.4 CH_2	27.7 CH_2
5	143.6 C	185.2 C	144.2 C
6	118.4 C	129.6 C	124.6 C
7	143.6 C	155.9 C	149.3 C
8	139.1 C	180.6 C	139.0 C
9	117.6 C	137.3 C	124.5 C
10	115.7 C	140.8 C	124.0 C
11	56.4 CH	54.6 CH	54.7 CH
13	55.3 CH	61.7 CH	54.8 CH
14	21.1 CH_2	61.4 CH	21.2 CH_2
15	143.6 C	184.1 C	186.1 C
16	118.8 C	128.1 C	128.9 C
17	143.9 C	155.1 C	155.4 C
18	140.9 C	182.4 C	182.8 C
19	118.0 C	135.7 C	135.4 C
20	116.6 C	140.2 C	141.8 C
21	60.7 CH	56.0 CH	60.0 CH
22	64.3 CH_2	63.2 CH_2	66.7 CH_2
6-CH_3	9.2 CH_3	8.7 CH_3	10.0 CH_3
16-CH_3	9.3 CH_3	8.7 CH_3	8.7 CH_3
7-OCH_3	60.9 CH_3	61.0 CH_3	60.7 CH_3
17-OCH_3	61.0 CH_3	61.0 CH_3	60.9 CH_3
N- CH_3	41.7 CH_3	41.5 CH_3	41.5 CH_3
21-CN	116.4 C	116.1 C	117.2 C
O<u>CO</u>CH_3	-	169.7 C	168.3 C
	-		168.2 C
OCO<u>CH_3</u>	-	20.7 CH_3	20.6 CH_3
	-		20.3 CH_3
24	167.8 C	166.7 C	167.0 C
25	127.6 C	126.3 C	126.7 C
26	137.7 CH	138.6 CH	140.4 CH
27	15.4 CH_3	15.6 CH_3	15.9 CH_3
28	20.1 CH_3	20.3 CH_3	20.6 CH_3

Table 20 ^{1}H-NMR spectral data for hydroquinone renieramycin acetates, **45**,**43** and **46** (in $CDCl_3$)

proton	**14,15,18-*O*-triacetyl renieramycin N(45)**	**5,8,15,18-*O*-tetraacetylbishydroquinone renieramycin M (43)**	**5,8,14,15,18-*O*-pentaacetyl bishydroquinone renieramycin M (46)**
1-H	4.02 (1H, m)	4.10 (1H, m)	4.08 (1H, m)
3-H	3.10 (1H, ddd, 11.3, 3.0, 2.7)	3.22 (1H, ddd, 11.6, 2.6, 2.3)	3.21 (1H, ddd, 11.3, 3.0, 2.7)
4-H β	1.53 (1H, ddd, 17.4, 11.3, 2.1)	1.89 (1H, dd, 15.5, 11.6)	1.73 (1H, dd, 17.4, 11.3)
4-H α	2.94 (1H, dd, 17.4, 2.6)	2.71 (1H, dd,15.5, 2.6)	2.65 (1H, dd, 17.4, 2.6)
11-H	3.84 (1H, d, 2.1)	3.68 (1H, d, 2.3)	3.82 (1H, d, 2.1)
13-H	3.30 (1H, br d)	3.33 (1H, ddd, 7.9, 2.6, 1.3)	3.52 (1H, br d)
14-H β	5.53 (1H, s)	2.27 (1H, d, 17.8)	5.59 (1H, s)
14-H α	-	2.82(1H, dd, 17.8, 7.9)	-
21-H	4.39 (1H, d, 2.4)	4.00 (1H, d, 2.6)	4.32 (1H, d, 2.4)
22-Ha	4.04 (1H, m)	3.68 (1H, m)	4.06 (1H, m)
22-Hb	4.09 (1H, dd, 11.0, 4.3)	4.10 (1H, m)	4.06 (1H, m)
6-CH_3	1.92 (3H, s)	2.06 (3H, s)	2.04 (3H, s)
16-CH_3	2.04(3H, s)	2.04(3H, s)	2.05 (3H, s)
7-OCH_3	4.01 (3H, s)	3.71 (3H, s)	3.75 (3H, s)
17-OCH_3	3.75 (3H, s)	3.74 (3H, s)	3.68 (3H, s)
N- CH_3	2.45 (3H, s)	2.23 (3H, s)	2.42 (3H, s)
OCO$\underline{CH_3}$	2.44 (3H, s), 2.17 (3H, s), 2.08 (3H, s) - -	2.38 (3H, s), 2.37 (3H, s), 2.33 (3H, s), 2.28 (3H, s) -	2.38 (3H, s), 2.38 (3H, s), 2.34 (3H, s), 2.33 (3H, s), 2.15 (3H, s)
26-H	5.94 (1H, qq, 6.4, 1.5)	6.05 (1H, qq, 7.3, 1.7)	6.06 (1H, qq, 7.3, 1.5)
27- H_3	1.83 (3H, dq, 7.3, 1.7)	1.96 (3H, dq, 7.3, 1.7)	1.96 (3H, dq, 7.3, 1.7)
28- H_3	1.51 (3H, dq, 1.7, 1.5)	1.70 (3H, dq, 1.7, 1.5)	1.82 (3H, dq, 1.7, 1.5)

Table 21 ^{13}C-NMR spectral data for Hydroquinone renieramycin acetates, **45**,**43** and **46** (in $CDCl_3$)

carbon	14,15,18-*O*-triacetyl renieramycin N (45)	5,8,15,18-*O*-tetraacetyl bishydroquinone renieramycin M (43)	5,8,14,15,18-*O*-penta acetylbishydroquinone renieramycin M (46)
1	55.8 CH	56.2 CH	56.6 CH
3	54.9 CH	56.0 CH	55.8 CH
4	24.1 CH_2	26.4 CH_2	26.2 CH_2
5	185.4 C	144.1 C	143.9 C
6	127.9 C	124.4 C	124.5 C
7	155.9 C	148.1 C	150.4 C
8	180.5 C	139.2 C	139.1 C
9	135.6 C	124.1 C	123.7 C
10	141.1 C	123.3 C	123.3 C
11	57.0 CH	57.2 CH	58.2 CH
13	61.7 CH	54.7 CH	62.0 CH
14	63.1 CH	20.9 CH_2	63.3 CH
15	145.9 C	144.9 C	145.8 C
16	125.6 C	124.5 C	125.5 C
17	150.7 C	148.1 C	149.1 C
18	139.8 C	140.2 C	139.6 C
19	123.1 C	124.3 C	123.9 C
20	122.3 C	123.6 C	122.1 C
21	57.0 CH	61.0 CH	57.4 CH
22	61.0 CH_2	67.9 CH_2	69.0 CH_2
6-CH_3	8.6 CH_3	9.8 CH_3	10.1 CH_3
16-CH_3	10.1 CH_3	10.0 CH_3	10.2 CH_3
7-OCH_3	60.9 CH_3	60.8 CH_3	60.9 CH_3
17-OCH_3	60.9 CH_3	60.8 CH_3	60.8 CH_3
N- CH_3	42.0 CH_3	41.5 CH_3	42.7 CH_3
21-CN	116.4 C	117.4 C	116.0 C
O<u>CO</u>CH_3	170.3 C	168.3 C	170.0 C
	168.4 C	168.0 C	168.1 C
	166.9 C	167.8 C	167.8 C
	-	167.8 C	167.2 C
	-	-	166.9 C
OCO<u>CH_3</u>	20.8 CH_3	20.7 CH_3	20.9 CH_3
	20.7 CH_3	20.5 CH_3	20.8 CH_3
	20.3 CH_3	20.3 CH_3	20.7 CH_3
	-	20.3 CH_3	20.5 CH_3
	-	-	20.4 CH_3
24	167.6 C	167.1 C	167.5 C
25	126.9 C	127.1 C	127.1 C
26	139.4 CH	139.5 CH	139.2 CH
27	15.5 CH_3	15.7 CH_3	15.9 CH_3
28	20.1 CH_3	20.4 CH_3	19.9 CH_3

3.6 Oxidative degradation of renieramycins

He and Faulkner suggested that renieramycin E (**1e)** undergoes oxidative cleavage to generate mimosamycin (**6**) and renierone (**4**) (Frincke and Faulkner, 1982; He and Faulkner, 1989). During the course of this investigation, the decomposition of **1e** was also observed. Saito *et al.* studied the oxidative degradation of saframycin S (Saito *et al.*, 2003) (Scheme 18). The *p*-quinone **47** was selected as a model compound for studying this degradation. Treatment of **49** with silver nitrate in aqueous acetonitrile gave the α-amino alcohol **50**, which was treated with a catalytic amount of TFA in chloroform at RT for 3 days afforded mimosamycin (**6**).

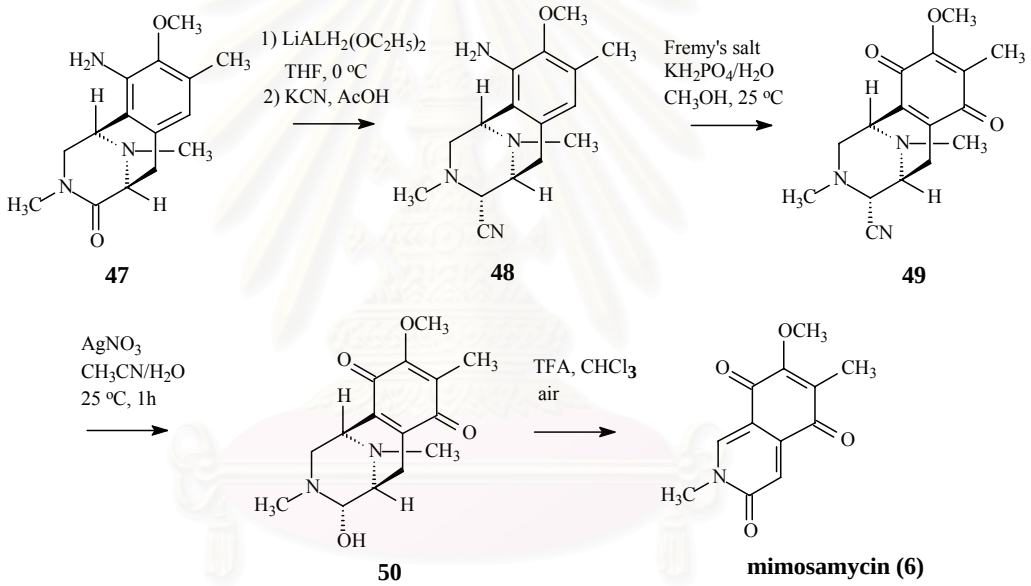

Scheme 18 The oxidative degradation study by using the *p*-quinone model compound (**47**).

The strategy was applied to the transformation of saframycin S resulting in the preparation of mimosamycin (**6**) and mimocin (**51**) as oxidative degradation products (Saito *et al.* 2003). Treatment of saframycin S with trifluoroacetic acid (TFA) in chloroform under reflux for 3 h gave **6** (16.7%) and **51** (16.2%) as shown in Scheme 19.

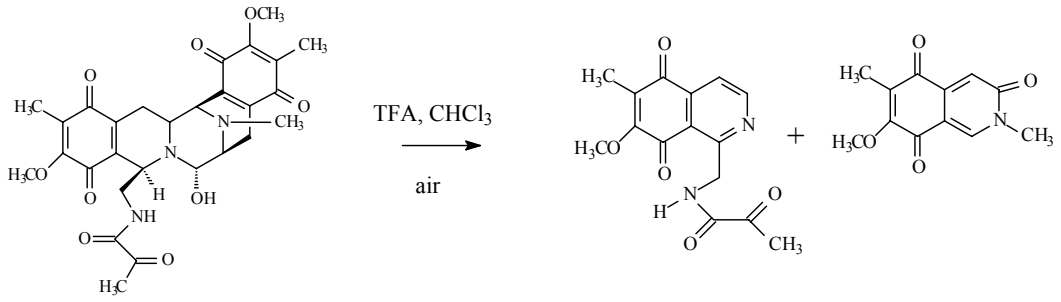

Scheme 19 The oxidative degradation of saframycin S into mimosamycin (**6**) and mimocin (**51**).

Although the mechanism of the oxidative degradation is not clear, one possible explanation for the cleavage of C3-C11 bond is the protonation of the quinone ring to generate the hydroquinone intermediate. The following steps including oxidative decarboxylation are unclear at this stage (Scheme 20).

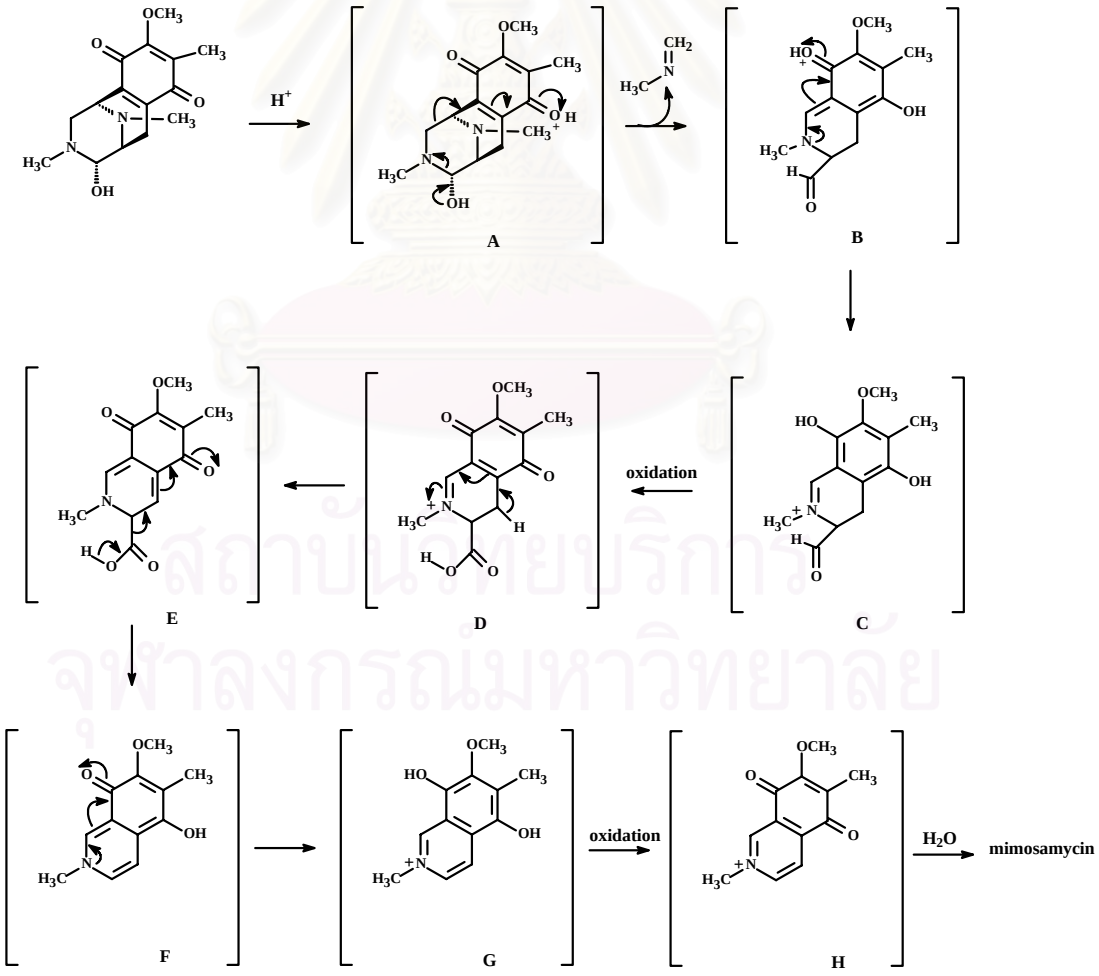

Scheme 20 One possible mechanism of oxidative degradation

Another possible mechanism of oxidative degradation was suggested by Professor Dr. Somsak Ruchirawat as shown in Scheme 21. After the generation of hydroquinone intermediate C, the peroxide intermediate D was formed by air oxidation. Loss of formic acid from intermediate D, initiated the formation of mimosamycin.

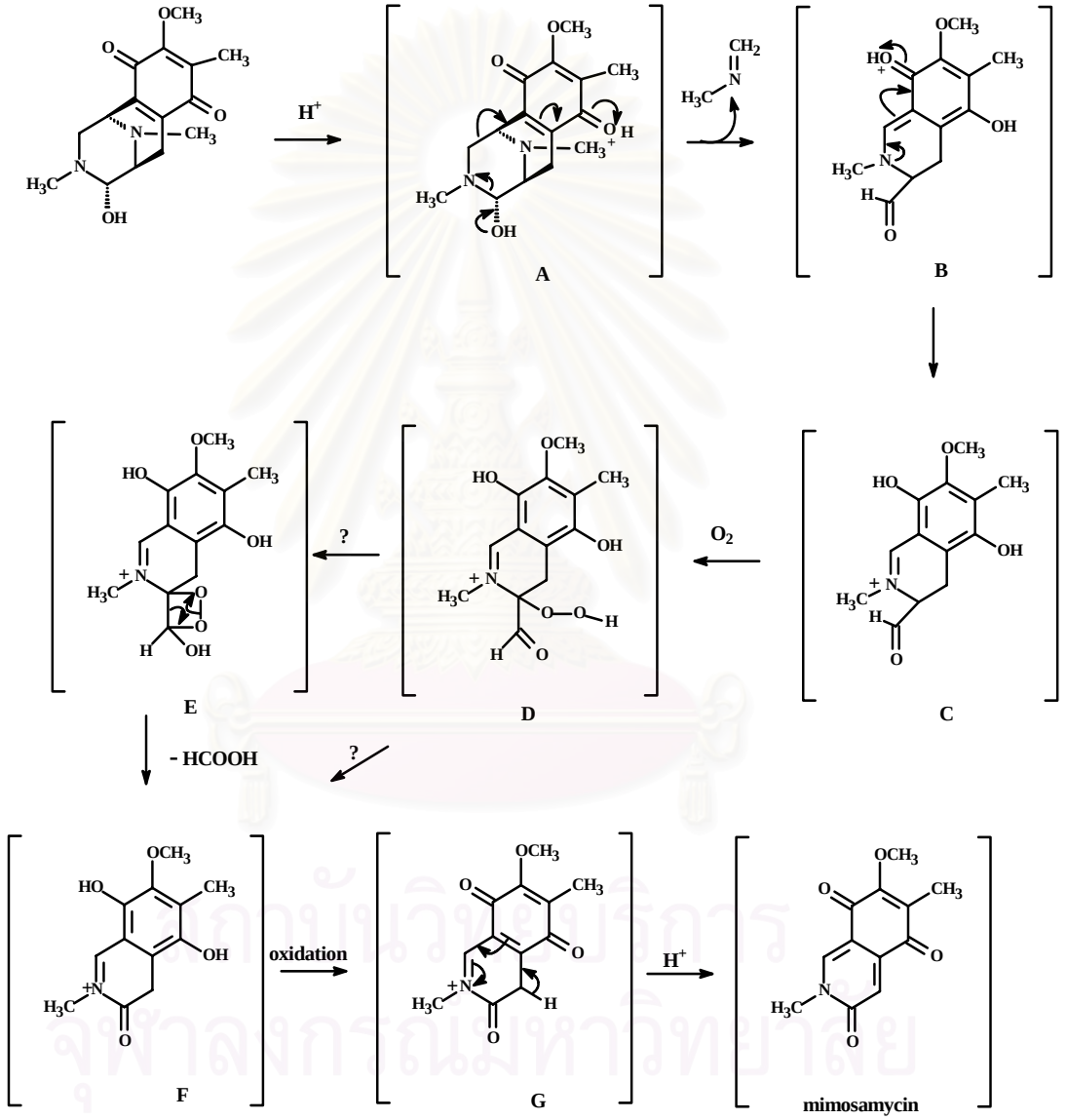

Scheme 21 Another possible mechanism of oxidative degradation

Degradation of renieramycin E (**1e)** was also studied by the same condition, with TFA in chloroform to give 1,6-dimethyl-7-methoxy-5,8 dihydroisoquinoline-5,8-

dione, **3** (4.4%), renierone, **4** (15.8%), *N*-formyl-1,2-dihydrorenierone, **5** (18.4%), and mimosamycin**, 6** (11.7%).

Furthermore, oxidation of **1e** with selenium oxide and *p*-toluenesulfonic acid (*p*-TsOH) in 1,4-dioxane at 80°C for 14 h afforded **4** (46.4%), **6** (43.9%), and *O*-demethylrenierone, **32** (21.8%). In contrast, treatment of jorumycin (**2)** under the same conditions generated **6** and renierol acetate (**34**) in 20.5% and 37.2% yields, respectively (see Table 19). These observations are evidence that such simple isoquinoline quinones as **3-6, 32** and **34** may be oxidative degradation products and/or artifacts of isolation procedures. The synthetic monomeric isoquinolinequinones, **3-6, 32** and **34** were identical with the reported spectroscopic data (see Tables 23, 24, and 25; Davidson, 1992; Edrada *et al.,*1996; Frincke and Faulkner, 1982; McIntyre *et al.,*1979; McKee and Ireland, 1987).

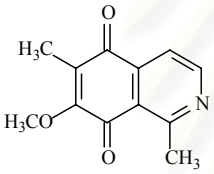

1,6-dimethyl-7-methoxy-5,8-dihydroisoquinoline-5,8-dione (**3**)

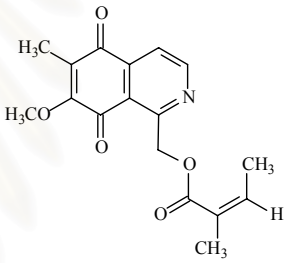

renierone (**4**)

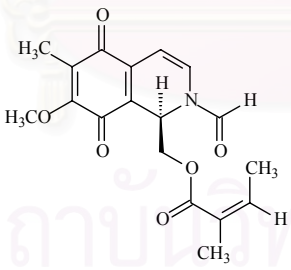

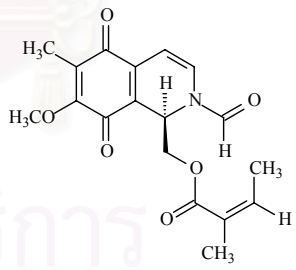

N-formyl-1,2-dihydrorenierone (**5**)

major isomer minor isomer

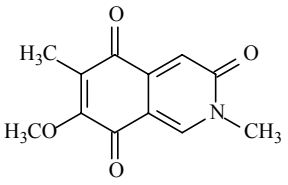

mimosamycin (**6**)

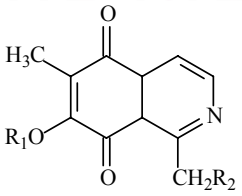

O-demethylrenierone (**32**);R_1 = H, R_2 = angelate ester
renierol acetate (**34**); $R_1 = CH_3$, $R_2 = OCOCH_3$

Table 22 Conditions and products of the oxidative degradation of some renieramycins

renieramycins	condition	Product (% yield)					
		3	**4**	**5**	**6**	**32**	**34**
1e	TFA, $CHCl_3$, reflux, 3h	4.4	15.8	18.4	11.7	0.0	
1e	*p*-TsOH, SeO_2, dioxane, 80°C, 14h	0.0	46.4	0.0	43.9	21.8	
2	*p*-TsOH, SeO_2, dioxane, 80°C, 12h				20.5		37.2

Table 23 ^{1}H-NMR spectral data for oxidative degradation products; renierone (**4)**, N-formyl-1,2-dihydrorenierone (**5)**, demethylrenierone (**32)**, and renierol acetate (**34)** in $CDCl_3$

proton	**4**	**5** (major)	**5** (minor)	**32**	**34**
1-H	-	5.99 (1H, dd, 4.5, 3.1)	5.36 (1H, dd, 5.0, 4.3)	-	-
3-H	8.92 (1H, d, 4.9)	6.91 (1H, d, 7.5)	7.44 (1H, d, 7.5)	8.97 (1H, d, 5.0)	8.94 (1H, d, 5.0)
4-H	7.88 (1H, d, 4.9)	6.03 (1H, d, 7.5)	6.23 (1H, d, 7.5)	7.95 (1H, d, 5.0)	7.90 (1H, d, 5.0)
6-CH_3	2.09 (3H, s)	1.95 (3H, s)	1.98 (3H, s)	2.12 (3H, s)	2.09 (3H, s)
7-OCH_3	4.15 (3H, s)	4.07 (3H, s)	4.06 (3H, s)	-	4.15 (3H, s)
N-CH_3	-	NCHO 8.43 (1H, s)	NCHO 8.22 (1H, s)	-	-
11-Ha	5.79 (1H, s)	4.36 (1H, dd, 12.0, 4.5)	4.21 (1H, dd, 12.5, 5.0)	5.80 (1H, s)	5.71 (1H, s)
11-Hb	5.79 (1H, s)	4.20 (1H, dd, 12.0, 3.1)	3.90 (1H, dd, 11.5, 4.3)	5.80 (1H, s)	5.71 (1H, s)
14-CH_3	1.98 (3H, dq, 1.5, 1.3)	1.77 (3H, dq, 1.5, 1.3)	2.00 (3H, dq, 1.5, 1.3)	1.98 (3H, dq, 1.5, 1.5)	2.22 (3H, s)
15-H	6.12 (1H, qq, 7.3, 1.3)	6.05 (1H, qq, 7.3, 1.5)	6.15 (1H, qq, 7.2, 1.5)	6.12 (1H, qq, 7.2, 1.5)	-
15-CH_3	2.01 (3H, dq, 7.3, 1.5)	1.91 (3H, dq, 7.3, 1.3)	1.87 (3H, dq, 7.3, 1.3)	2.01 (3H, dq, 7.2, 1.5)	-

Table 24 ^{1}H-NMR spectral data for oxidative degradation products; 1, 6-dimethyl-7-methoxy-5, 6-dihydroisoquinoline-5, 8-dione (**3)** and mimosamycin (**6)** in $CDCl_3$

proton	3	6
1-H	-	8.27 (1H, s)
3-H	8.84 (1H, d, 4.9)	-
4-H	7.80 (1H, d, 4.9)	7.10 (1H, s)
6-CH_3	2.08 (3H, s)	2.06 (3H, s)
7-OCH_3	4.14 (3H, s)	4.17 (3H, s)
N-CH_3	-	3.67 (3H, s)
1-CH_3	2.99 (3H, s)	-

Table 25 ^{13}C-NMR spectral data for oxidative degradation products; renierone (**4)**, mimosamycin (**6)**, and renierol acetate (**34)** in $CDCl_3$

CH_3

carbon	4	6	34
1	158.5 C	142.1 CH	158.5 C
3	153.9 CH	162.8 C	153.8 CH
4	118.3 CH	116.7 CH	118.6 CH
5	184.5 C	183.5 C	184.4 C
6	122.6 C	133.1 C	122.8 C
7	156.8 C	159.5 C	156.6 C
8	181.7 C	177.3 C	181.7 C
9	128.0 C	111.3 C	128.0 C
10	138.5 C	138.9 C	139.1 C
11	65.3 CH_2	-	65.5 CH_2
13	167.8 C	-	171.0 C
14	130.5 C	-	130.6 C
15	138.0 CH	-	-
7-OCH_3	61.2 CH_3	61.3 CH_3	61.3 CH_3
6-CH_3	9.0 CH_3	9.5 CH_3	9.1 CH_3
14- CH_3	20.6 CH_3	-	20.9 CH_3
15-CH_3	15.7 CH_3	-	-
N- CH_3	-	38.4 CH_3	-

4. Cytotoxic activity of renieramycins

The *in vitro* cytotoxicities of renieramycins and their derivatives against some human carcinoma cell lines including HCT116 (colon carcinoma), NCI-H460 (lung carcinoma), DLD1 (colon carcinoma), QG56 (lung carcinoma), and DU145 (prostate cancer), are summarized in Table 26. Among the renieramycins, renieramycin E (**1e),** jorumycin (**2),** deangeloyl renieramycin M (**38),** and 21-cyanojorumycin (**41)** are the most cytotoxic compounds with similar potency. The IC_{50} values for cytoxicity of the main isolated renieramycins, renieramycin M (**1m)** and N (**1n)** were almost equal to those of the reference 5-fluorouracil and the other tetrahydroisoquinoline alkaloids, saframycin A and ecteinascidin 770. From the available data, it is worth to note that compounds with the acetate ester (**41**) and without the ester side chain (**38**) displayed cytotoxicity more potent than **1m** which contains the angelate ester. However, **40** and renieramycin J (**1j)**, which lack a leaving group at C-21, have much less activities. To realize good cytotoxic activity, a cyano or a hydroxyl group at C-21 position is essential, confirming that the elimination of this functional group under physiological conditions results in the formation of a reactive iminium species that is responsible for covalent bond formation with the target as previously described in saframycins and ecteinascidins. The presence of the oxygen containing functionalities (OH, OCH_3, OCH_2CH_3 and OAc) at position 14 (eg. Renieramycins O (**1o)**, Q (**1q)**, R (**1r)**, R' (**1r')**, 14-*O*-acetylrenieramycin O (**44**), and 14,15,18-*O*-triacetylrenieramycin N (**45**) also causes much less cytotoxic activity; however, it is quite interesting to note that 5,8-*O*-diacetylhydroquinone renieramycin M (**42**) and 5,8,15,18-*O*-tetraacetylbishydro quinone renieramycin M (**43**) are more active than the corresponding **1m**.

Further anticancer evaluations of these renieramycins against more carcinoma cell lines and in animal models, as well as mechanisms of action are underway.

Table 26 Cytotoxicity of renieramycins and derivatives against human tumor cell lines.

Compound	IC_{50} (nM)				
	HCT 116	**QG 56**	**NCI-H 460**	**DLD1**	**DU 145**
5-Fluorouracil	2.0	2.6	NT	NT	3.5
saframycin A	0.4	5.5	NT	NT	NT
ecteinascidin 770	1.2	3.9	NT	NT	NT
renieramycin E (**1e**)	< 0.38	1.0	NT	NT	< 0.38
renieramycin J (**1j**)	730.0	510.0	NT	NT	370.0
renieramycin M (**1m**)	7.9	19.0	59.0	96.0	NT
renieramycin N (**1n**)	5.6	11.0	67.0	57.0	NT
renieramycin O (**1o**)	28.0	40.0	NT	NT	NT
renieramycin Q (**1q**)	59.0	71.0	NT	NT	NT
renieramycin R (**1r**)	23.0	29.0	NT	NT	NT
renieramycin R' (**1r'**)	33.0	99.0	NT	NT	NT
renieramycin S (**1s**)	15.0	26.0	NT	NT	NT
jorumycin (**2**)	0.57	0.76	NT	NT	0.49
deangeloyl RM (**38**)	< 0.38	2.9	NT	NT	2.6
decyano deangeloyl RM (**40**)	32.0	130.0	NT	NT	10.0
21-cyanojorumycin (**41**)	< 0.38	0.68	NT	NT	< 0.38
5,8-*O*-diacetyl hydroquinone renieramycin M (**42**)	1.9	3.9	NT	NT	NT
5,8,15,18-*O*-tetra acetyl bishydroquinone renieramycin M (**43**)	3.0	7.9	NT	NT	NT
14-*O*-acetyl renieramycin O (**44**)	120.0	300.0	NT	NT	NT
14,15,18-*O*-triacetyl renieramycin N (**45**)	630.0	1,600.0	NT	NT	NT

NT = not tested

CHAPTER V

CONCLUSION AND RECOMMENDATION

Six tetrahydroisoquinoline alkaloids were isolated from the Thai marine sponge, *Xestospongia* sp., collected from Si Chang Island, in the Gulf of Thailand, including renieramycins M, N, O, Q, R, and S, in 11.25, 1.52, 0.27, 0.11, 0.62, and 0.09 % yield of the ethyl acetate extract, respectively. With the KCN-pretreated strategy, large-scale preparation of the labile renieramycins in the stabilized forms from the Thai sponge, *Xestospongia* sp. was achieved. This result is opening new opportunities in marine biomedical research collaborations for further chemical, pharmacological, and biological investigations required for future development of renieramycin alkaloids as a new frontier of anticancer agents from the Thai *Xestospongia* sponge.

The chemical transformations of renieramycin M are summarized as following :

1. Renieramycin M was transformed to renieramycins R and R', allylic oxidation with alcoholic solvent introduced the α-alkoxy substitution at carbon 14.

2. The transformation of renieramycin M to the naturally occurring renieramycin E was treated by silver nitrate and aqueous acetonitrile.

3. From the ABC ring model studies and the possible transformation of renieramycin M to renieramycin J showed that renieramycin J be the C-21 acetone adduct derivative resulting from the extraction and isolation using acetone solvent.

4. The angeloyl ester side chain cleavage at C-22 of renieramycin M was studied by several methods of hydrogenation and reduction using either lithium aluminium hydride or aluminium hydride to afford deangeloyl renieramycin M (**38**). Two-step hydrogenation and reduction by aluminium hydride at very low temperature (-20^{o}C) gave the highest yield of **38**. This compound will be an important intermediate for further modification to new promising series of ester derivatives. The first modification came from the effort to synthesis the nudibranch renieramycin, jorumycin which was an acetyl ester *via* an cyanojorumycin, **(41)**.

5. The bisquinones, renieramycin M was transformed to the hydroquinone acetates by reductive acetylation to obtain 5,8-*O*-diacetylhydroquinone renieramycin M (**42**) and the 5,8,15,18-*O*-tetraacetylbishydroquinone renieramycin M (**43**). 14-*O*-acetylrenieramycin O (**44**), 14,15,18-*O*-triacetyl renieramycin N (**45**), and 5,8,14,15,18-*O*-pentaacetylbishydroquinone renieramycin M (**46**) were transformed from renieramycins N and O by acetylation and reductive acetylation.

6. Oxidative degradation of renieramycin E was studied by using TFA in $CHCl_3$, to obtain 1,6-dimethyl-7-methoxy-5,8-dihydroisoquinoline-5,8-dione (**3**), renierone (**4**), *N*-formyl-1,2-dihydrorenierone (**5**), mimosamycin (**6**) in 4, 16, 18 and 12% yield, respectively. By using *p*-TsOH, SeO_2, dioxane, renierone, mimosamycin and *O*-demethylrenierone (**32**) were obtained in 46, 44 and 22 % yield, respectively. The oxidative degradation of jorumycin was also studied using *p*-TsOH, SeO_2, dioxane to obtain mimosamycin, and renierol acetate (**34**) in 21 and 37 % yield, respectively.

Cytotoxic activity evaluation of all the isolated and transformed compounds revealed the following characters.

1. Renieramycin E (**1e**), jorumycin (**2**), deangeloyl renieramycin M (**38**), and 21-cyanojorumycin **(41)** exhibited the most cytoxic activity with similar potency.

2. The leaving group (OH, CN) at C-21 is essential for cytotoxic activity.

3. The acetylated hydroquinone derivatives are more potent than the quinone derivatives.

4. The deangeloyl derivatives or deesterified derivatives at C-22 (free alcohol at C-22) are more potent than the parent compounds.

5. The acetyl derivatives are more potent than the angeloyl derivatives.

6. The oxygenated substituents at C-14 decrease the cytotoxic activity.

According to the cytotoxic activity, further transformation of renieramycin M especially the deangelate derivative should be studied on new esters or ethers, both aliphatics and aromatics. The anticancer evaluations of these renieramycins against more carcinoma cell lines and in animal models, as well as toxicity and mechanisms of action are recommended for future drug development.

REFERENCES

Arai, T. and Kubo, A. 1983. Isoquinolinequinones from Actinomycetes and sponges. In Brossi, A. Ed. The Alkaloids. vol. 21. New York: Academic Press, pp. 55-100.

Arai, T., Takahashi, K. , Ishiguro, K., and Yazawa, K. 1980a. Increase production of saframycin A and isolation of saframycin S. J. Antibiot. 33: 951-960.

Arai, T., Takahashi, K., and Kubo, A. 1977. New antibiotics, saframycins A, B, C, D and E. J. Antibiot. 30: 1015-1018.

Arai, T., Takahashi, K., Nakahara, S., and Kubo, A. 1980b. The structure of a novel antitumor antibiotic, saframycin. Experentia 36: 1025-1027.

Arai, T.; Yazawa, K.; Takahashi, K.; Maeda, A.; Mikami, Y. 1985. Direct biosynthesis of new saframycin derivatives with resting cell *of Streptomyces lavendulae*. Antimicrob. Agents Chemother. 28: 5-11.

Cuevas, C., Perez, M., Martin, M.J., Chicharro, J.L., Fernandez-Rivas, C., Flores, M., Francesch, A., Gallego, P., Zarzuelo, M., de la Calle, F., Garcia, J., Polanco, C., Rodriguez, I. And Mazanares, I. 2000. Synthesis of ecteinascidin ET–743 and phthalascidin Pt–650 from cyanosafracin B. Org.Lett. 2(16): 2545-8.

Davidson, B.S. 1992. Renieramycin G, a new alkaloid from the sponge *Xestospongia caycedoi*. Tetrahedron Lett 33: 3721-3724.

Edrada, R.A., Proksch, P., Gras, V., Christ, R., Witte, L., and Soest, R.W.M.V. 1996. Bioactive isoquinolinequinone from an undescribed Phillippine marine sponge of the genus *Xestospongia*. J. Nat. Prod. 59: 973-976.

Fontana, A., Cavaliere, P., Wahidulla, S., Naik, C.G., and Cimino, G. 2000. A new antitumor isoquinoline alkaloid from the marine nudibranch *Jorunna funebris*. Tetrahedron 56: 7305-7308.

Frincke, J.M., Faulkner, D.J. 1982. Antimicrobial metabolites of the sponge *Reniera* sp. J. Am. Chem. Soc. 104: 265-269.

Fukuyama, T., Linton, S.D., and Tun, M.M. 1990. A stereocontrolled total synthesis of (±)-renieramycin A. Tetrahedron Lett. 31(42): 5989-5992.

Fukuyama, T., and Sachleben, R.A. 1982. Stereocontrolled total synthesis of (±)-saframycin B. J. Am. Chem. Soc. 104: 4957-4958.

Fukuyama, T., Yang, L., Ajeck, K.L., and Sachleben, R.A. 1990. Total synthesis of (±)-saframycin A. J. Am. Chem. Soc. 112: 3712-3713.

Garcia-Nieto, R.; Manzanares, I.; Cuevas, C.; Gago, F. 2000. Bending of DNA upon binding of ecteinascidin 743 and phthalascidin 650 studied by unrestrained molecular dynamics simulations. J. Am. Chem.Soc. 122: 7172-7182.

He, H., and Faulkner, D.J. 1989. Renieramycins E and F from the sponge *Reniera* sp.: reassignment of the stereochemistry of the renieramycins. J. Org. Chem. 54: 5822-5824.

Hooper, J.N.A. 2000. Sponguide : Guide to sponge collection and identification. http://www.qmuseum.qld.gov.au/organisation/sections/SessileMarineInvertebrates/index.asp.

Inouye, Y., Oogose, K., Take, Y., Kubo, T., and Nakamura, S. 1987. Role of single-electron reduction potential in inhibition of reverse transcriptase by streptonigrin and sakyomicin A. J. Antibiot. 40(5): 702-705.

Jeedigunta, S.; Krenisky, J. M.; Kerr, R. G. 2000. Diketopiperazines as advanced intermediates in the biosynthesis of ecteinascidins. Tetrahedron 56(21): 3303-3307.

Kaneda, S., Hour-Young, C., Yazawa, K., Takahashi, K., Mikami, Y. and Arai, T.1986. Antitumour activity of new semisynthetic saframycin derivatives. Jpn. J .Cancer Res. (Gann) 77: 1043-1049.

Kaneda, S., Hour-Young, C., Yazawa, K., Takahashi, K., Mikami, Y. and Arai, T. 1987. Biological activities of newly prepared saframycins. J. Antibiot. XL(11): 1640-1642.

Kerr, R. G., and Miranda, N. F. 1995. Biosynthetic studies of ecteinascidins in the marine tunicate *Ecteinascidia turbinata.* J. Nat. Prod. 58(10): 1618-1621.

Kishi, K., Yazawa, K., Takahashi, K., Mikami, Y., and Arai, T. 1984. Structure-acitvity relationships of saframycins. J. Antibiot. 37(8): 847-852.

Kobayashi, M., Rao, S.R., Chavakula, R., and Sarma, N.S. 1994. Mimosamycin, 4-aminomimosamycin and 7-amino-7-demethoxymimosamycin from the *Petrosia* sp. sponge. J. Chem. Res.(S): 282-3.

Koizumi, Y., Kubo, A., Suwanborirux, K., Saito, N. 2002. Chemistry of renieramycins. Part 2. Partial reduction and nucleophilic substitution of hexahydro-1,5-imino-4-oxo-3-benzazocine-7,10-dione: promising method to construct renieramycin J from renieramycin G via renieramycin E. Heterocycles 57: 2345-2355.

Kubo, A. and Saito, N. 1992. Studies in Natural Products Chemistry. vol. 10. Atta-ur-Rahman, Ed., Amsterdam: Elsevier, pp. 77-145.

Kubo, A., Saito, N., Yamato, Masubuchi, K., and Nakamura, M. 1988. Stereoselective total synthesis of (±)-saframycin B. J. Org. Chem 53: 4295-4310.

Kubo, A., Saito, N., Yamauchi, R., and Sakai, S. 1987b. Synthesis of saframycins. I. Total synthesis of (±)-saframycin B and its congeners. Chem. Pharm. Bull. 35(5): 2158-2161.

Kubo, A.; Saito, N.; Yamato, H.; Kawakami, Y. 1987a. Preparations and reactions of (Z)-3-arylidene-6-arylmethyl-2,5-piperazinediones having highly oxygenated benzene rings. Chem. Pharm. Bull. 35(6): 2525-2532.

Kubo, A., Kitahara, Y., and Nakahara, S. 1989. Synthesis of new isoquinoline quinone metabolites of a marine sponge, *Xestospongia* sp., and the nudibranch *Jorunna funebris*. Chem. Pharm. Bull. 37(5): 1384-1386.

Lown, J. W.; Joshua, A. V., and Chen, H.-H. 1981. Studies related to antitumor antibiotics. Part XXIV. High field ^{1}H-NMR analysis and conformations of saframycins A and C. Can. J. Chem. 59: 2945-2951.

Lown, J. W.; Joshua, A. V.; Lee, J. S. 1982. Molecular mechanisms of binding and single-strand scission of deoxyribonucleic acid by antitumor antibiotics saframycins A and C. Biochemistry 21: 419-428.

Martinez, E.J., and Corey, E.J. 2000. A new, more efficient, and effective process for the synthesis of a key pentacyclic intermediate for production of ecteinascidin and phthalascidin antitumor agents. Org. lett. 2(7): 993-996.

Martinez, E.J., Owa, T., Schreiber, S.L., and Corey, E.J. 1999. Phthalascidin, a synthetic antitumor agent with potency and mode of action comparable to ecteinascidin 743. Proc. Natl. Acad. Sci. USA. 96: 3496-3501.

McIntyre, D.E., Faulkner, D.J., Engen, D.V., and Clardy, J. 1979. Renierone, an antimicrobial metabolite from a marine sponge. Tetrahedron Lett. 20: 4163-4166.

Mckee, T.C., and Ireland, C.M. 1987. Cytotoxic and antimicrobial alkaloids from the Fijian sponge *Xestospongia caycedoi.* J. Nat. Prod. 50(4): 754-756.

Mikami, Y.; Takahashi, K.; Yazawa, K.; Arai, T.; Namikoshi, M.; Iwasaki, S.; Okuda, S. 1985. Biosynthetic studies on saframycin A, a quinine antitumor antibiotic produced by *Streptomyces lavendulae*. J. Biol. Chem. 260: 344-348.

Moore, R. M., II; Seaman, F. C.; Wheelhouse, R. T.; Hurley, L. H. 1998. Mechanism for the catalytic activation of Ecteinascidin 743 and its subsequent alkylation of guanine N2. J. Am. Chem. Soc. 120: 2490-2491.

Myers, A.G., and Kung, D.W. 1999. A concise, stereocontrolled synthesis of (-)-saframycin A by the directed condensation of α-amino aldehyde precursors. J. Am. Chem. Soc. 121: 10828-10829.

Myers, A.G., and Lanman, B.A. 2002. A solid-supported, enantioselective synthesis suitable for the rapid preparation 0f large number of diverse structural analogues of (-)-saframycin A. . J. Am. Chem. Soc. 124: 12969-12971.

Myers, A.G., and Plowright, A.T. 2001. Synthesis and evaluation of bishydroquinone derivatives of (-)-saframycin A: identification of a versatile molecular template imparting potent antiproliferative activity. J. Am. Chem. Soc. 123: 5114-5115.

Myers, A. G.; Kung, D. W.; Zhong, B.; Movassaghi, M.; Kwon, S. 1999a. Preparation of chiral, C-protected α-amino aldehydes of high optical purity and their use as condensation components in a linear synthesis strategy. J. Am. Chem. Soc. 121: 8401-8402.

Myers, A. G.; Schnider, P.; Kwon, S.; Kung, D. W. 1999b. Greatly simplified procedures for the synthesis of α-amino acids by the direct alkylation of pseudoephedrine glycinamide hydrate. J. Org. Chem. 64: 3322-3327.

Oku, N., Matsunaga, S., Van Soest, R.W.M., Fusetani, N.J. 2003. Renieramycin J, a highly cytotoxic tetrahydroisoquinoline alkaloid, from a marine sponge *Neopetrosia* sp. J. Nat. Prod. 66: 1136-1139.

Ozturk, T. 2000. The Alkaloids. vol. 53. Cordell, G. A., Ed.; New York: Academic, pp 119-238.

Parameswarn, P.S., Naik, C.G., Kamat, S.Y., Pramanik, B.N. 1998. Renieramycins H and I, two novel alkaloids from the sponge *Haliclona cribricutis* Dendy. Indian J. Chem. 37B: 1258-1263.

Pettit, G.R., Collins, J.C., Herald, D.L., Doubek, D.L., Boyd, M.R., Schmidt, J.M., Hooper, J.N.A., Tackett, L.P. 1992. Isolation and structure of cribrostatins 1 and 2 from the blue marine sponge, *Cribrochalina* sp. Can. J. Chem. 70: 1170-1175;

Pettit, G.R., Knight, J.C., Collins, J.C., Herald, D.L., Pettit, R.R., Boyd, M.R. and Young, V.G. 2000. Antineoplastic agents 430. Isolation and structure of cribrostatins 3, 4 and 5 from the Republic of Maldives *Cribrochalina* species. J. Nat. Prod. 63: 793-798.

Pospiech, A.; Cluzel, B.; Bietenhader, J.; Schupp, T. 1995. A new *Myxococcus xanthus* gene cluster for the biosynthesis of the antibiotic saframycin Mx1 encoding a peptide synthetase. Microbiology 141: 1793-1803.

Pospiech, A.; Bietenhader, J.; Schupp, T. 1996. Two multifunctional peptide synthetases and an *O*-methyltransferase are involved in the biosynthesis of the DNA-binding antibiotic and antitumor agent saframycin Mx1 from *Myxococcus xanthus*. Microbiology 142: 741-746.

Reid, J. M.; Walker, D. L.; Ames, M. M. 1996. Preclinical pharmacology of ecteinascidin 729, a marine natural product with potent antitumor activity. Cancer Chemother. Pharmacol. 38: 329-334.

Rinehart, K.L. 2000. Antitumour Compounds from Tunicates. Med. Res. Rev. 20(1): 1-27.

Rinehart, K.L.Holt, T.G., Fregeau, N.L., Keifer, P.A., Wilson, G.R., Perun Jr., T.J., Sakai, R., Thompson, A.G., Stroh, J.G., Shield, L., Seigler, D.S., Li, L.H., Martin, D.G., Grimmelikhuijzen, C.J.P. and Gade, G. 1990a. Bioactive compounds from aquatic and terrestrial sources. J. Nat. Prod. 53(4): 771-792.

Rinehart, K.L., Holt, T.G., Fregeau, N.L., Stroh, J.G., Keifer, P.A., Sun, F., Li, L.H.and Martin, D.G. 1990b. Ecteinascidins 729, 743, 745,759A, 759B and 770 : Potent antitumour agents from the Caribbean tunicate . *Ecteinascidia turbinata* . J. Org. Chem. 55: 4512-4515.

Roman, L.U., del Rio, R.E., Hernandez, J.D., Cerda, C.M., Cervantes, D., Castaneda, R., and Joseph-Nathan, P. 1985. Structural and stereochemical studies of naturally occurring longipinene derivatives. J. Org. Chem. 50: 3965-3972.

Saito, N., Koizumi, Y., Tanaka, C., Suwanborirux, K., Amnuoypol, S., and Kubo, A. 2003. Chemistry of antitumor isoquinolinequinone alkaloids: unexpected oxidative degradation of saframycin S to generate simple isoquinoline alkaloids, mimosamycin and mimocin. Heterocycles 61: 79-86.

Saito, N., Sakai, H., Suwanborirux, K., Pummangura, S., and Kubo, A. 2001. ^{13}C NMR spectral assignment of 5-hydroxy-1,5-imino-3-benzazocin-4,7,10-trione derivatives: The revised structure of renieramycin H. Heterocycles 55: 21-28.

Sakai, R., Jares-Erijman, E.A., Manzanares, I., Silva Elipe, M.V. and Rinehart, K.L. 1996. Ecteinascidins: Putative biosynthetic precursors and absolute stereochemistry. J.Am.Chem.Soc. 118: 9017-9023.

Sakai, R., Rinehart, K.L., Guan, Y. and Wang, A.H.-J. 1992. Additional antitumour ecteinascidins from a Caribbean tunicate: Crystal structures and activities in vivo. Proc. Natl. Acad . Sci. USA. 89: 11456-11460.

Scott, J.D.; Williams, R.M. 2002. Tetrahydroisoquinolinequinones antitumor antibiotics. Chem. Rev. 102: 1669-1730.

Suwanborirux, K., Charupant, K., Amnuoypol, S., Pummangura, S., Kubo, A., and Saito, N. 2002. Ecteinascidins 770 and 786 from the Thai tunicate *Ecteinascidia thurstoni*. J. Nat. Prod. 65: 935-937.

Suwanborirux, K., Amnuoypol, S., Plubrukarn, A., Pummangura, S., Kubo, A., Tanaka, C., and Saito, N. 2003. Chemistry of renieramycins. Part 3. Isolation and structure of stabilized renieramycin type derivatives possessing antitumor activity from Thai sponge *Xestospongia* species, pretreated with potassium cyanide. J. Nat. Prod. 66: 1441-1446.

Takebayashi, Y.; Pourquier, P.; Zimonjic, D. B.; Nakayama, K.; Emmert, S.;Ueda, T.; Urasaki, Y.; Kanzaki, A.; Akiyama, S.; Popescu, N.; Kraemer, K. H.; Pommier, Y. 2001b. Antiproliferative activity of ecteinascidin 743 is dependent upon transcription - coupled nucleotide – excision repair. Nat. Med. 7: 961.

Takebayashi, Y.; Goldwasser, F.; Urasaki, Y.; Kohlhagen, G.; Pommier, Y. 2001a. Ecteinascidin 743 induced protein-linked DNA breaks in human colon carcinoma HCT116 cells and its cytotoxic independently of topoisomerase I expression. Clin.Cancer Res. 7: 185-191.

Take, Y., Oogose, K., Kubo, T., Inouye, Y., Nakamura, S., Kitahara, Y., and Kubo, A. 1987. Comparative study on biological activities of heterocyclic quinines and streptonigrin. J. Antibiot. 40(5): 679-684.

Tomson, R. H. 1987. Naturally Occurring Quinones III. New York: Chapman and Hall, pp. 633-686.

Venkateswarlu, Y., Reddy, V.R., Srinivas, K.V.N.S., and Rao, J.V. 1993. A new isoquinolinequinone from a sponge *Petrosia* sp. Ind. J. Chem. 32B: 704.

Wright, A.E., Forleo, D.A., Gunawardana, S.P., Gunasekera, S.P., Koehn, F.E. and McConnell, O.J. 1990. Antitumour tetrahydroisoquinoline alkaloids from the colonial ascidian *Ecteinascidia turbinata.* J. Org. Chem. 55: 4508-4512.

Yazawa, K., Takahashi, K., Mikami, Y., Arai, T., Saito, N., and Kubo, A. 1986. Isolation and structural elucidation of new saframycins Y3, Yd-1, Yd-2, Ad-1, Y2b and Y2b-d. J. Antibiot. 39(12): 1639-1650.

Zewail-Foote, M.; Hurley, L. H. 1999. Ecteinascidin 743: a minor groove alkylator that bends DNA toward the major groove. J. Med. Chem. 42: 2493-2497.

Zewail-Foote, M.; Hurley, L. H. 2001. Differential rates of reversibility of ecteinascidin 743-DNA covalent adducts from different sequences lead to migration to favored bonding sites. J. Am. Chem. Soc. 123: 6485-6495.

APPENDICES

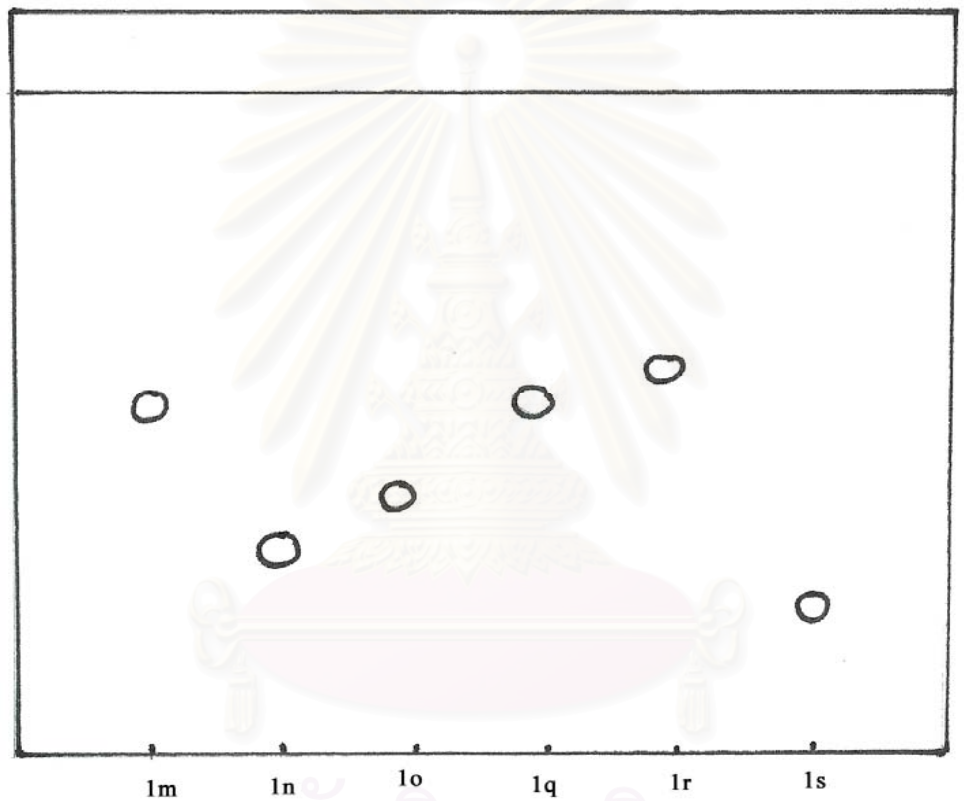

Si/hexane:ethyl acetate 1:1

Figure 16 The TLC chromatogram of the isolated renieramycins, M, N, O, Q, R, and S.

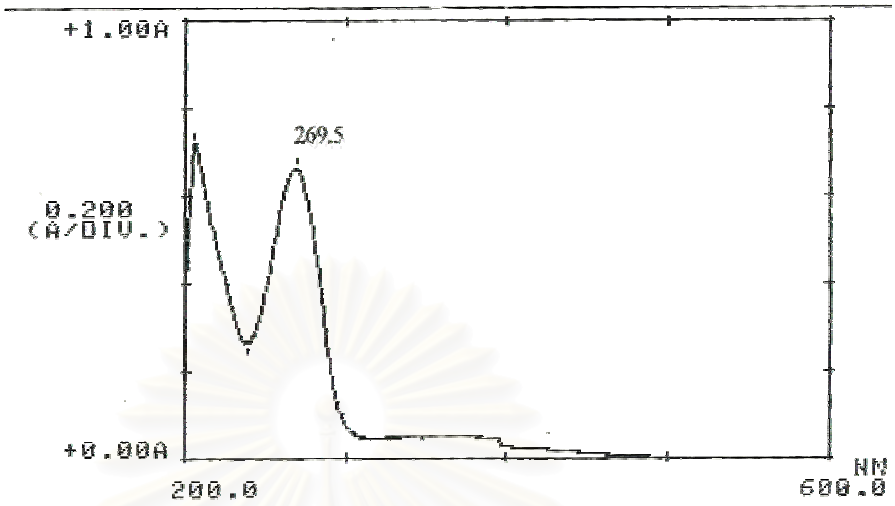

Figure 17 The UV spectrum of renieramycin M in methanol

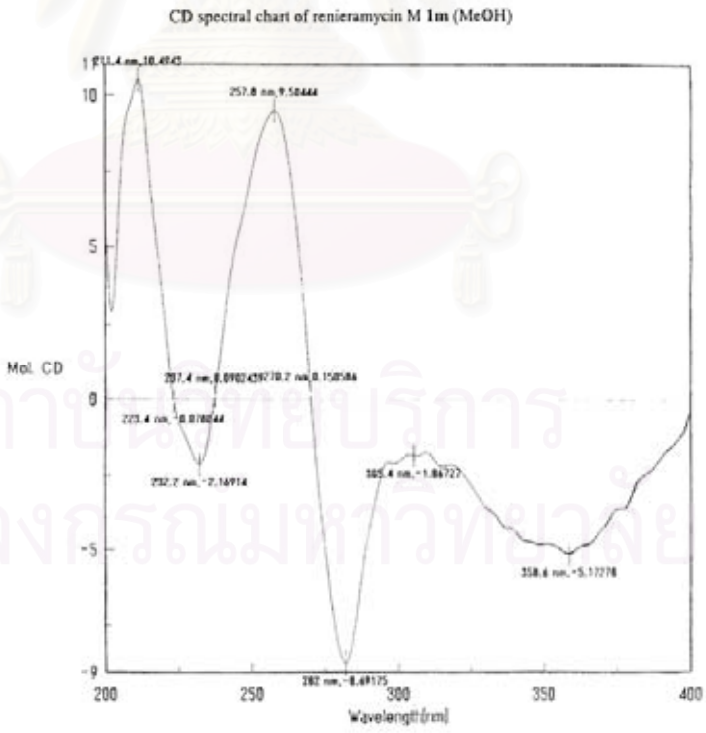

Figure 18 The circular dichroism spectrum of renieramycin M in methanol

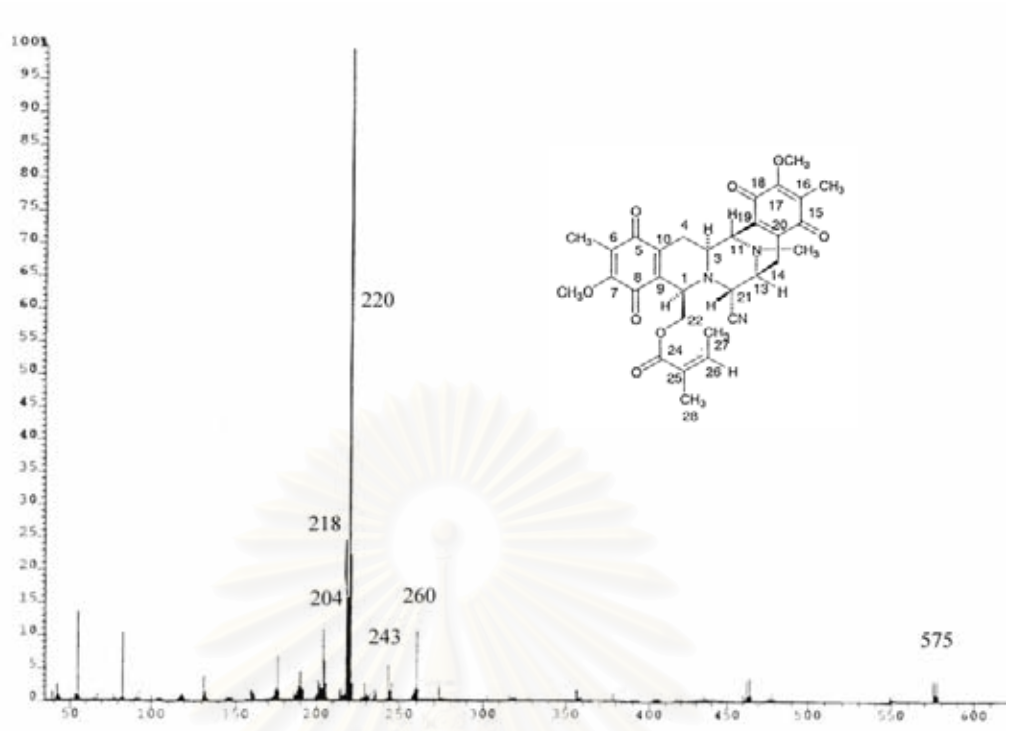

Figure 19 The EI-mass spectrum of reniramycin M

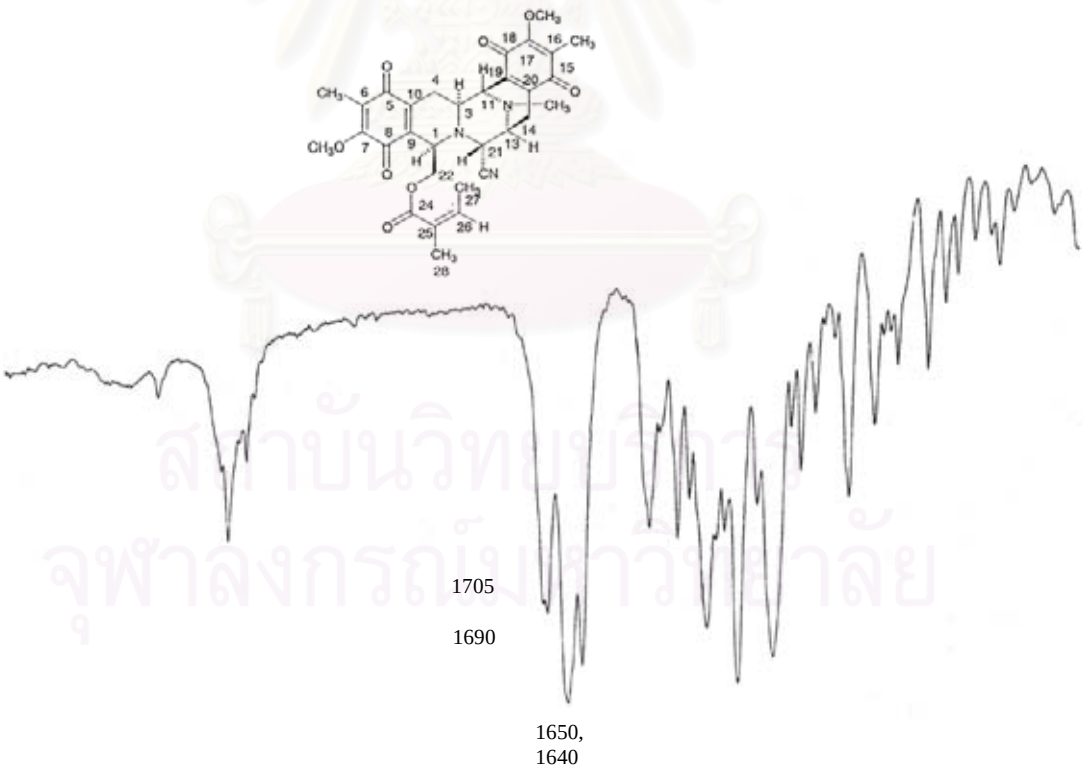

Figure 20 The IR spectrum of renieramycin M (KBr)

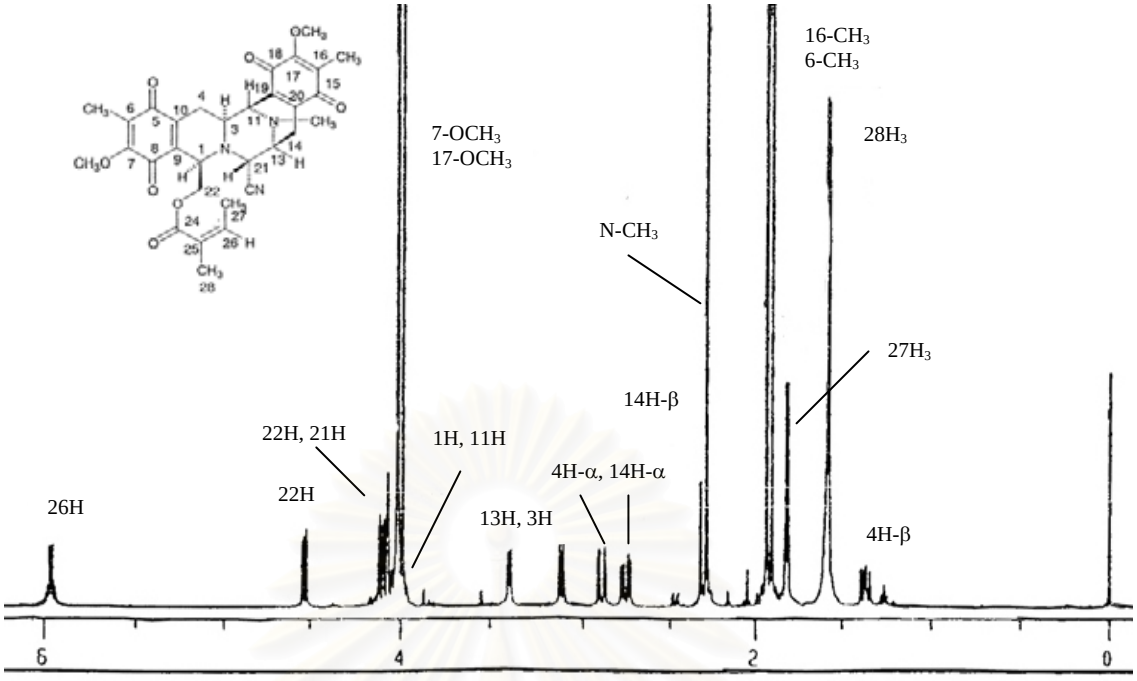

Figure 21 The 500MHz ^{1}H-NMR spectrum of renieramycin M in $CDCl_3$

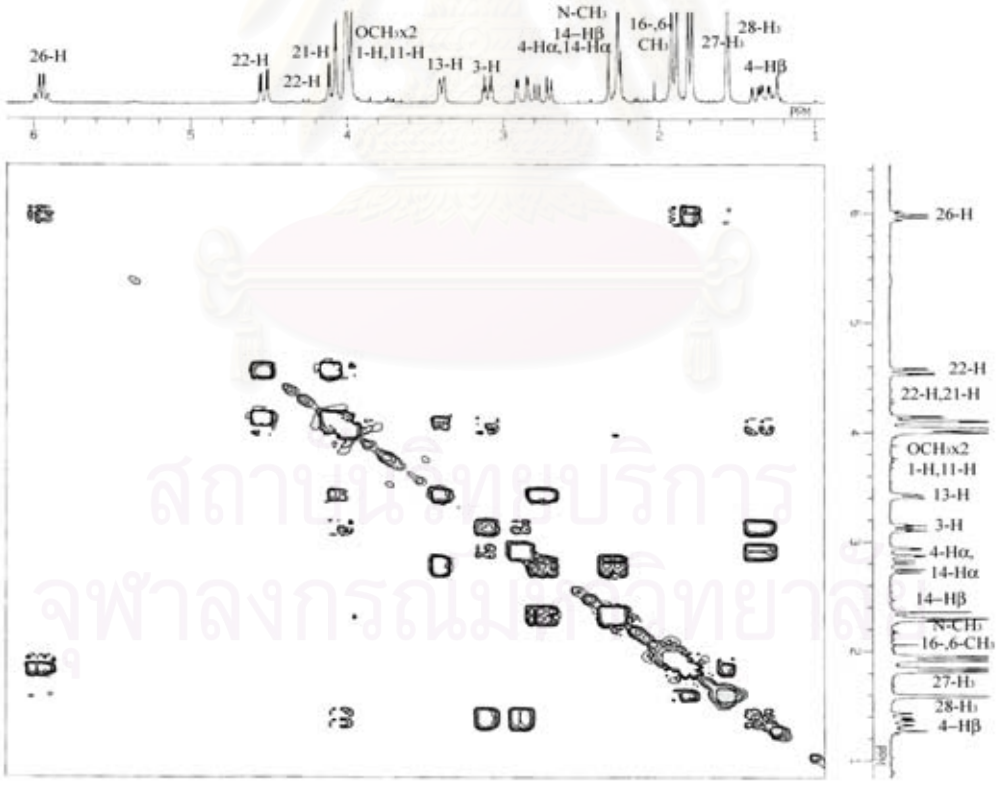

Figure 22 The 500 MHz ^{1}H,^{1}H-COSY spectrum of renieramycin M in $CDCl_3$

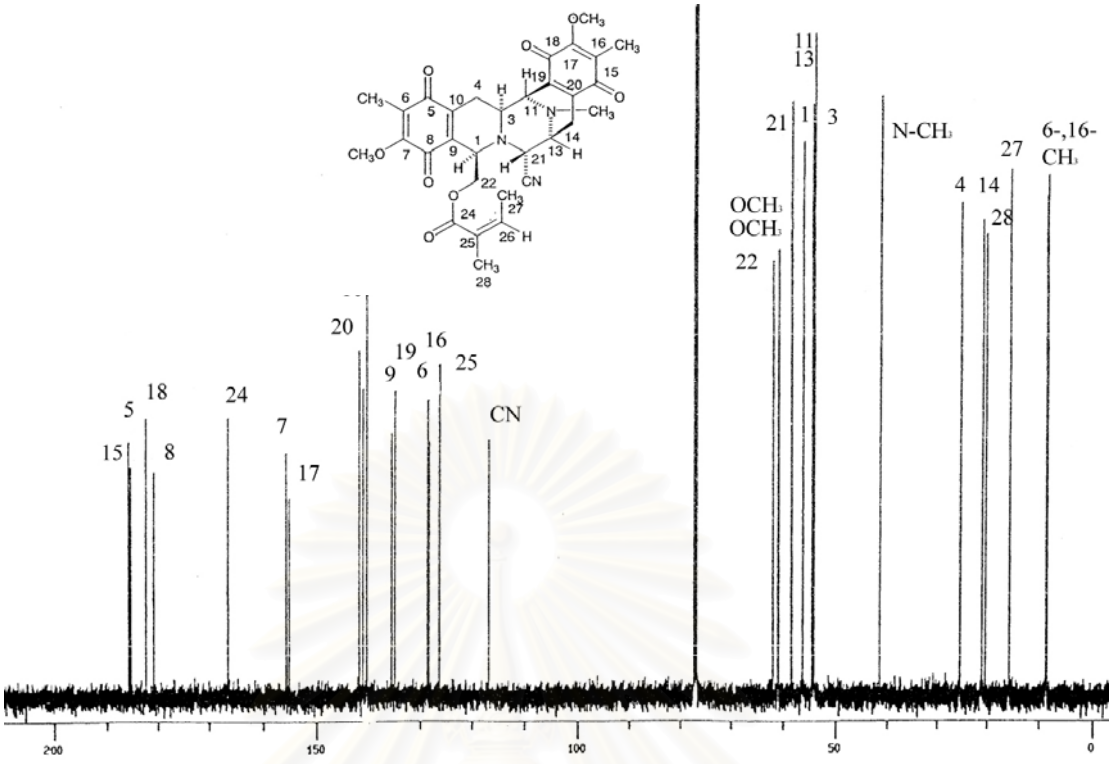

Figure 23 The 125 MHz ^{13}C-NMR spectrum of renieramycin M in $CDCl_3$

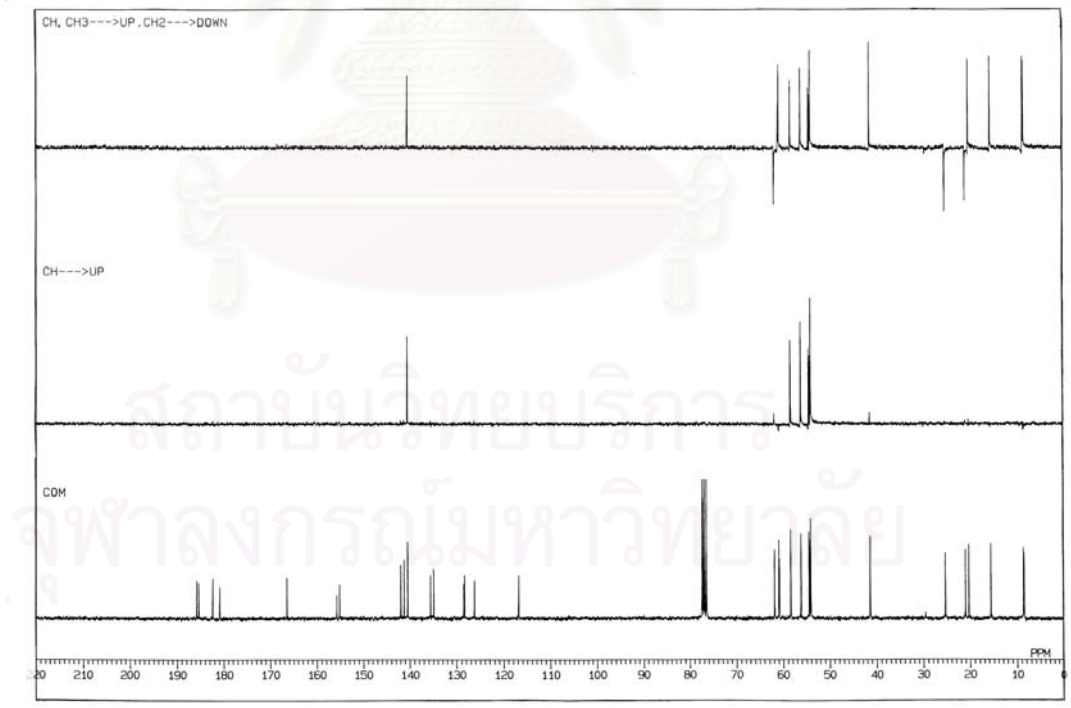

Figure 24 The 125 MHz DEPT spectrum of renieramycin M in $CDCl_3$

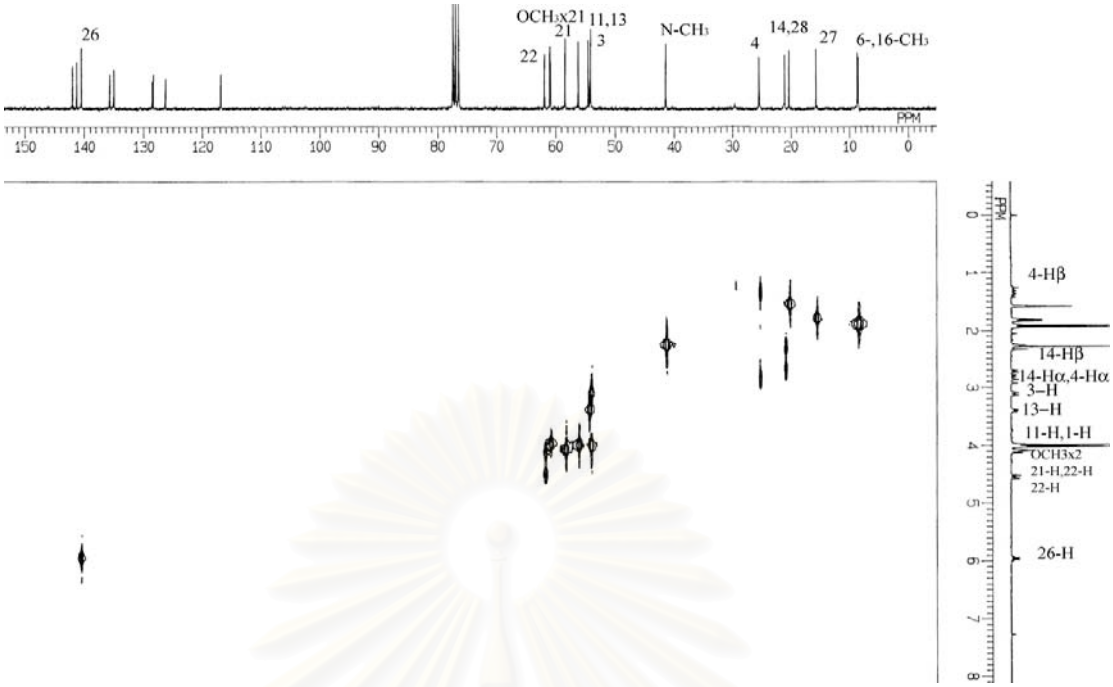

Figure 25 The 500 MHz HMQC spectrum of renieramycin M in $CDCl_3$

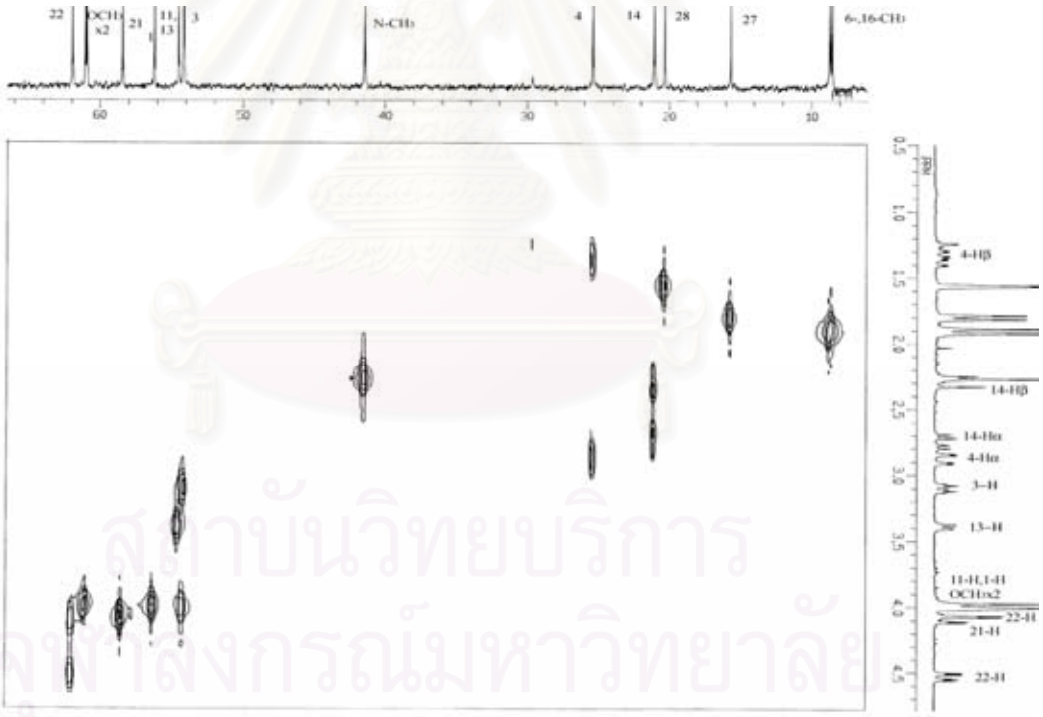

Figure 26 The 500 MHz HMQC spectrum of renieramycin M in $CDCl_3$ (expanded from δ_H 0.50-4.70ppm and δ_C 8.00-66.00 ppm)

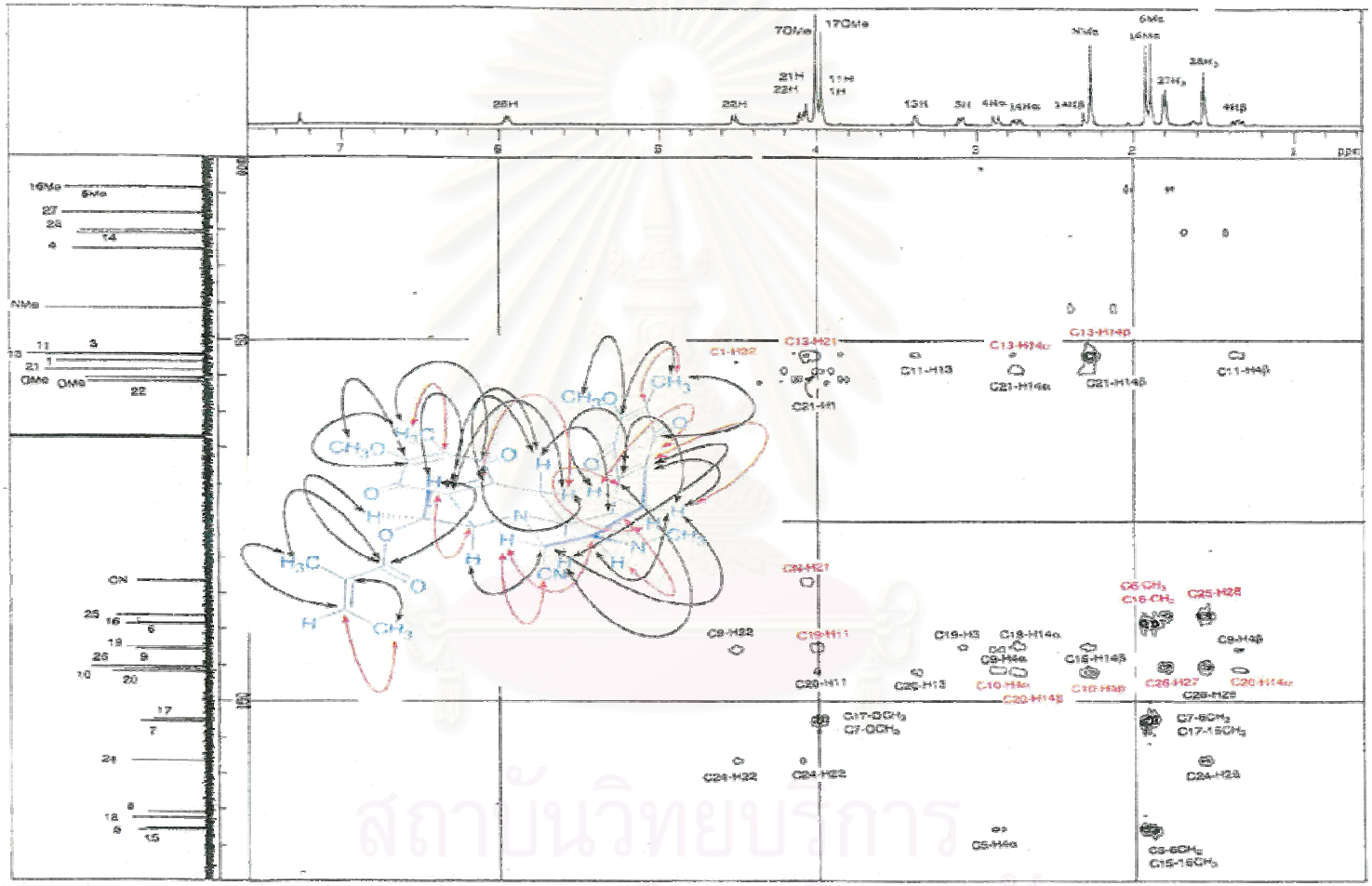

Figure 27 The 500 MHz HMBC spectrum of renieramycin M in $CDCl_3$

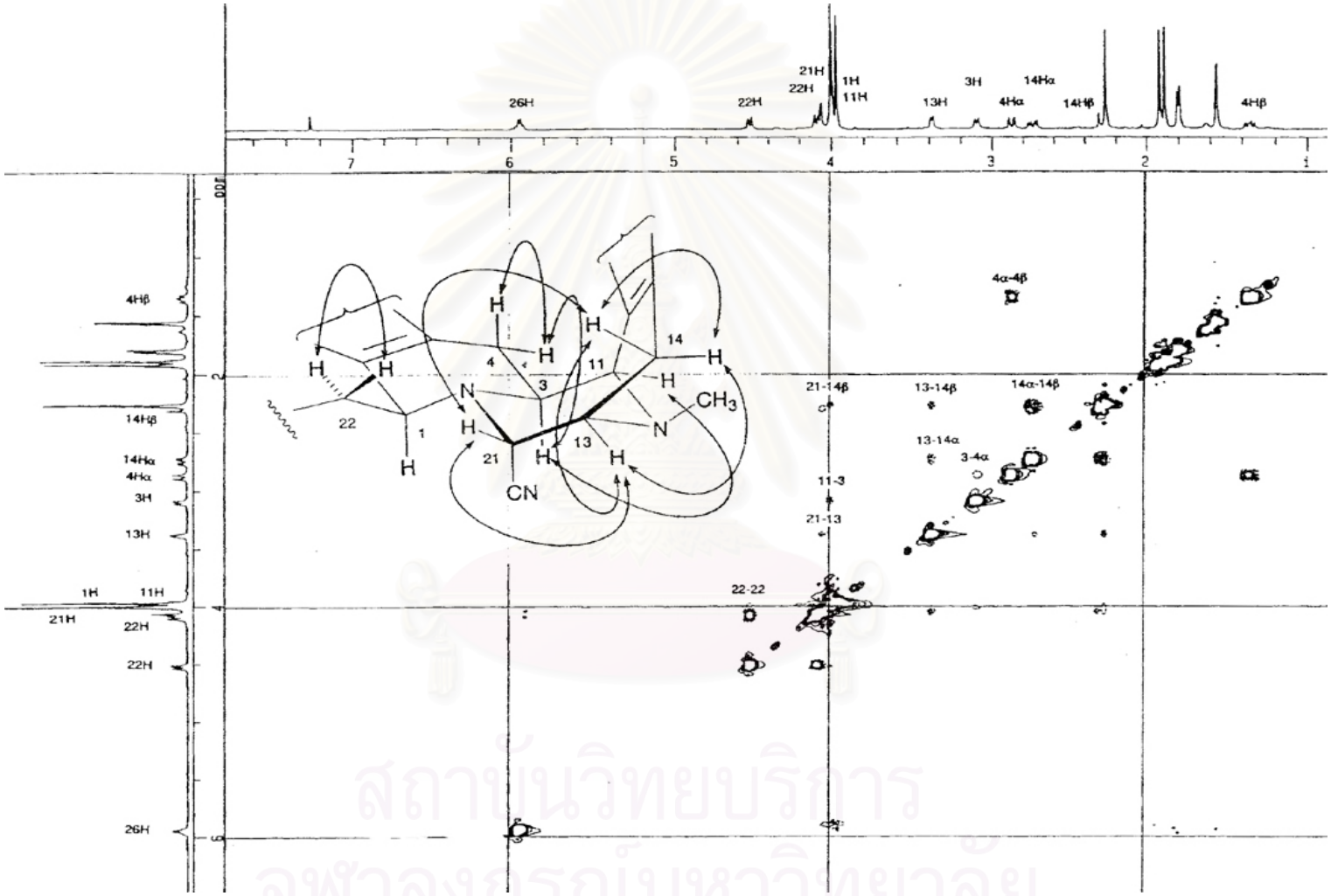

Figure 28 The 500 MHz NOESY spectrum of renieramycin M in $CDCl_3$

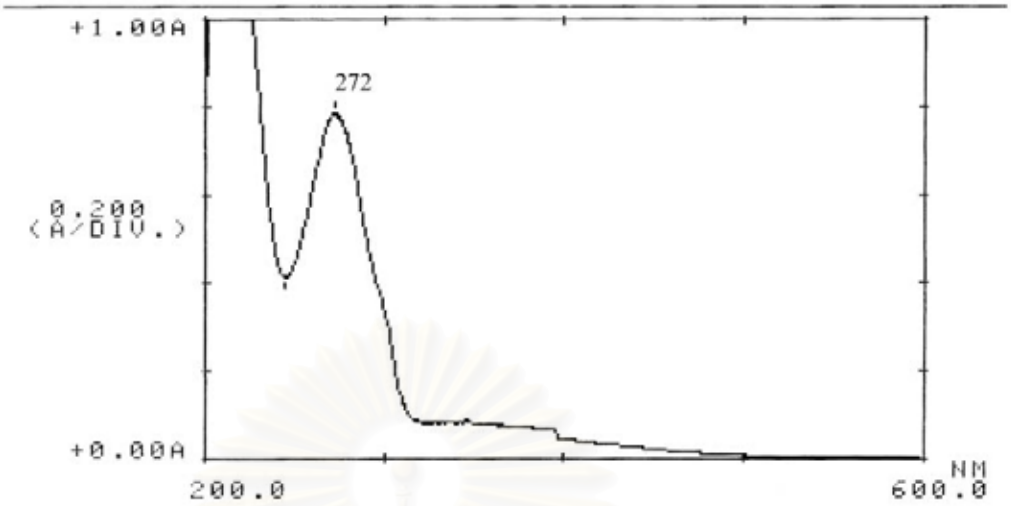

Figure 29 The UV spectrum of renieramycin N (c=0.035 mg/ml) in methanol

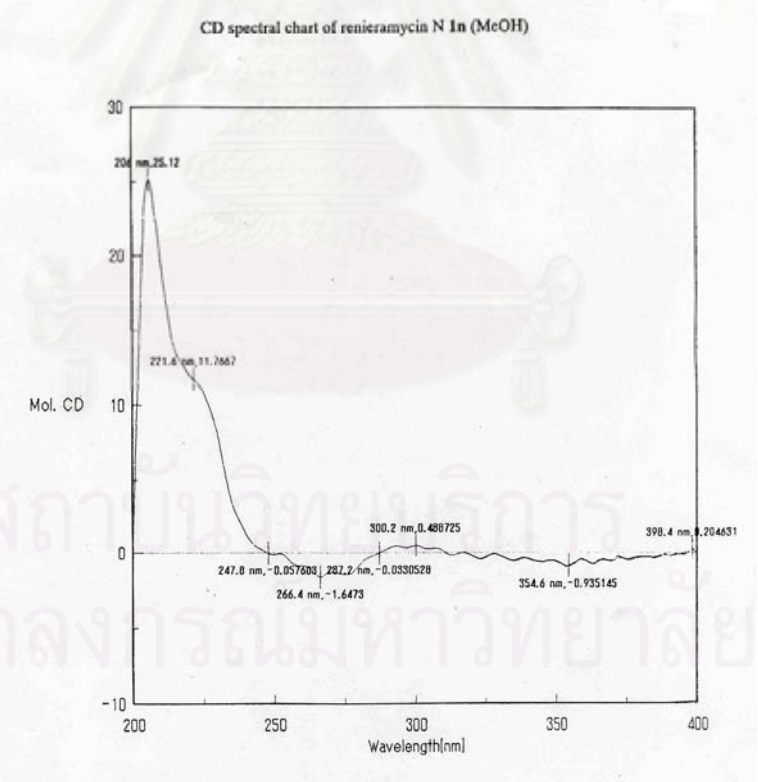

Figure 30 The circular dichroism spectrum of renieramycin N in methanol

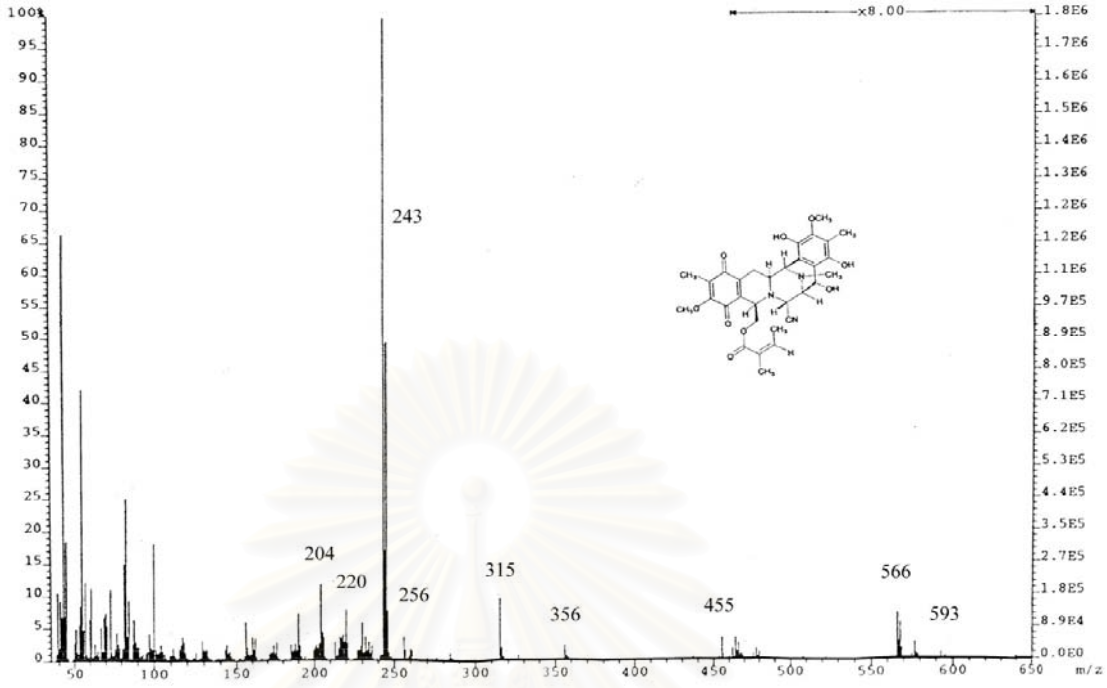

Figure 31 The EI-mass spectrum of reniramycin N

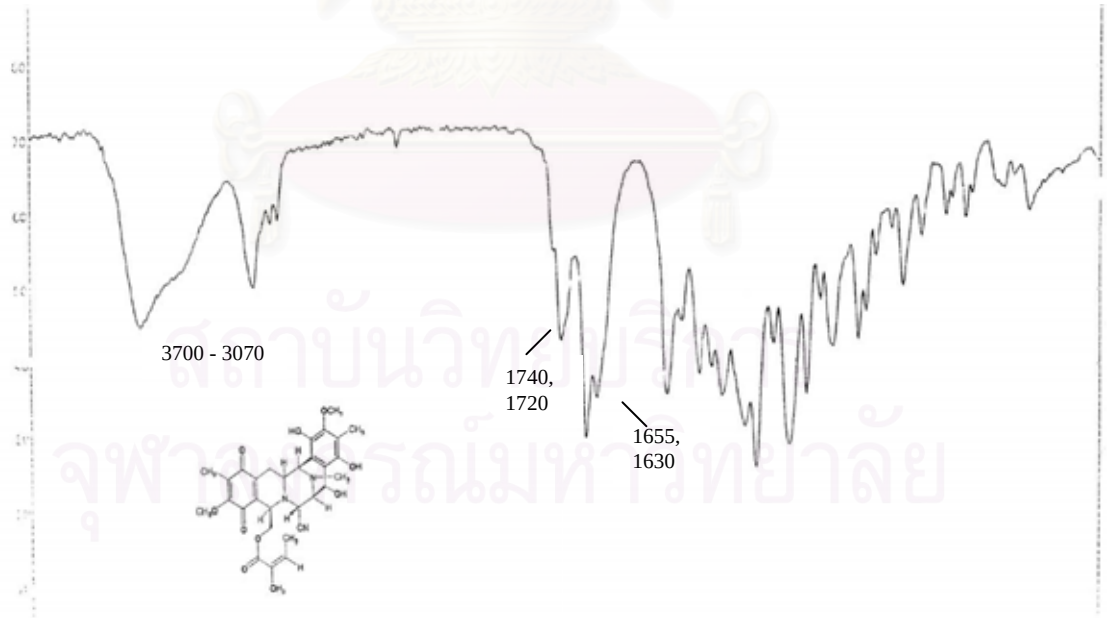

Figure 32 The IR spectrum of renieramycin N (KBr)

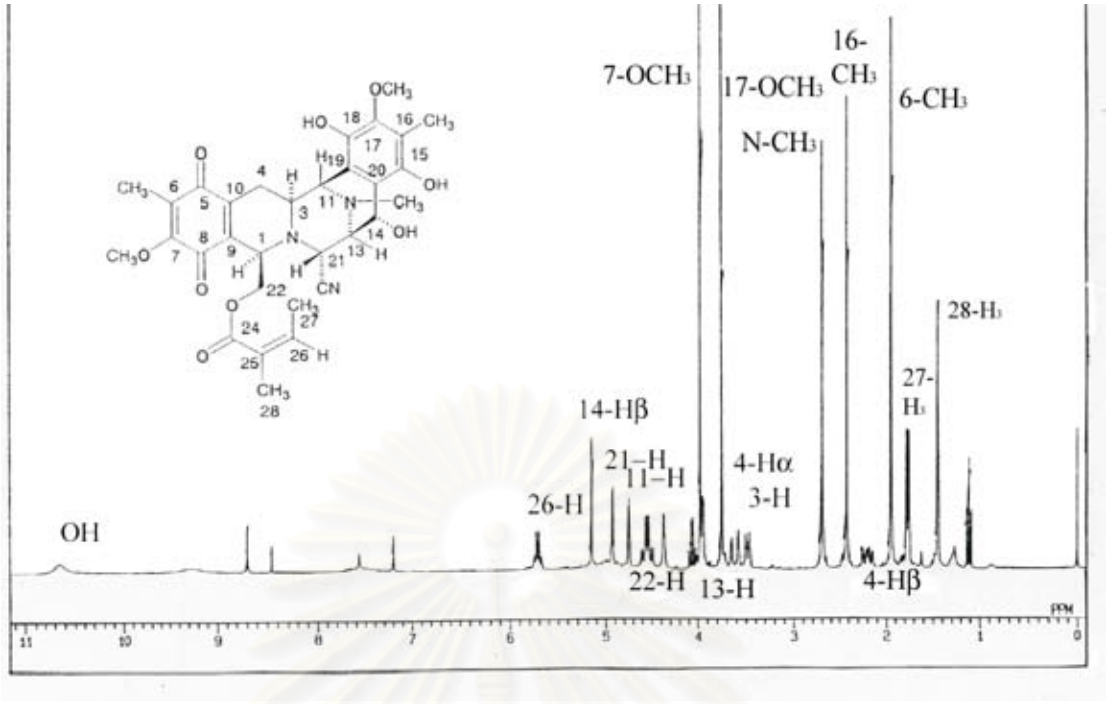

Figure 33 The 500 MHz ^{1}H-NMR spectrum of renieramycin N in pyridine-d_5

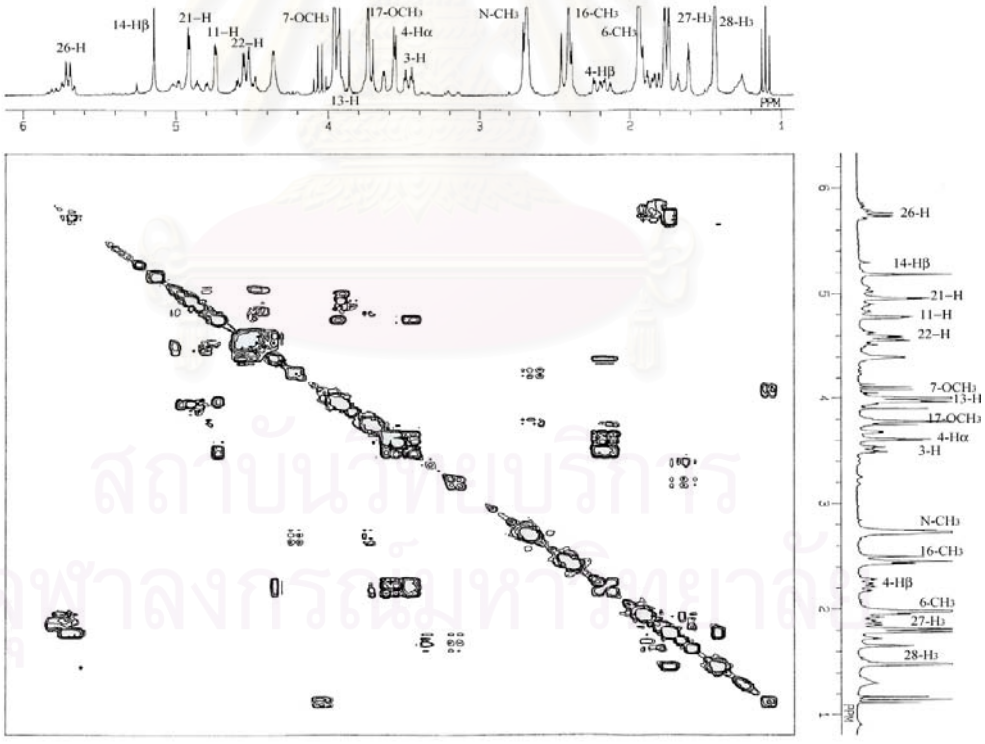

Figure 34 The 500 MHz ^{1}H,^{1}H-COSY spectrum of renieramycin N in pyridine-d_5

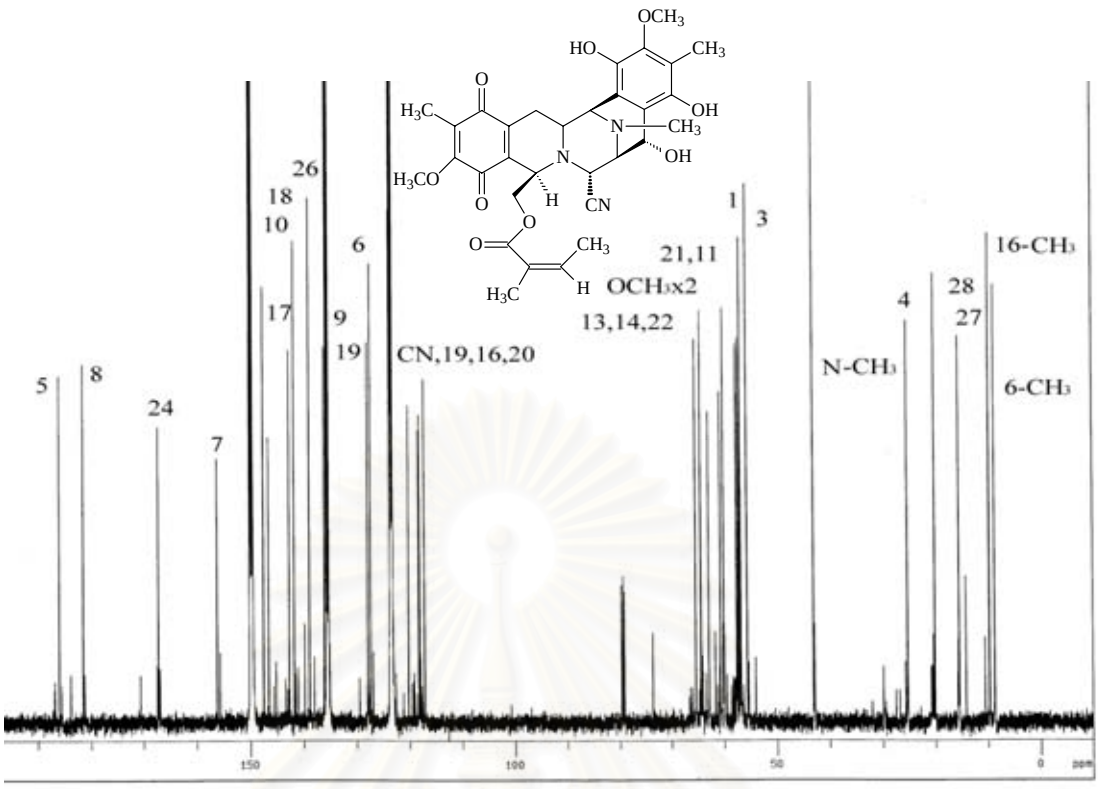

Figure 35 The 125 MHz ^{13}C-NMR spectrum of renieramycin N in pyridine-d_5

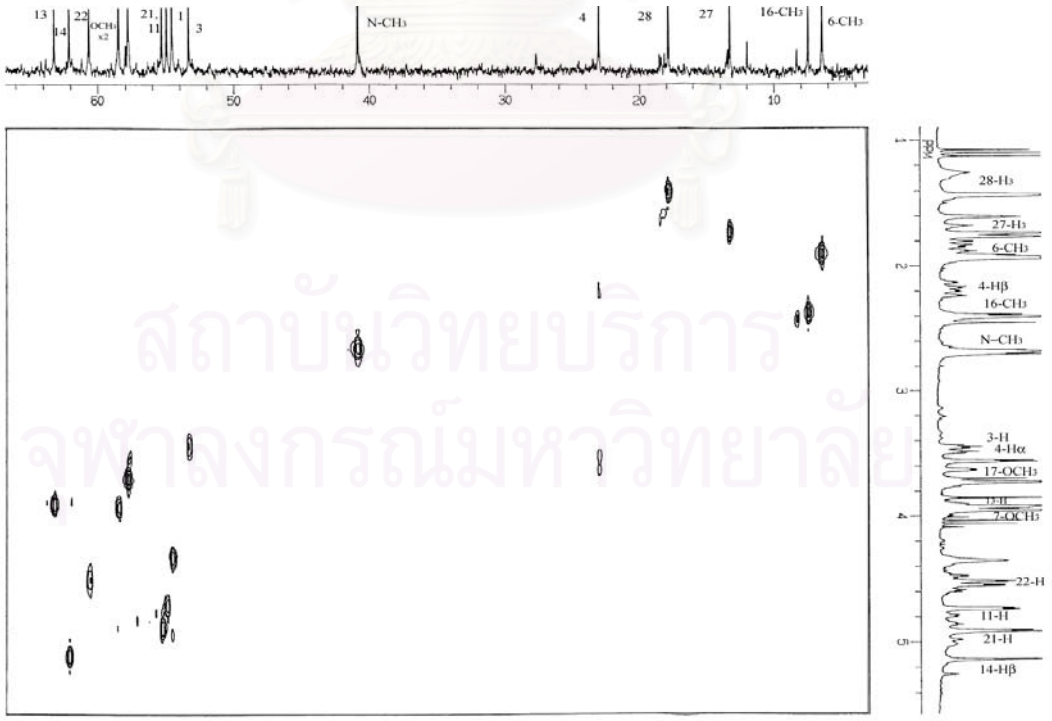

Figure 36 The 500 MHz HMQC spectrum of renieramycin N in pyridine-d_5

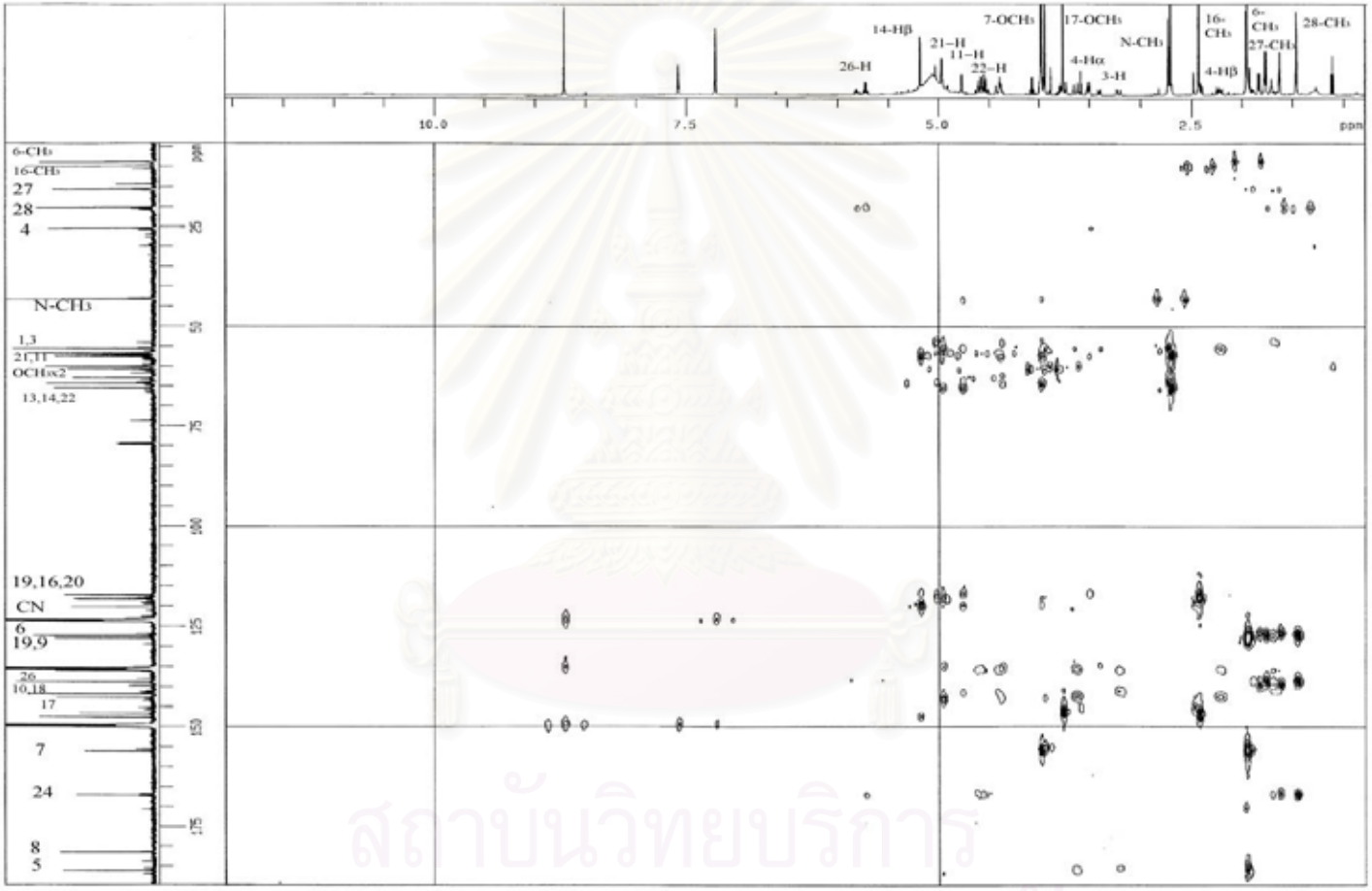

Figure 37 The 500 MHz HMBC spectrum of renieramycin N in pyridine-d_5

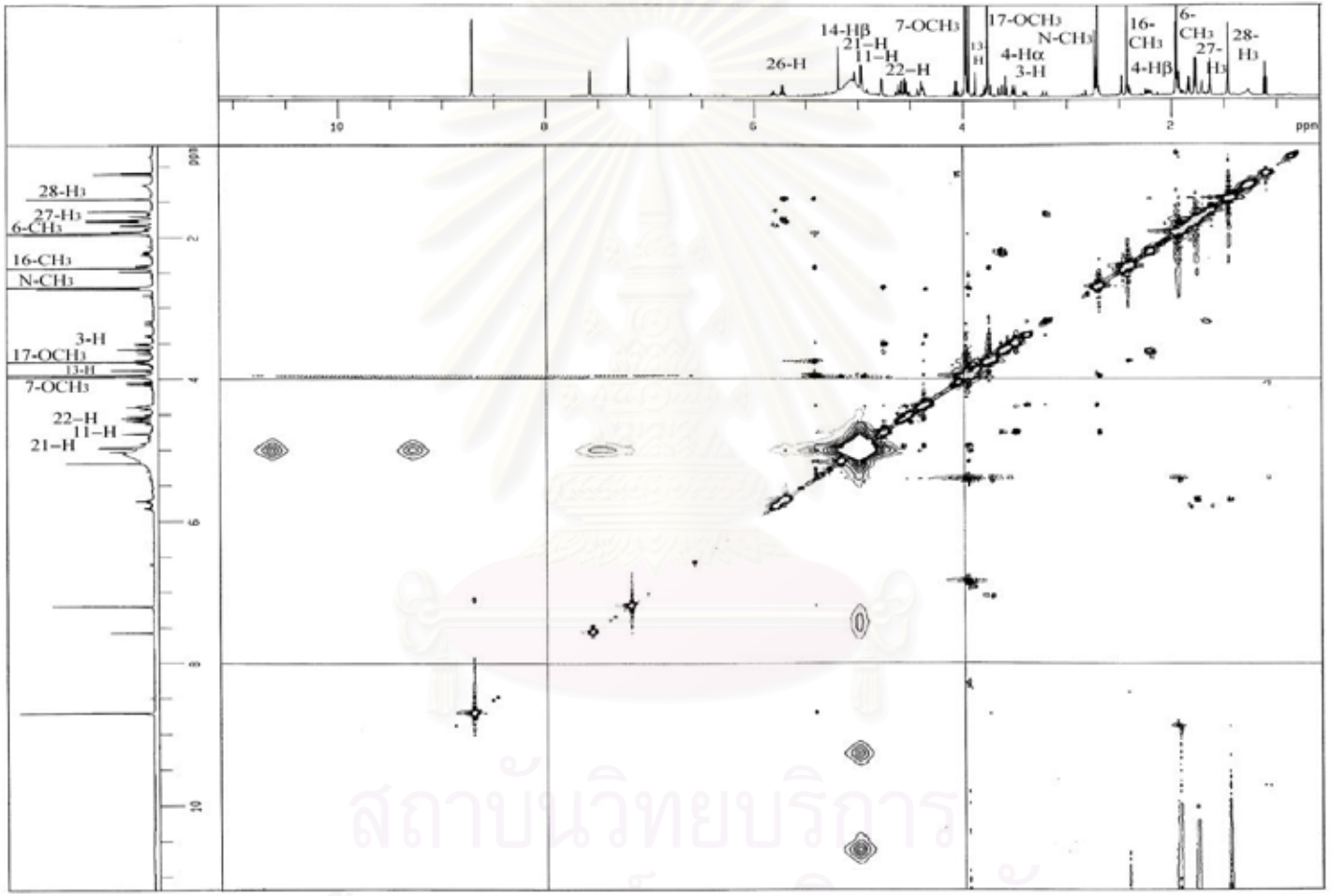

Figure 38 The 500 MHz NOESY spectrum of renieramycin N in pyridine-d_5

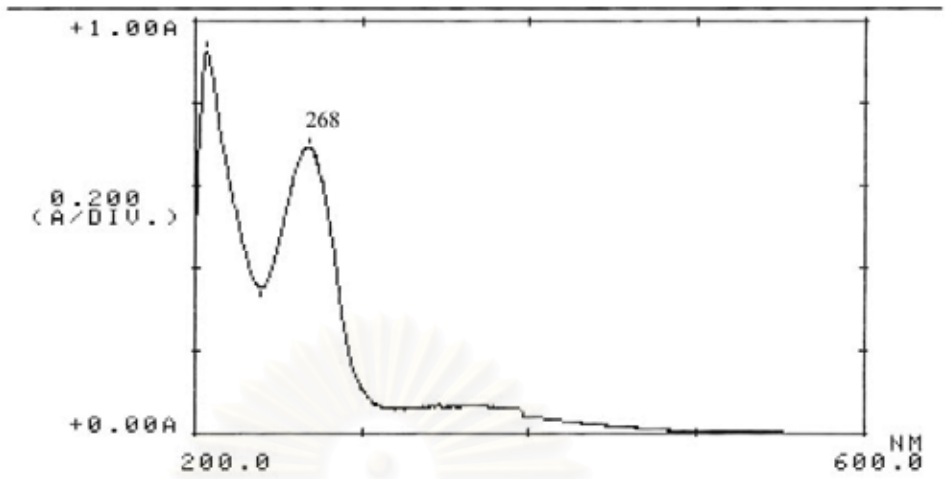

Figure 39 The UV spectrum of renieramycin O in methanol

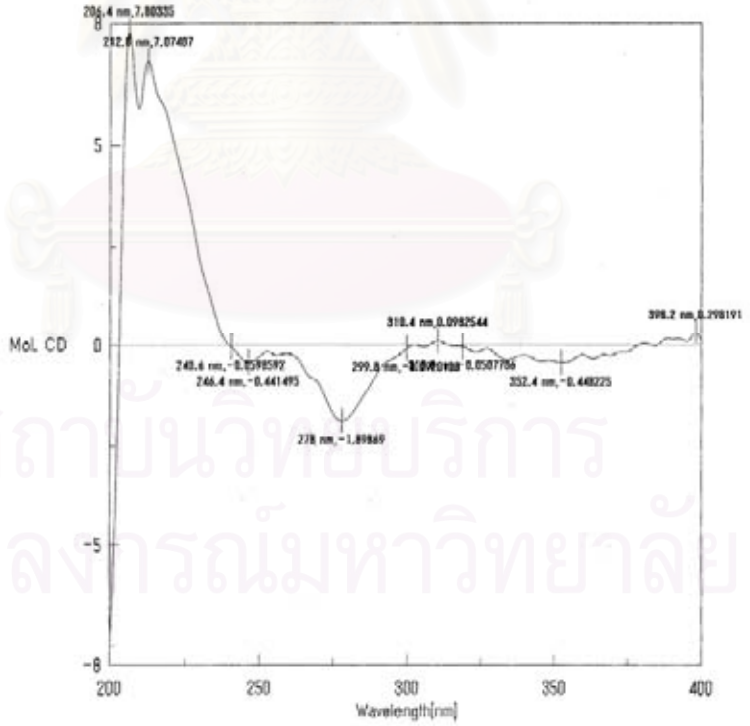

Figure 40 The circular dichroism spectrum of renieramycin O in methanol

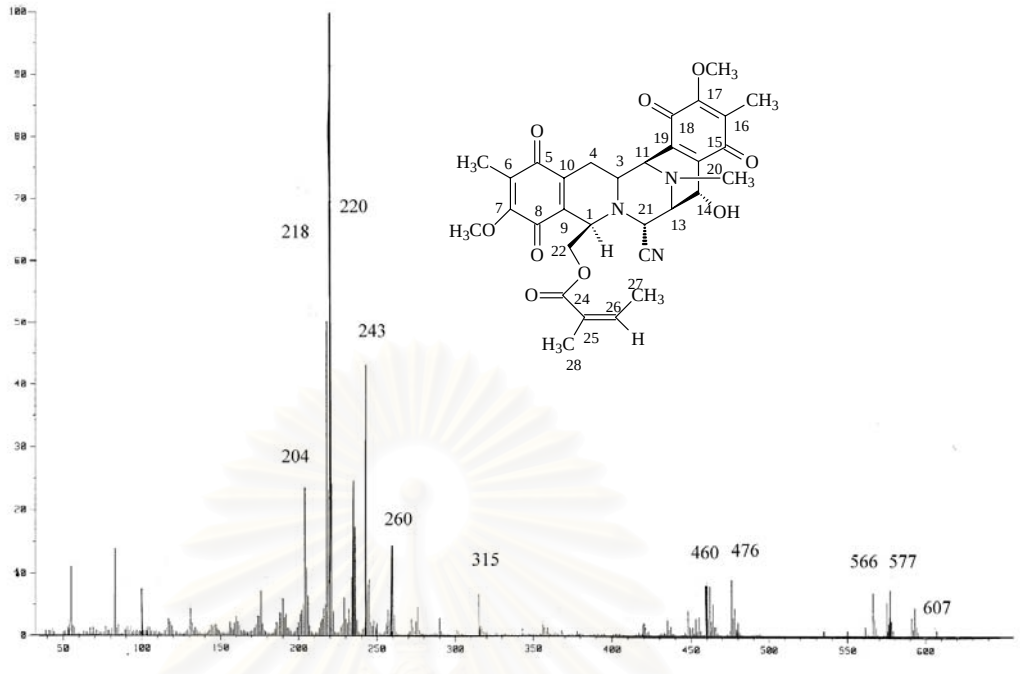

Figure 41 The EI-mass spectrum of reniramycin O

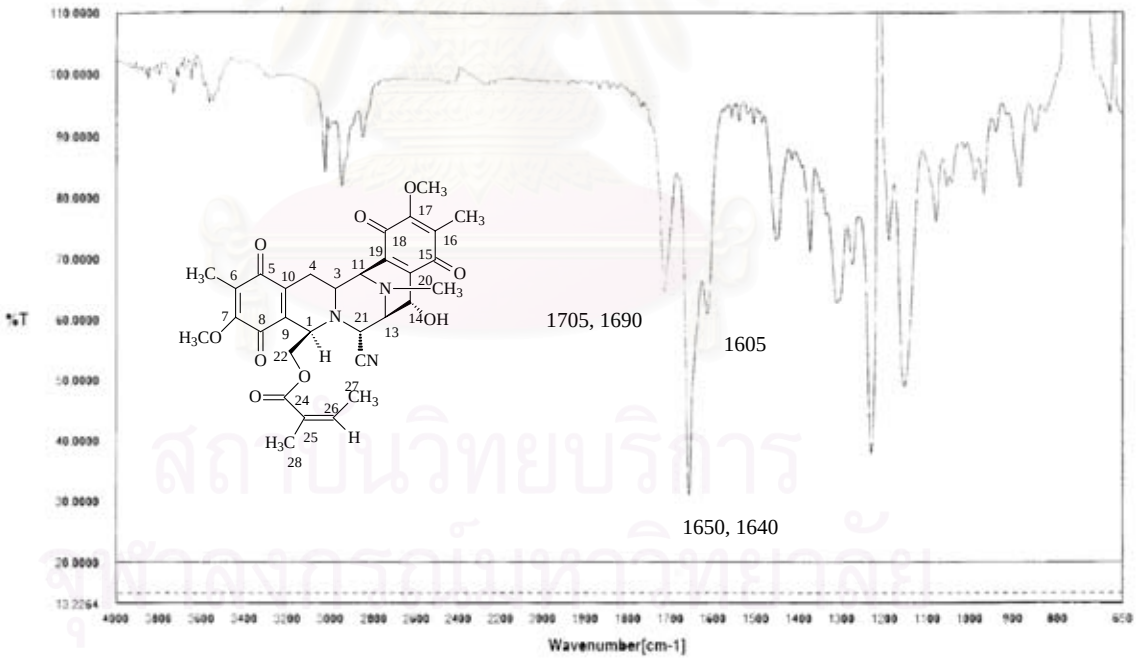

Figure 42 The IR spectrum of renieramycin O in $CHCl_3$

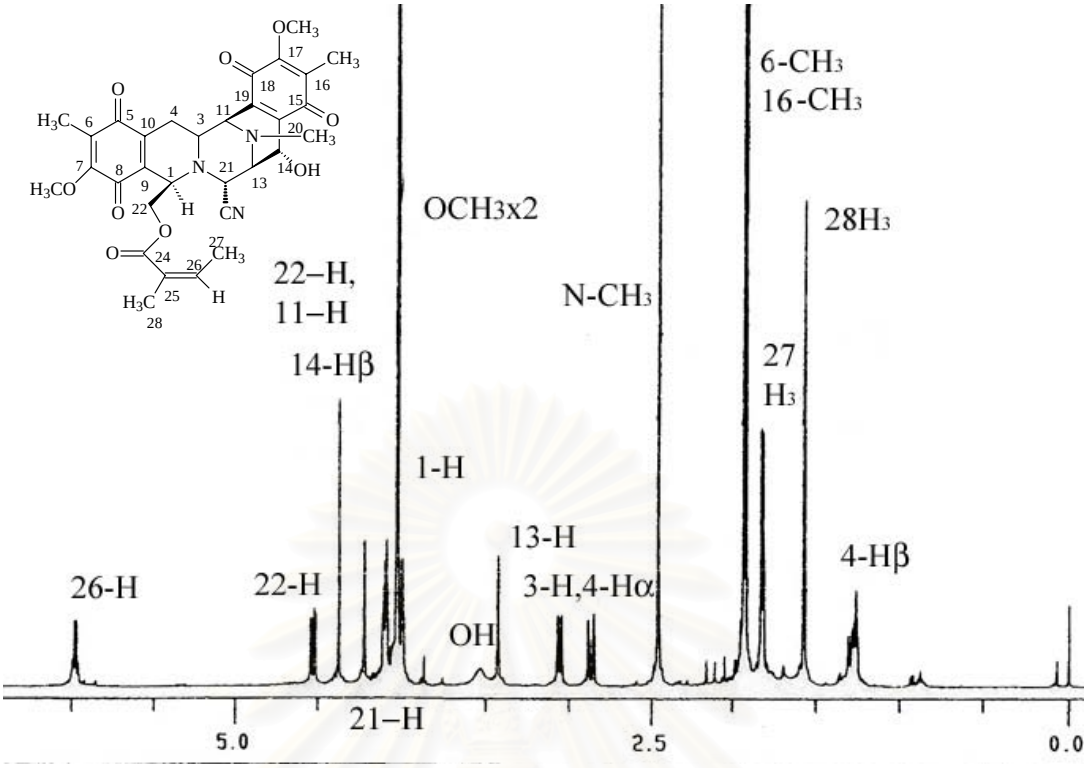

Figure 43 The 270 MHz ^{1}H-NMR spectrum of renieramycin O in $CDCl_3$

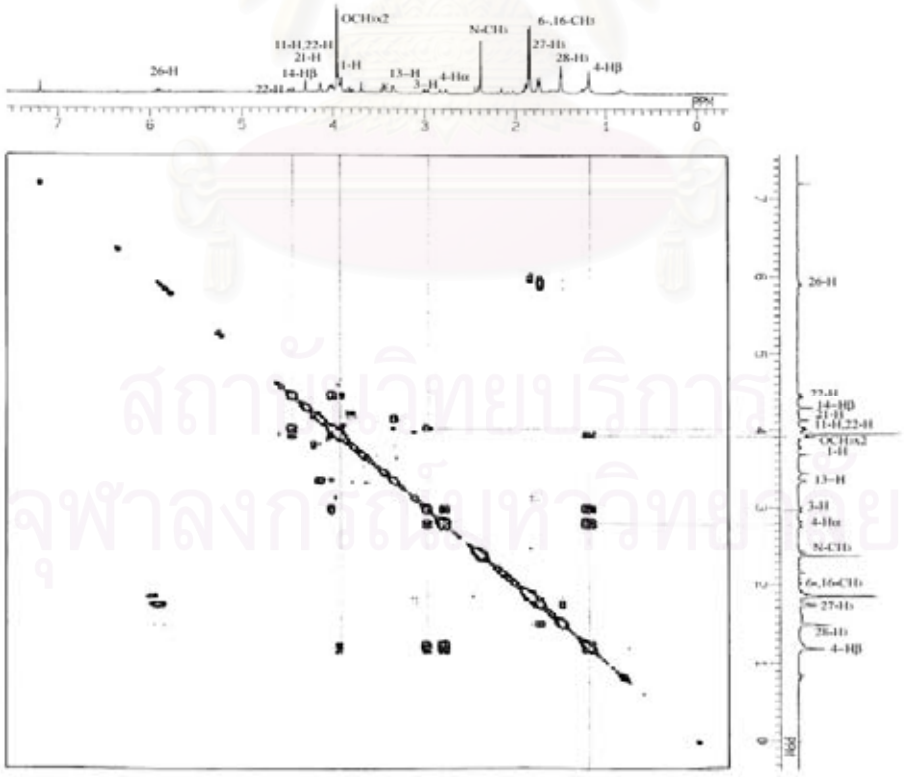

Figure 44 The 270 MHz ^{1}H,^{1}H-COSY spectrum of renieramycin O in $CDCl_3$

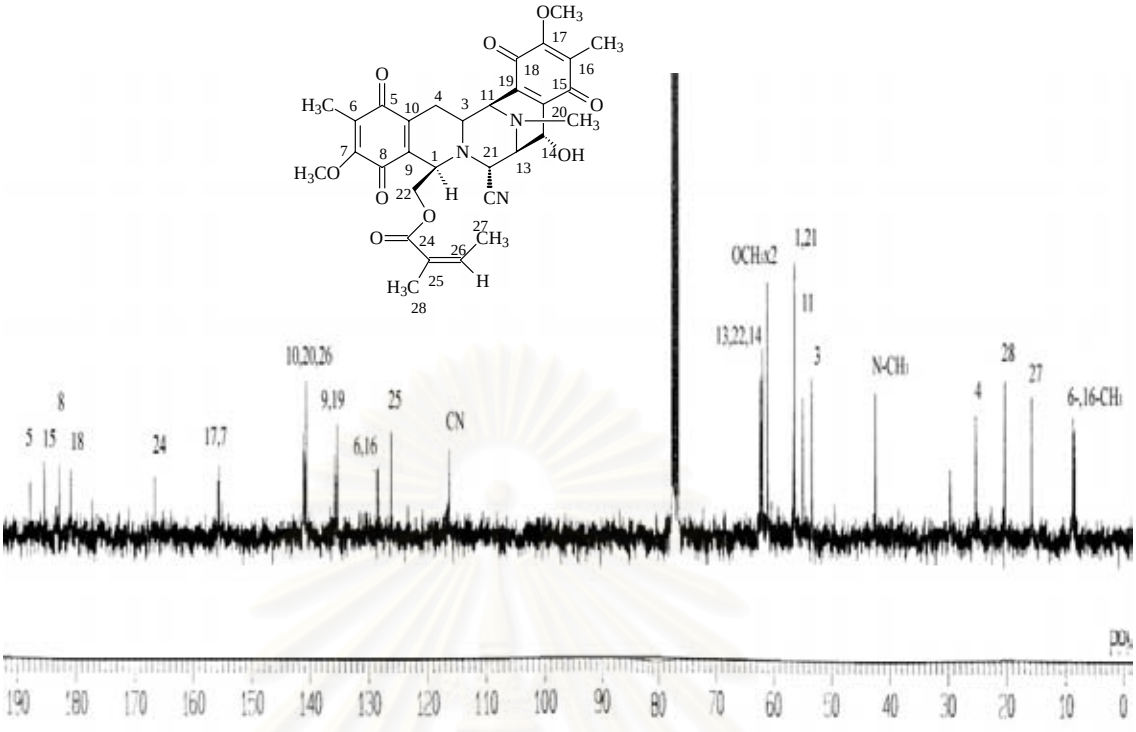

Figure 45 The 67.5 MHz ^{13}C-NMR spectrum of renieramycin O in $CDCl_3$

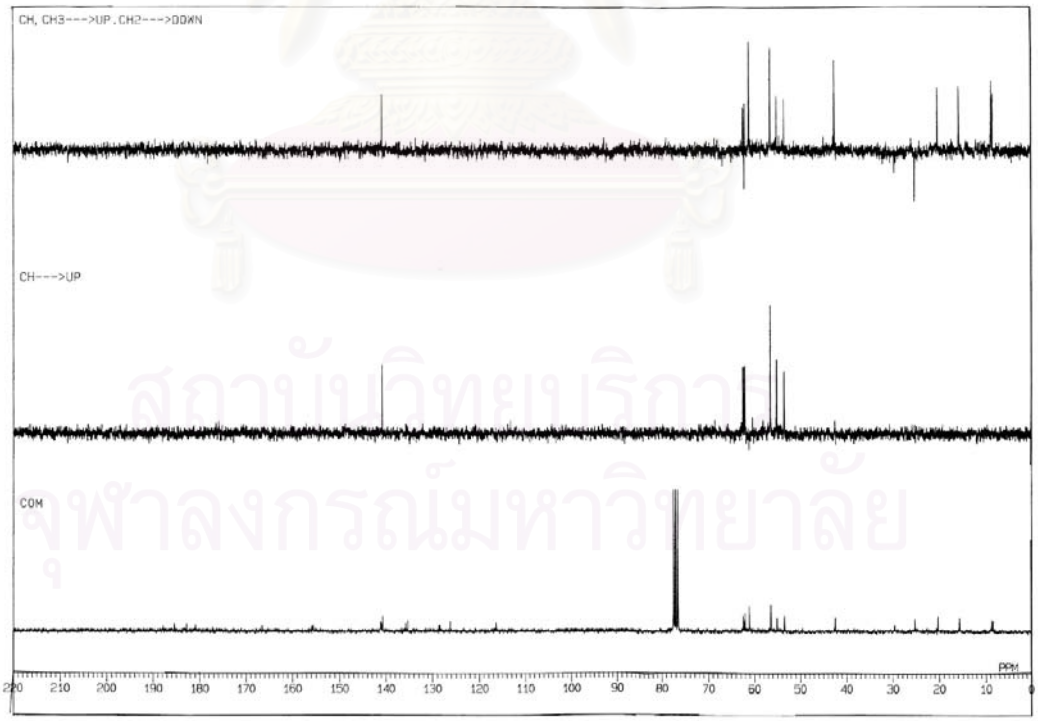

Figure 46 The 67.5 MHz DEPT spectrum of renieramycin O in $CDCl_3$

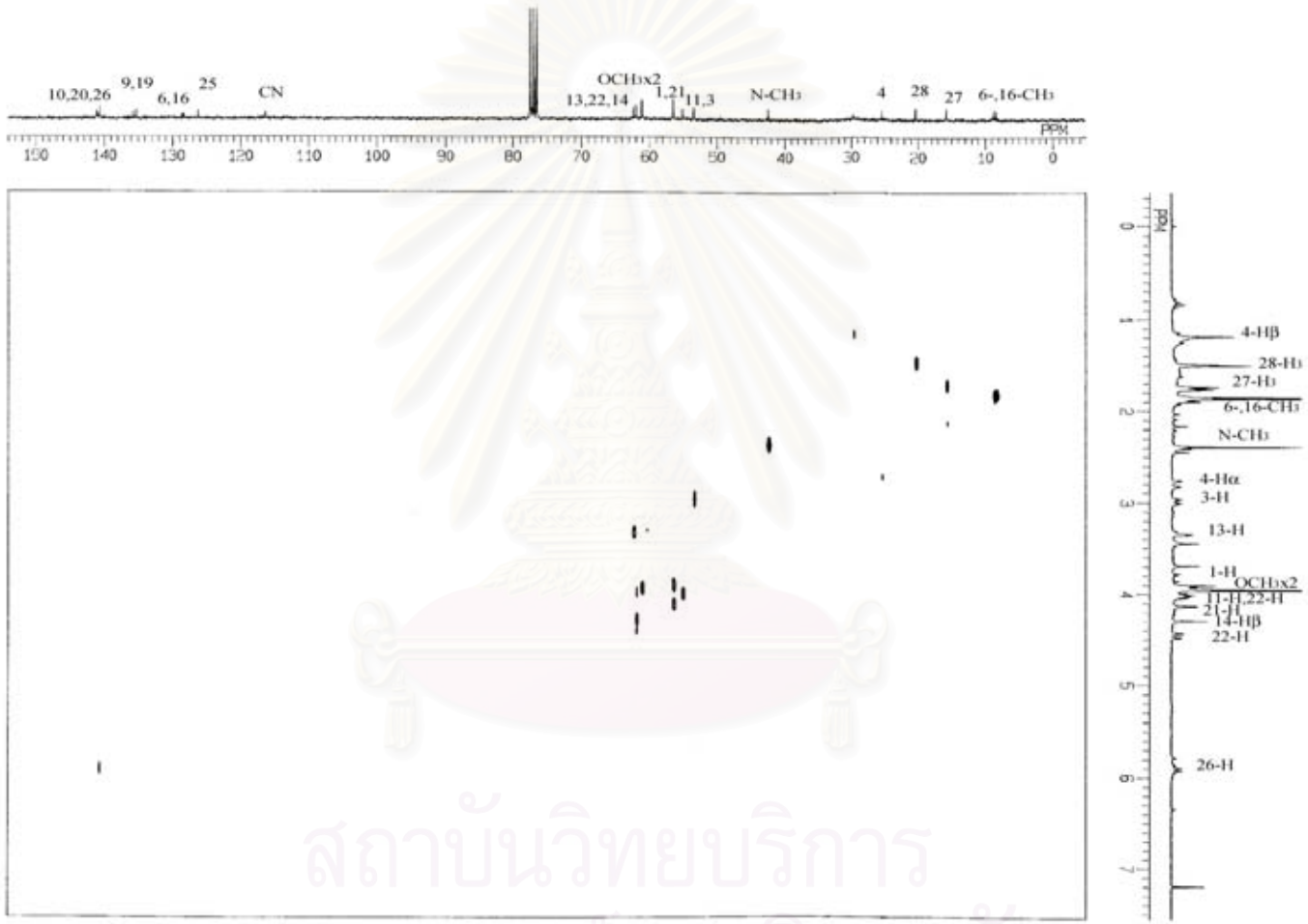

Figure 47 The 270 MHz HMQC spectrum of renieramycin O in $CDCl_3$

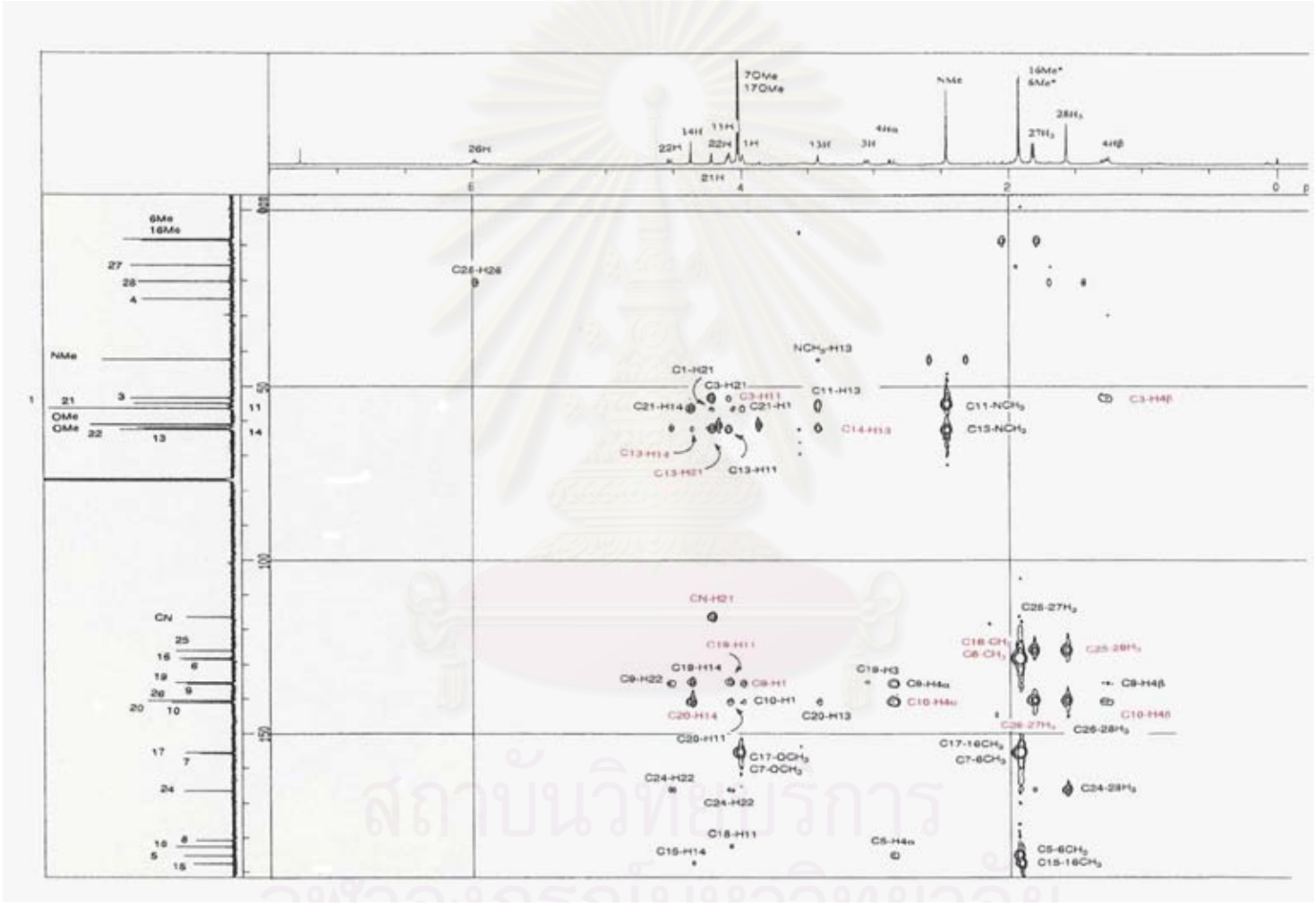

Figure 48 The 500 MHz HMBC spectrum of renieramycin O in $CDCl_3$

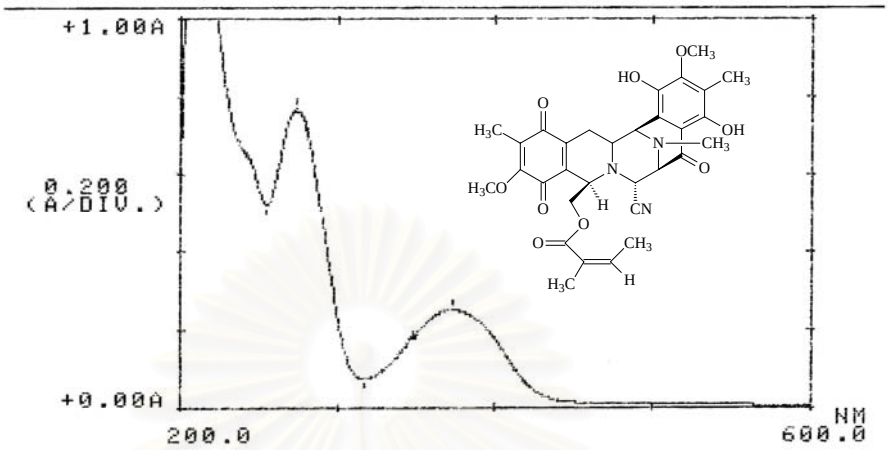

Figure 49 The UV spectrum of renieramycin Q in methanol

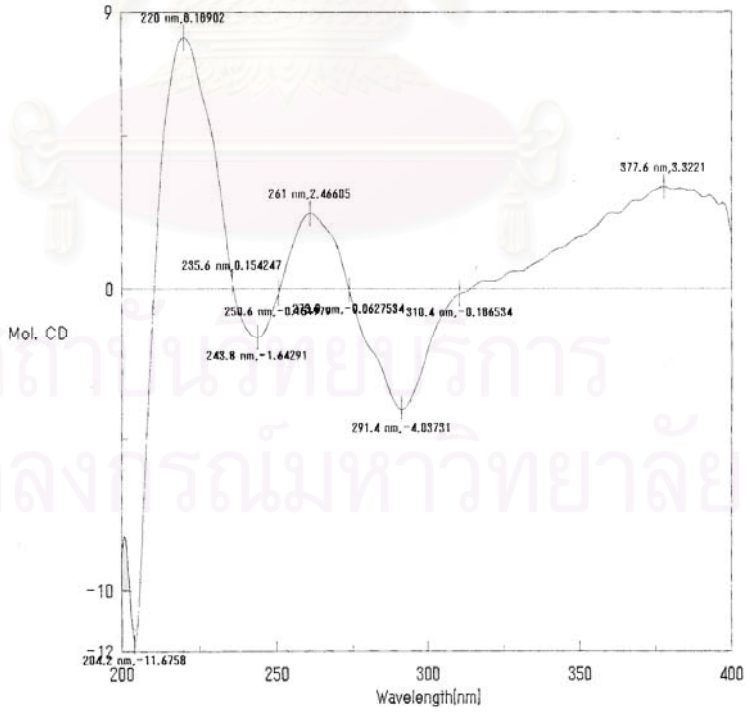

Figure 50 The circular dichroism spectrum of renieramycin Q in methanol

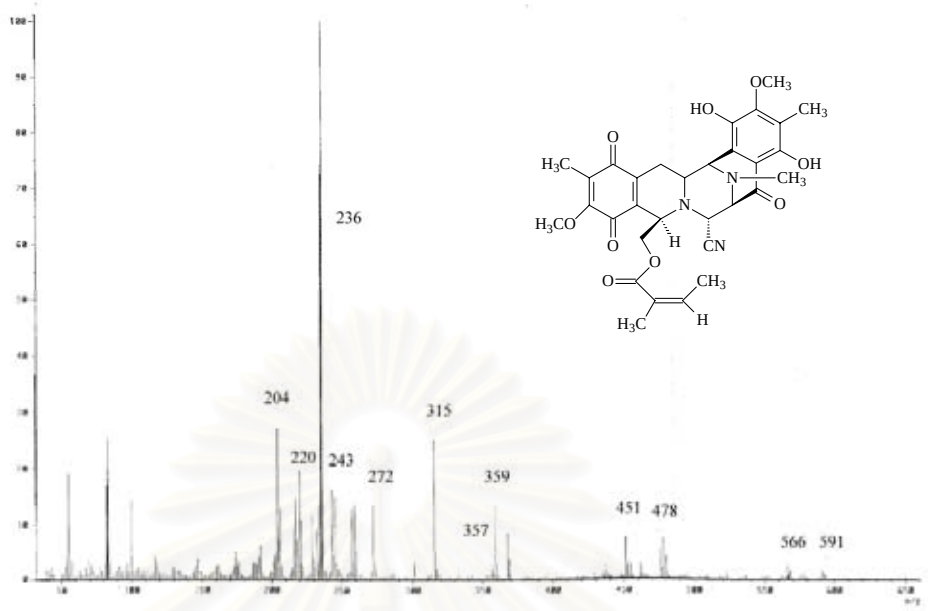

Figure 51 The ESI-Mass spectrum of reniramycin Q

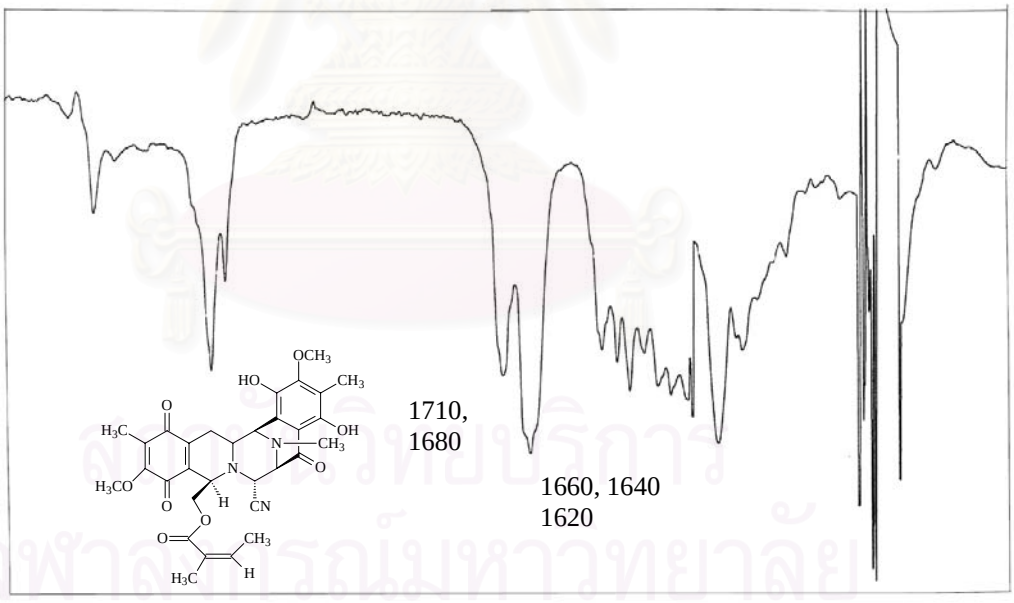

Figure 52 The IR spectrum of renieramycin Q in $CHCl_3$

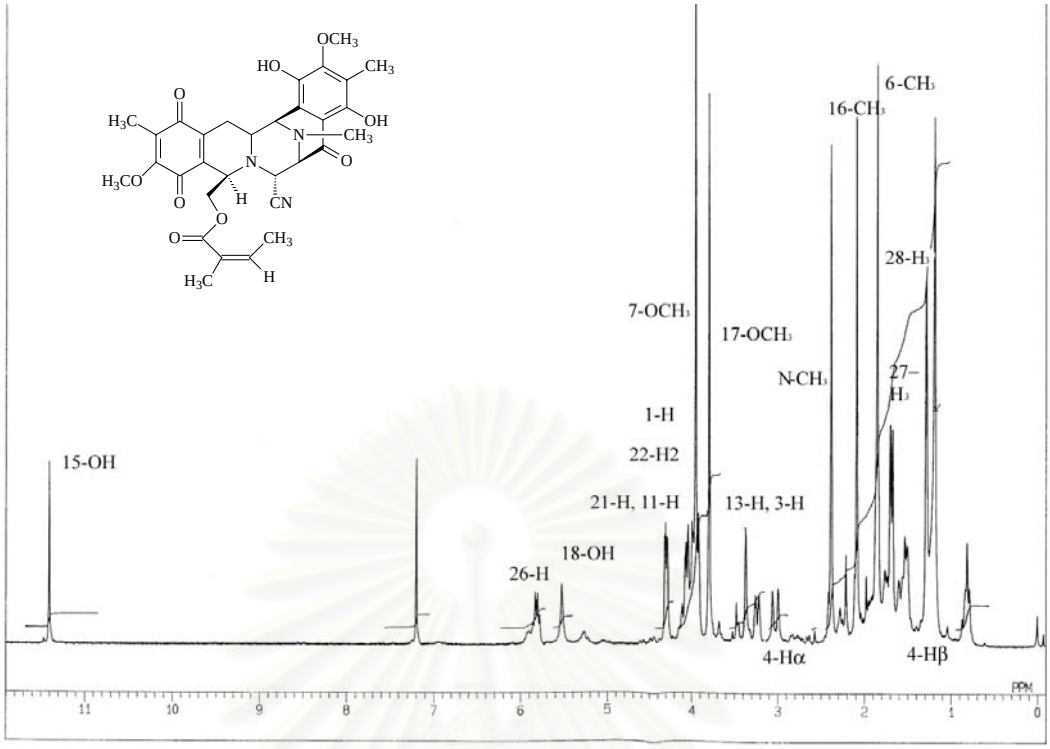

Figure 53 The 500 MHz ^{1}H-NMR spectrum of renieramycin Q in $CDCl_3$

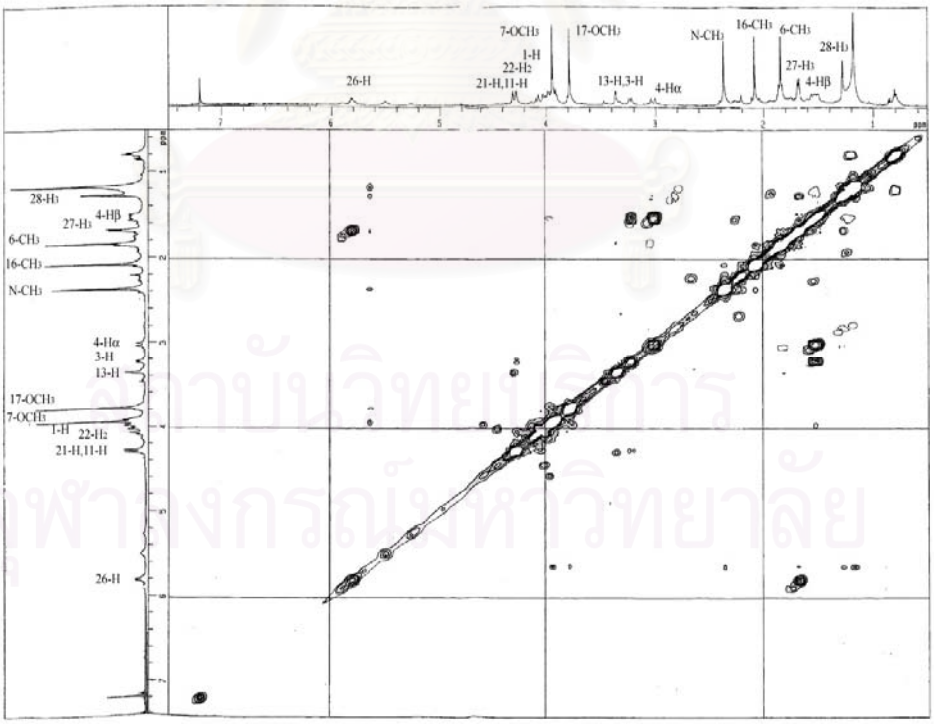

Figure 54 The 500 MHz ^{1}H,^{1}H-COSY spectrum of renieramycin Q in $CDCl_3$

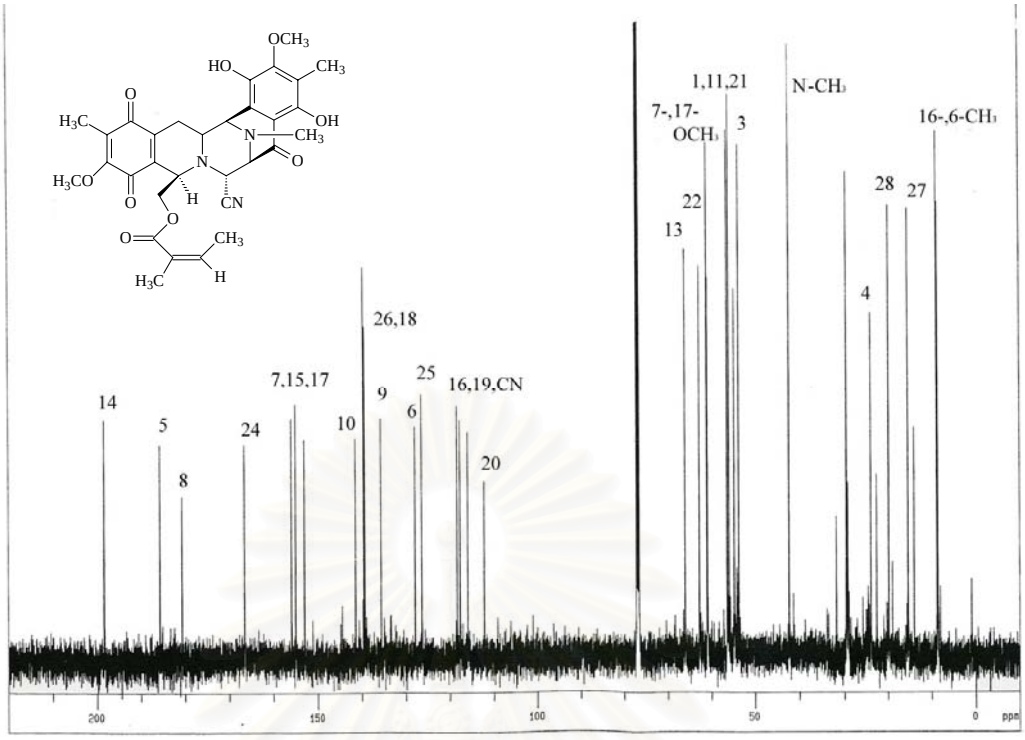

Figure 55 The 125 MHz ^{13}C-NMR spectrum of renieramycin Q in $CDCl_3$

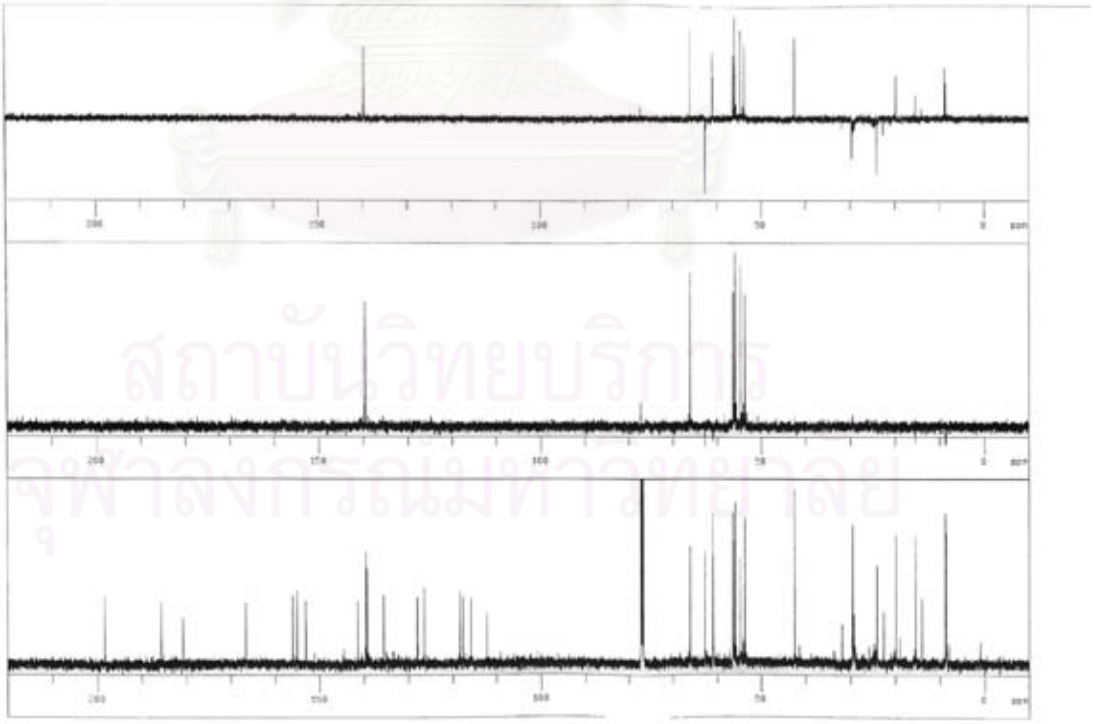

Figure 56 The 125 MHz DEPT spectrum of renieramycin Q in $CDCl_3$

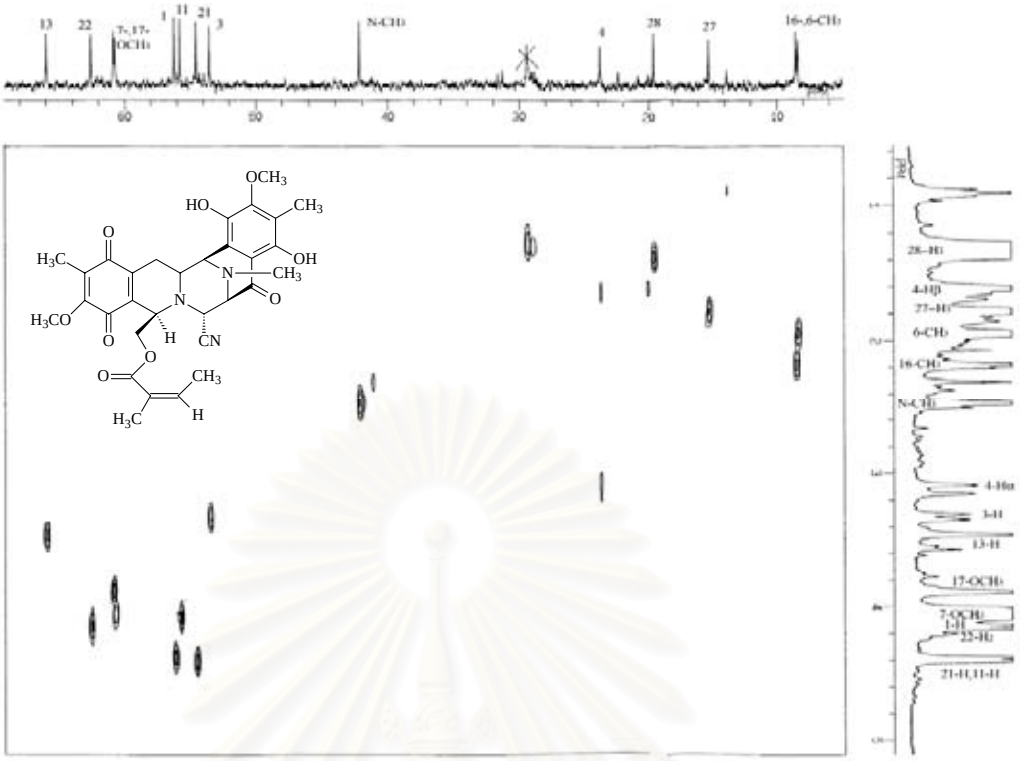

Figure 57 The 500 MHz HMQC spectrum of renieramycin Q in $CDCl_3$ (expanded from δ_H 0.60-5.00 ppm and δ_C 6.00-68.00 ppm)

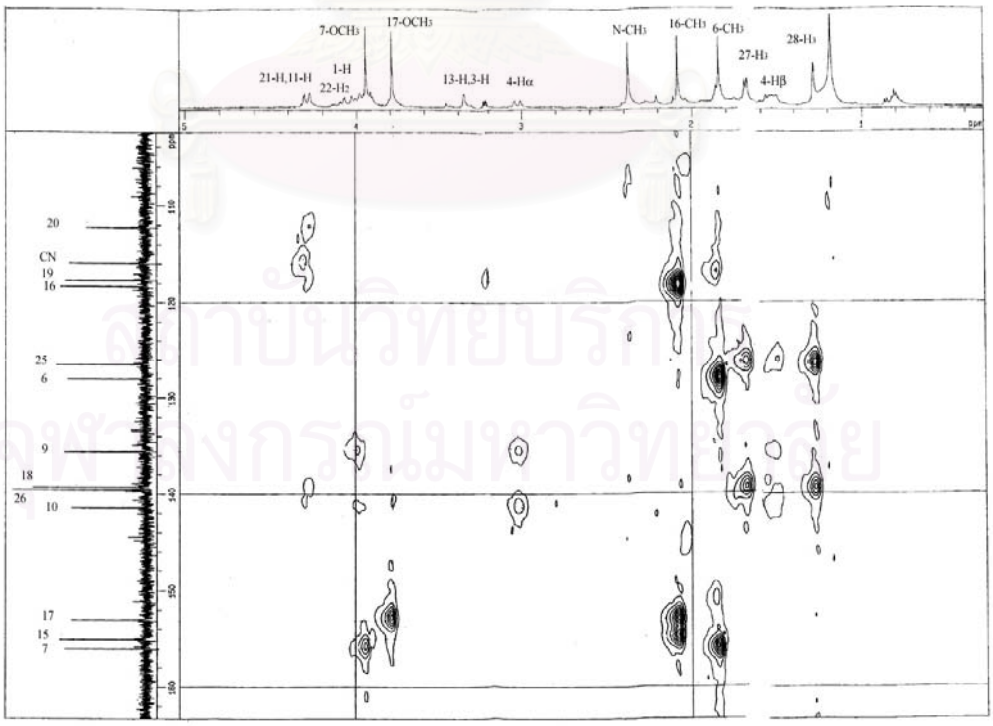

Figure 58 The 500 MHz HMBC spectrum of renieramycin Q in $CDCl_3$

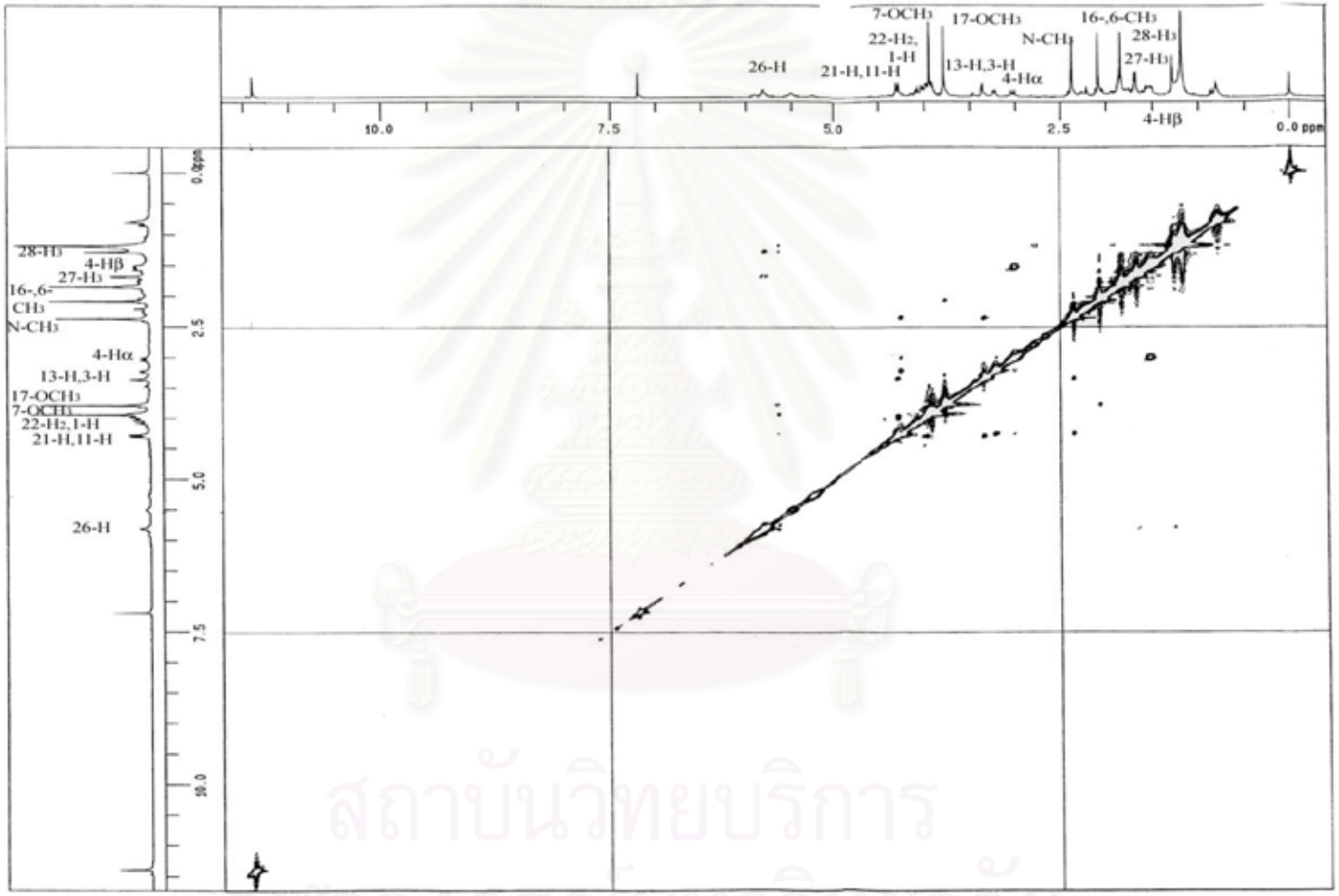

Figure 59 The 500 MHz NOESY spectrum of renieramycin Q in $CDCl_3$

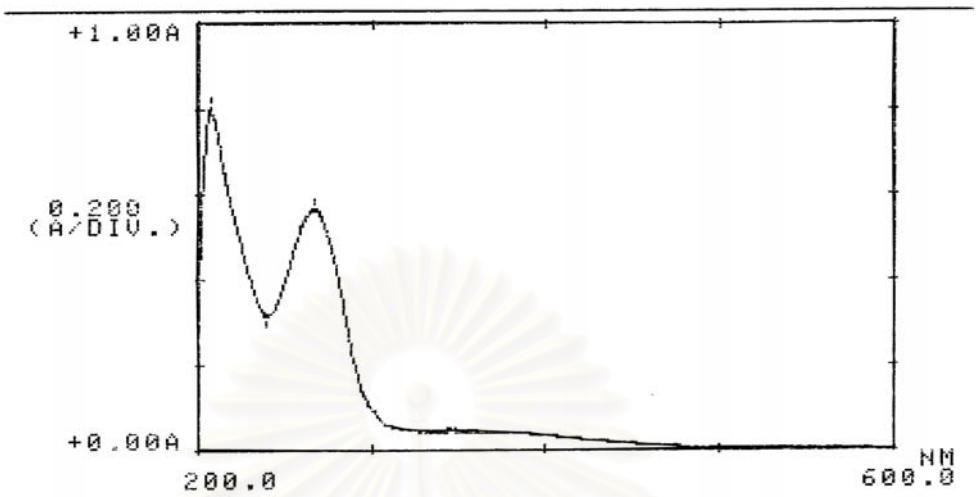

Figure 60 The UV spectrum of renieramycin R in methanol

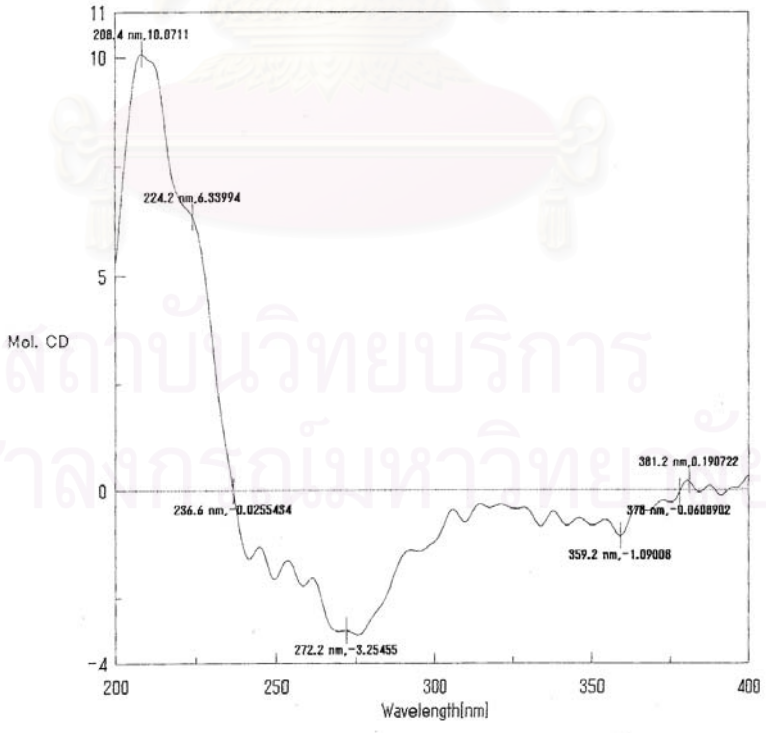

Figure 61 The circular dichroism spectrum of renieramycin R in methanol

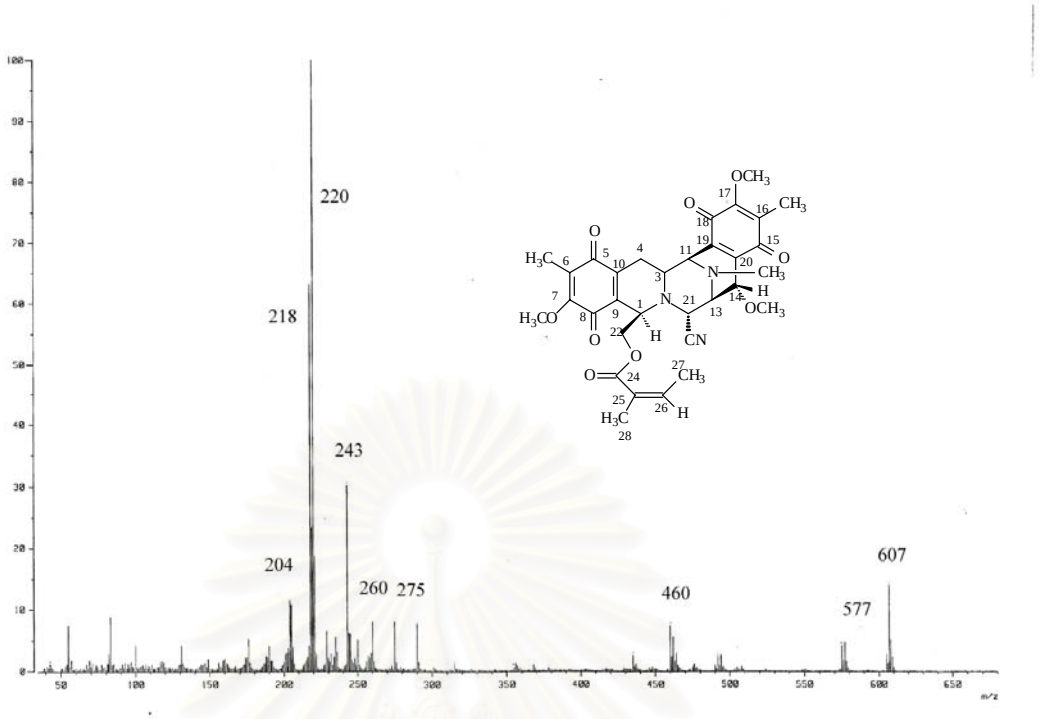

Figure 62 The ESI-mass spectrum of reniramycin R

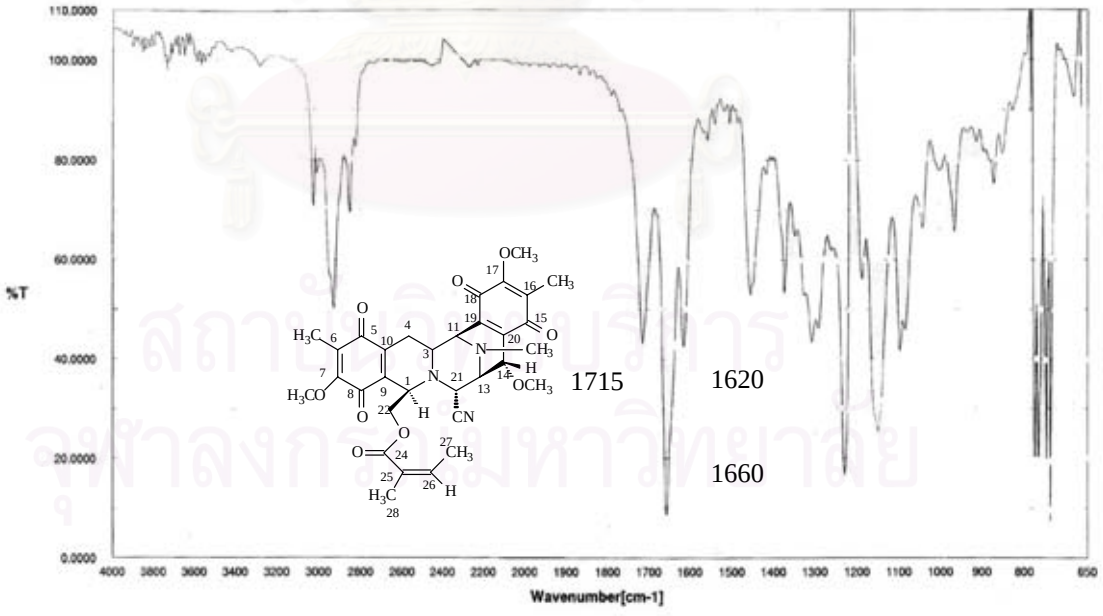

Figure 63 The IR spectrum of renieramycin R in $CHCl_3$

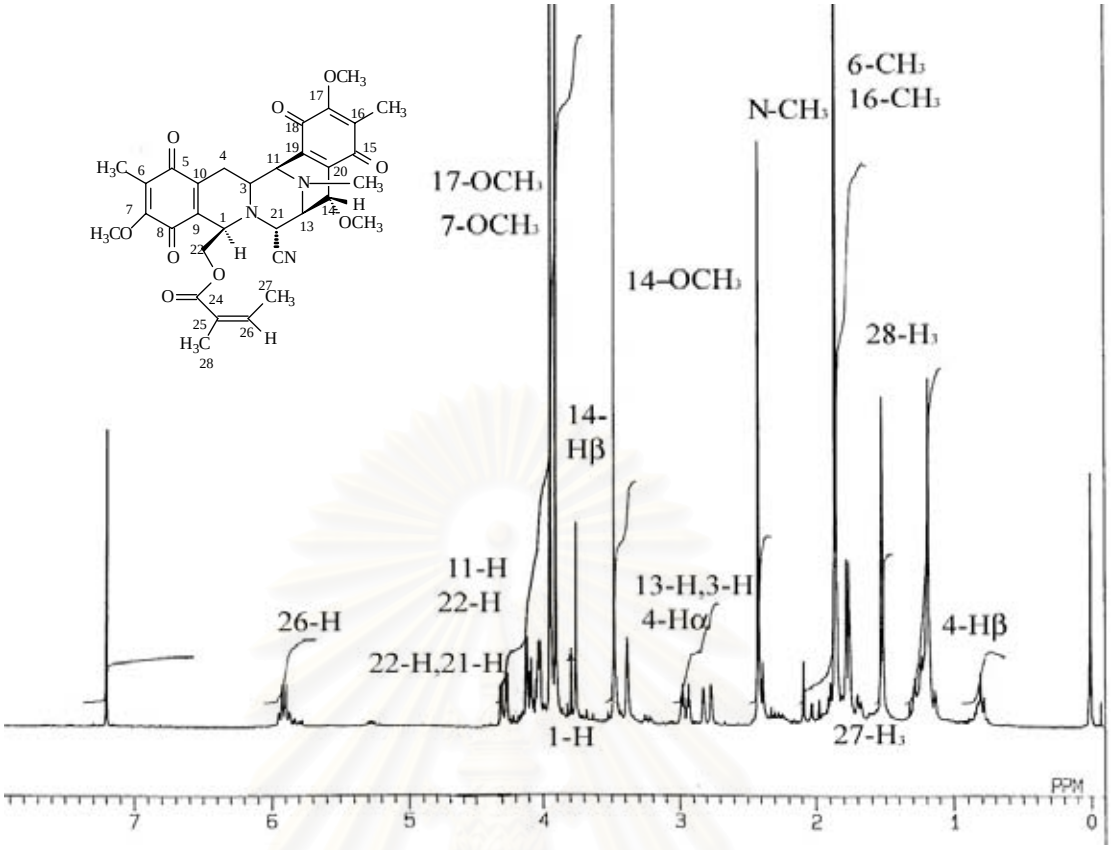

Figure 64 The 500 MHz ^{1}H-NMR spectrum of renieramycin R in $CDCl_3$

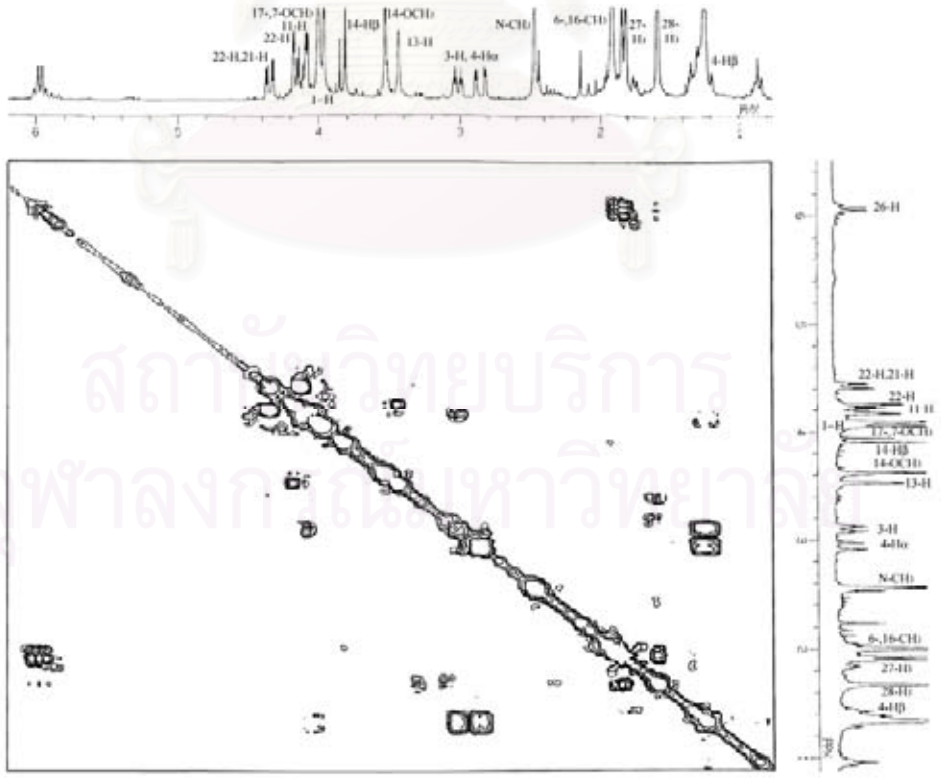

Figure 65 The 500 MHz ^{1}H,^{1}H-COSY spectrum of renieramycin R in $CDCl_3$

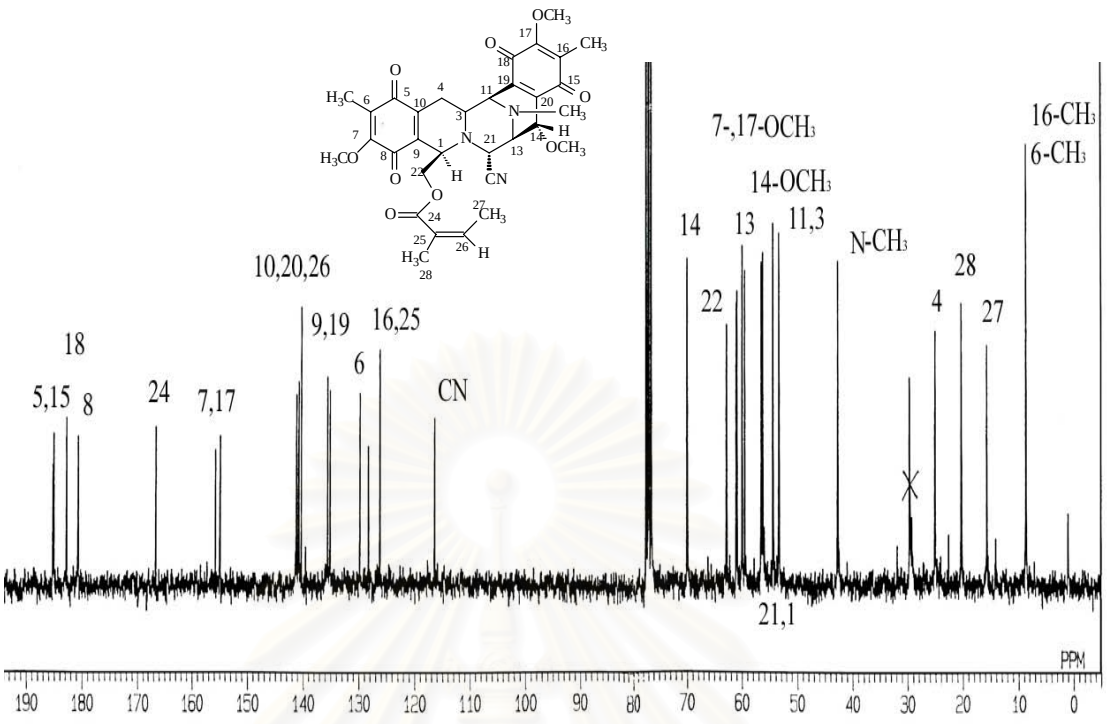

Figure 66 The 125 MHz ^{13}C-NMR spectrum of renieramycin R in $CDCl_3$

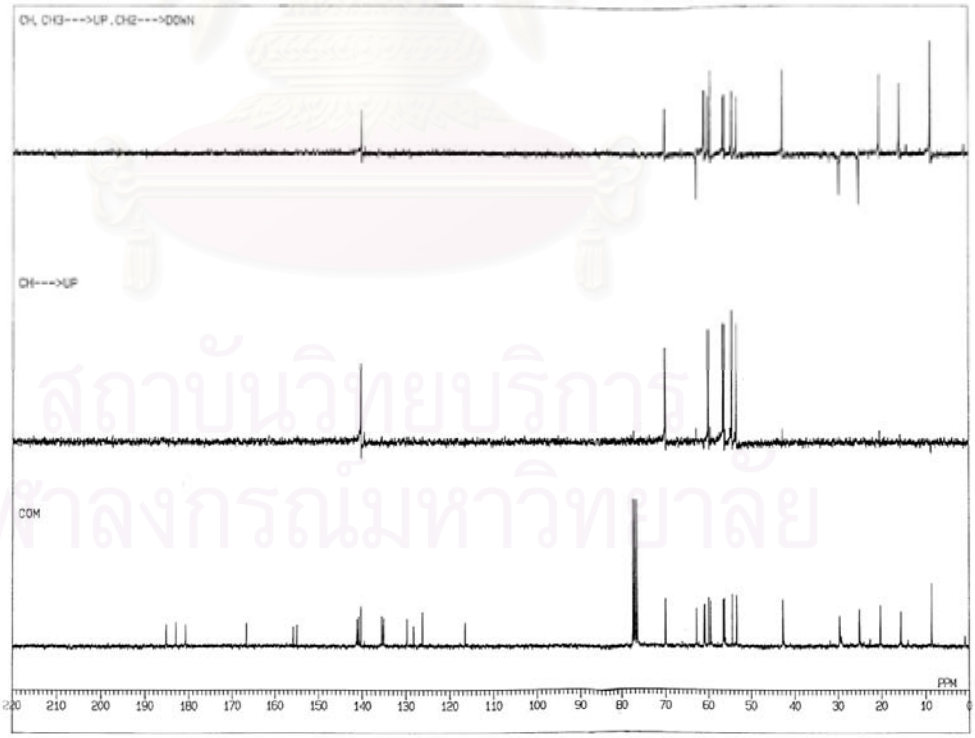

Figure 67 The 125 MHz DEPT spectrum of renieramycin R in $CDCl_3$

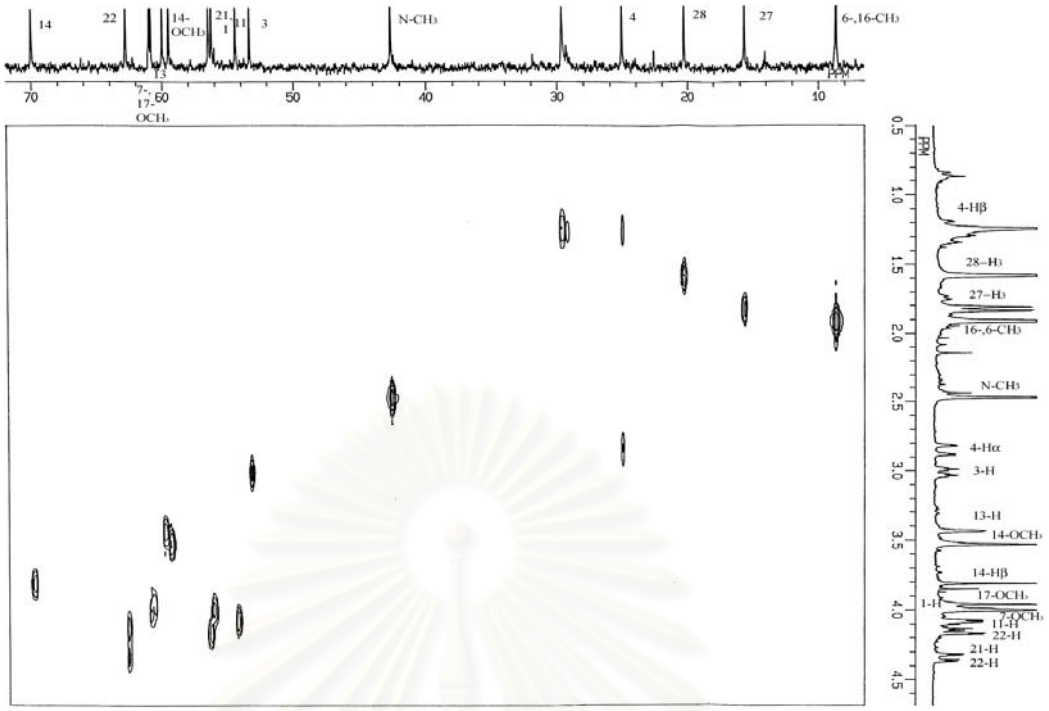

Figure 68 The 500 MHz HMQC spectrum of renieramycin R in $CDCl_3$

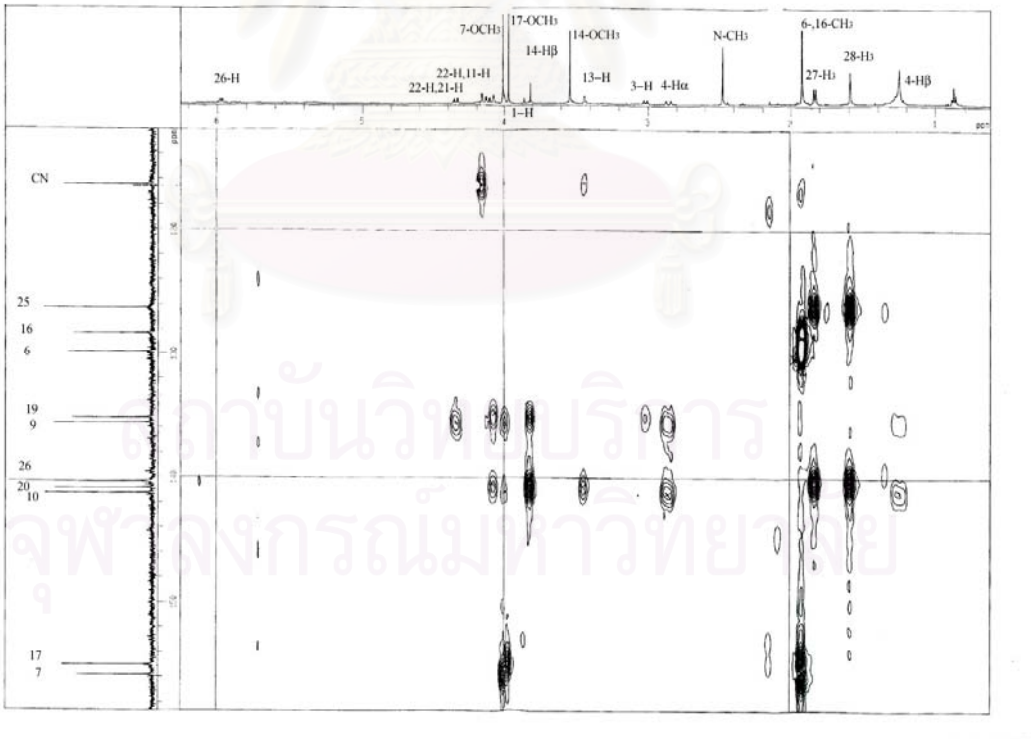

Figure 69 The 500 MHz HMBC spectrum of renieramycin R in $CDCl_3$ (expanded from δ_H 0.80-6.20 ppm and δ_C 110.0-160.0 ppm)

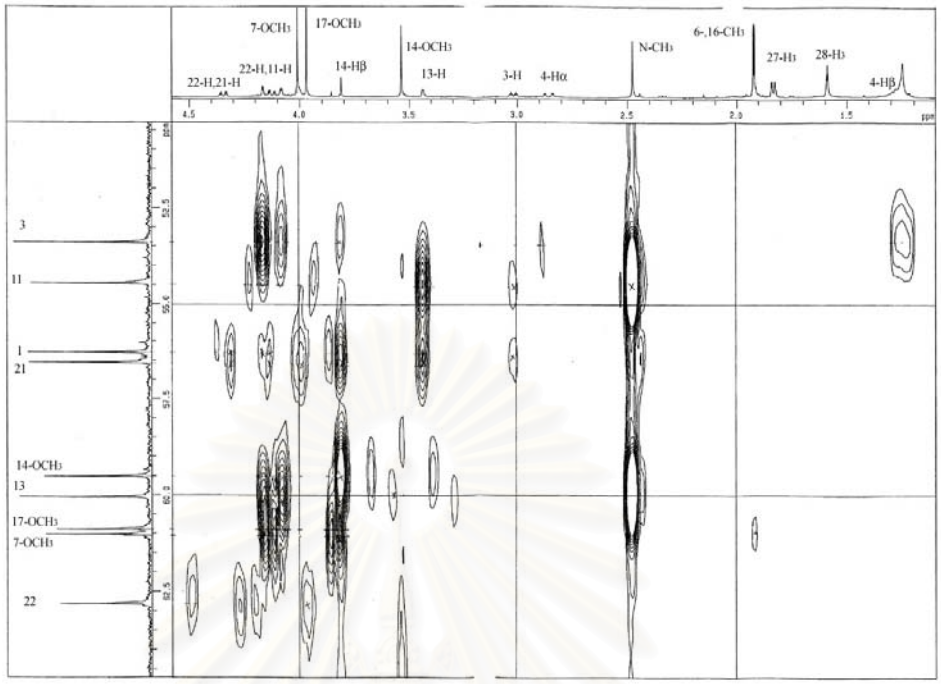

Figure 70 The 500 MHz HMBC spectrum of renieramycin R in $CDCl_3$ (expanded from δ_H 1.2-4.5 ppm and δ_C 50.5-64.5 ppm)

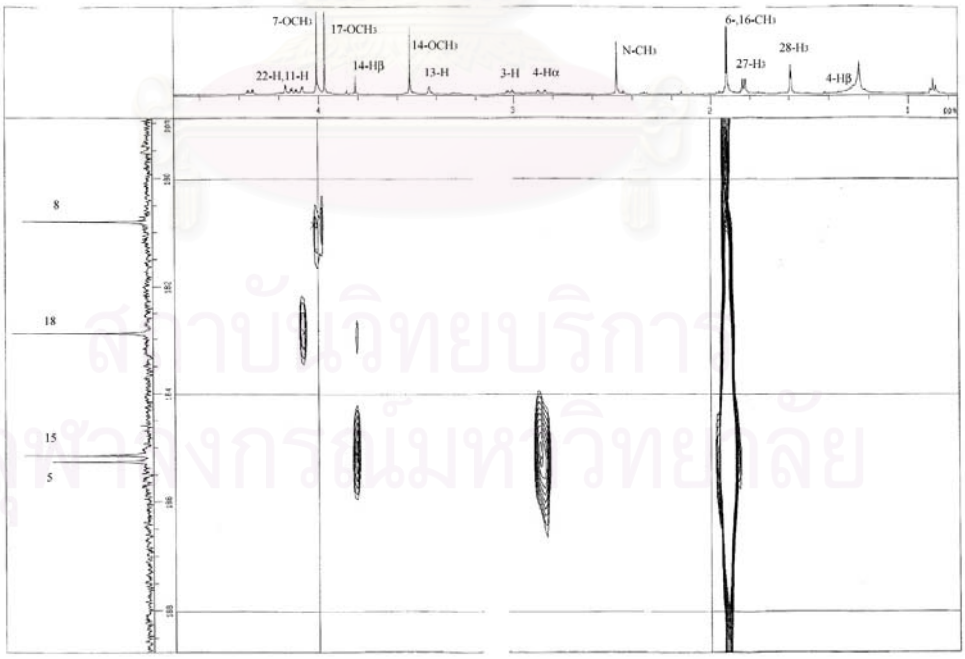

Figure 71 The 500 MHz HMBC spectrum of renieramycin R in $CDCl_3$ (expanded from δ_H 0.80-4.60 ppm and δ_C 179.0-189.0 ppm)

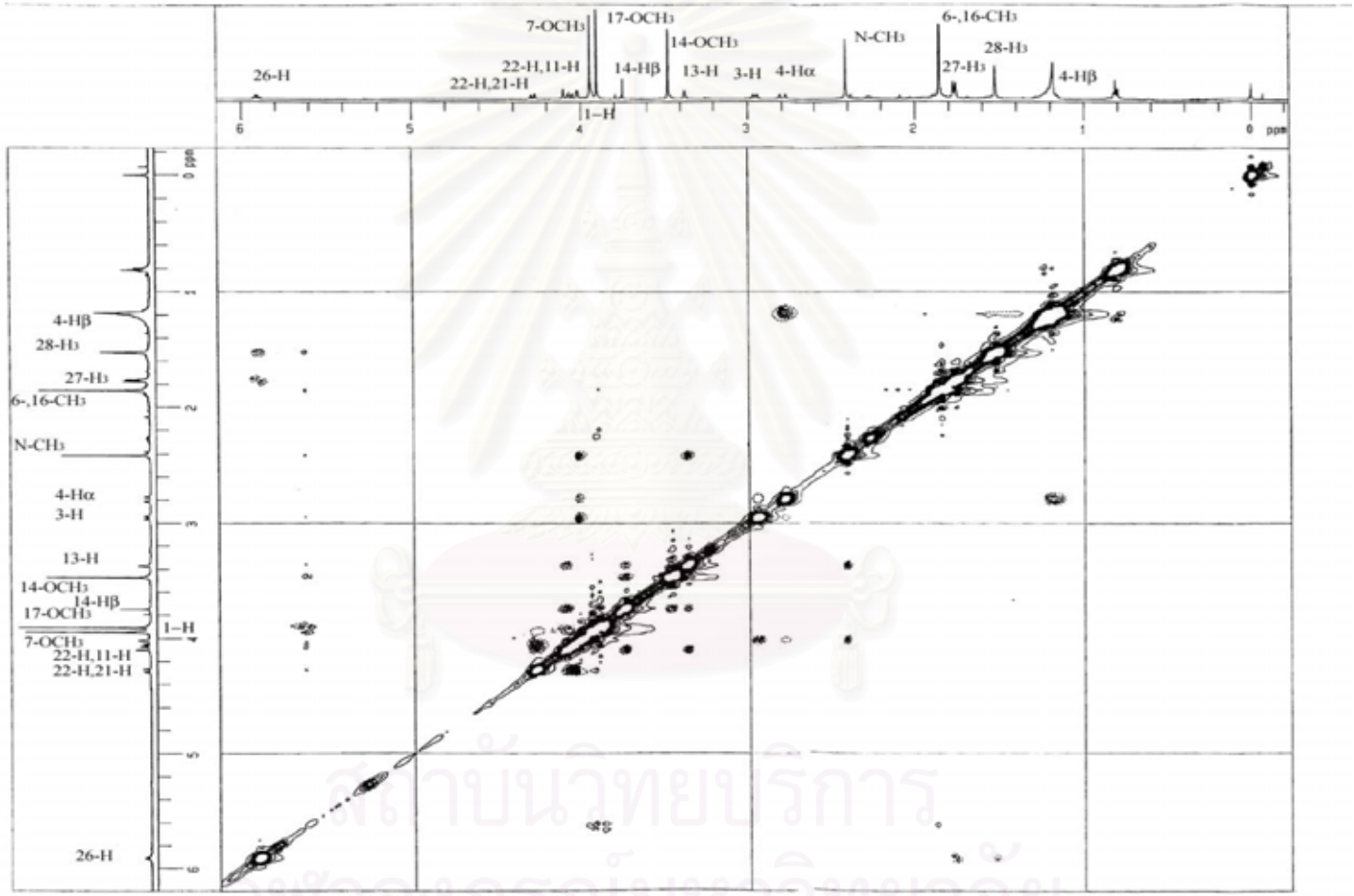

Figure 72 The 500 MHz NOESY spectrum of renieramycin R in $CDCl_3$

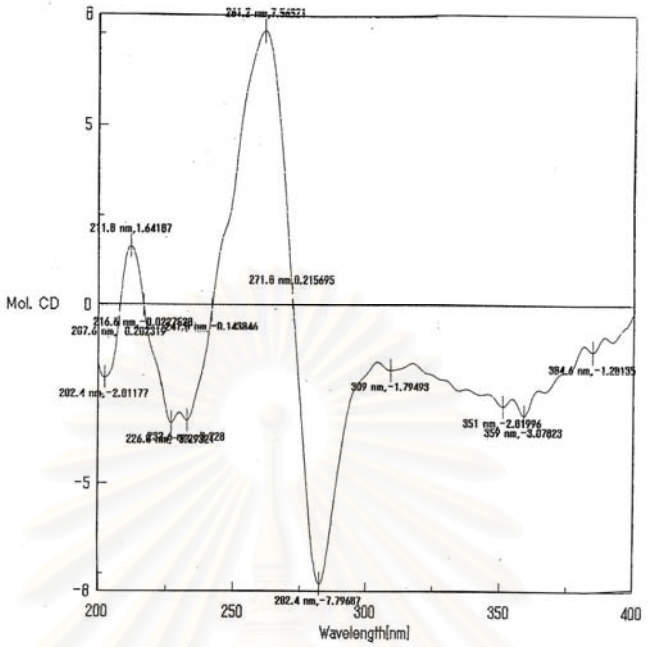

Figure 73 The circular dichroism spectrum of renieramycin S in methanol

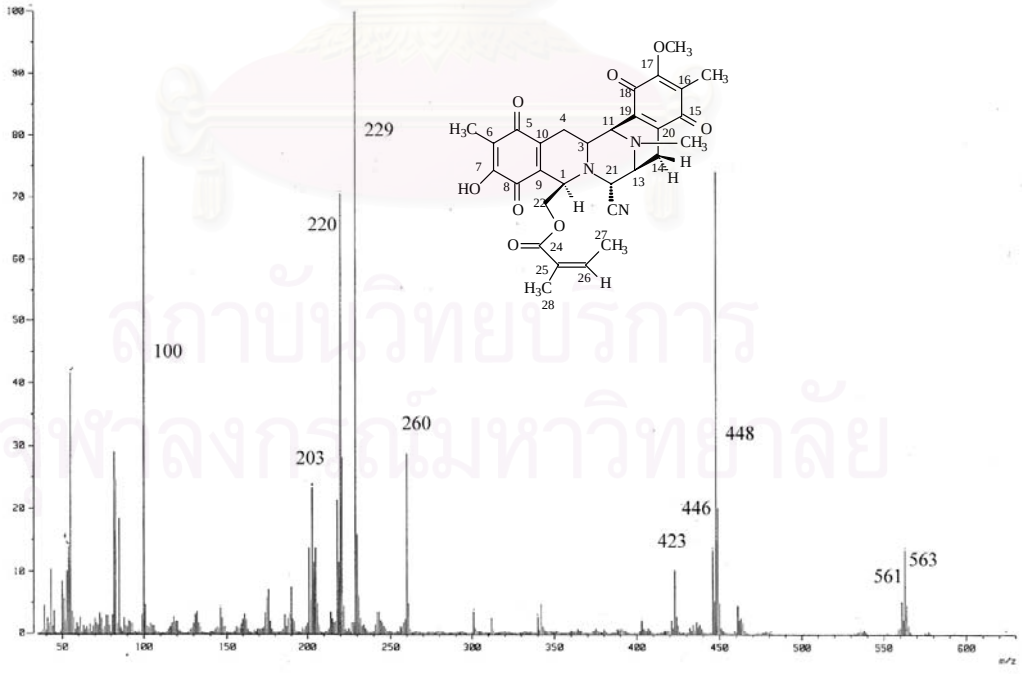

Figure 74 The EI-mass spectrum of reniramycin S

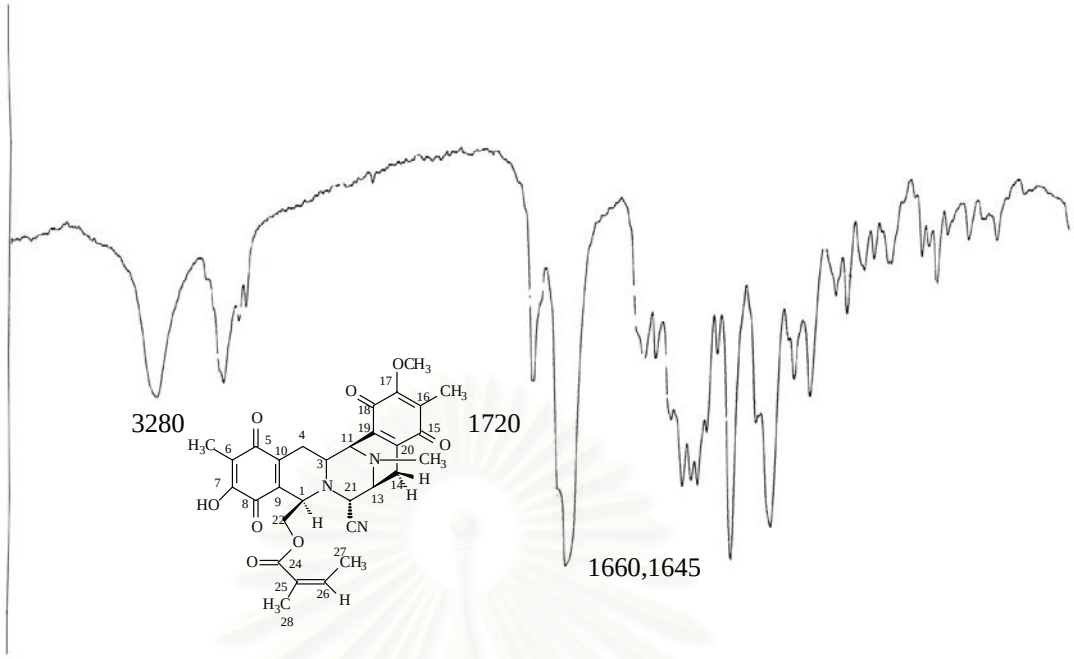

Figure 75 The IR spectrum of renieramycin S (KBr)

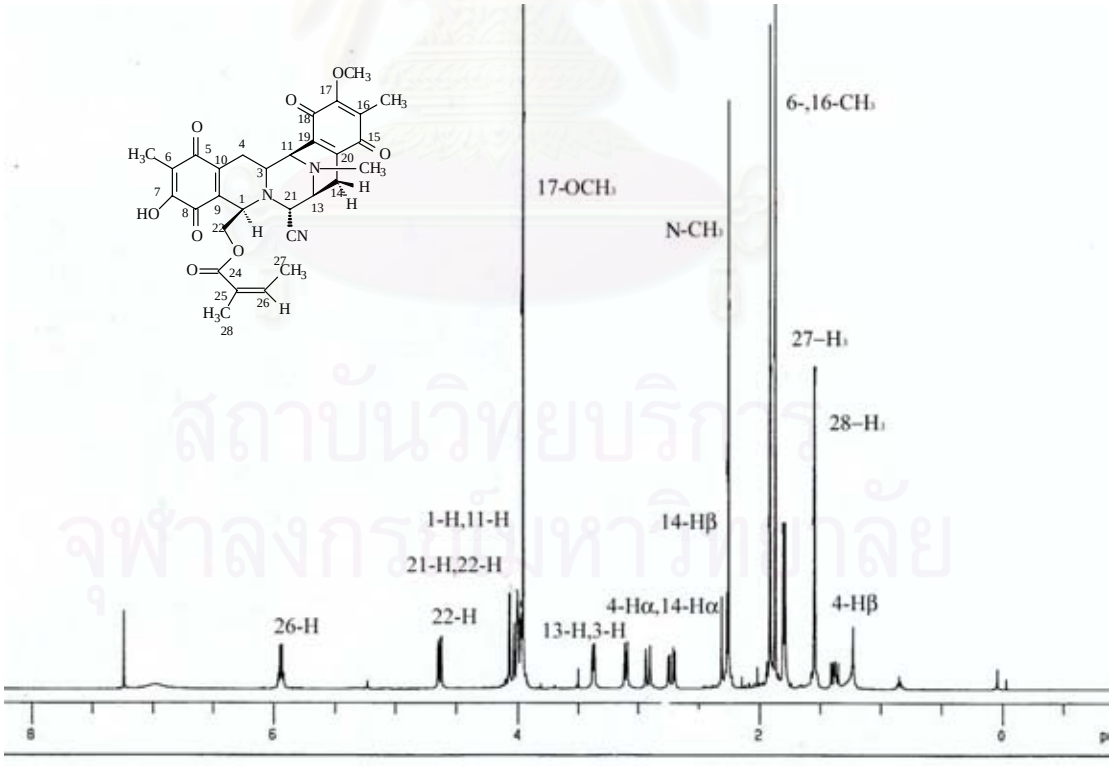

Figure 76 The 300 MHz ^{1}H-NMR spectrum of renieramycin S in $CDCl_3$

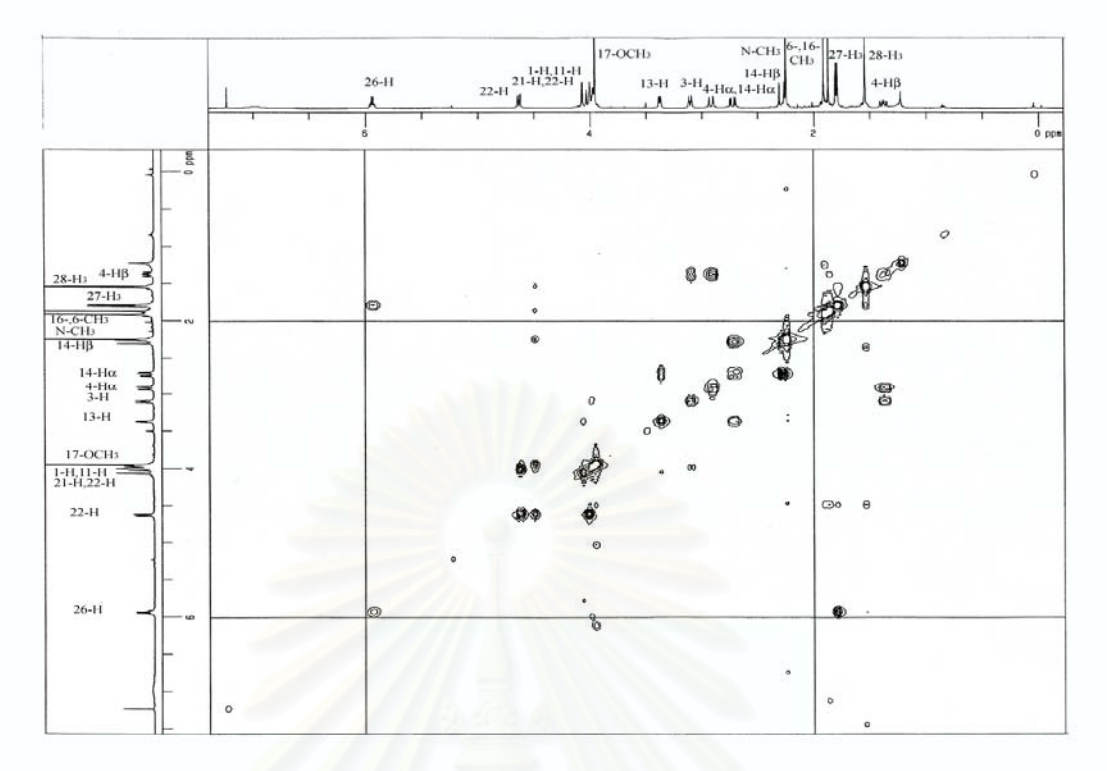

Figure 77 The 300 MHz $^{1}H,^{1}H$-COSY spectrum of renieramycin S in $CDCl_3$

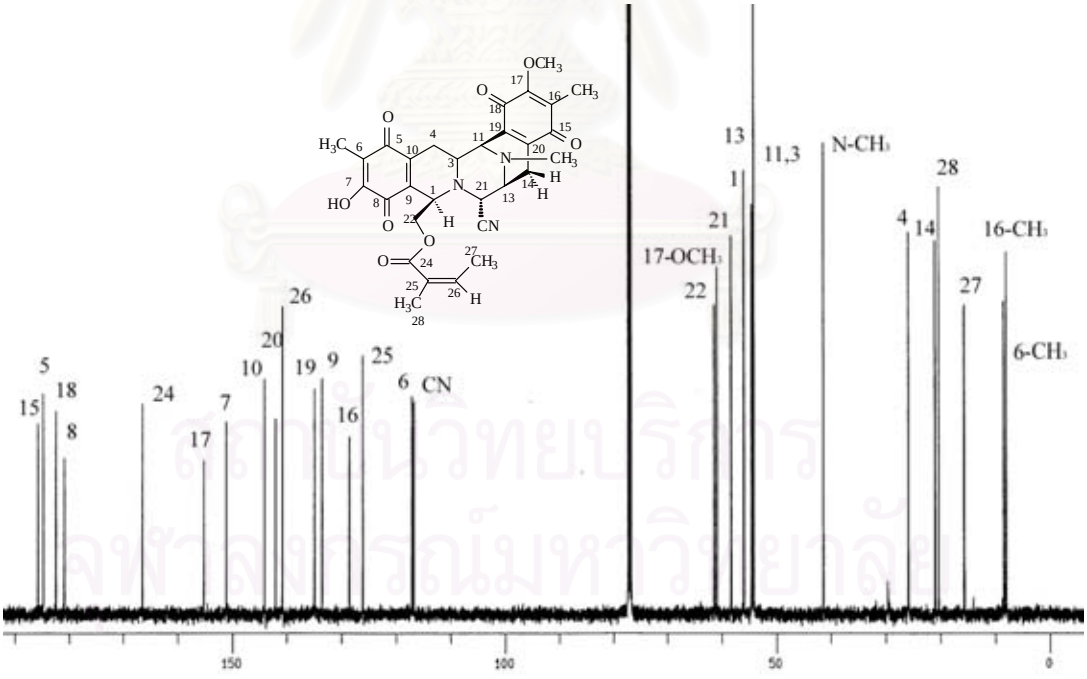

Figure 78 The 75 MHz ^{13}C-NMR spectrum of renieramycin S in $CDCl_3$

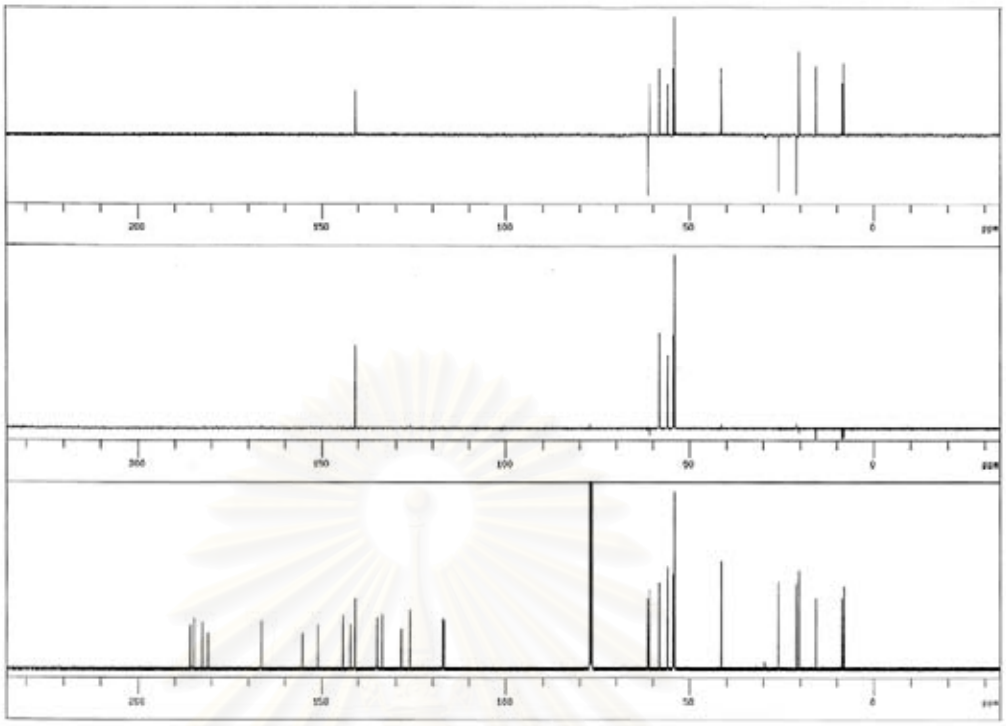

Figure 79 The 300 MHz DEPT spectrum of renieramycin S in $CDCl_3$

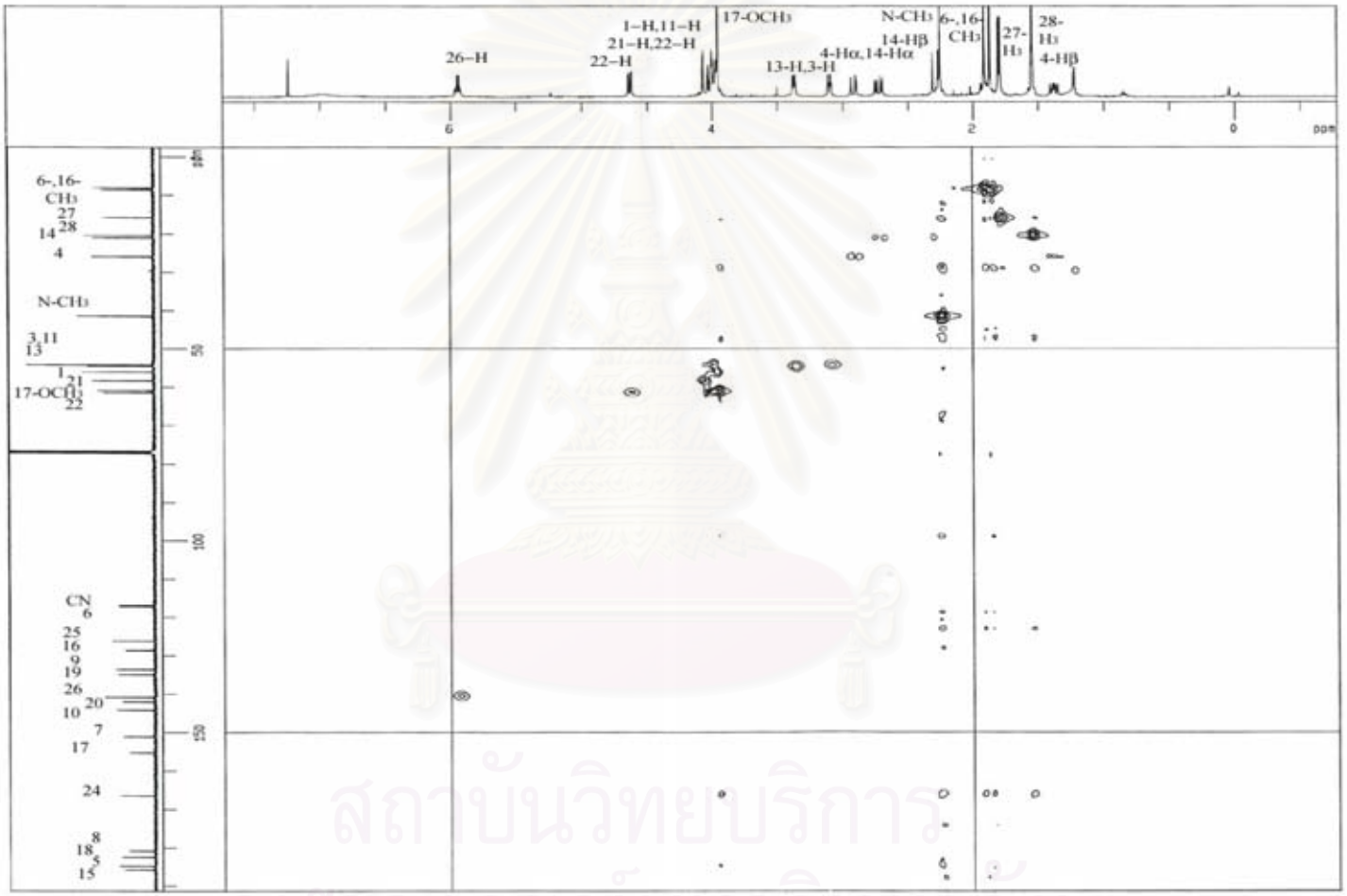

Figure 80 The 300 MHz HMQC spectrum of renieramycin S in $CDCl_3$

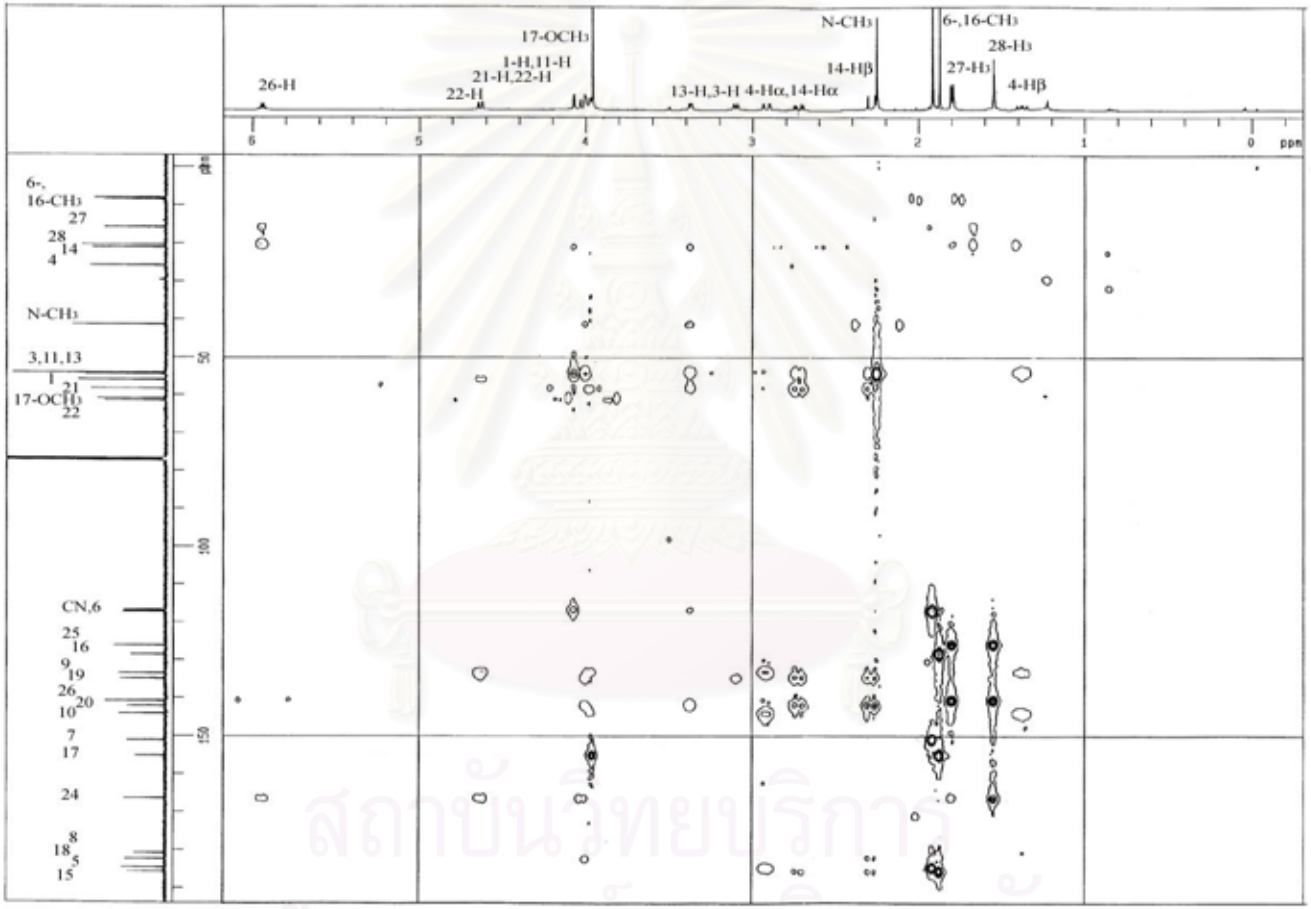

Figure 81 The 300 MHz HMBC spectrum of renieramycin S in $CDCl_3$

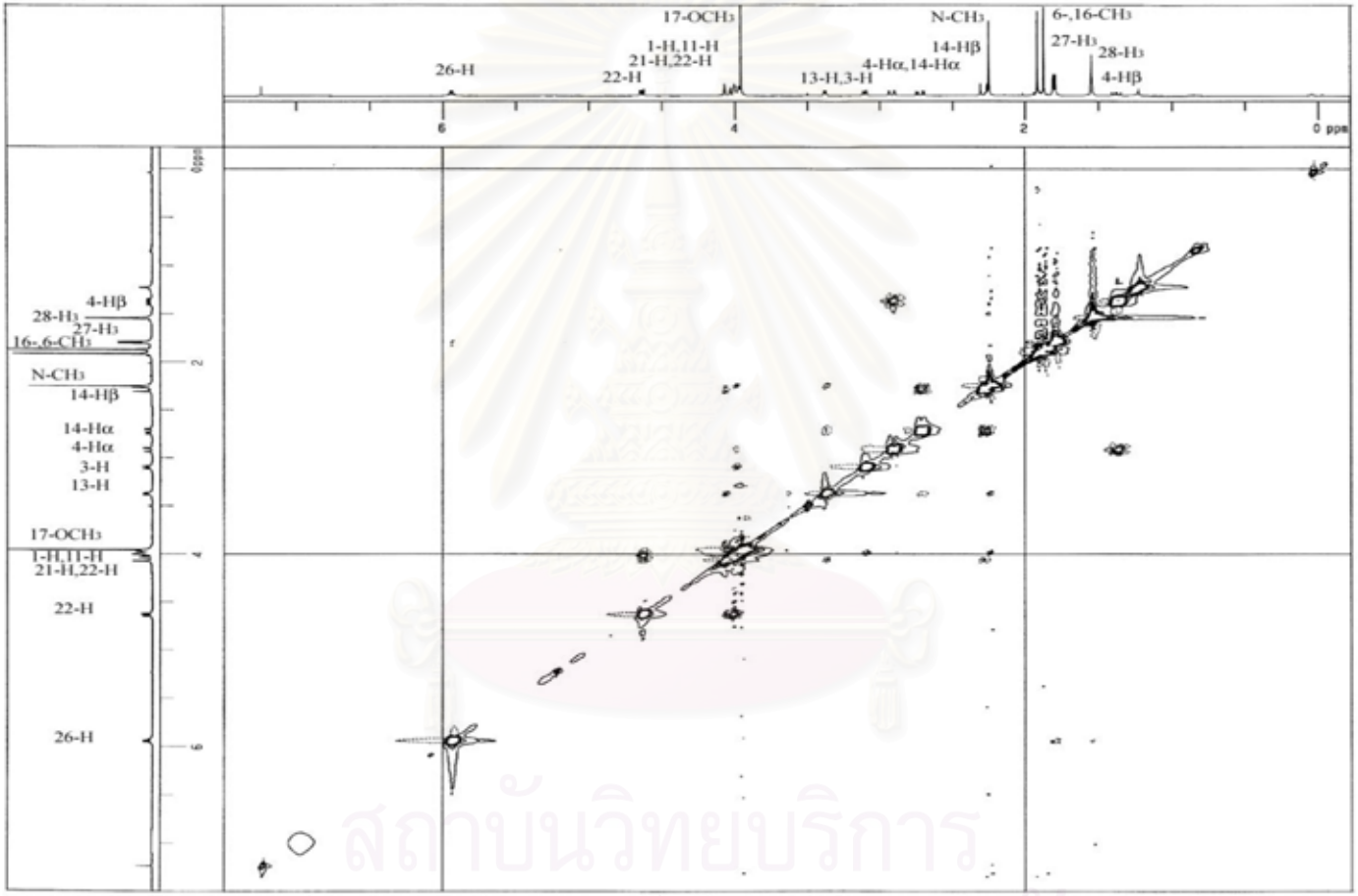

Figure 82 The 300 MHz NOESY spectrum of renieramycin S in $CDCl_3$

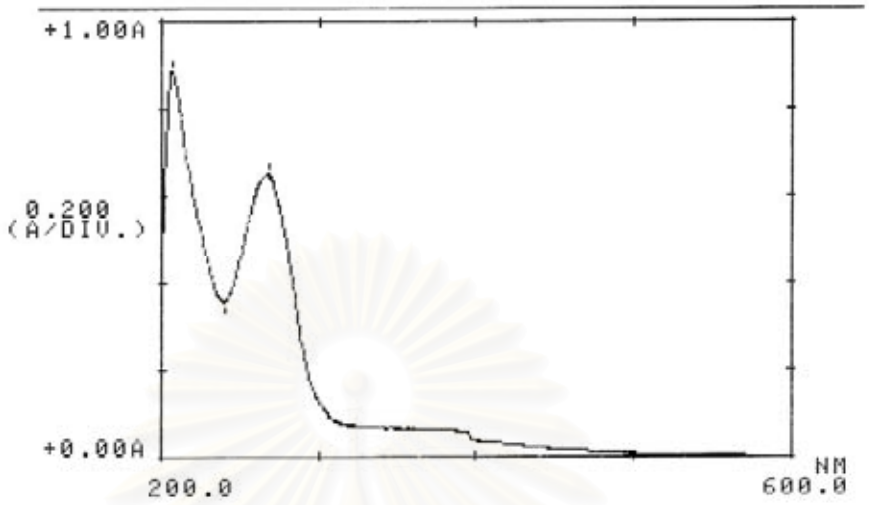

Figure 83 The UV spectrum of renieramycin R' in methanol

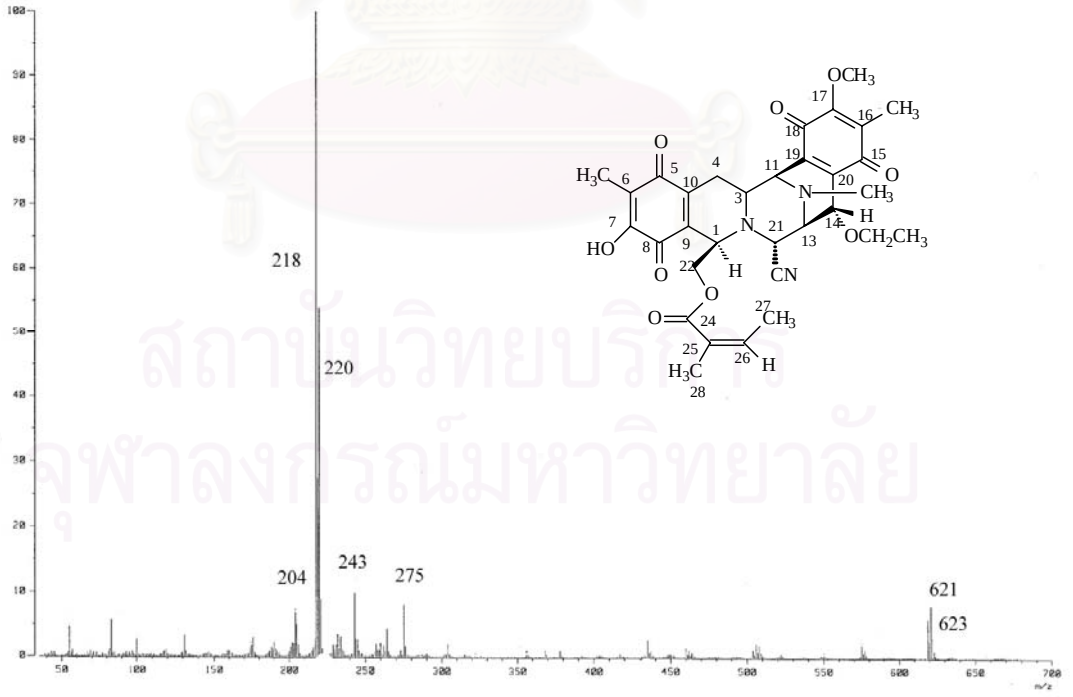

Figure 84 The ESI-mass spectrum of reniramycin R'

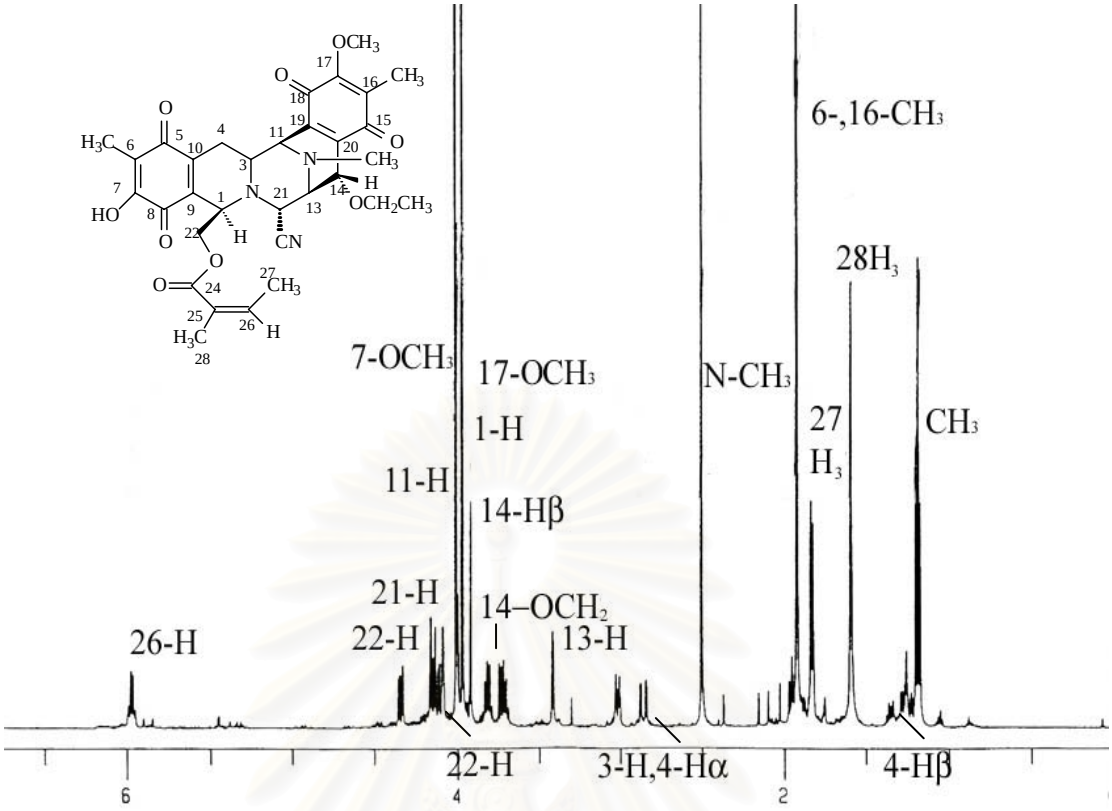

Figure 85 The 500 MHz ^{1}H-NMR spectrum of renieramycin R' in $CDCl_3$

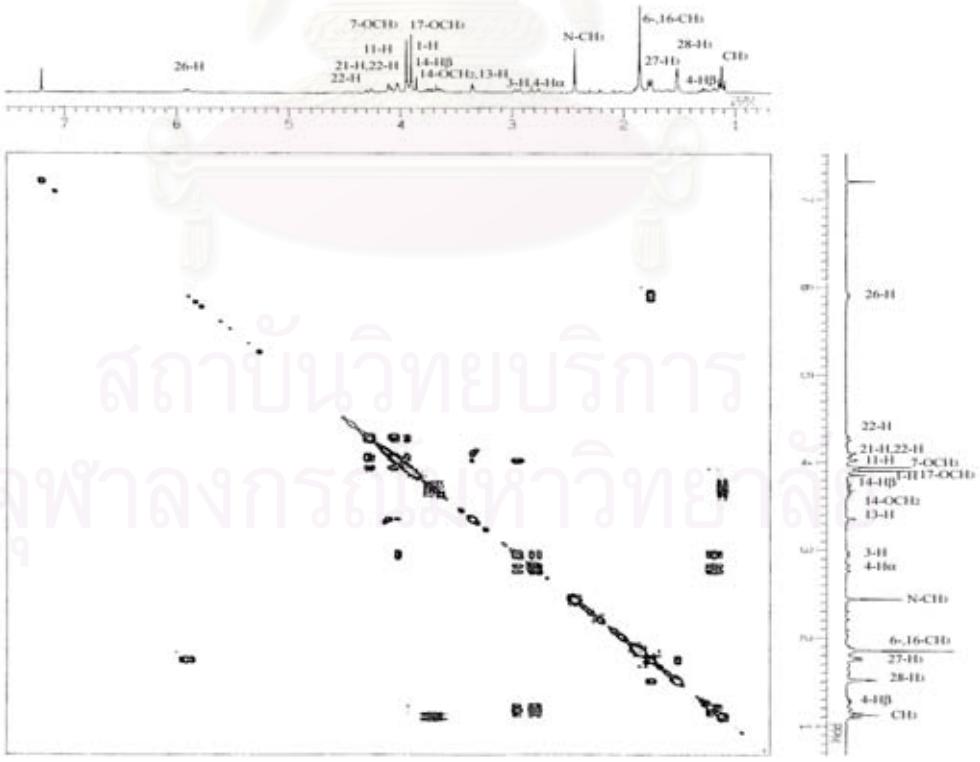

Figure 86 The 500 MHz ^{1}H,^{1}H-COSY spectrum of renieramycin R' in $CDCl_3$

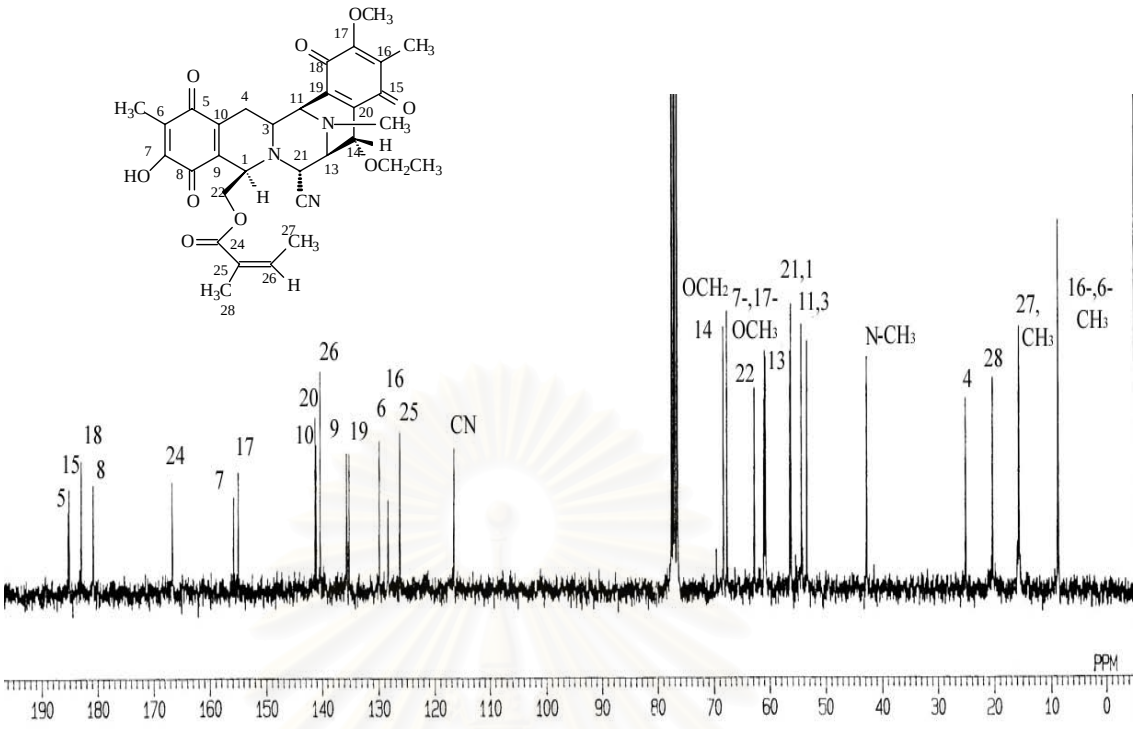

Figure 87 The 125 MHz ^{13}C-NMR spectrum of renieramycin R' in $CDCl_3$

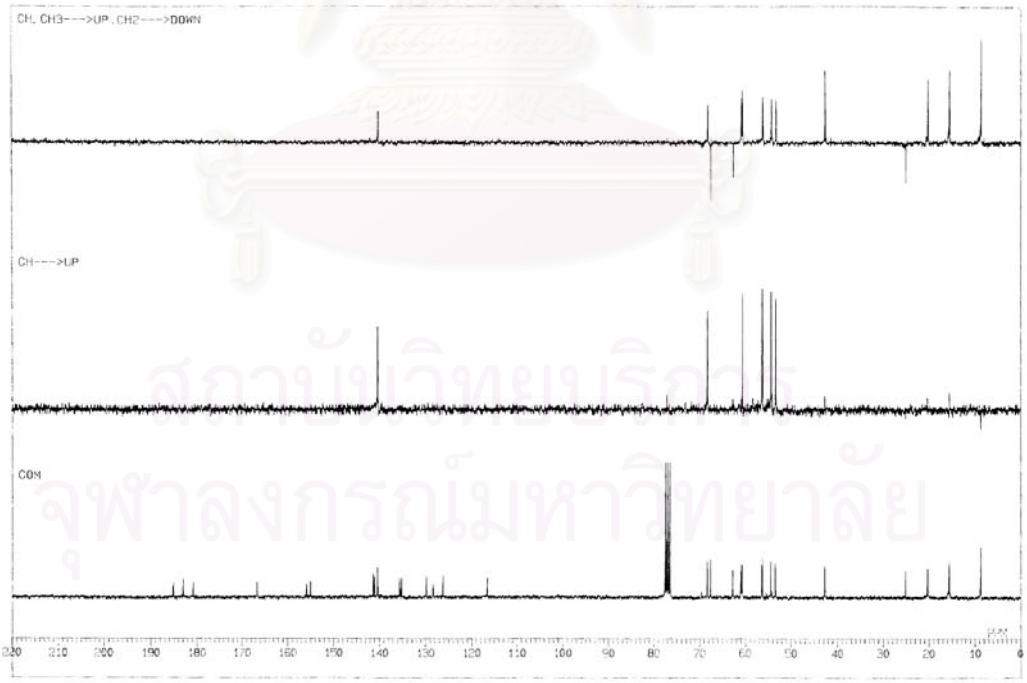

Figure 88 The 125 MHz DEPT spectrum of renieramycin R' in $CDCl_3$

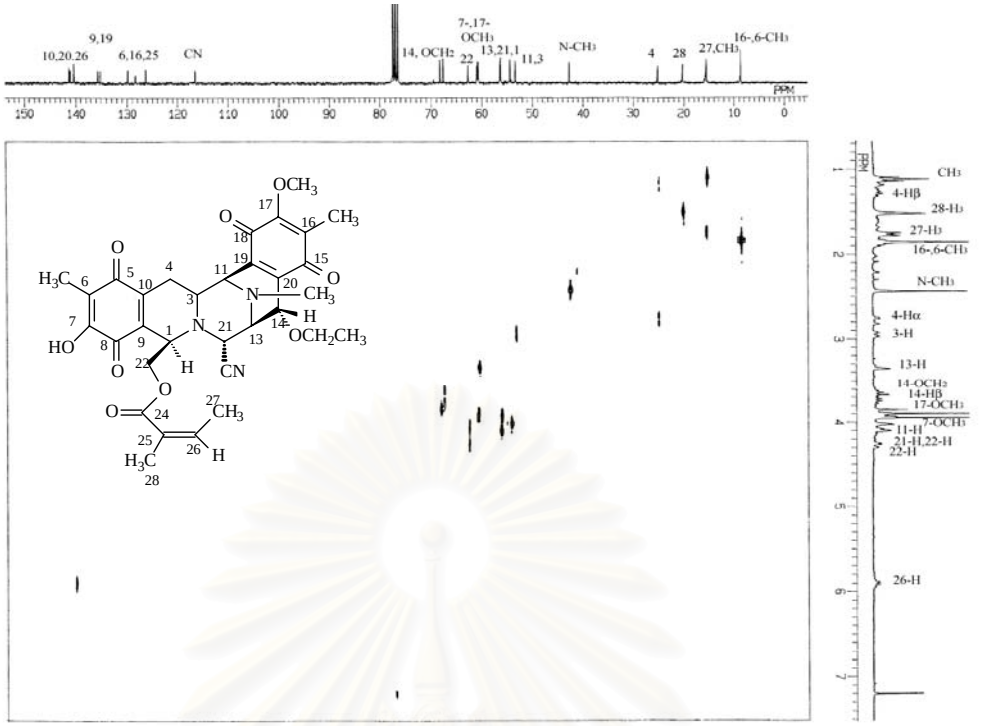

Figure 89 The 500 MHz HMQC spectrum of renieramycin R' in $CDCl_3$

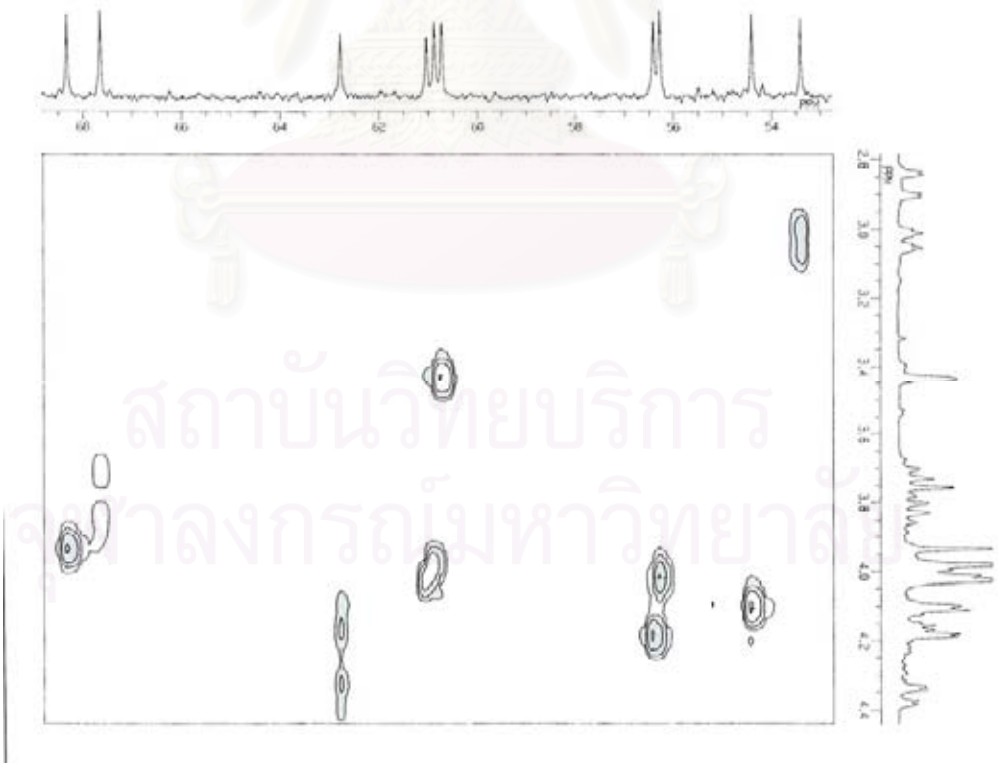

Figure 90 The 500 MHz HMQC spectrum of renieramycin R' in $CDCl_3$ (expanded from δ_H 2.80-4.40 ppm and δ_C 53.00-69.00 ppm)

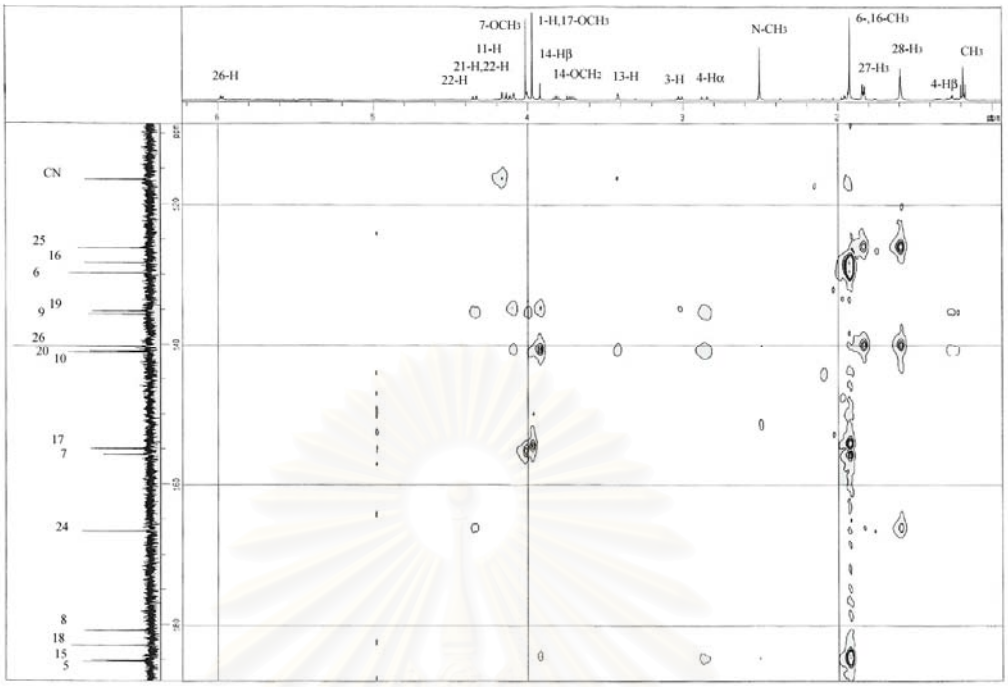

Figure 91 The 500 MHz HMBC spectrum of renieramycin R' in $CDCl_3$ (expanded from δ_H 1.00-6.00 ppm and δ_C 110.00-188.00 ppm)

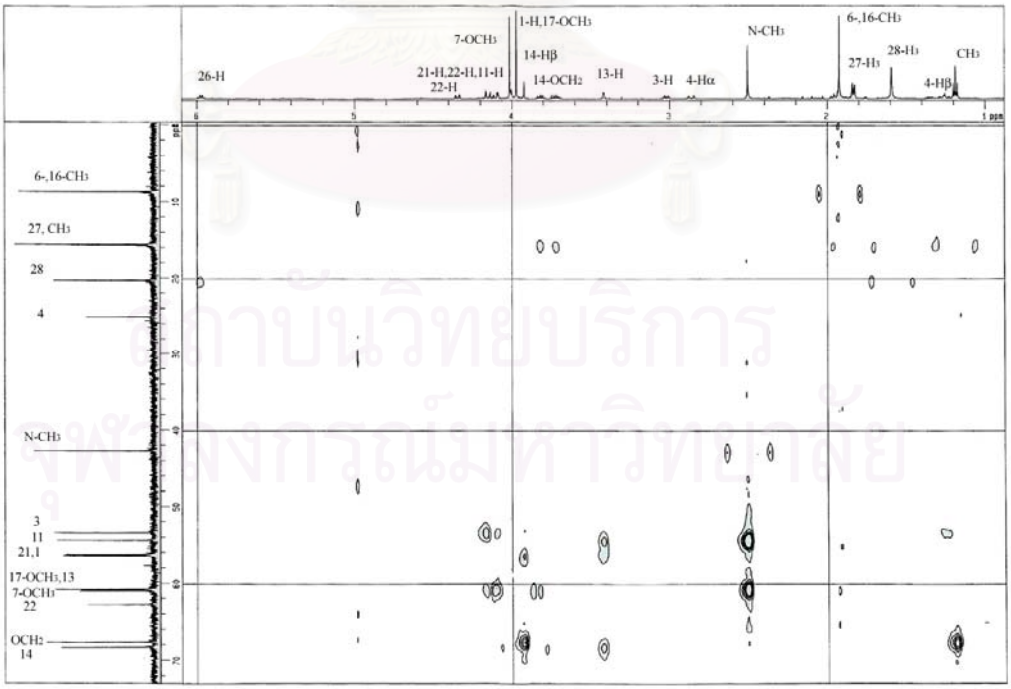

Figure 92 The 500 MHz HMBC spectrum of renieramycin R' in $CDCl_3$ (expanded from δ_H 0.00-6.00 ppm and δ_C 0.00-72.00 ppm)

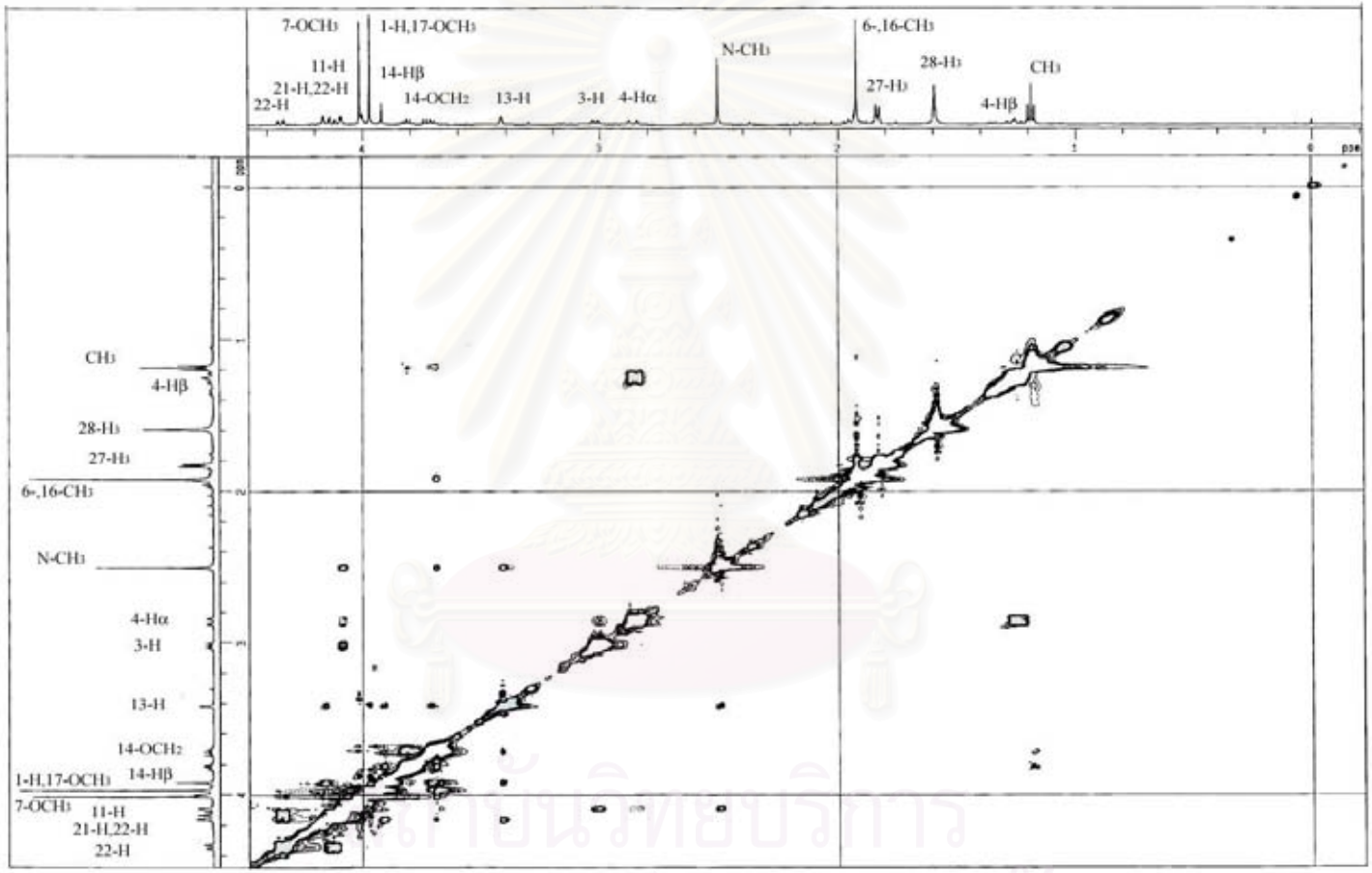

Figure 93 The 500 MHz NOESY- NMR spectrum of renieramycin R' in $CDCl_3$

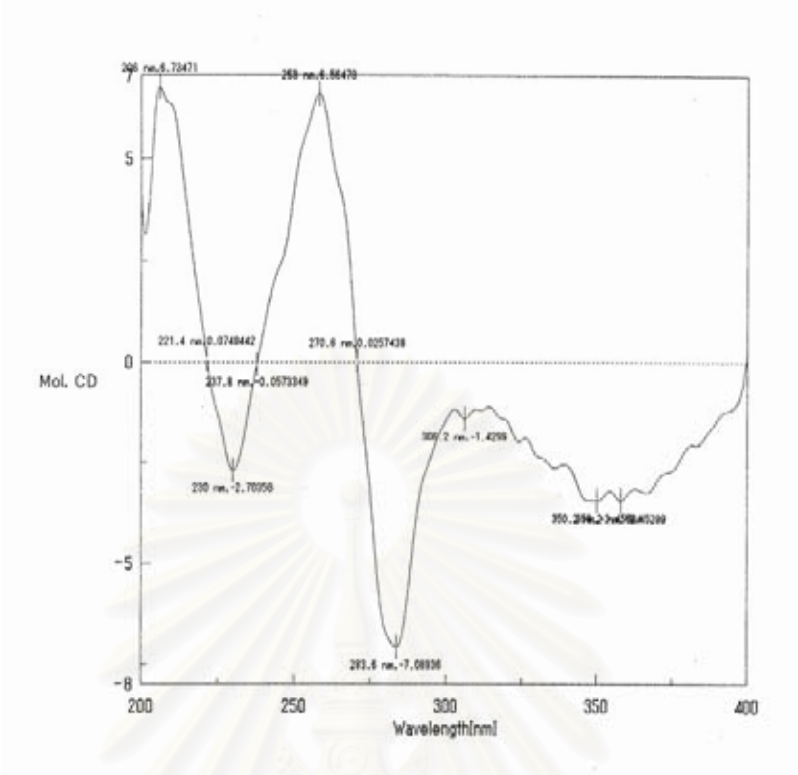

Figure 94 The circular dichroism spectrum of renieramycin E in methanol

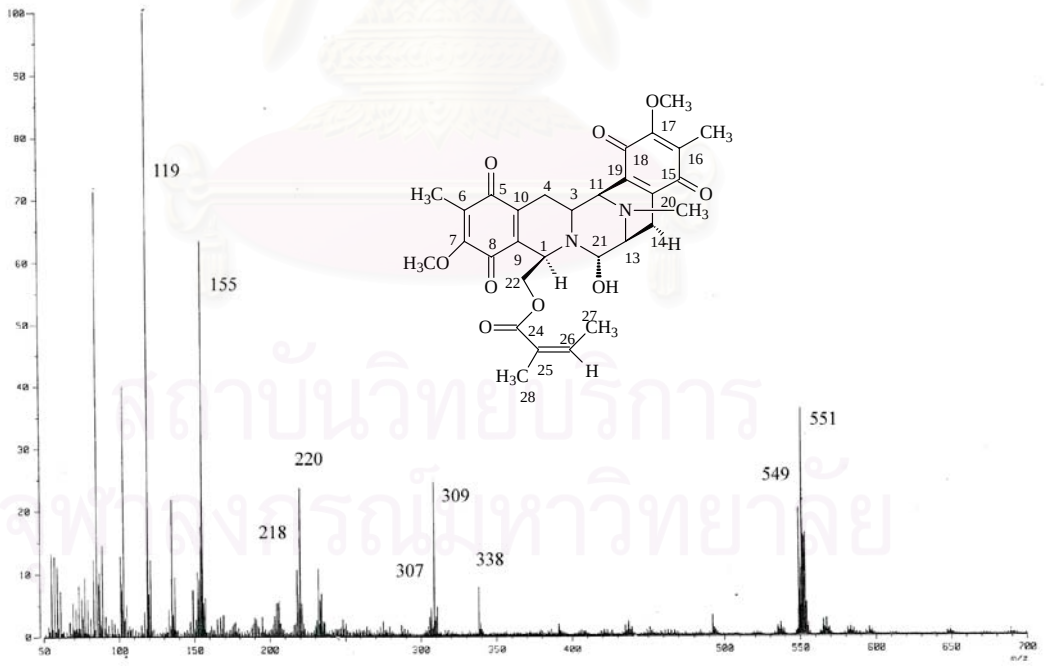

Figure 95 The FAB-mass spectrum of reniramycin E

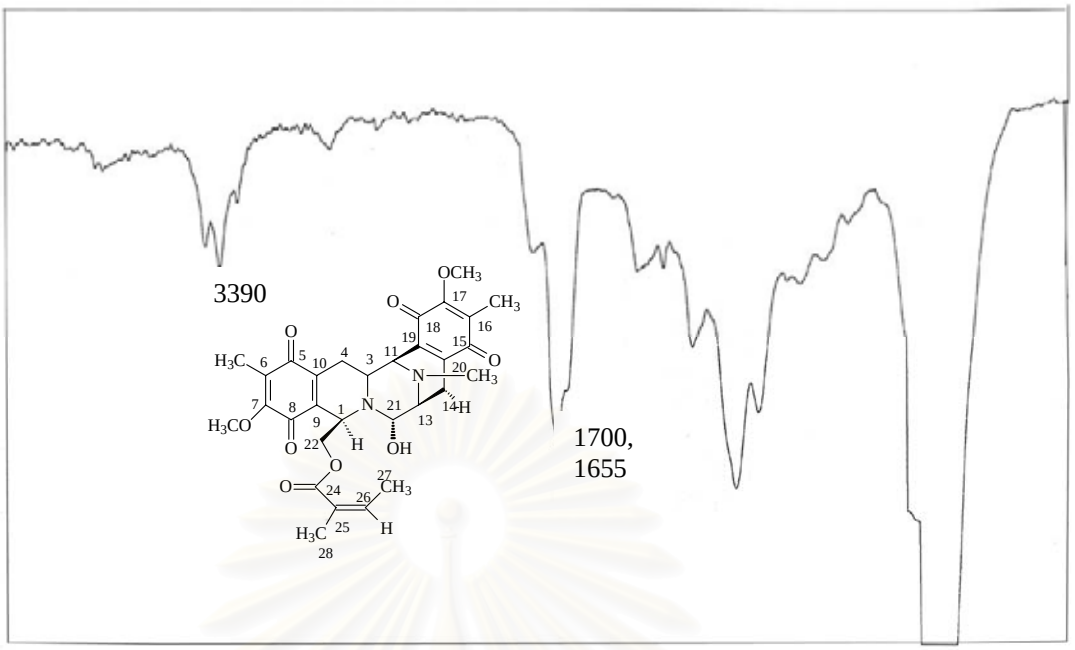

Figure 96 The IR spectrum of renieramycin E in $CHCl_3$

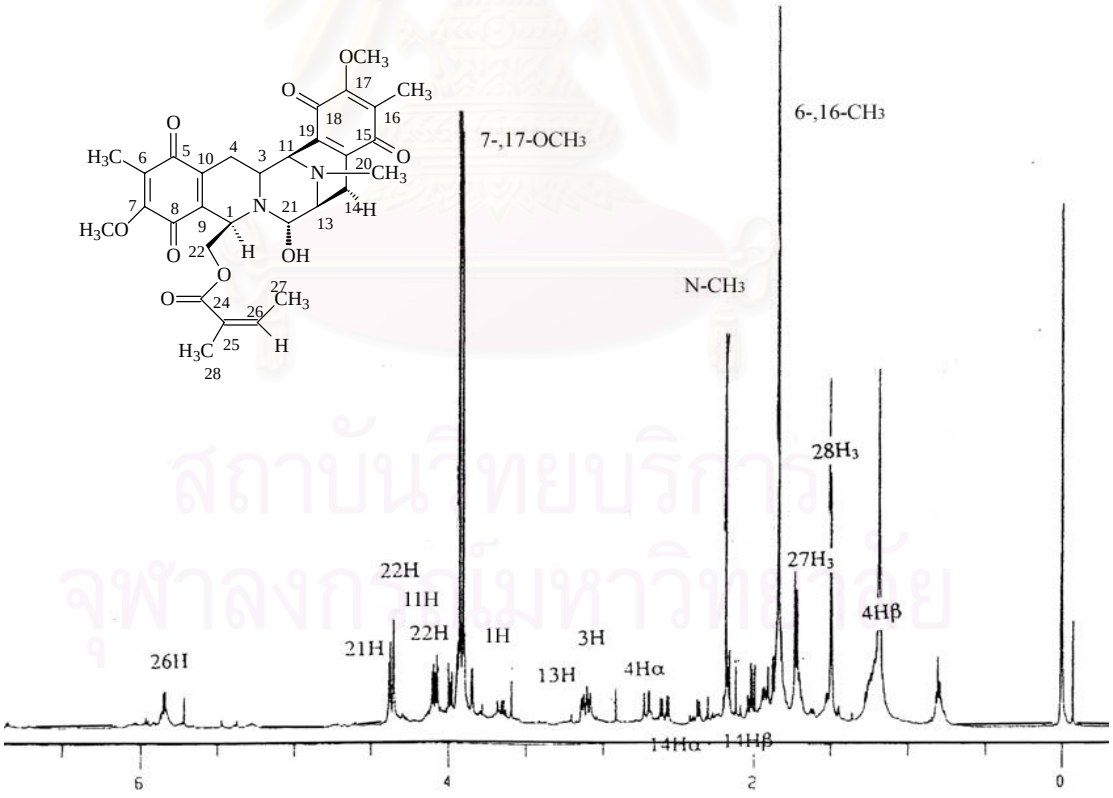

Figure 97 The 500 MHz ^{1}H-NMR spectrum of renieramycin E in $CDCl_3$

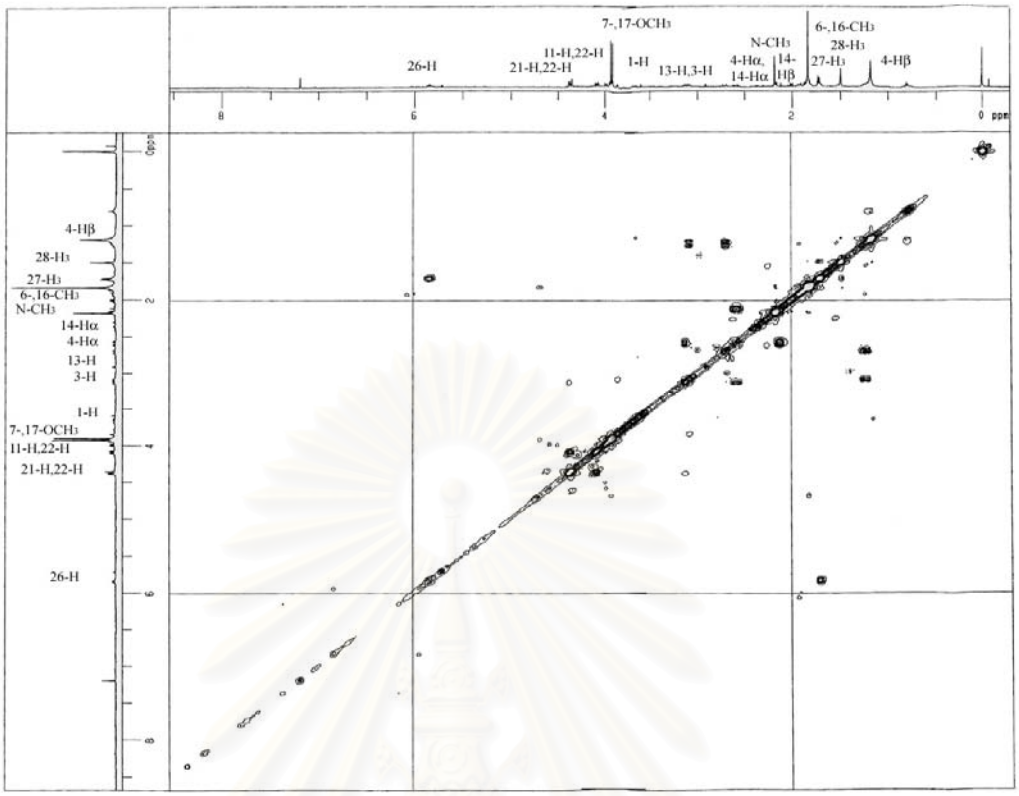

Figure 98 The 500 MHz $^{1}H,^{1}H$-COSY NMR spectrum of renieramycin E in $CDCl_3$

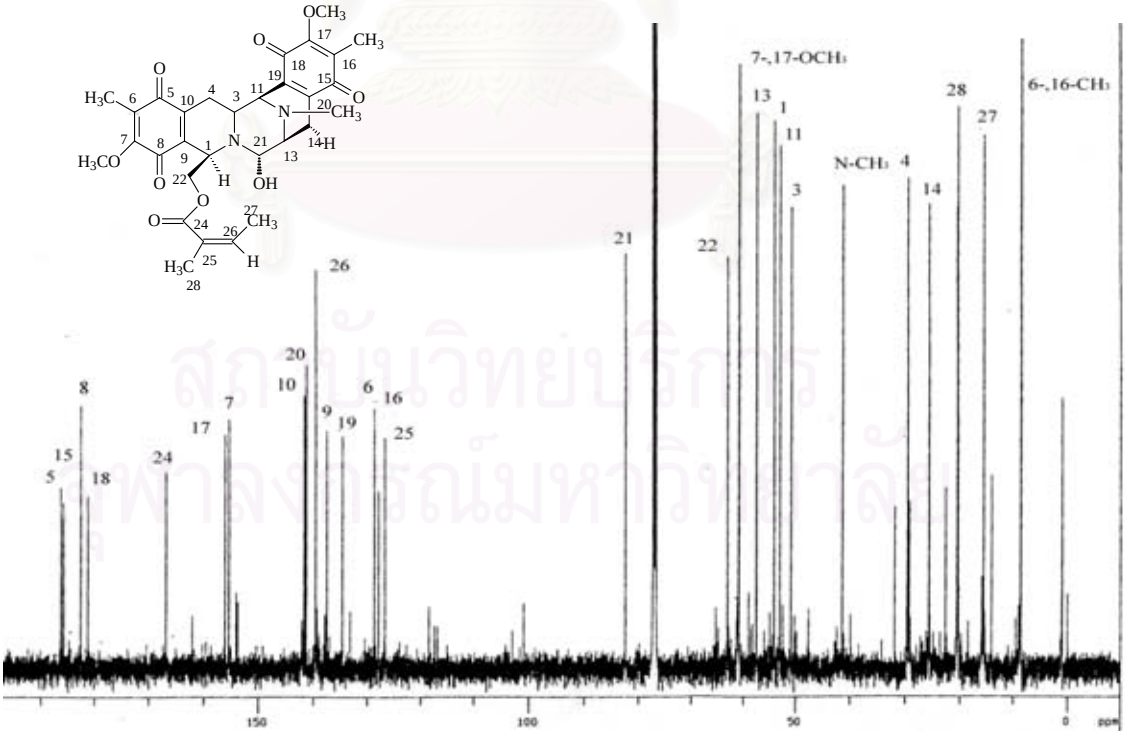

Figure 99 The 125 MHz ^{13}C-NMR spectrum of renieramycin E in $CDCl_3$

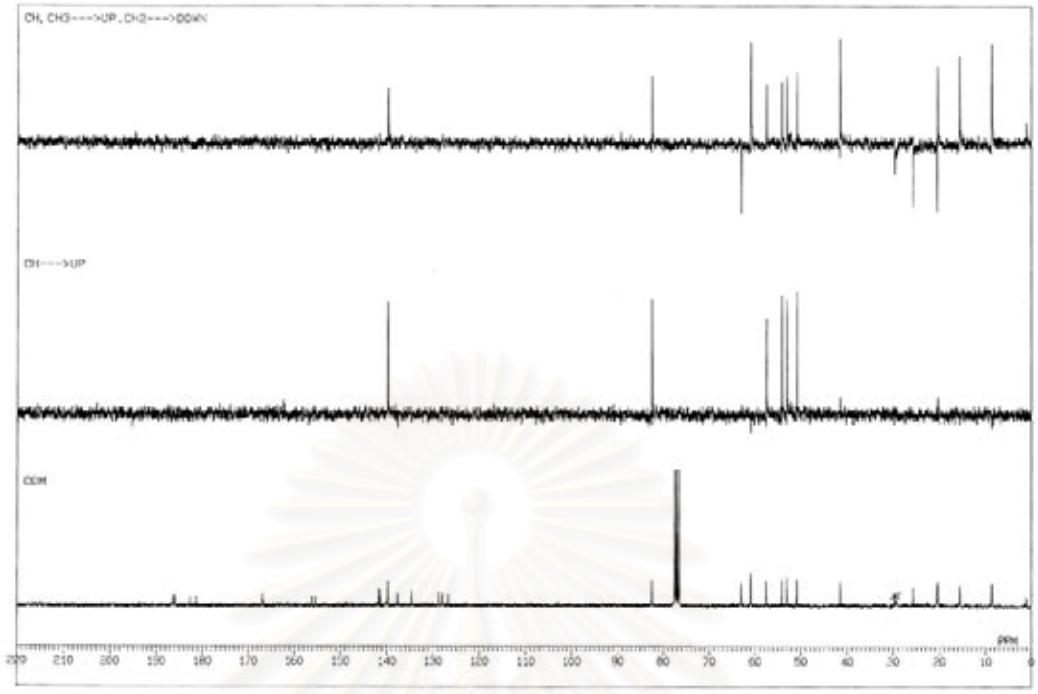

Figure 100 The 125 MHz DEPT carbon NMR spectrum of renieramycin E in $CDCl_3$

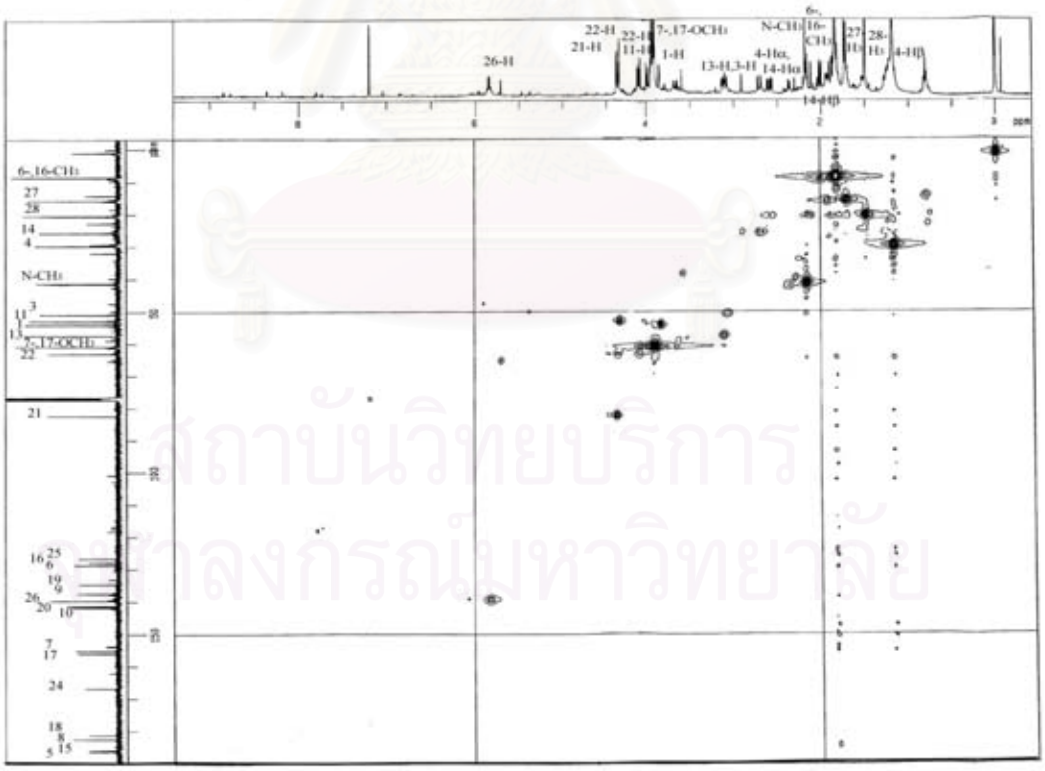

Figure 101 The 500 MHz HMQC spectrum of renieramycin E in $CDCl_3$

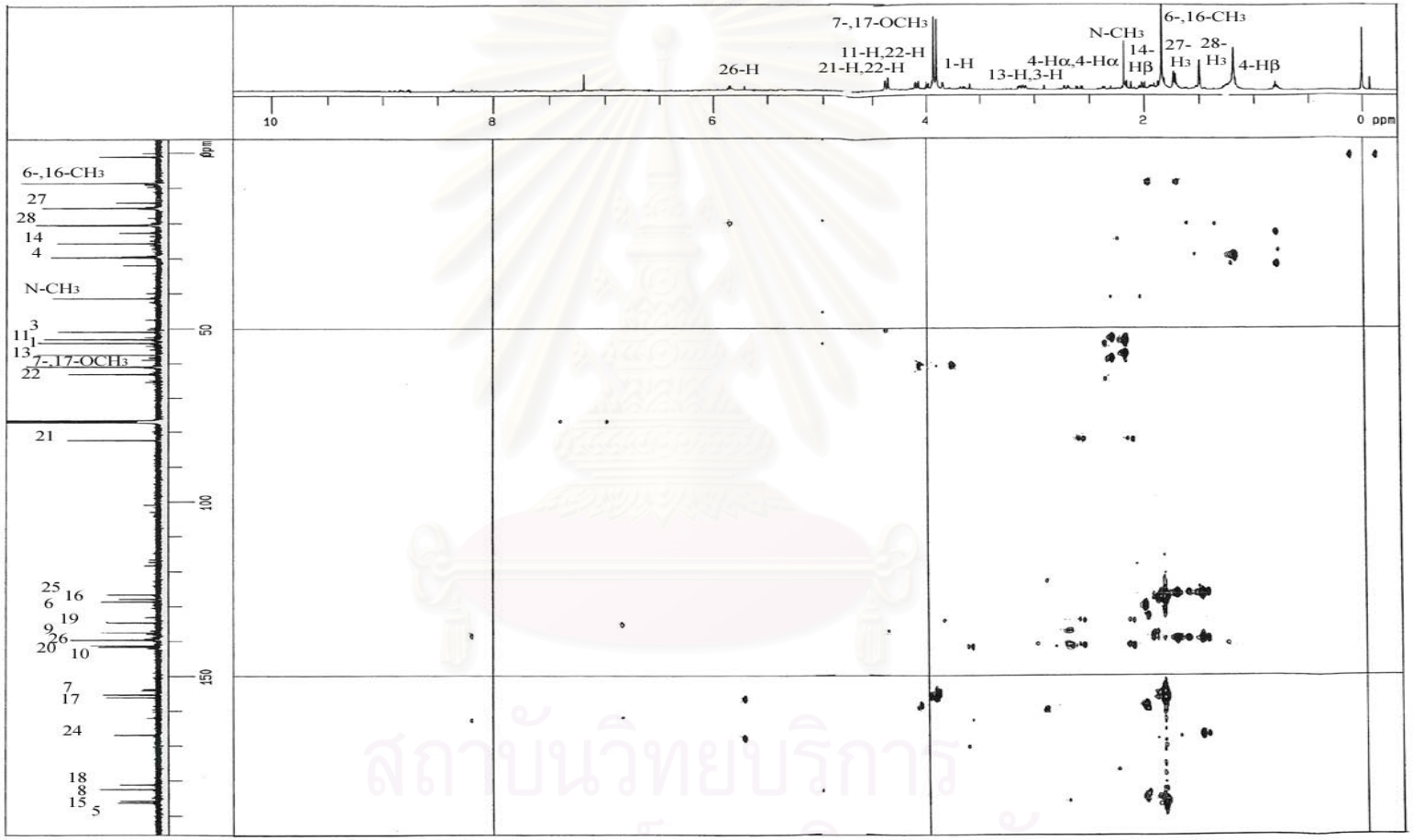

Figure 102 The 500 MHz HMBC spectrum of renieramycin E in $CDCl_3$

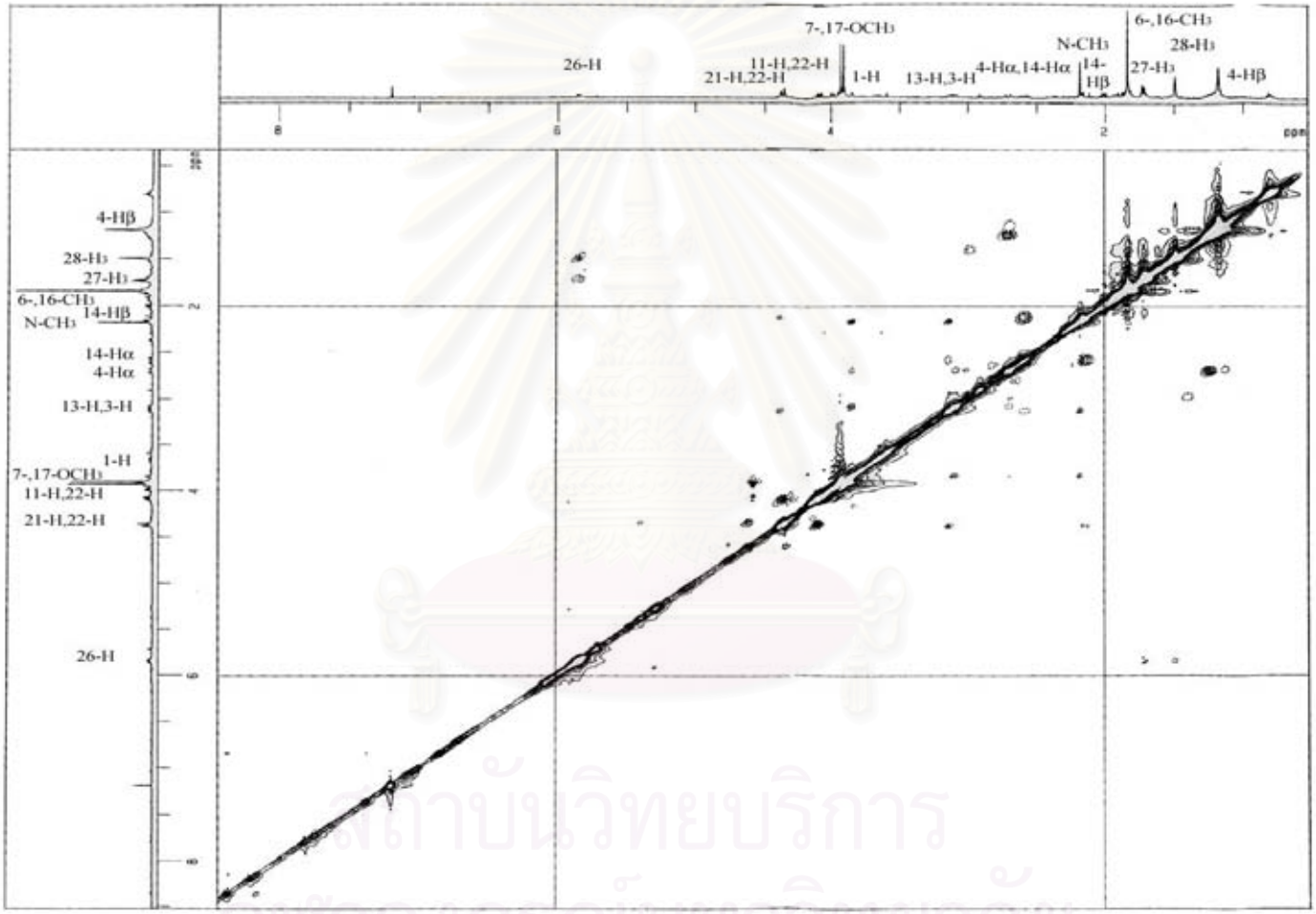

Figure 103 The 500 MHz NOESY- NMR spectrum of renieramycin E in $CDCl_3$

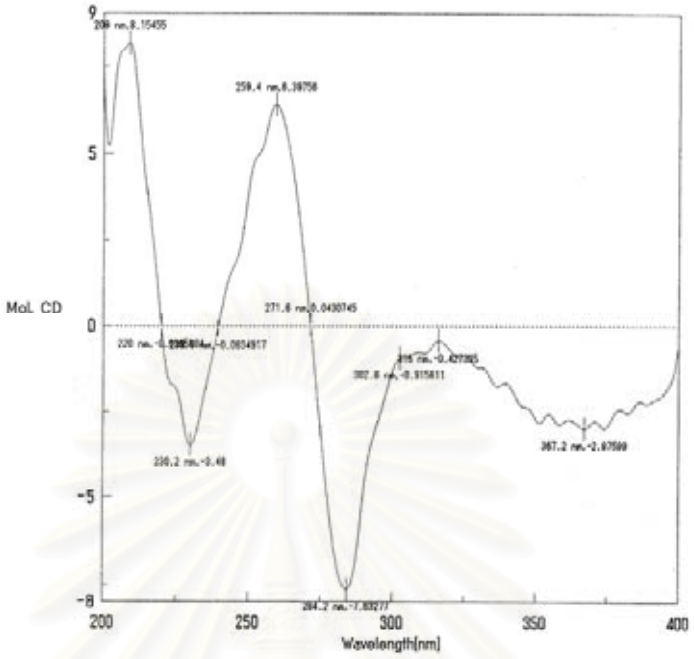

Figure 104 The circular dichroism spectrum of renieramycin J in methanol

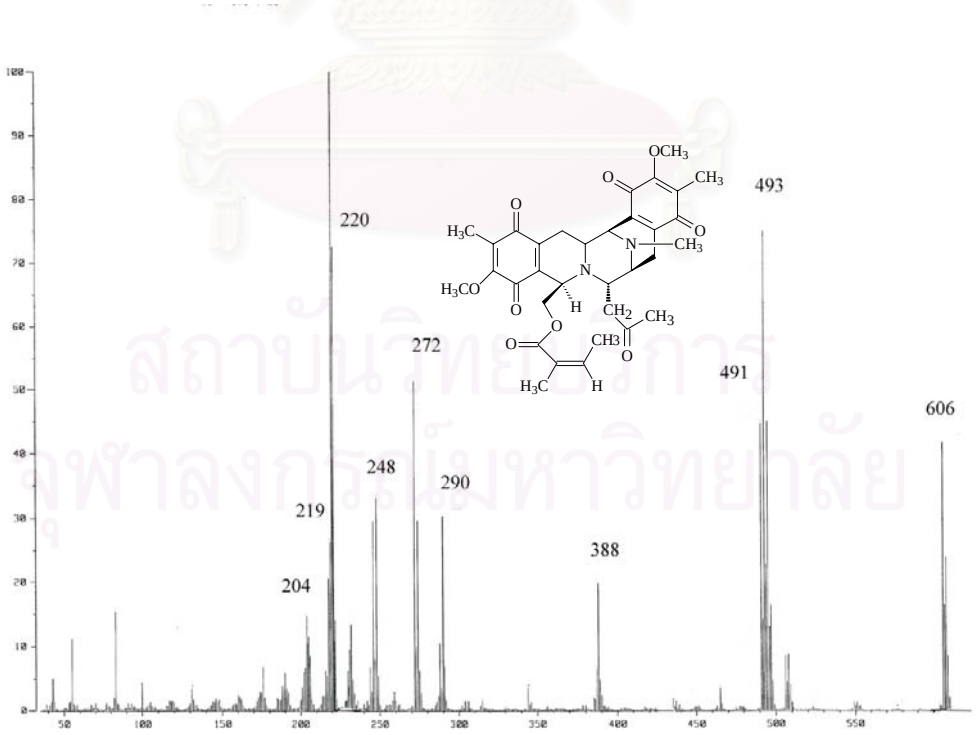

Figure 105 The EI-mass spectrum of reniramycin J

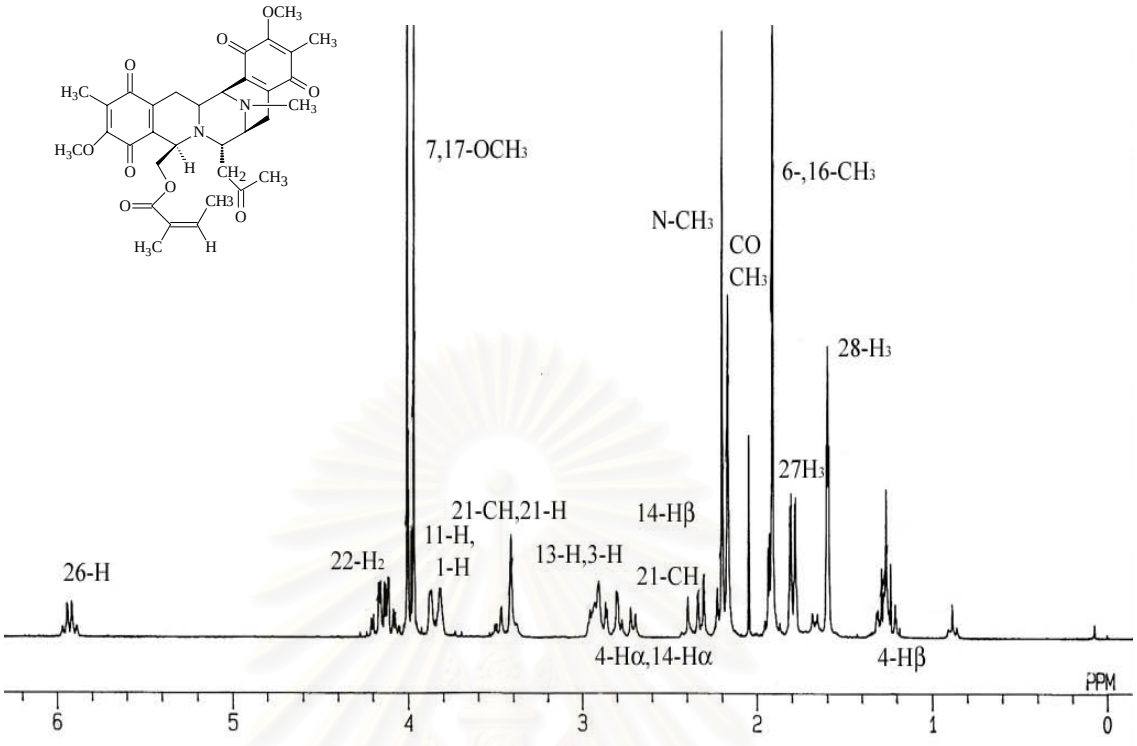

Figure 106 The 500 MHz ^{1}H-NMR spectrum of renieramycin J in $CDCl_3$

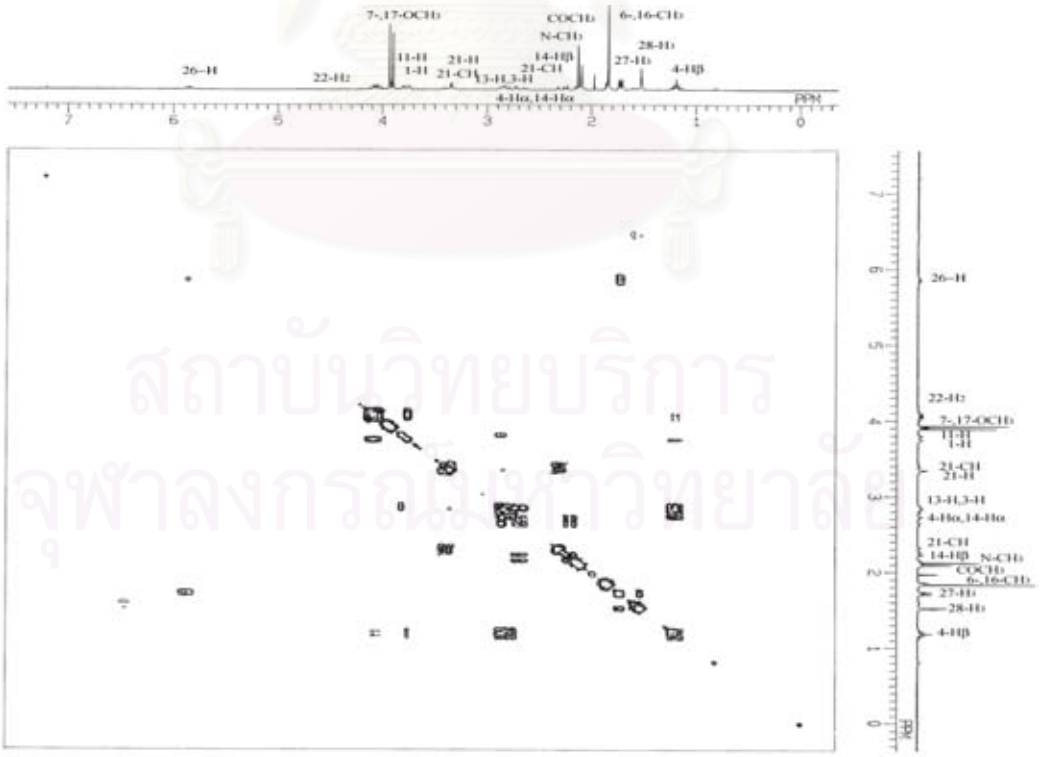

Figure 107 The 500 MHz ^{1}H,^{1}H-COSY NMR spectrum of renieramycin J in $CDCl_3$

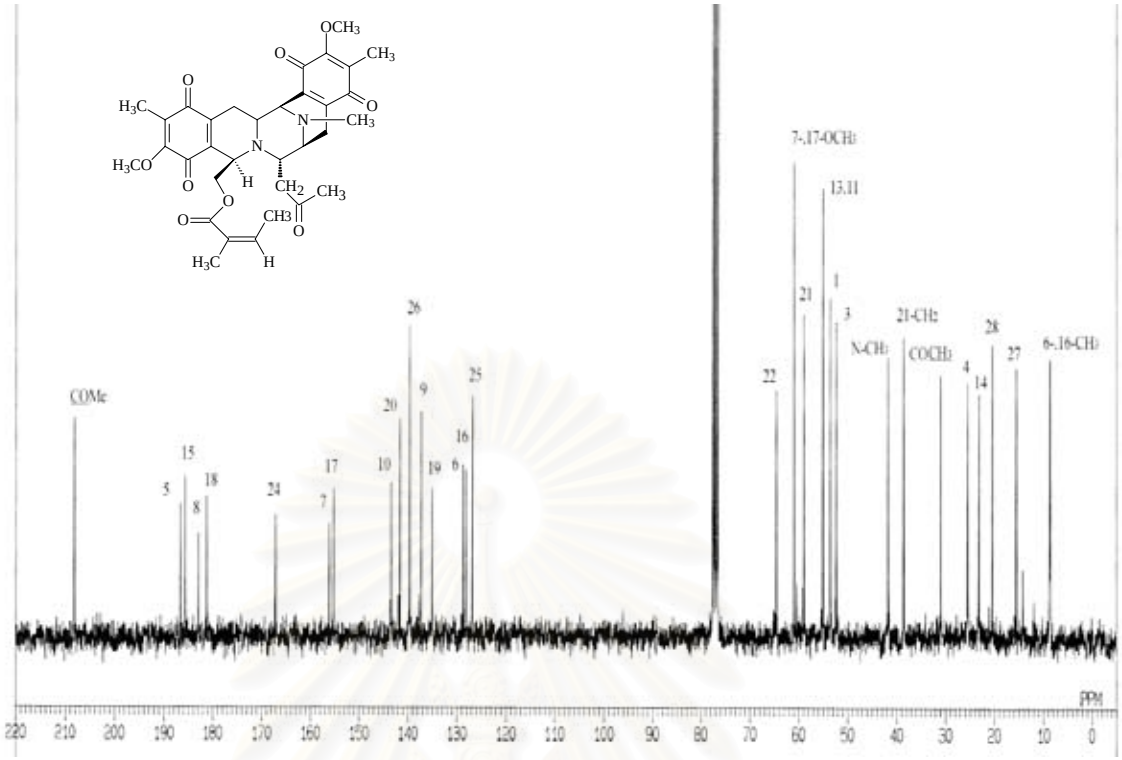

Figure 108 The 125 MHz ^{13}C-NMR spectrum of renieramycin J in $CDCl_3$

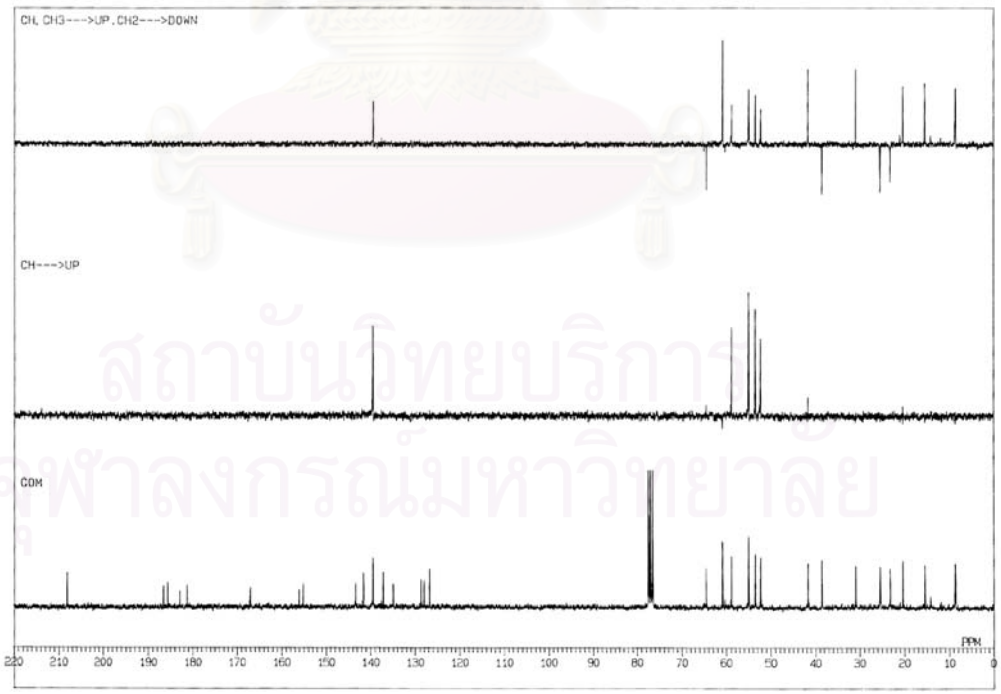

Figure 109 The 125 MHz DEPT carbon NMR spectrum of renieramycin J in $CDCl_3$

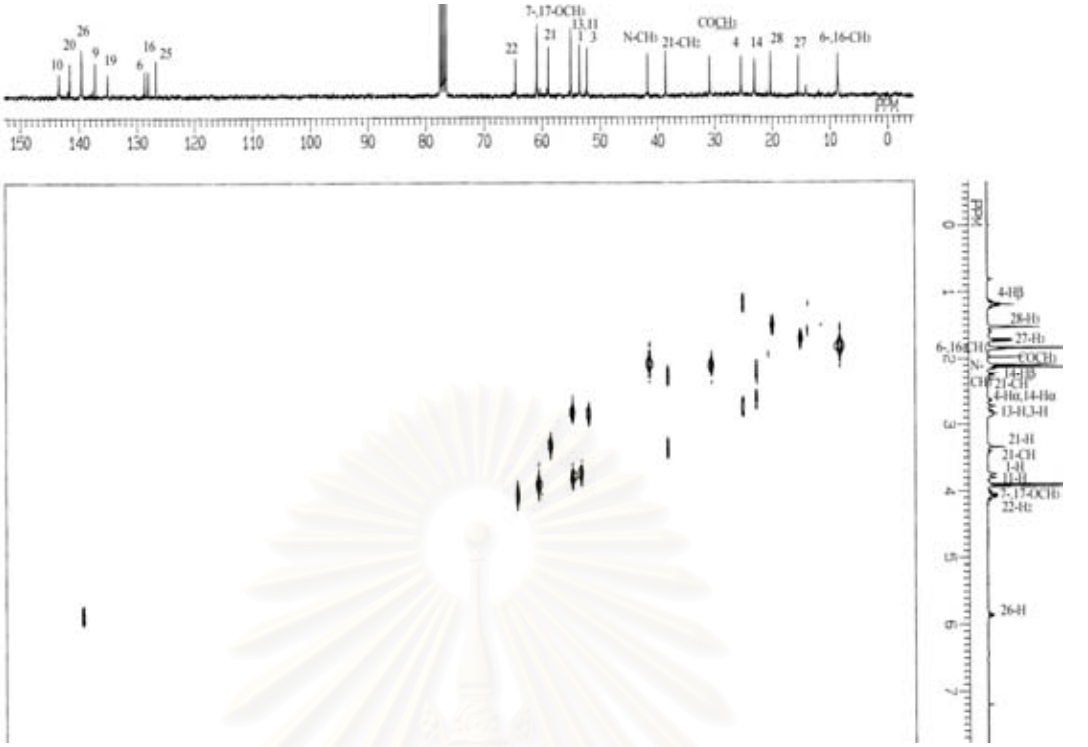

Figure 110 The 500 MHz HMQC spectrum of renieramycin J in $CDCl_3$

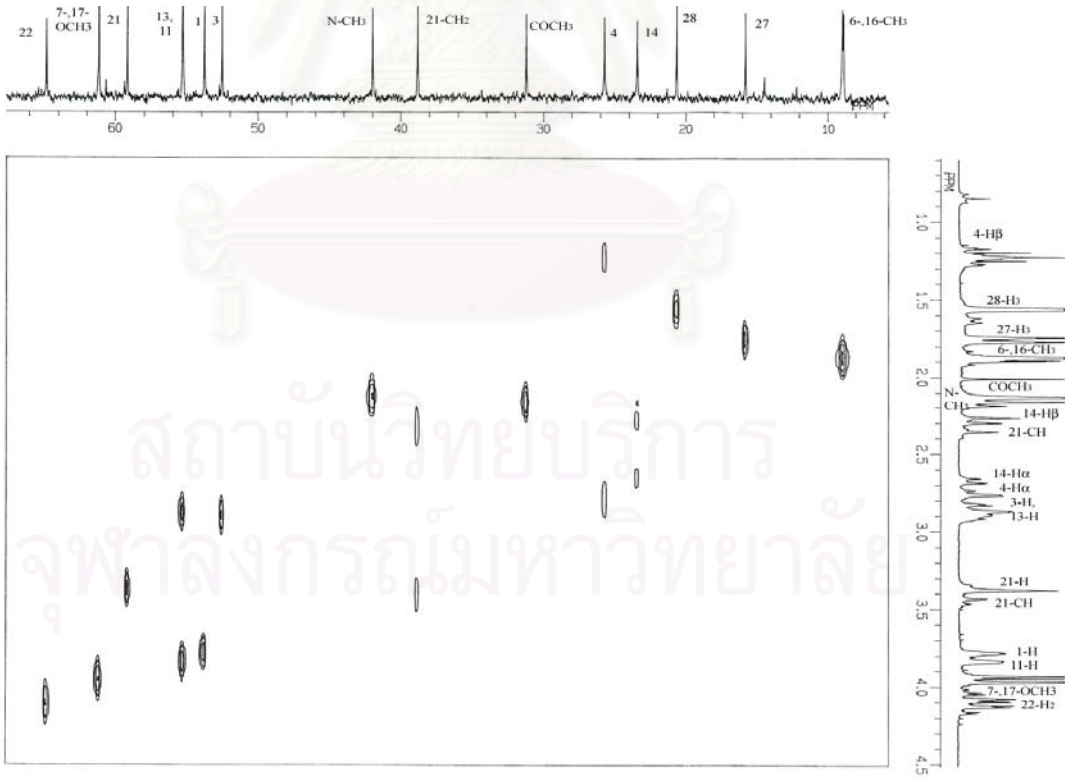

Figure 111 The 500 MHz HMQC spectrum of renieramycin J in $CDCl_3$ (expanded from δ_H 0.60-4.50 ppm and δ_C 6.00-66.00 ppm)

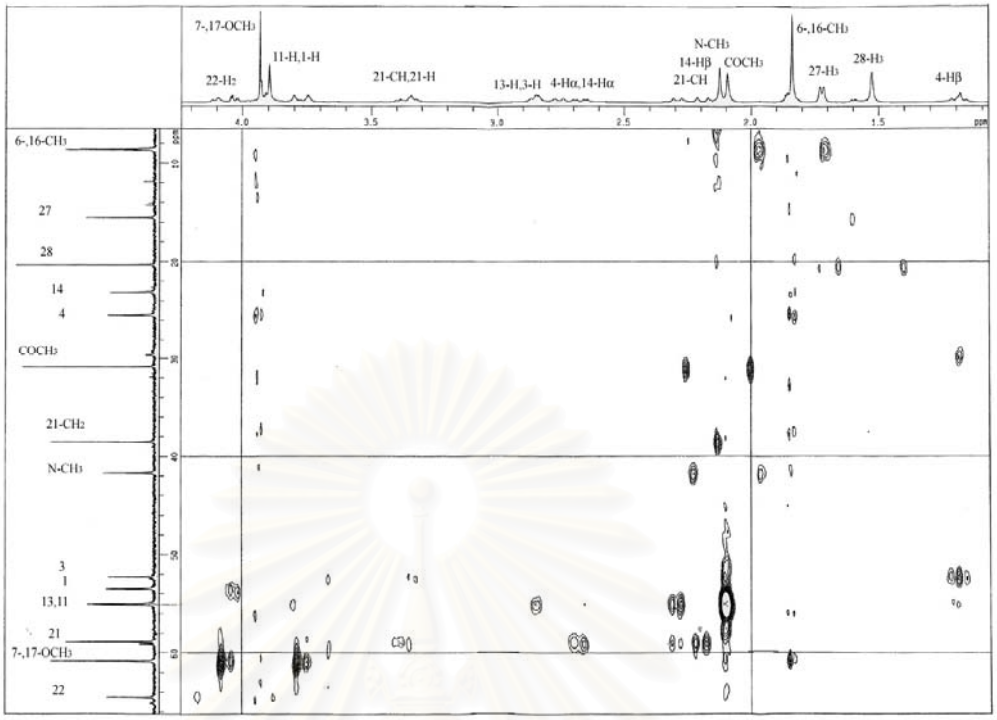

Figure 112 The 500 MHz HMBC spectrum of renieramycin J in $CDCl_3$

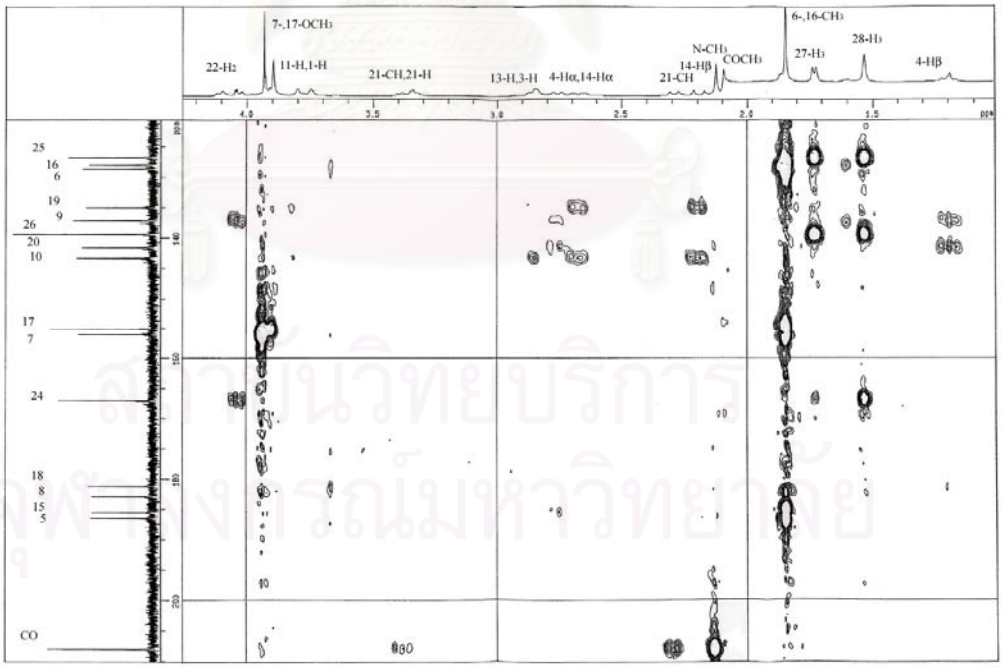

Figure 113 The 500 MHz HMBC spectrum of renieramycin J in $CDCl_3$ (expanded from δ_H 1.10-4.20 ppm and δ_C 120.00-210.00 ppm)

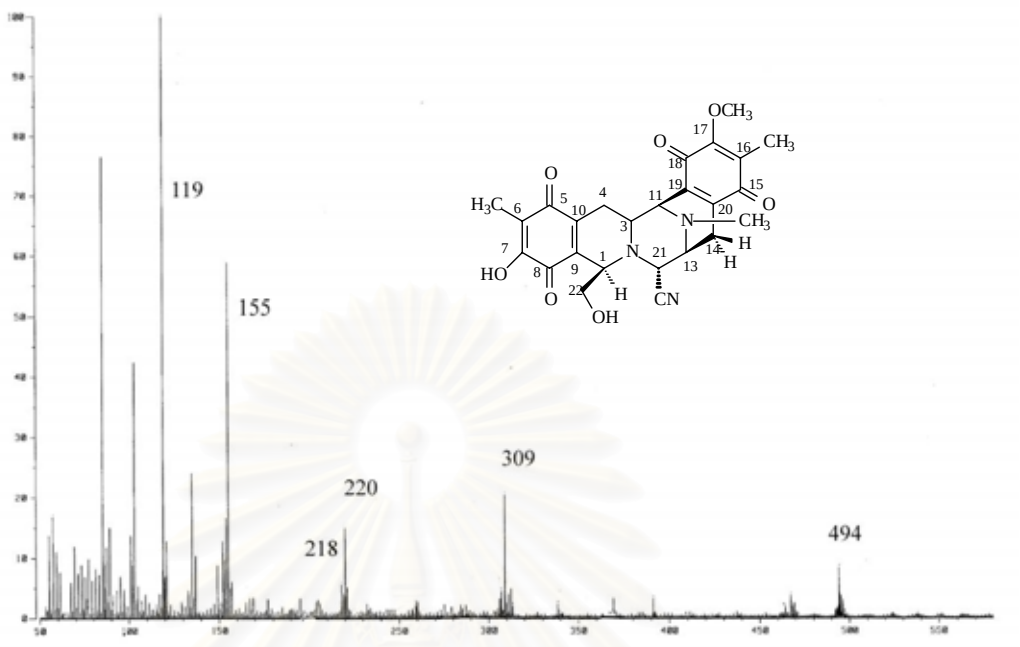

Figure 114 The FAB-mass spectrum of deangeloyl reniramycin M

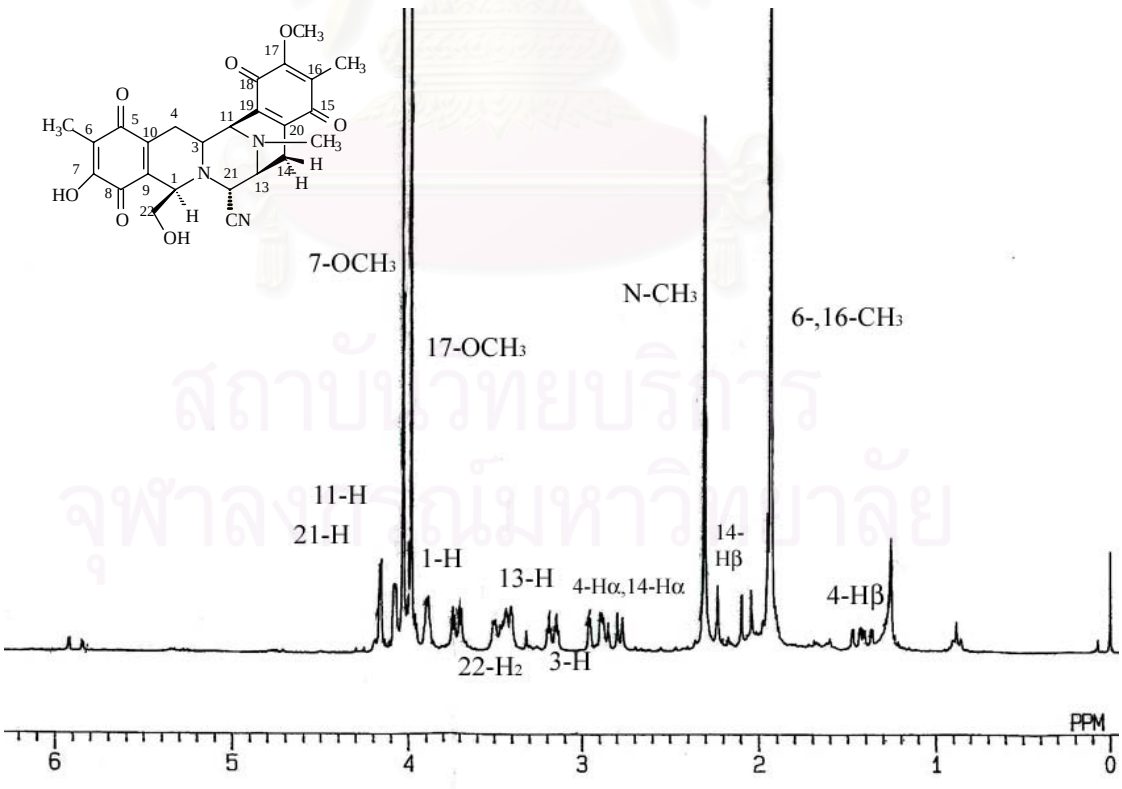

Figure 115 The 500 MHz ^{1}H-NMR spectrum of deangeloyl renieramycin M in $CDCl_3$

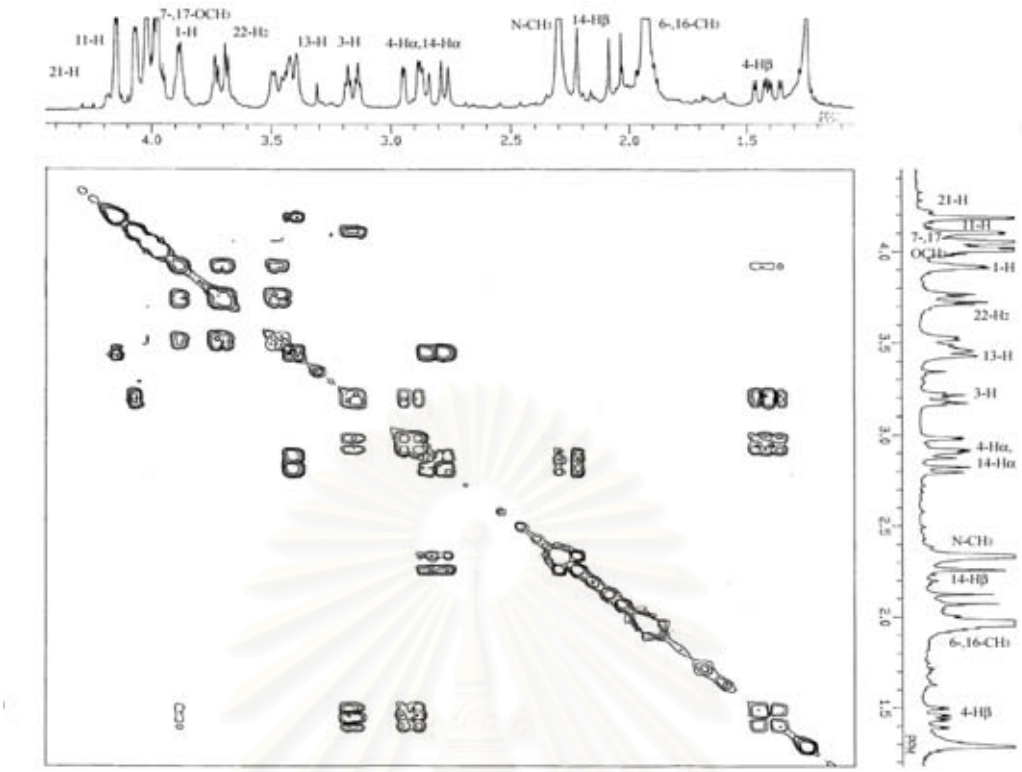

Figure 116 The 500 MHz $^{1}H,^{1}H$-COSY spectrum of deangeloyl renieramycin M in $CDCl_3$ (expanded from δ_H 1.10-4.40 ppm)

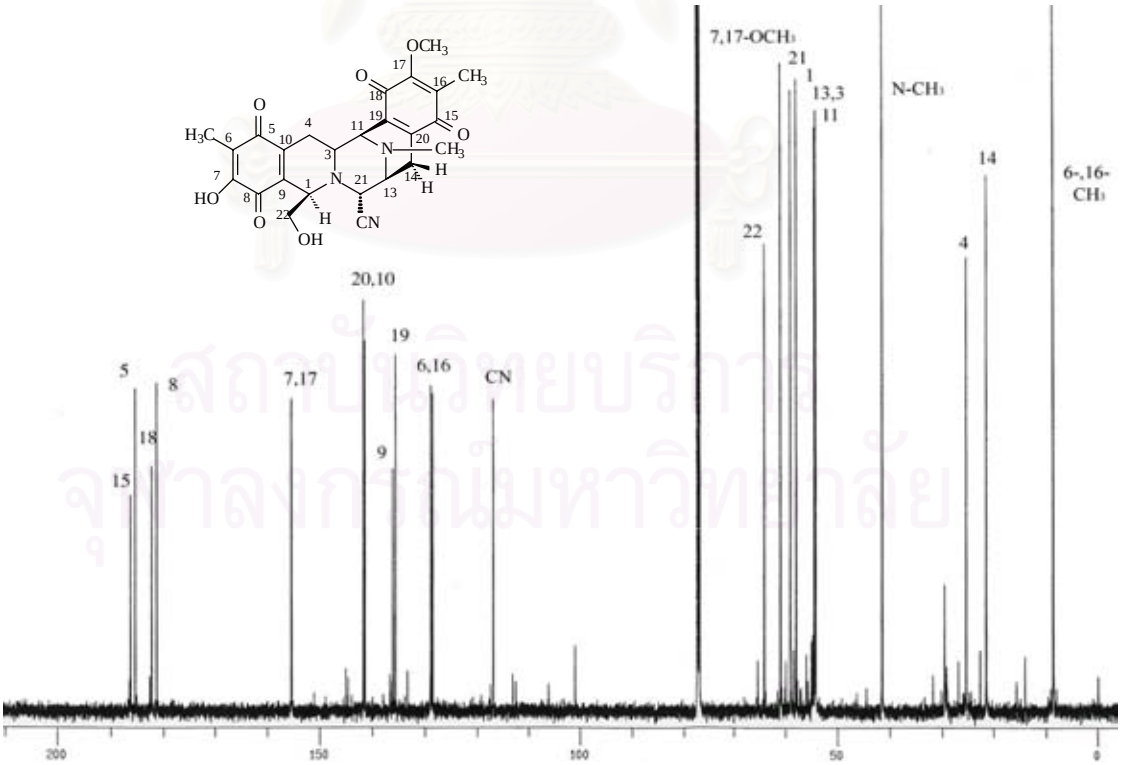

Figure 117 The 125 MHz ^{13}C-NMR spectrum of deangeloyl renieramycin M in $CDCl_3$

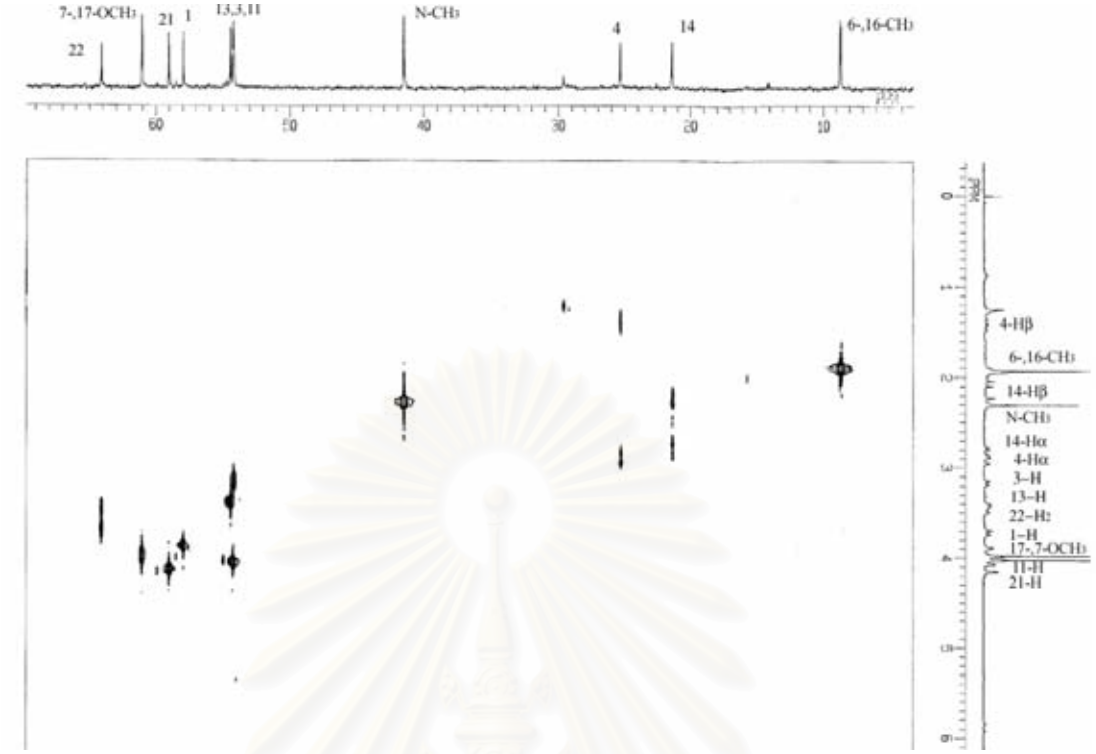

Figure 118 The 500 MHz HMQC spectrum of deangeloyl renieramycin M in $CDCl_3$

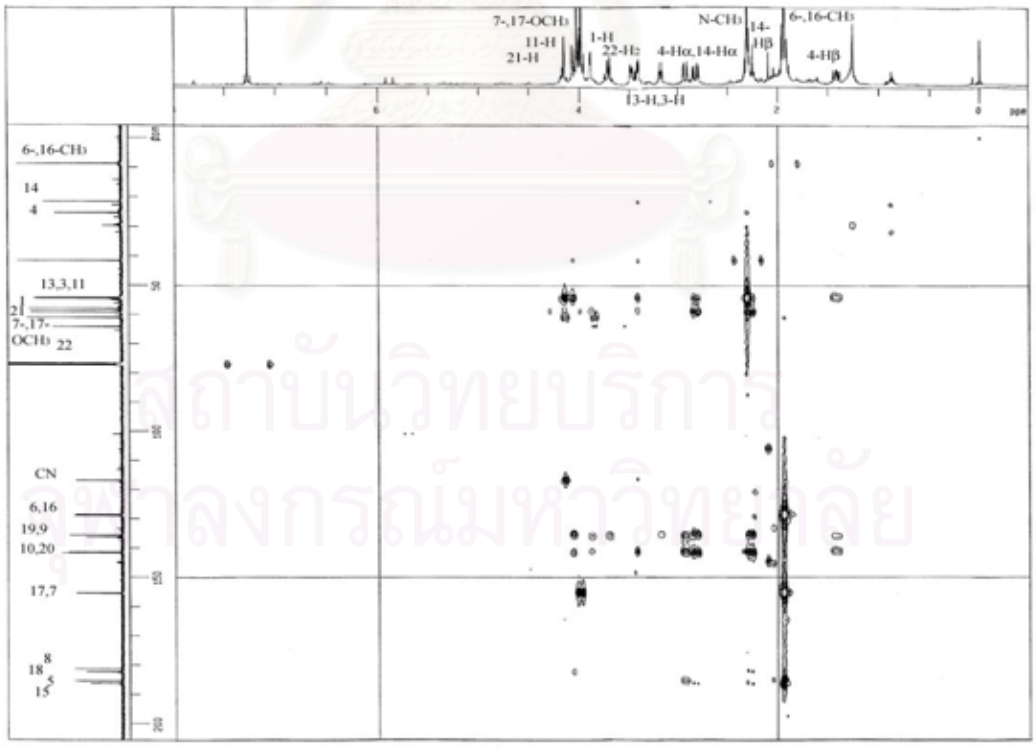

Figure 119 The 500 MHz HMBC spectrum of deangeloyl renieramycin M in $CDCl_3$

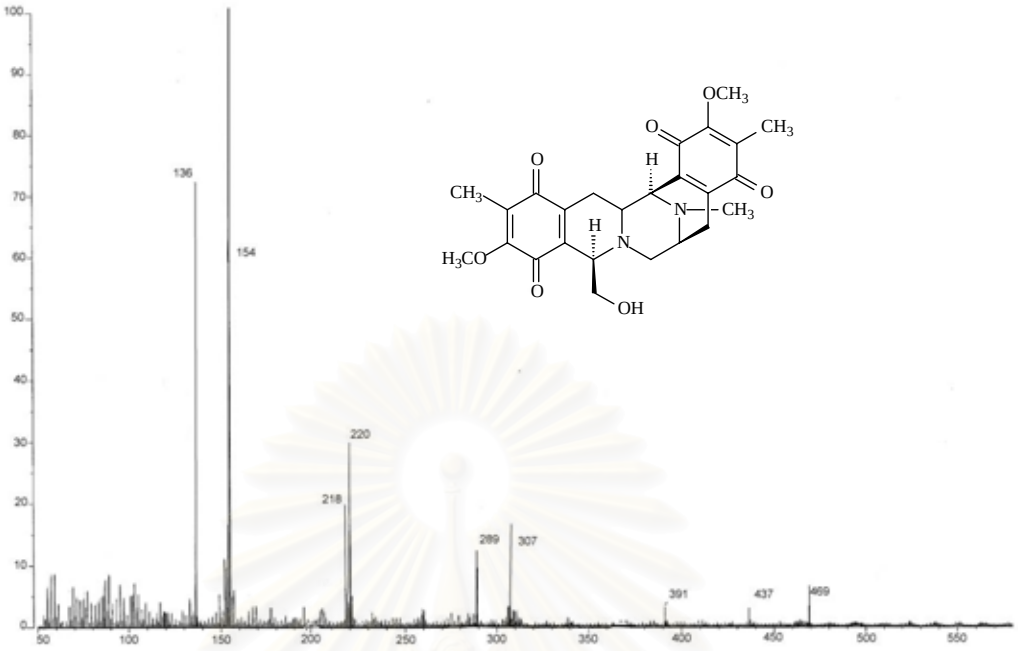

Figure 120 The FAB-mass spectrum of decyano deangeloyl reniramycin M

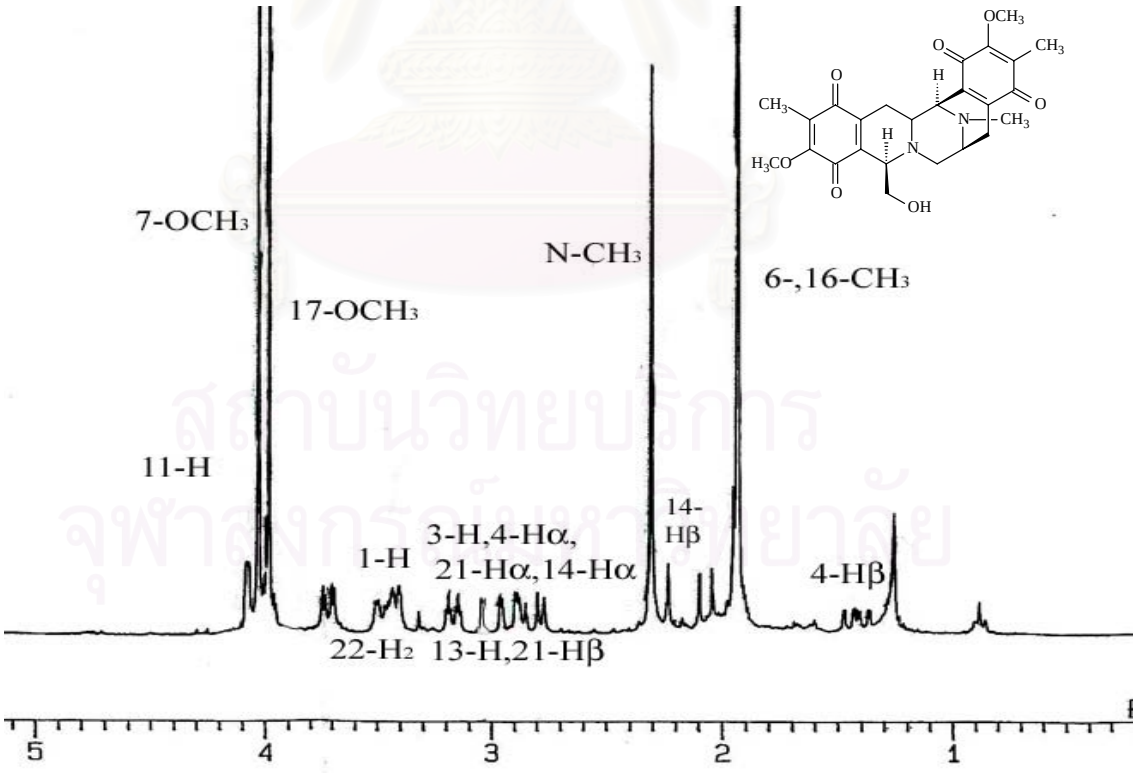

Figure 121 The 500 MHz ^{1}H-NMR spectrum of decyano deangeloyl renieramycin M in $CDCl_3$

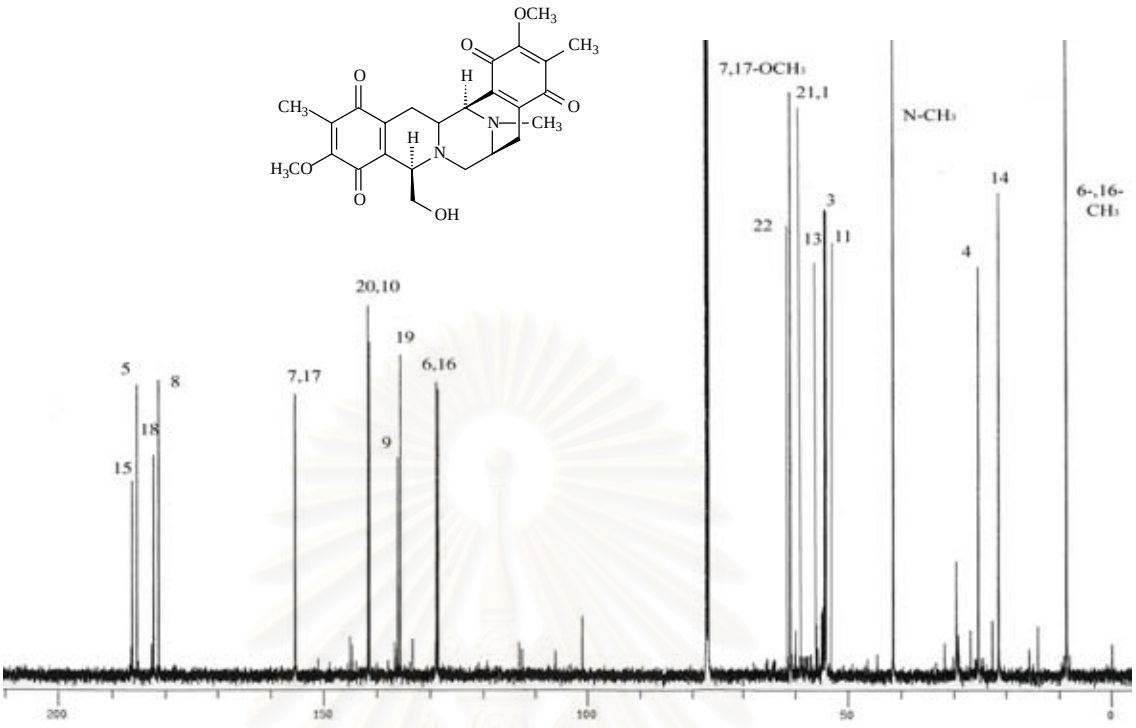

Figure 122 The 125 MHz ^{13}C-NMR spectrum of decyano deangeloyl renieramycin M in $CDCl_3$

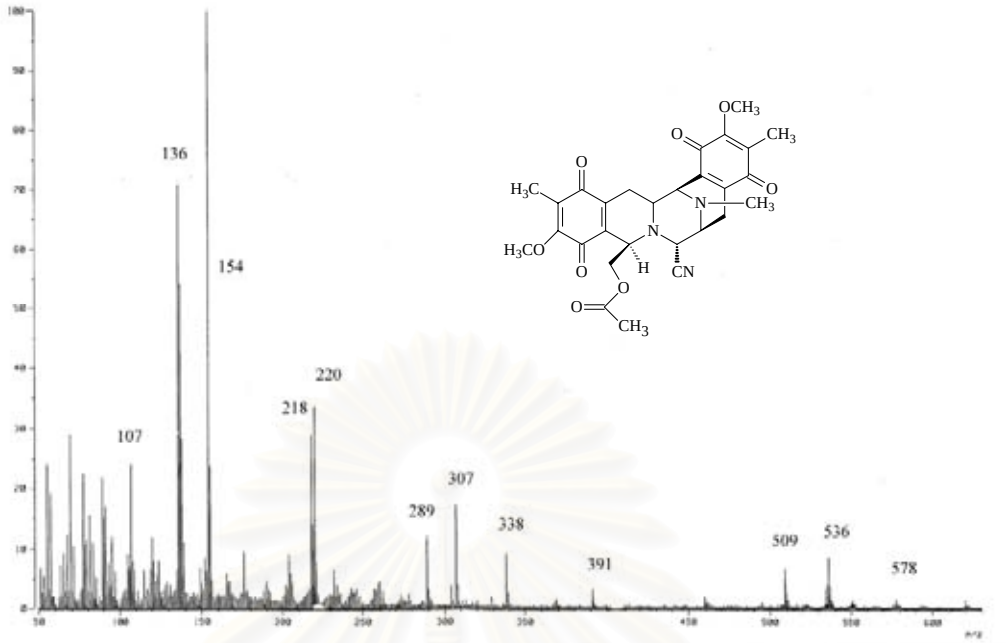

Figure 123 The EI-mass spectrum of cyanojorumycin

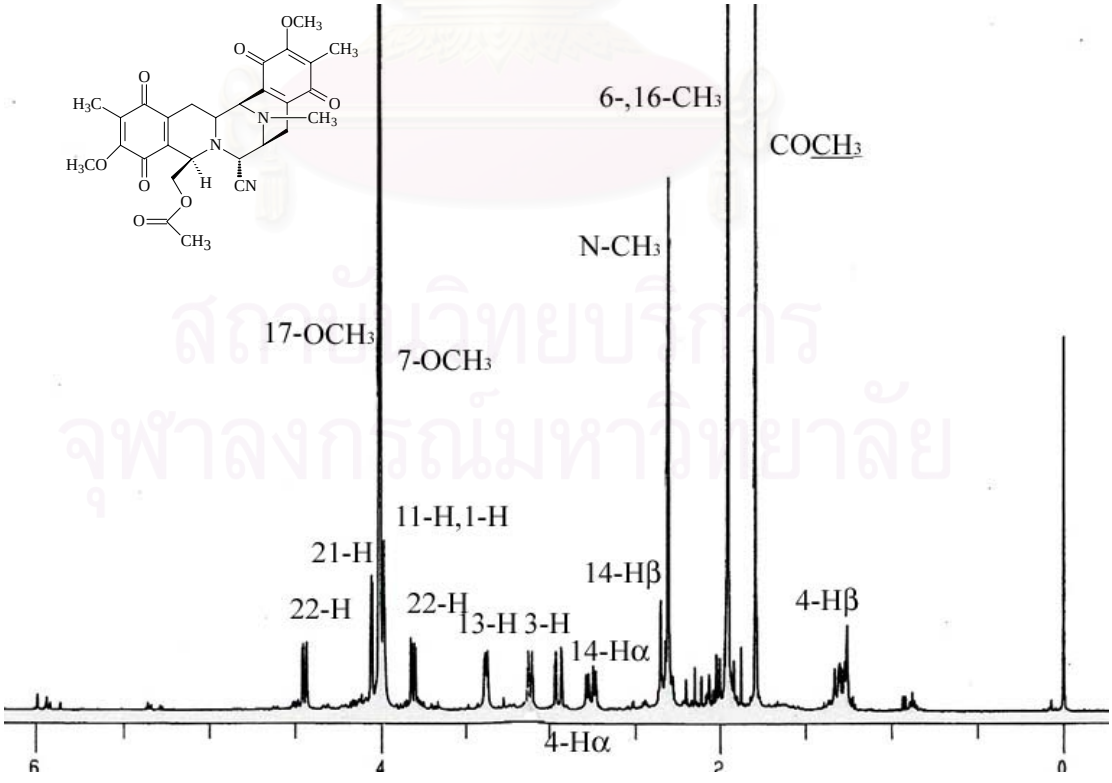

Figure 124 The 500 MHz ^{1}H-NMR spectrum of cyanojorumycin in $CDCl_3$

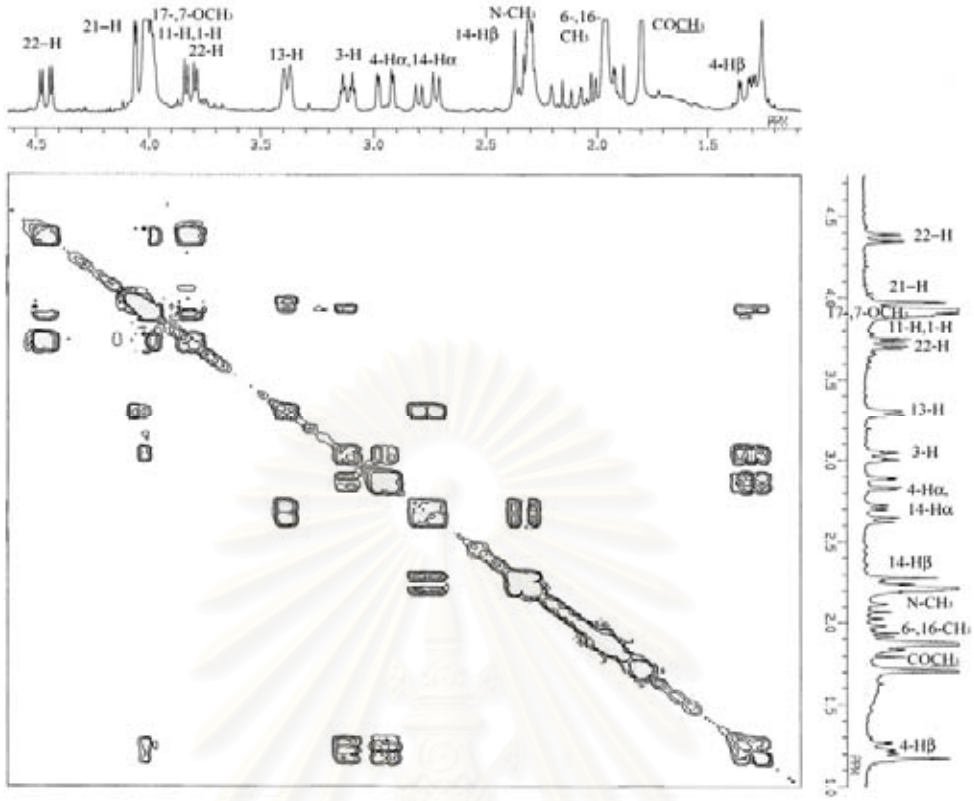

Figure 125 The 500 MHz $^{1}H,^{1}H$-COSY spectrum of cyanojorumycin in $CDCl_3$

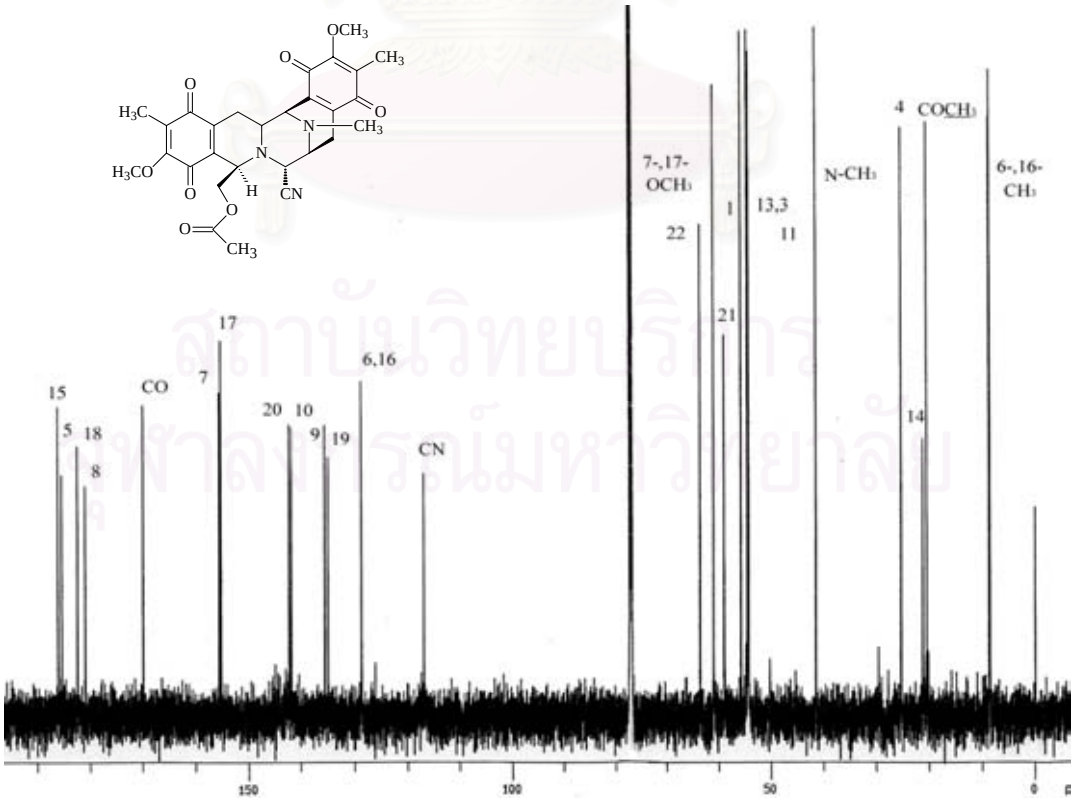

Figure 126 The 125 MHz ^{13}C-NMR spectrum of cyanojorumycin in $CDCl_3$

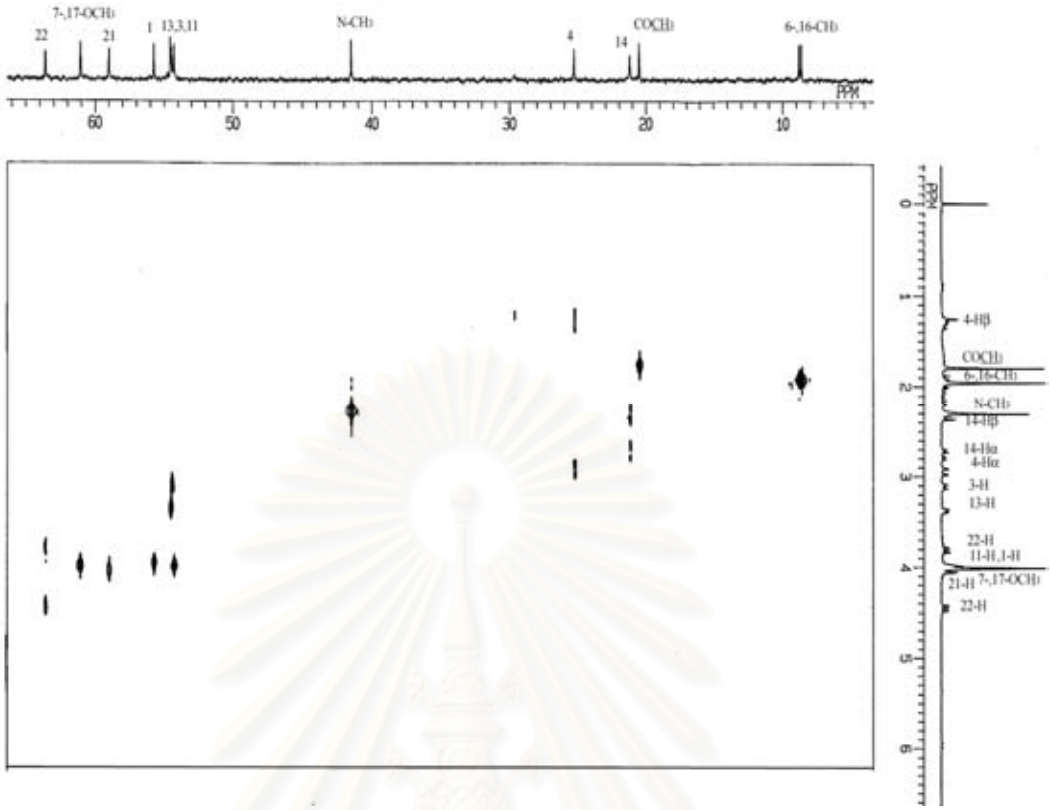

Figure 127 The 500 MHz HMQC spectrum of cyanojorumycin in $CDCl_3$

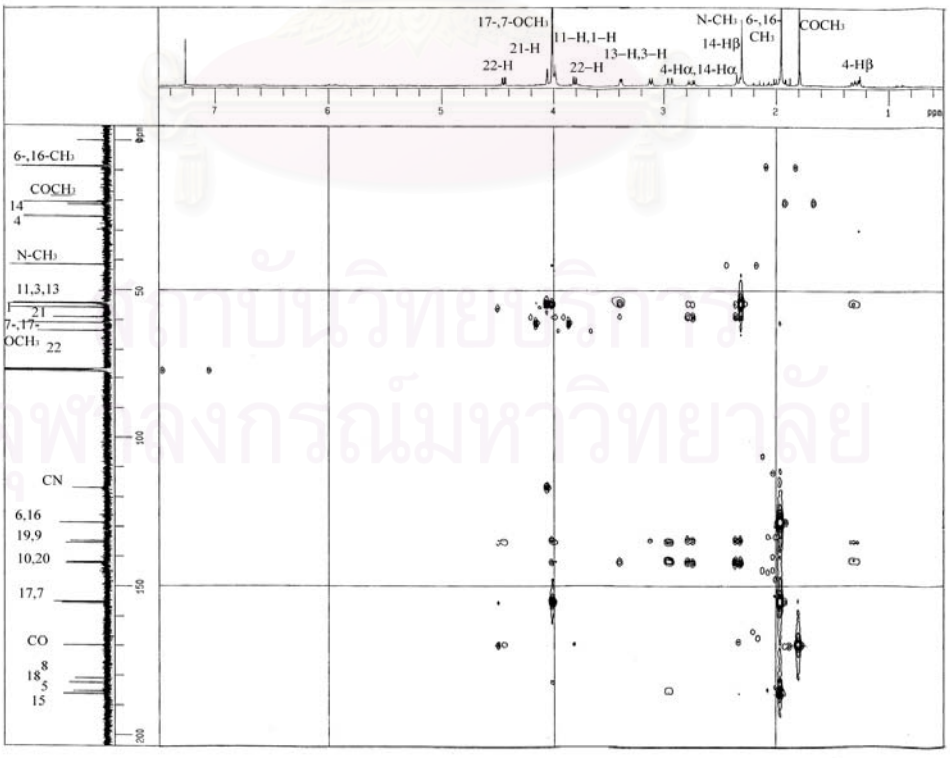

Figure 128 The 500 MHz HMBC spectrum of cyanojorumycin in $CDCl_3$

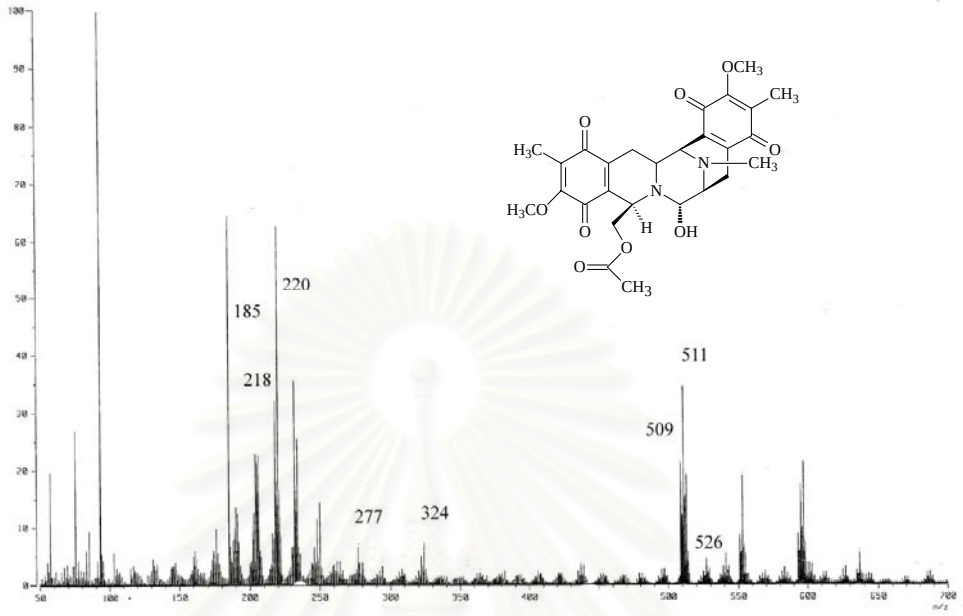

Figure 129 The EI-mass spectrum of jorumycin

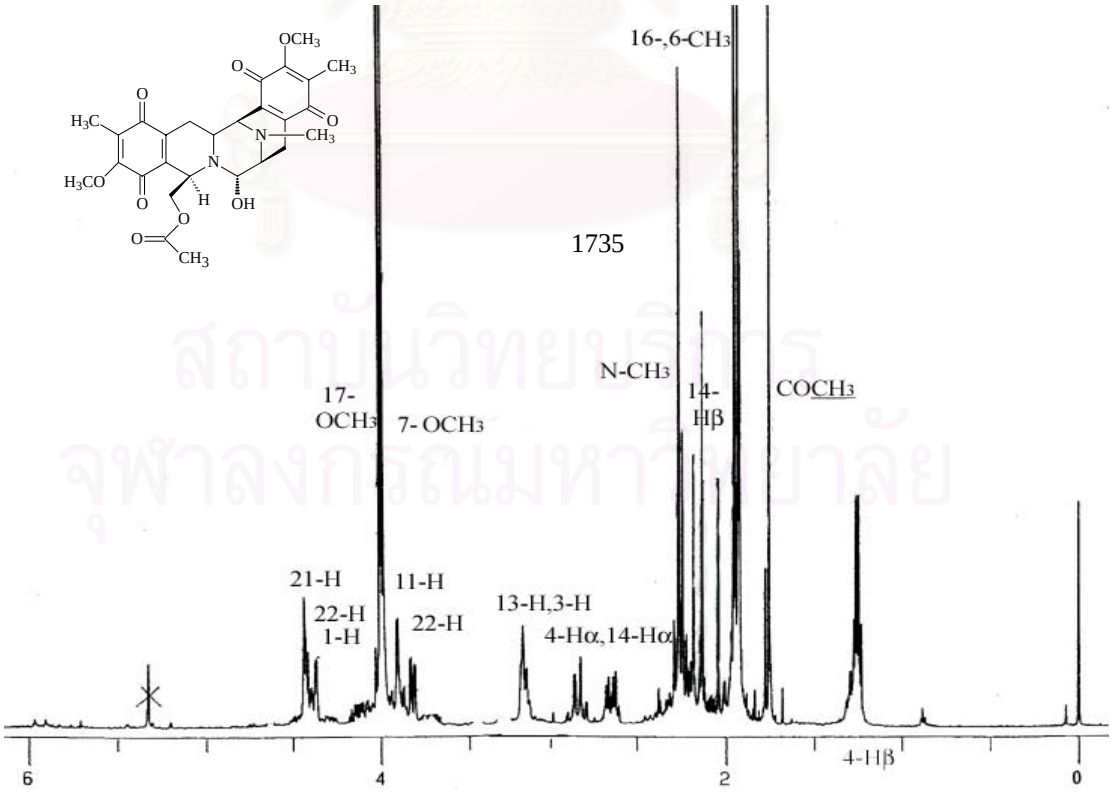

Figure 130 The 500 MHz ^{1}H-NMR spectrum of jorumycin in $CDCl_3$

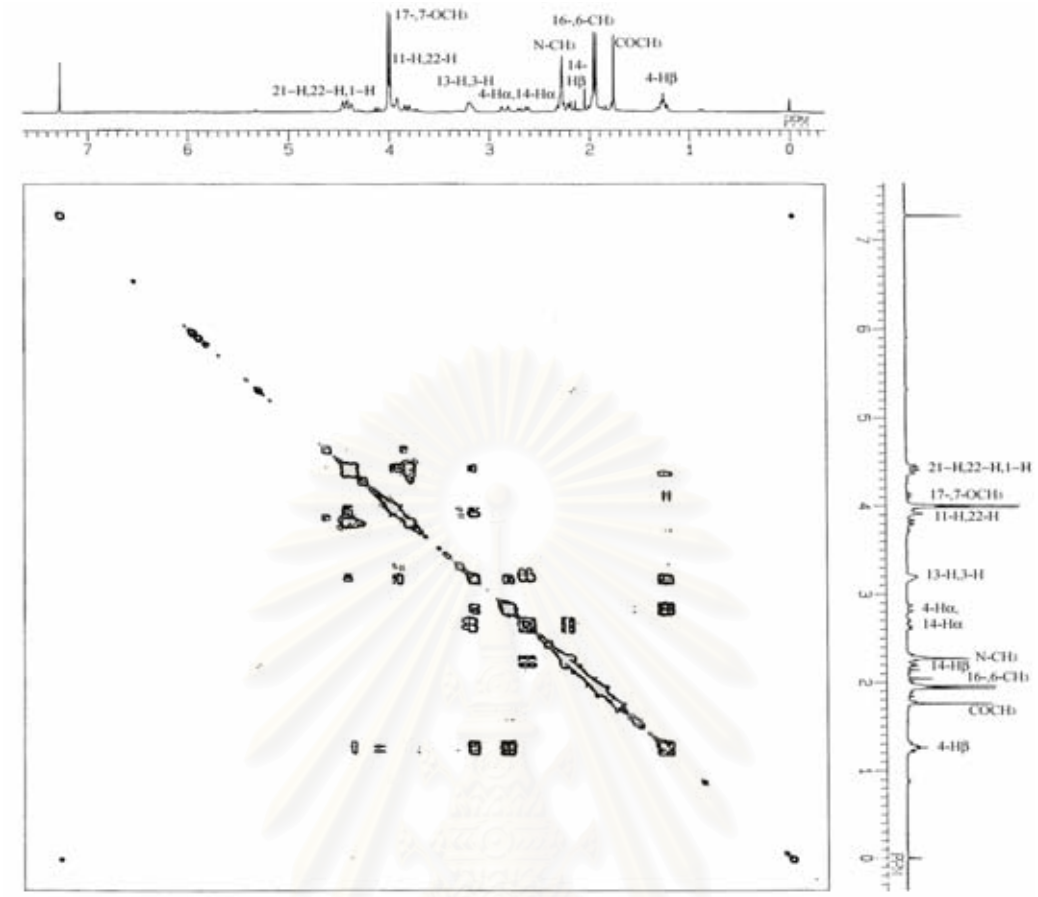

Figure 131 The 500 MHz $^{1}H,^{1}H$-COSY spectrum of jorumycin in $CDCl_3$

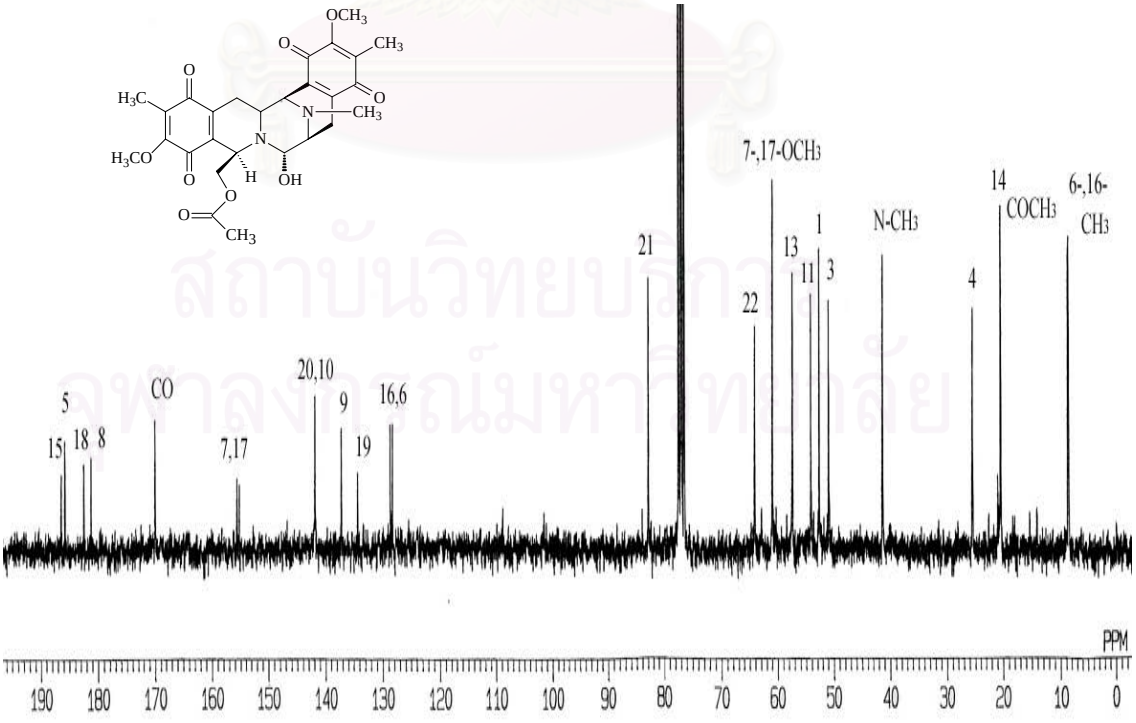

Figure 132 The 125 MHz ^{13}C-NMR spectrum of jorumycin in $CDCl_3$

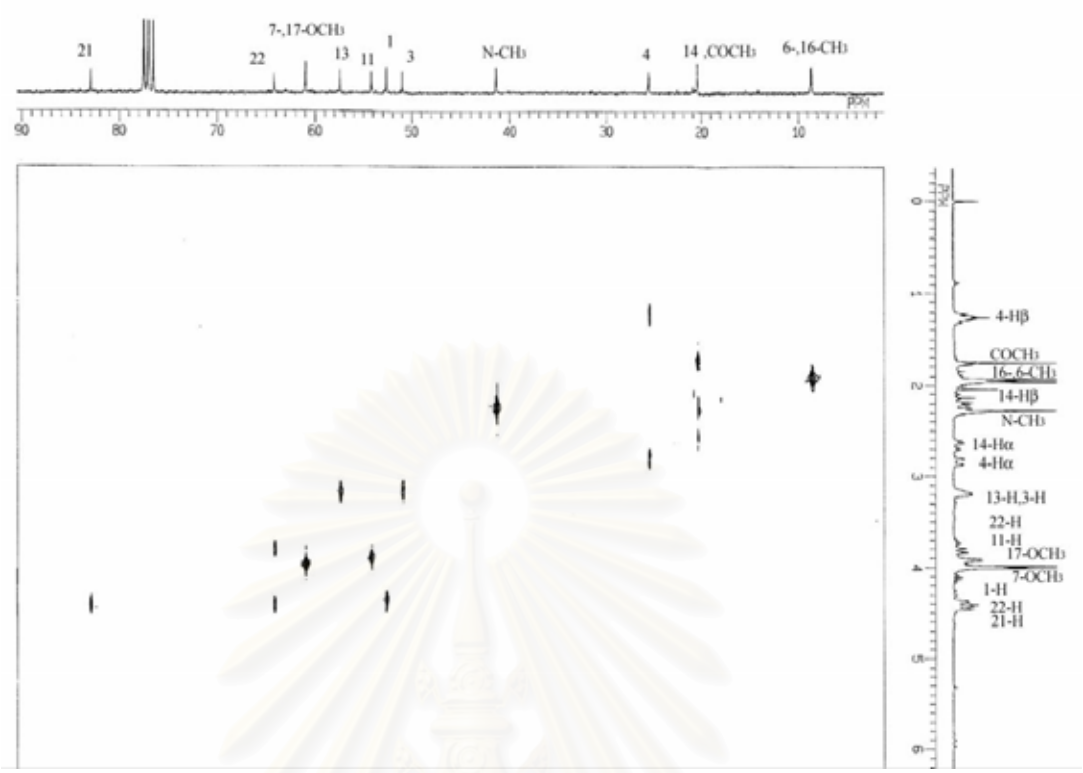

Figure 133 The 500 MHz HMQC spectrum of jorumycin in $CDCl_3$

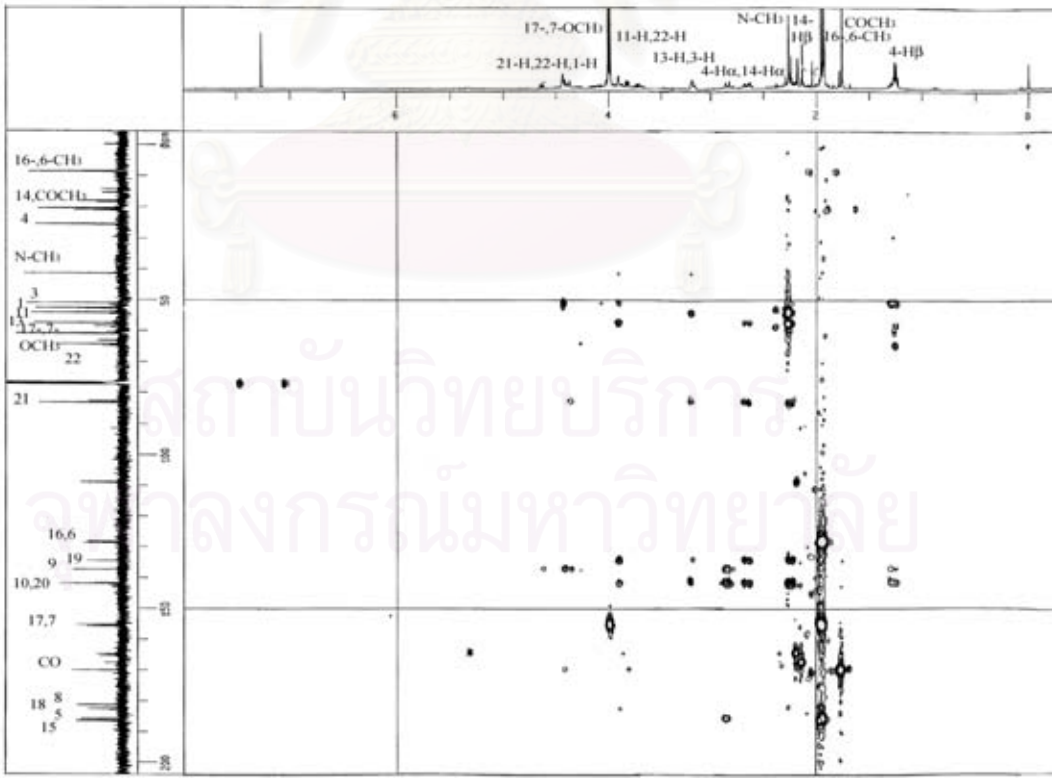

Figure 134 The 500 MHz HMBC spectrum of jorumycin in $CDCl_3$

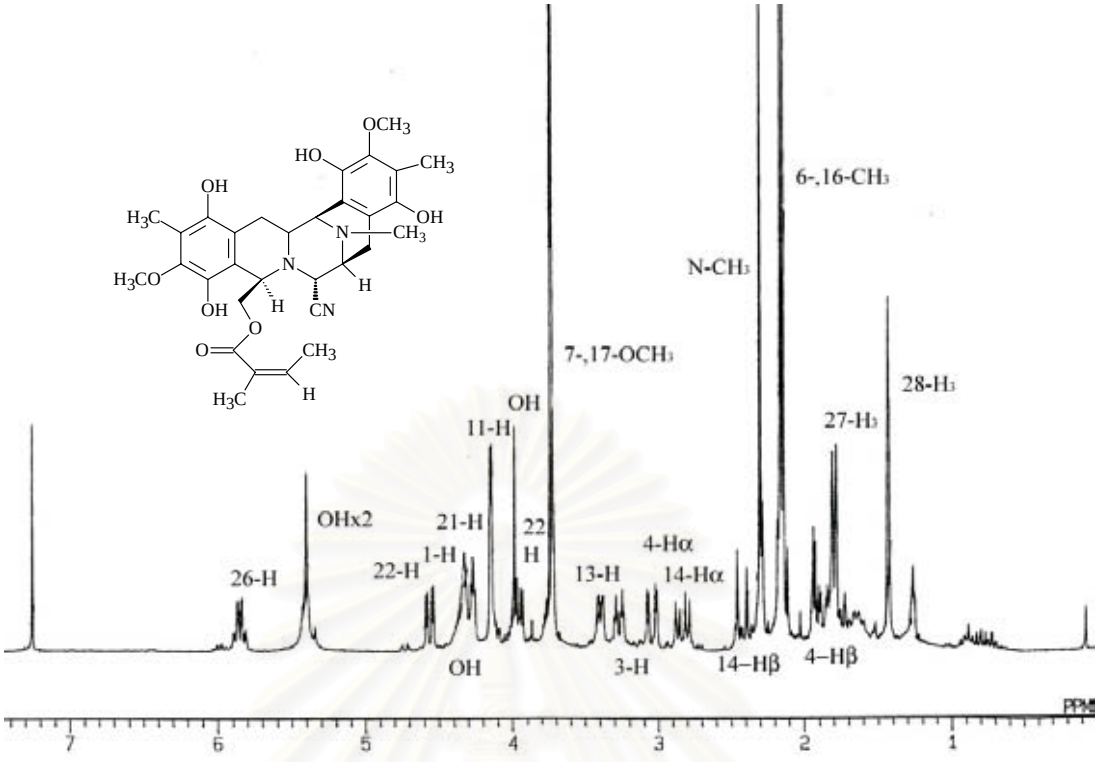

Figure 135 The 270 MHz ^{1}H-NMR spectrum of bishydroquinone renieramycin M in $CDCl_3$

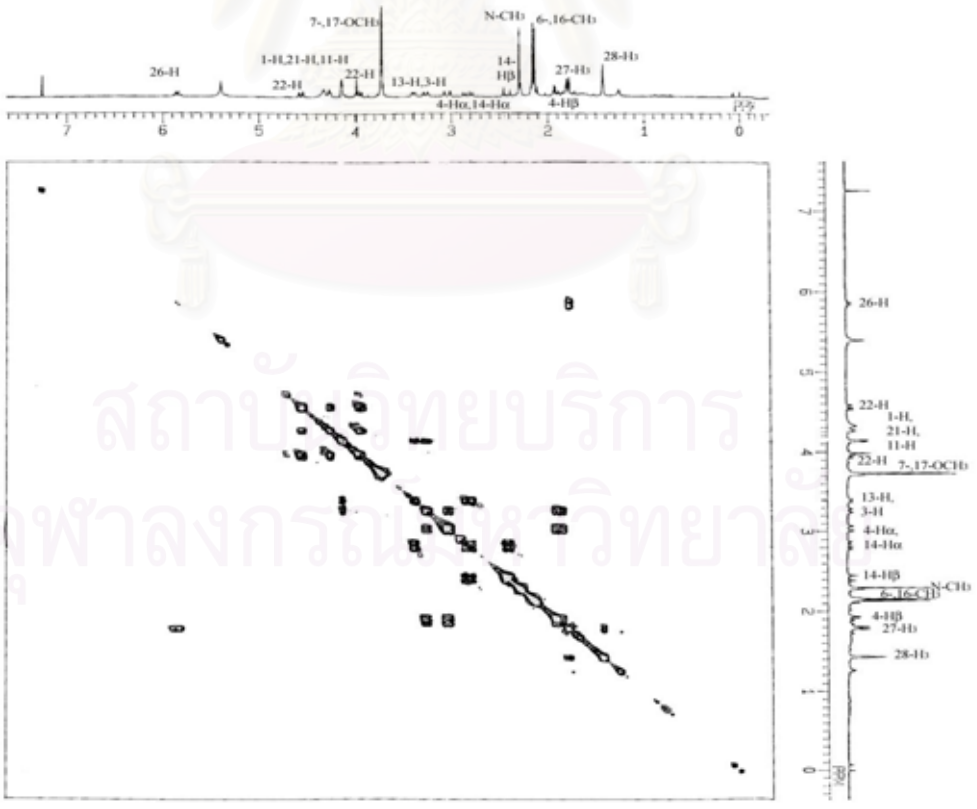

Figure 136 The 270 MHz ^{1}H,^{1}H-COSY NMR spectrum of bishydroquinone renieramycin M in $CDCl_3$

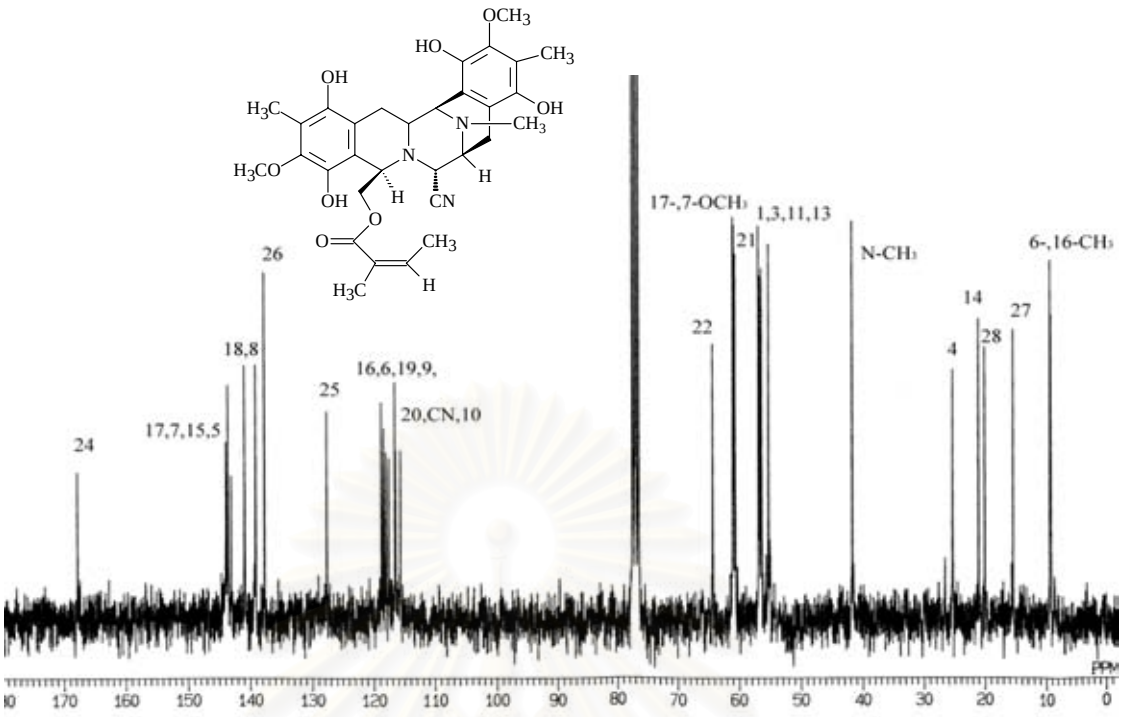

Figure 137 The 67.5 MHz ^{13}C-NMR spectrum of bishydroquinone renieramycin M in $CDCl_3$

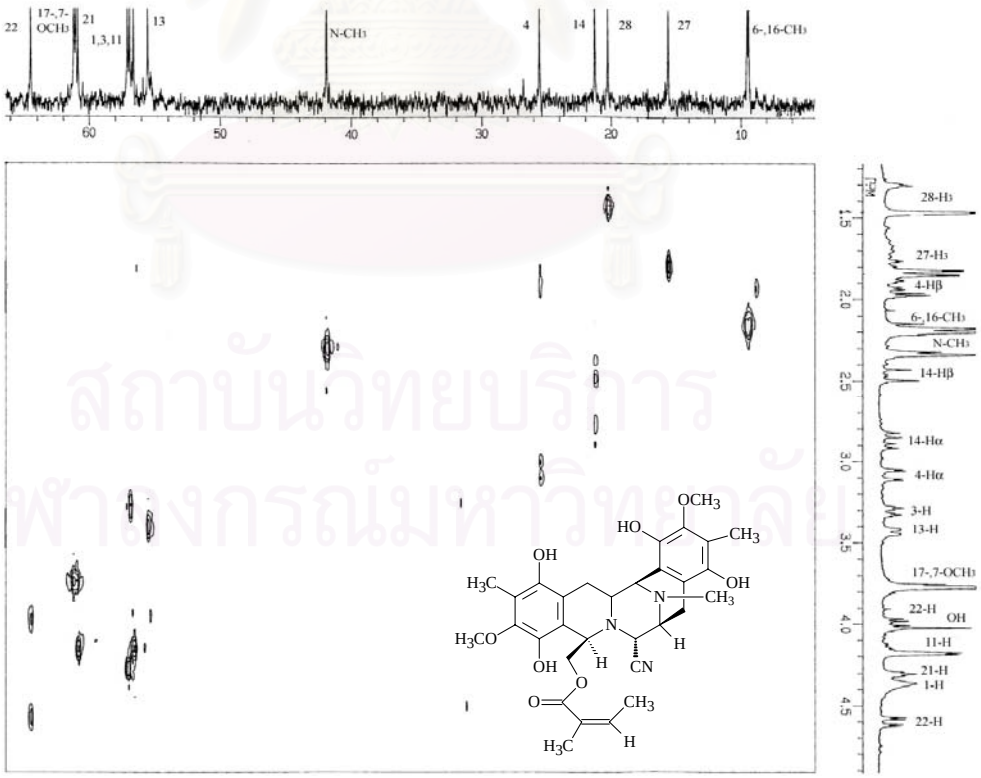

Figure 138 The 270 MHz HMQC spectrum of bishydroquinone renieramycin M in $CDCl_3$ (expanded from δ_H 1.20-4.90 ppm and δ_C 6.00-66.00 ppm)

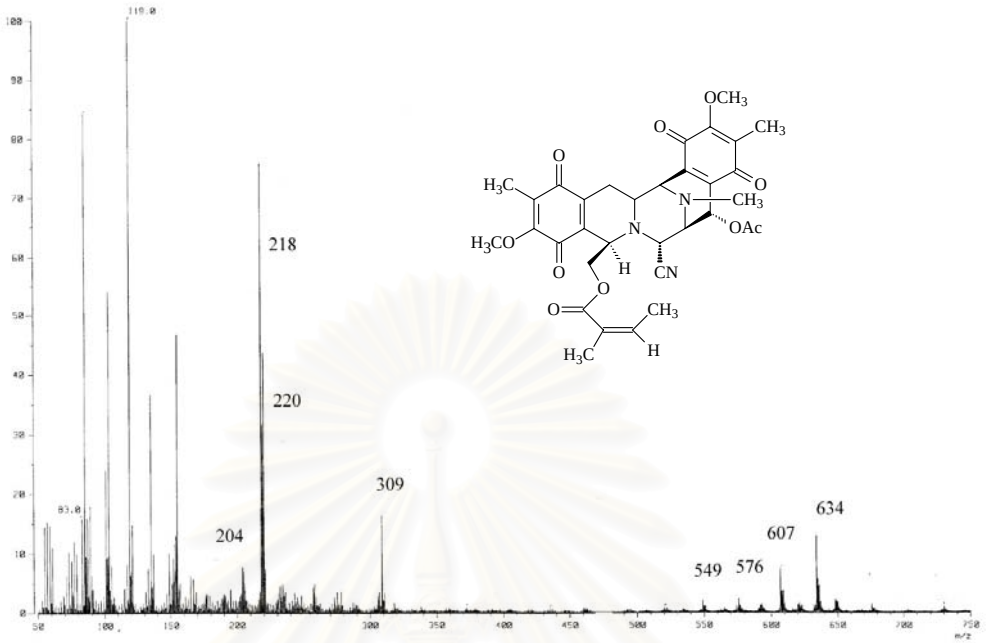

Figure 139 The EI-mass spectrum of 14-*O*-acetyl renieramycin O

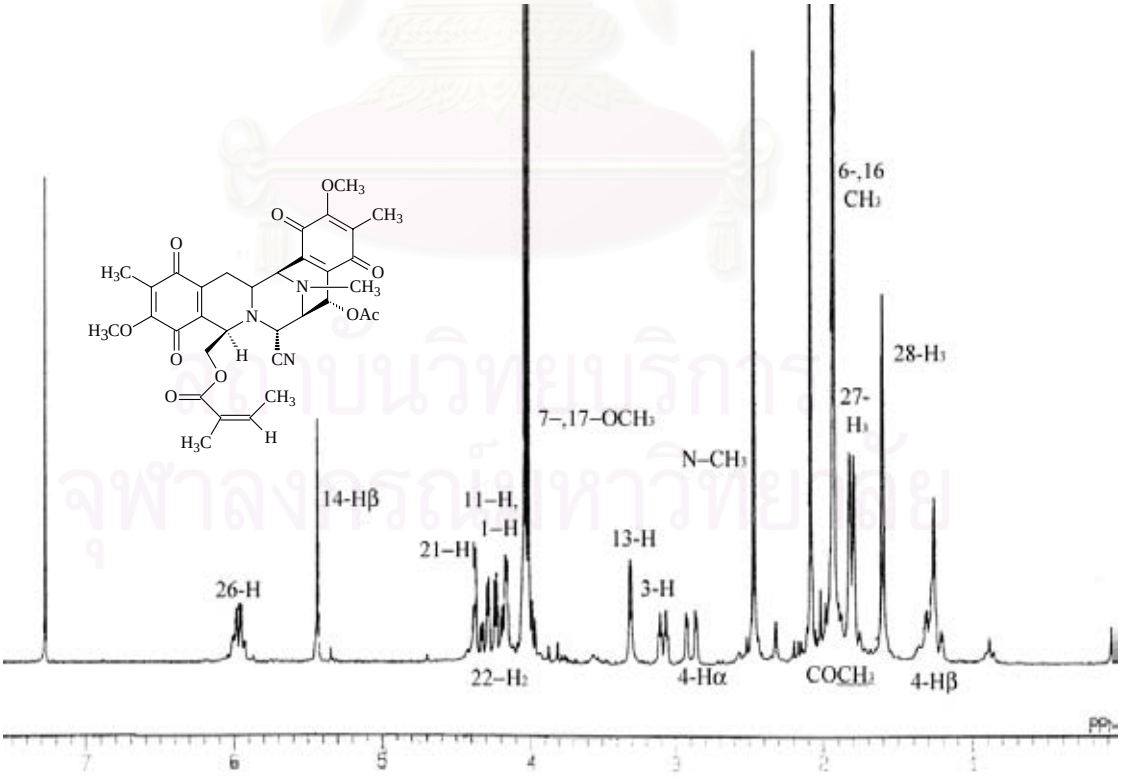

Figure 140 The 270 MHz ^{1}H-NMR spectrum of 14-*O*-acetyl renieramycin O in $CDCl_3$

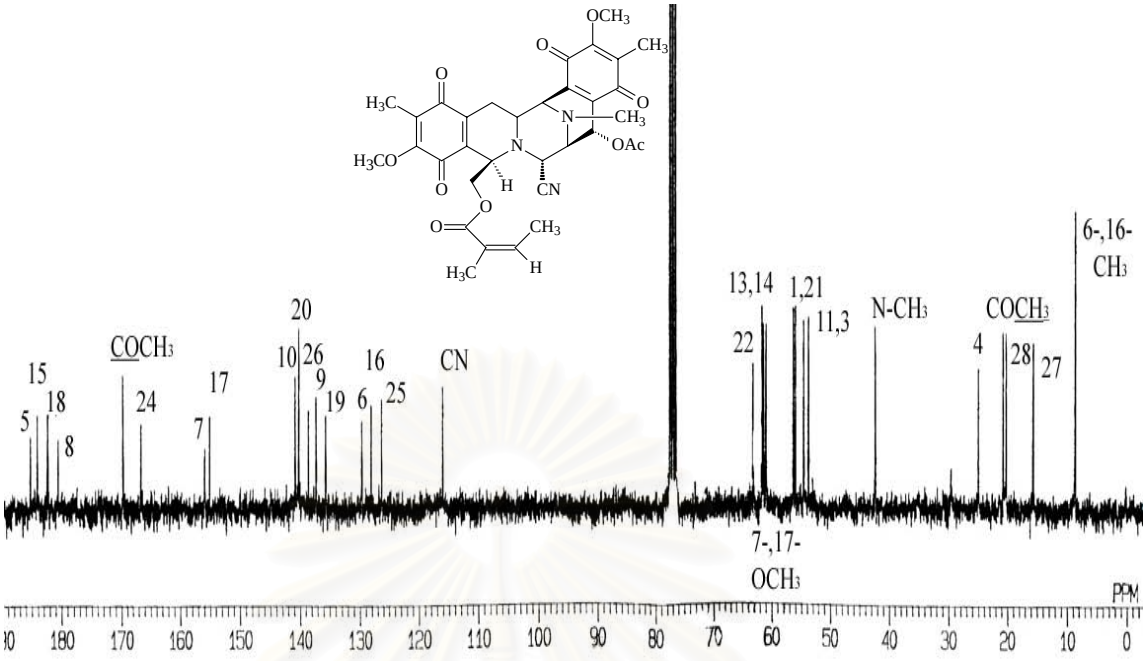

Figure 141 The 67.5 MHz ^{13}C-NMR spectrum of 14-*O*-acetyl renieramycin O in $CDCl_3$

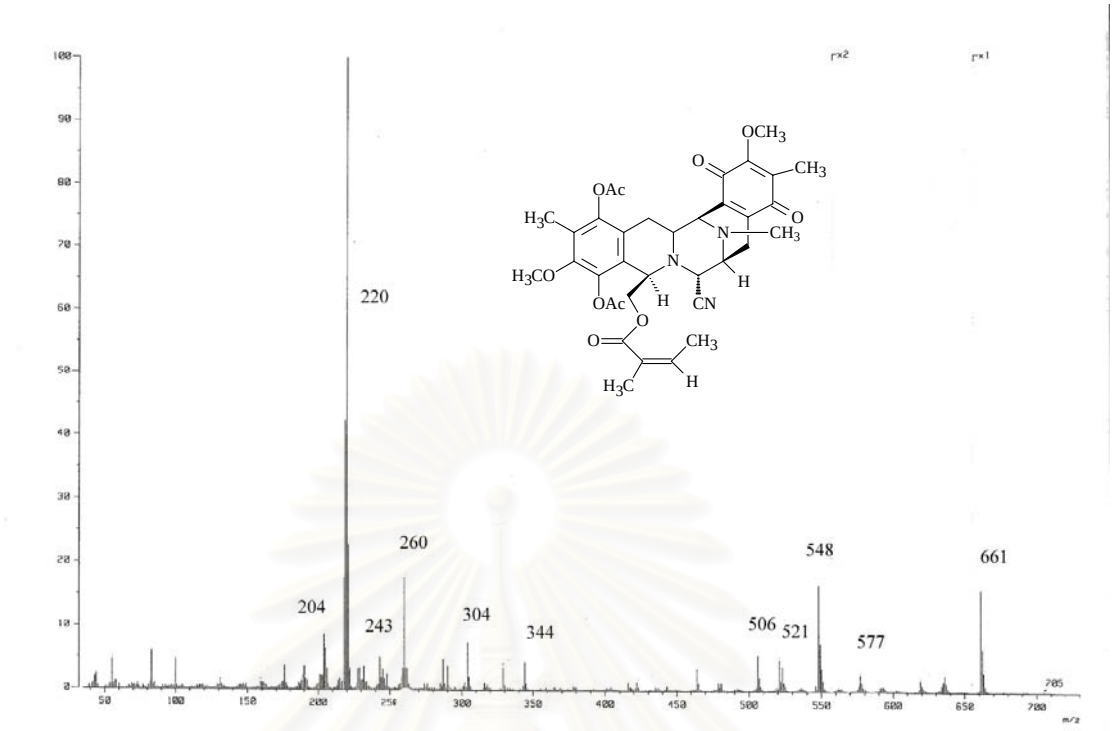

Figure 142 The EI mass spectrum of 5,8-*O*-diacetylhydroquinone renieramycin M

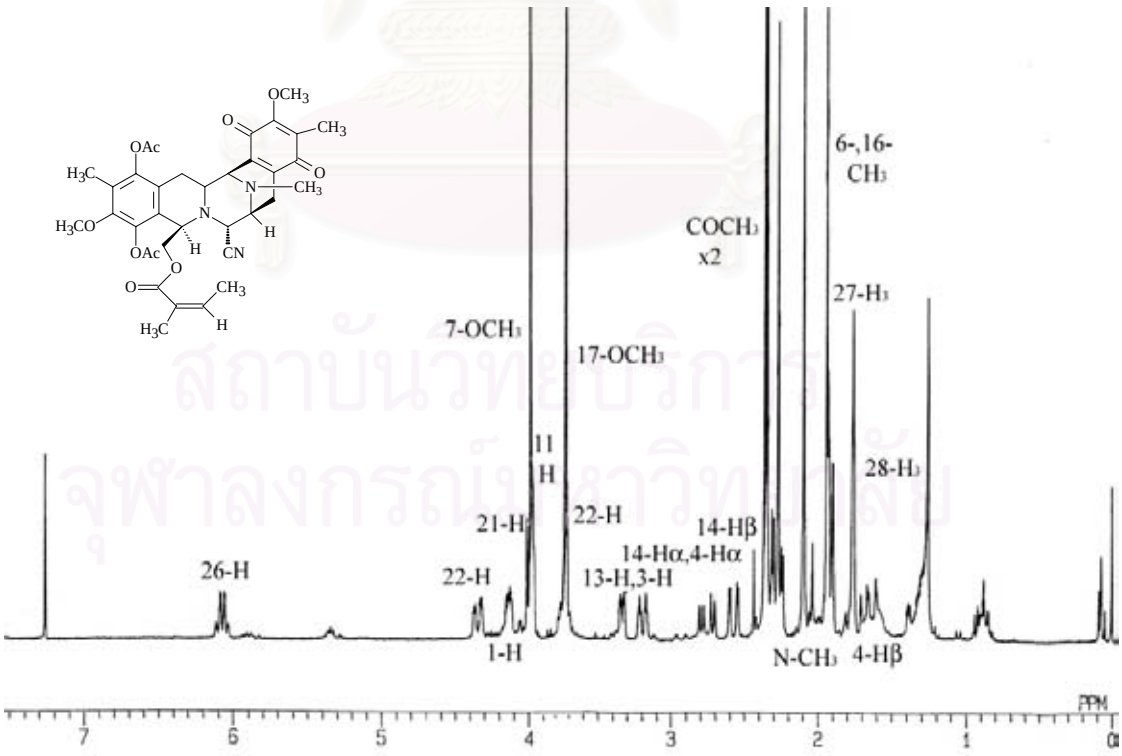

Figure 143 The 270 MHz ^{1}H-NMR spectrum of 5,8-di-*O*-acetyl hydroquinone renieramycin M in $CDCl_3$

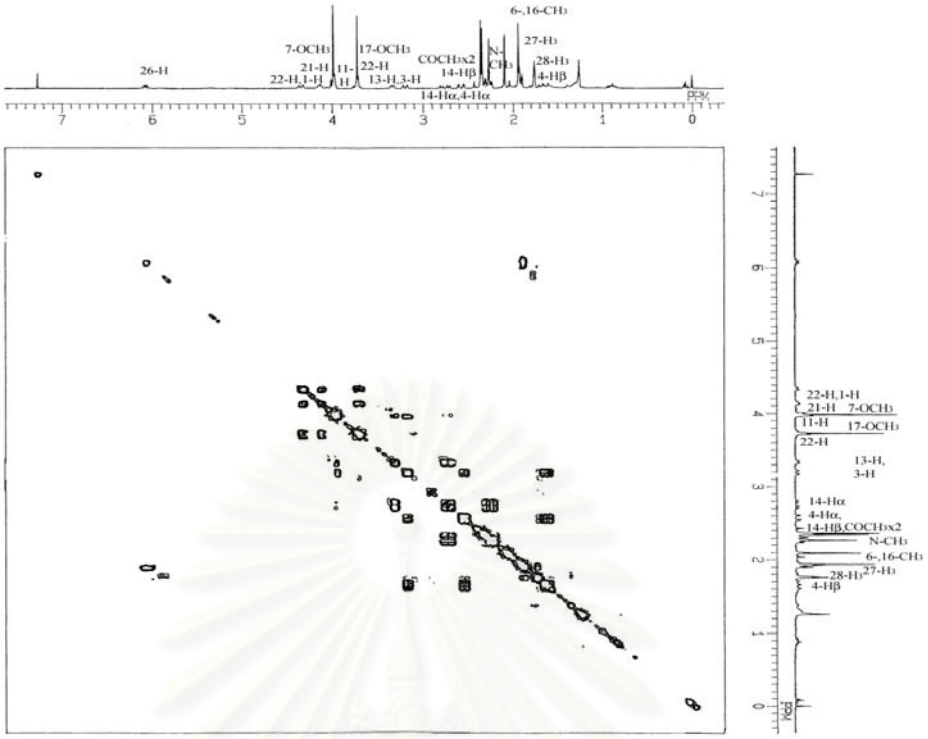

Figure 144 The 270 MHz $^{1}H,^{1}H$-COSY spectrum of 5,8-di-*O*-acetylhydroquinone renieramycin M in $CDCl_3$

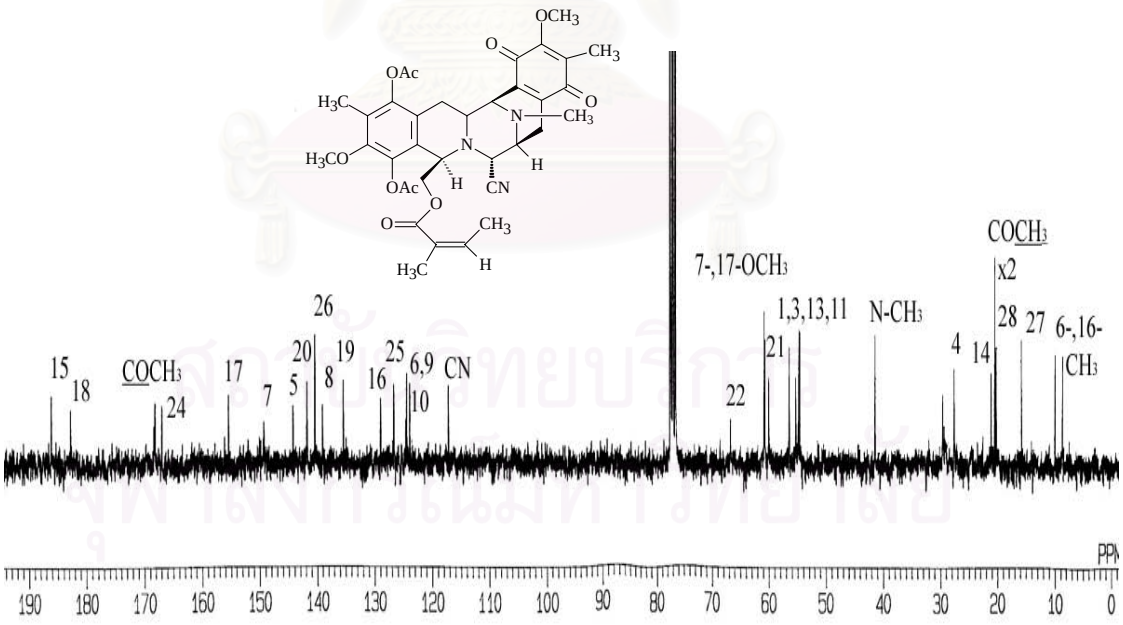

Figure 145 The 67.5 MHz ^{13}C-NMR spectrum of 5,8-di-*O*-acetylhydroquinone renieramycin M in $CDCl_3$

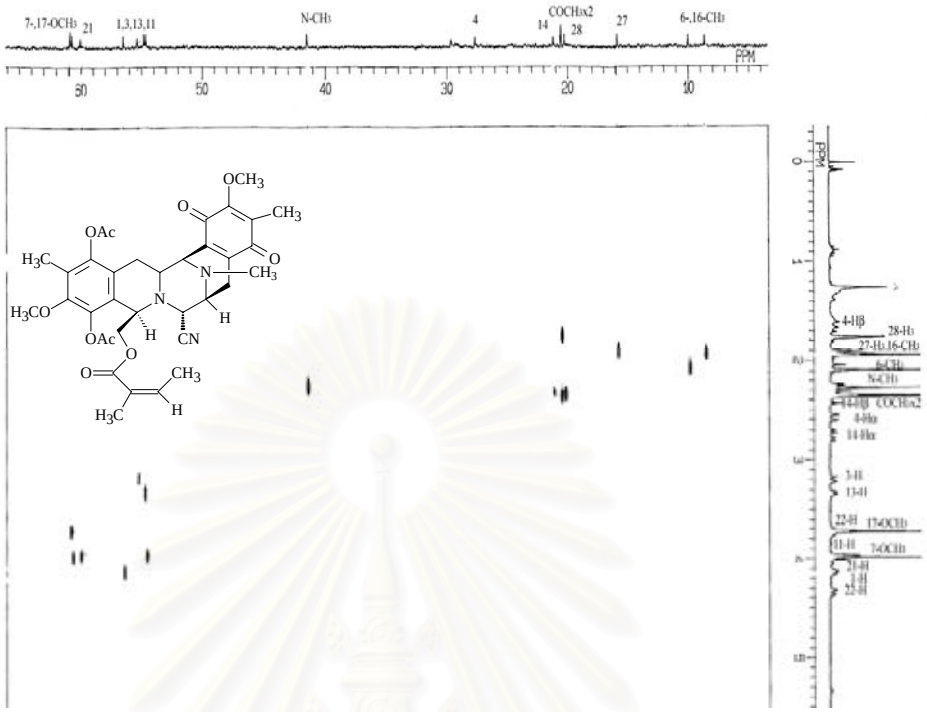

Figure 146 The 270 MHz HMQC spectrum of 5,8-di-*O*-acetylhydroquinone renieramycin M in $CDCl_3$

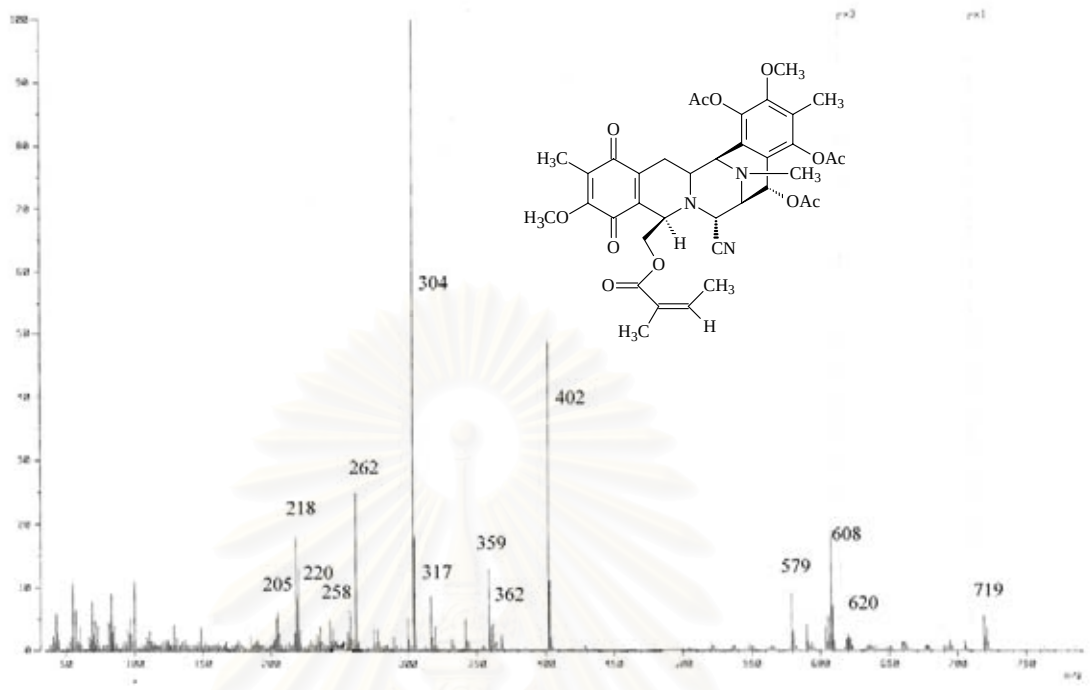

Figure 147 The EI-mass spectrum of 14,15,18-tri-*O*-acetyl renieramycin N

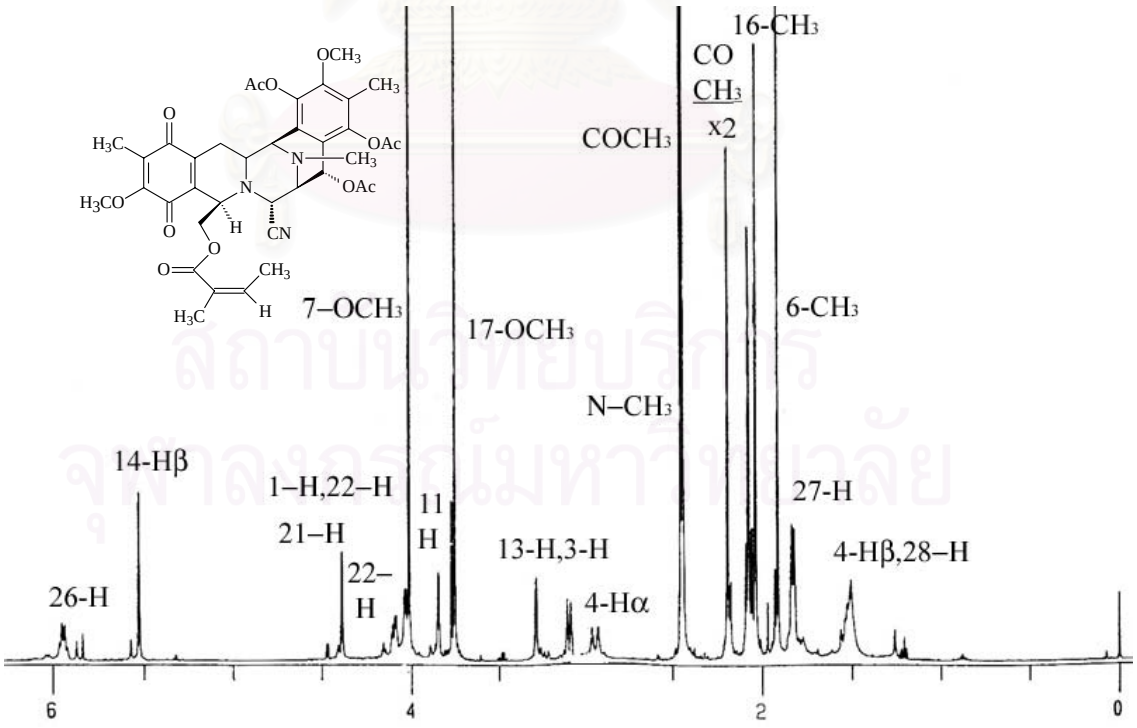

Figure 148 The 500 MHz ^{1}H-NMR spectrum of 14,15,18-tri-*O*-acetyl renieramycin N in $CDCl_3$

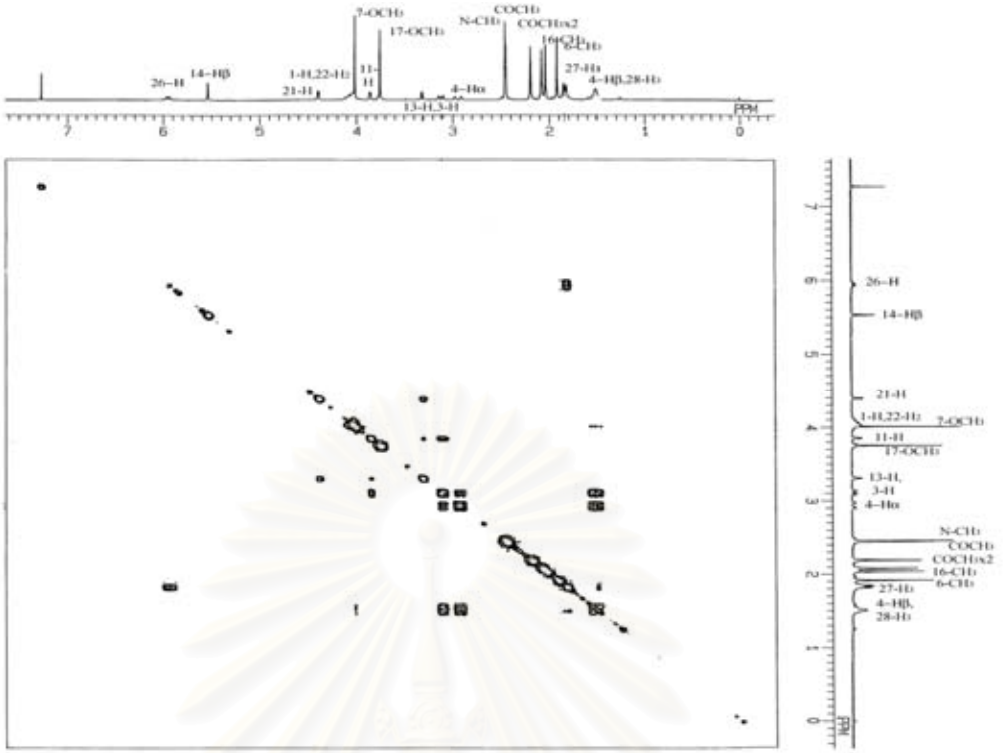

Figure 149 The 500 MHz $^{1}H,^{1}H$-COSY spectrum of 14,15,18-tri-*O*-acetyl renieramycin N in $CDCl_3$

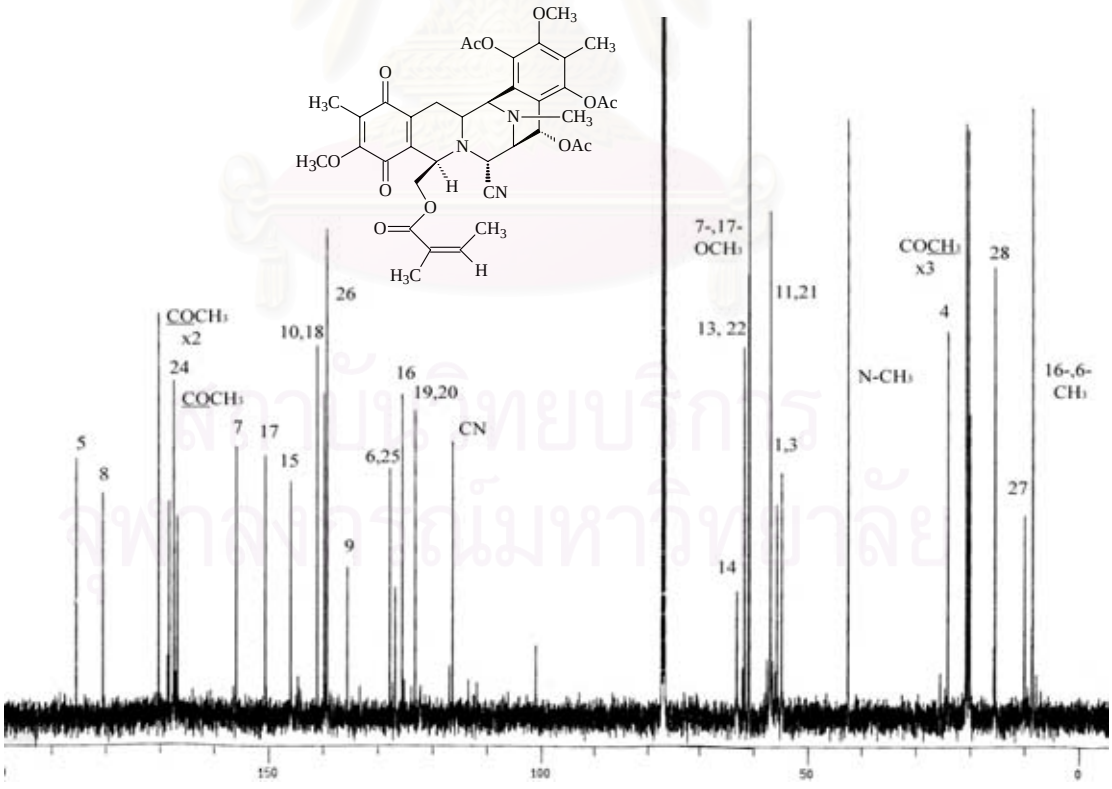

Figure 150 The 125 MHz ^{13}C-NMR spectrum of 14,15,18-tri-*O*-acetyl renieramycin N in $CDCl_3$

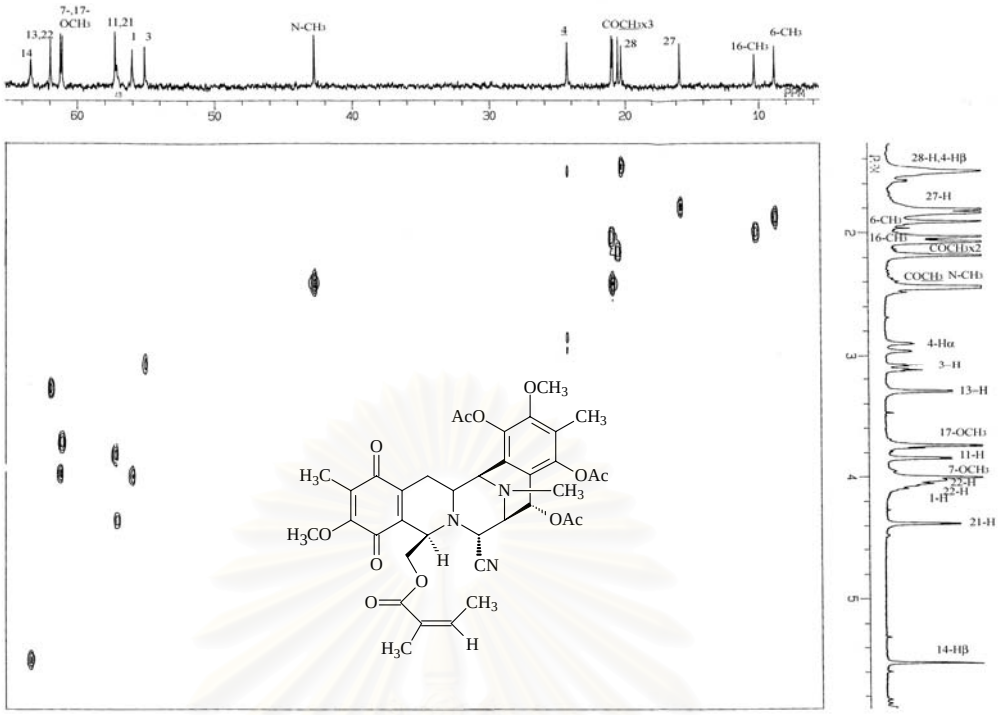

Figure 151 The 500 MHz HMQC spectrum of 14,15,18-tri-*O*-acetyl renieramycin N in $CDCl_3$(expanded from δ_H 1.40-5.80 ppm and δ_C 6.00-64.00 ppm)

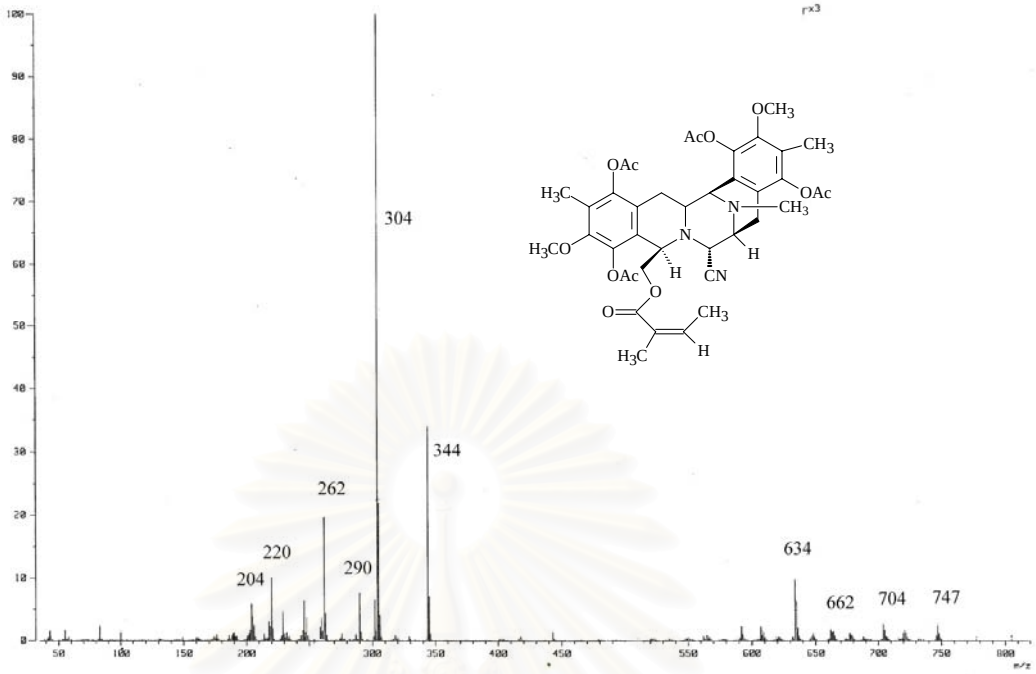

Figure 152 The EI-mass spectrum of 5,8,15,18-tetra-*O*-acetyl bishydroquinone renieramycin M

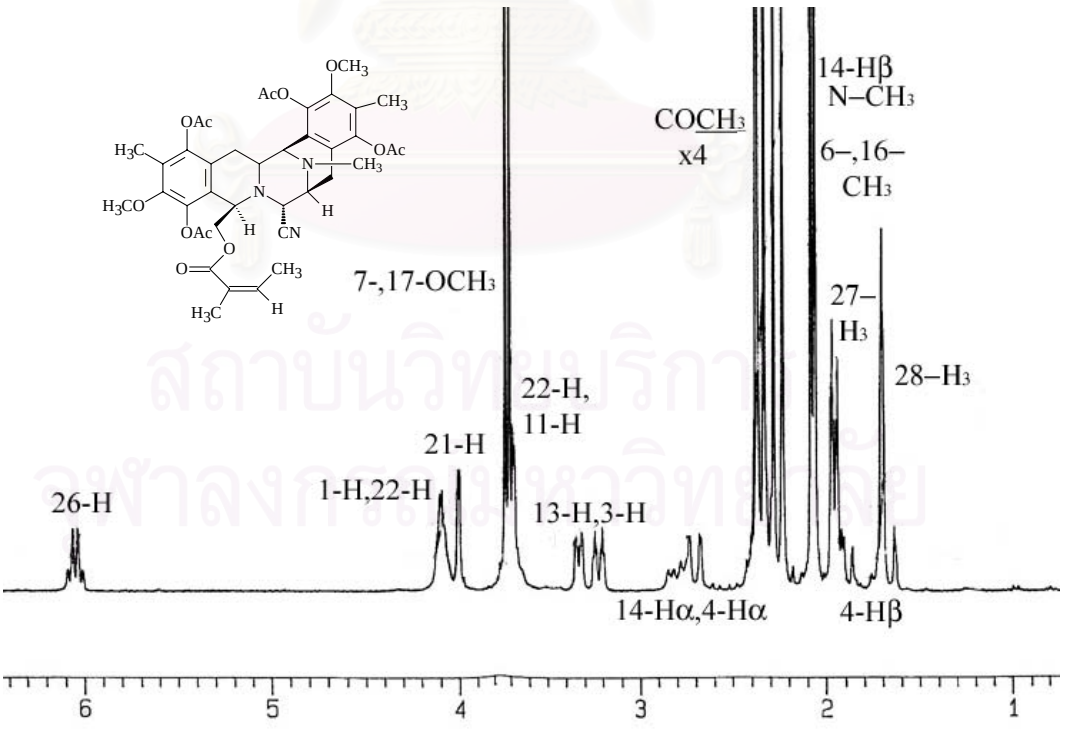

Figure 153 The 270 MHz ^{1}H-NMR spectrum of 5,8,15,18-tetra-*O*-acetyl bishydroquinone renieramycin M in $CDCl_3$

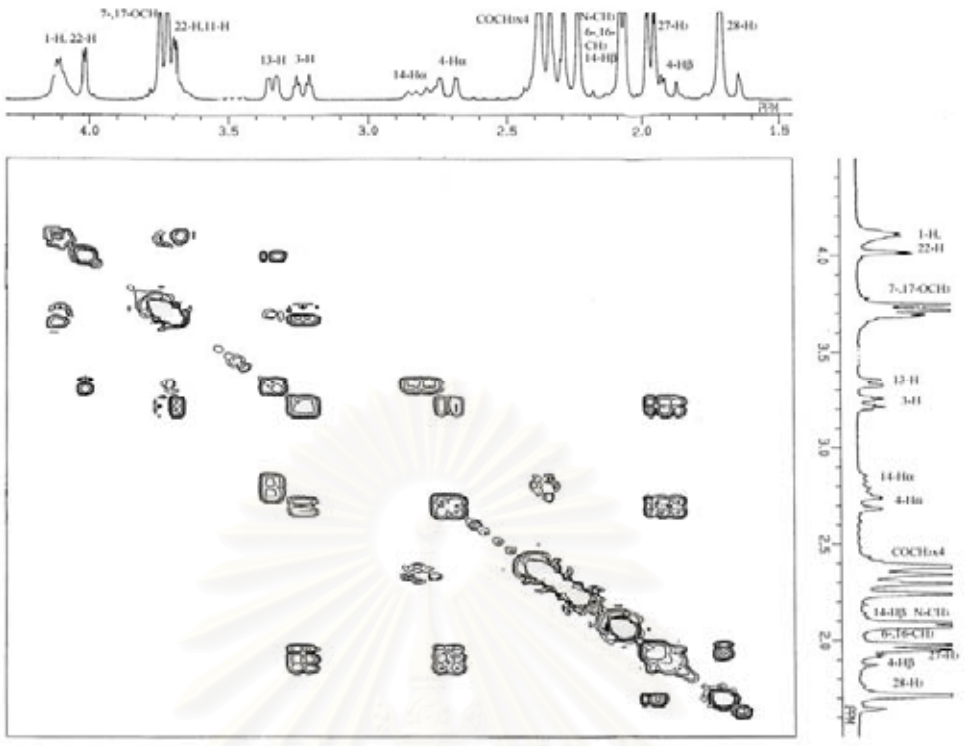

Figure 154 The 270 MHz ^{1}H,^{1}H-COSY spectrum of 5,8,15,18-tetra-*O*-acetyl bishydroquinone renieramycin M in $CDCl_3$ (expanded from δ_H 1.50-4.50 ppm)

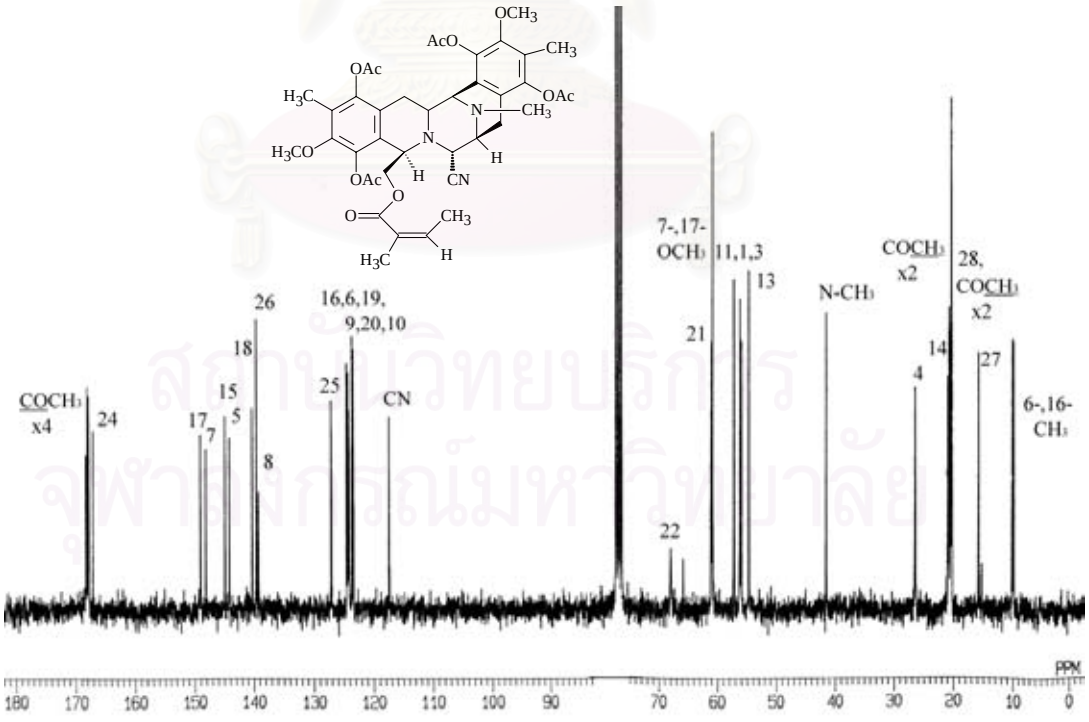

Figure 155 The 67.5 MHz ^{13}C-NMR spectrum of 5,8,15,18-tetra-*O*-acetyl bishydroquinone renieramycin M in $CDCl_3$

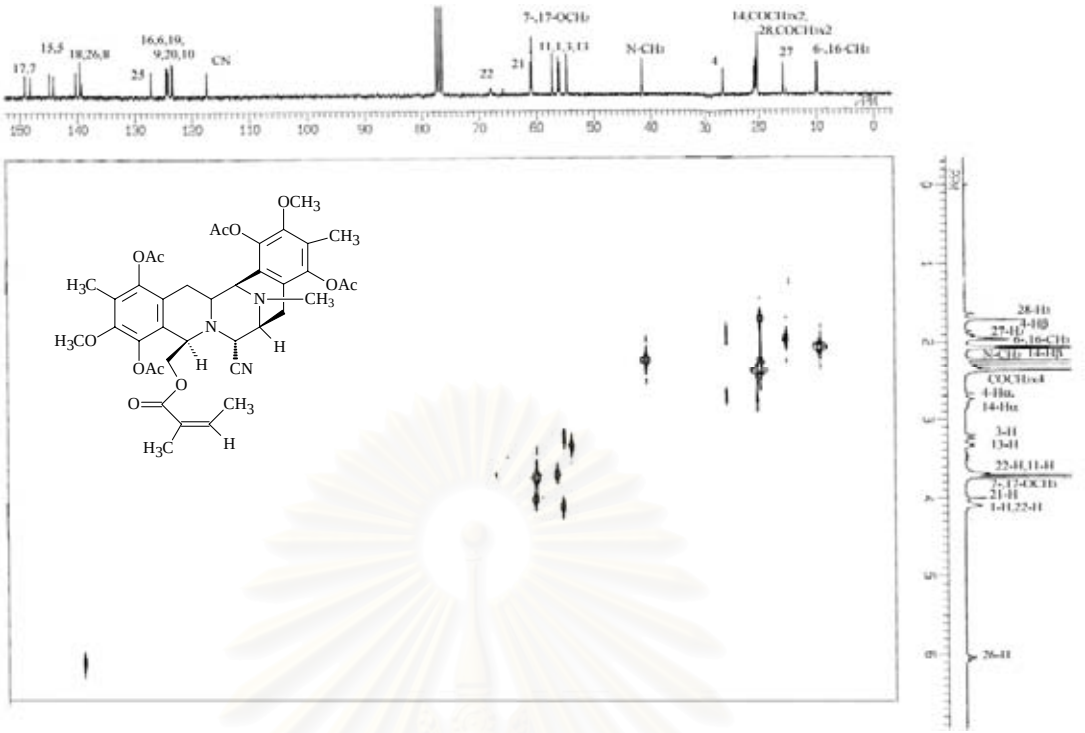

Figure 156 The 270 MHz HMQC spectrum of 5,8,15,18-tetra-*O*-acetyl bishydroquinone renieramycin M in $CDCl_3$

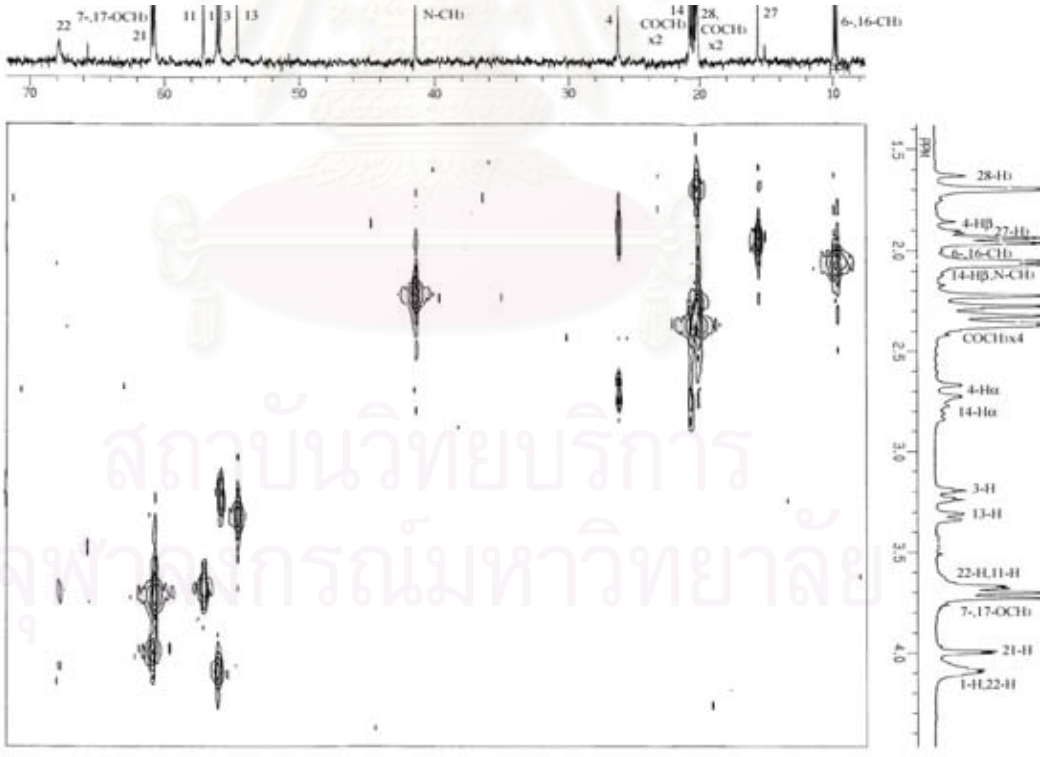

Figure 157 The 270 MHz HMQC spectrum of 5,8,15,18-tetra-*O*-acetyl bishydroquinone renieramycin M in $CDCl_3$ (expanded from δ_H 1.40-4.40 ppm and δ_C 8.00-70.00 ppm)

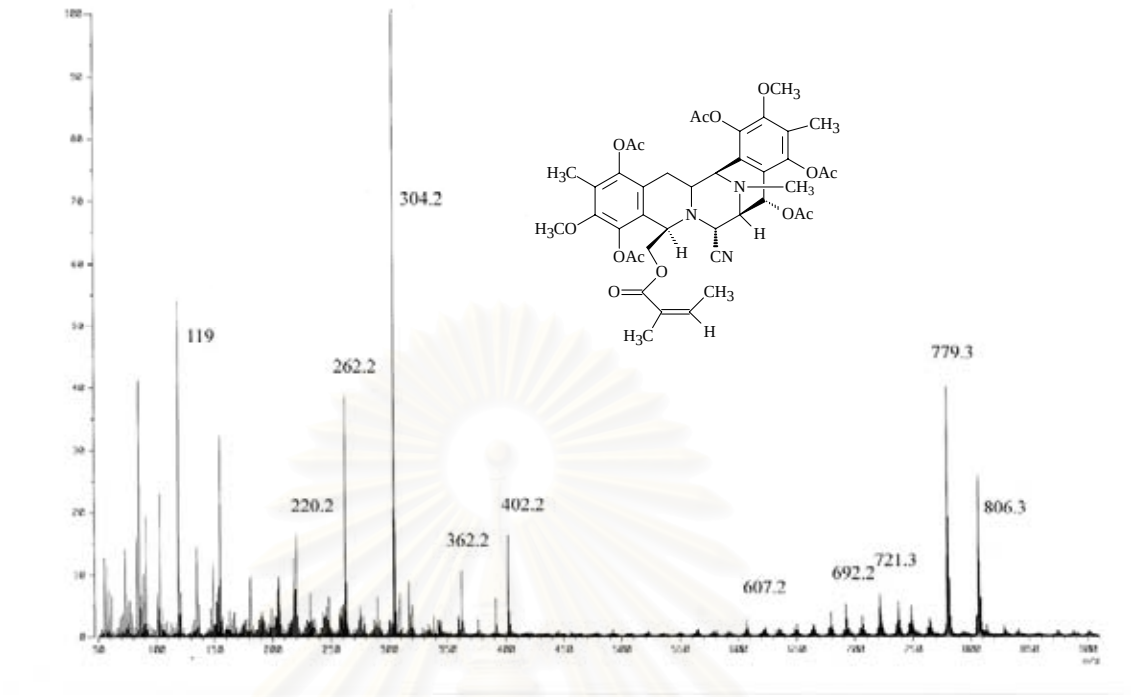

Figure 158 The EI-mass spectrum of 5,8,14,15,18-penta-*O*-acetyl bishydroquinone renieramycin M

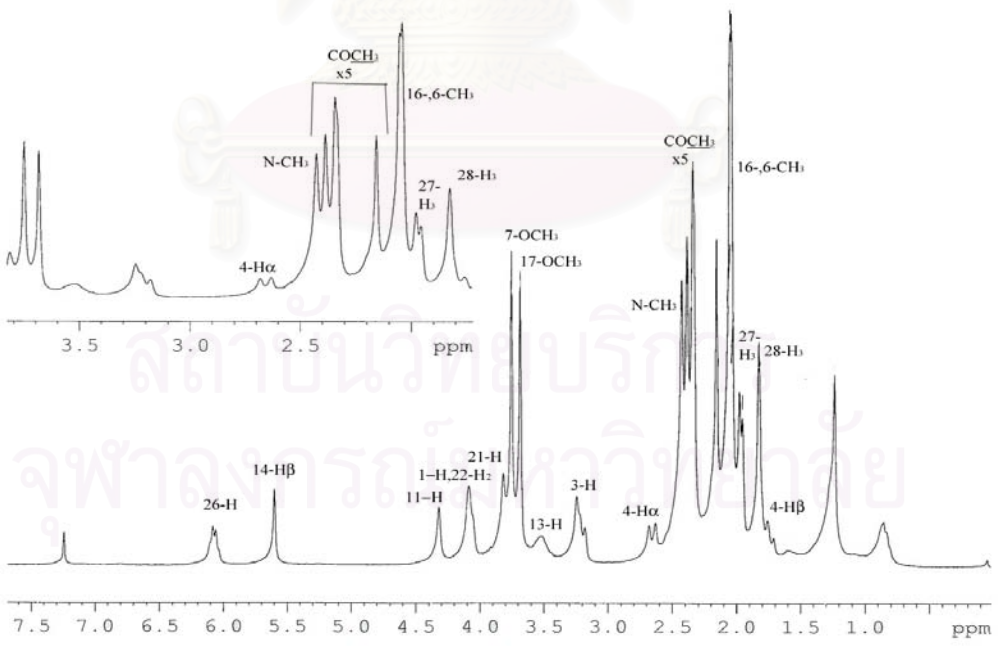

Figure 159 The 300 MHz ^{1}H-NMR spectrum of 5,8,14,15,18-penta-*O*-acetyl bishydroquinone renieramycin M in $CDCl_3$

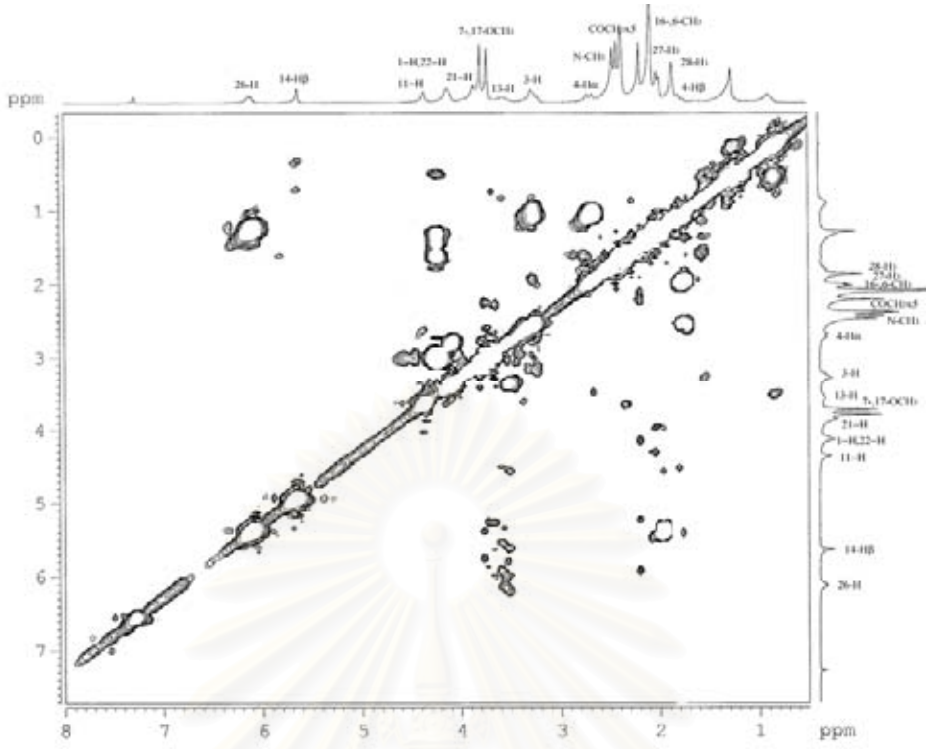

Figure 160 The 300 MHz ^{1}H,^{1}H-COSY spectrum of 5,8,14,15,18-penta-*O*-acetyl bishydroquinone renieramycin M in $CDCl_3$

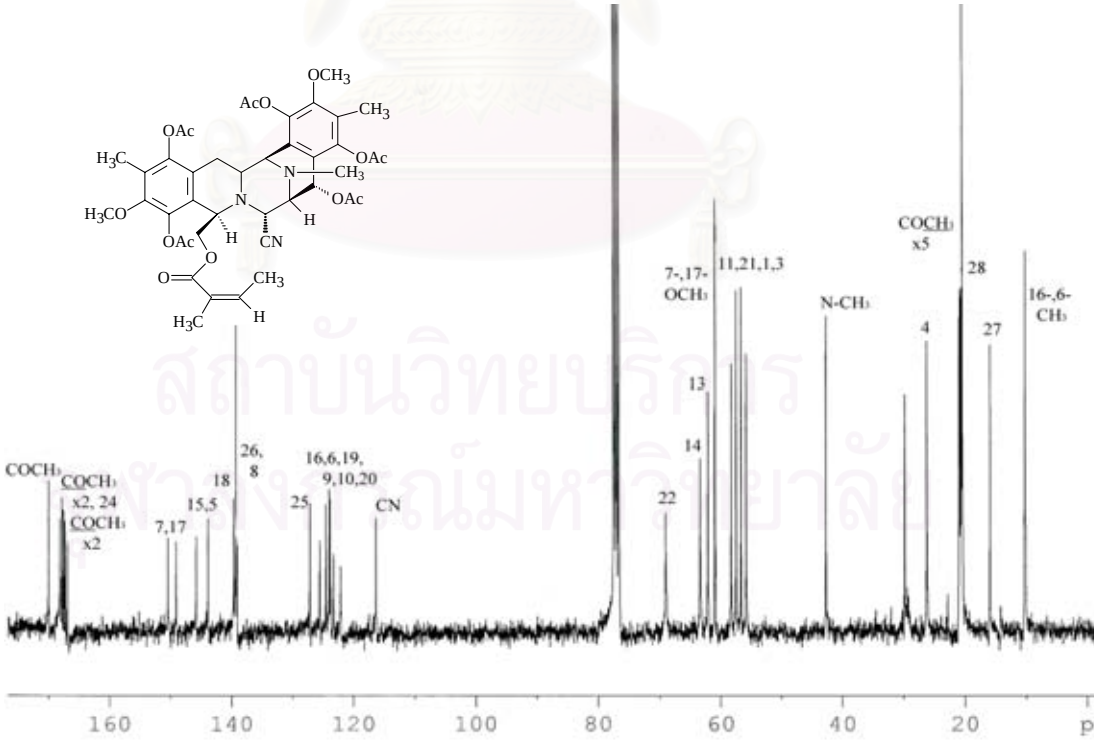

Figure 161 The 75 MHz ^{13}C-NMR spectrum of 5,8,14,15,18-penta-*O*-acetyl bishydroquinone renieramycin M in $CDCl_3$

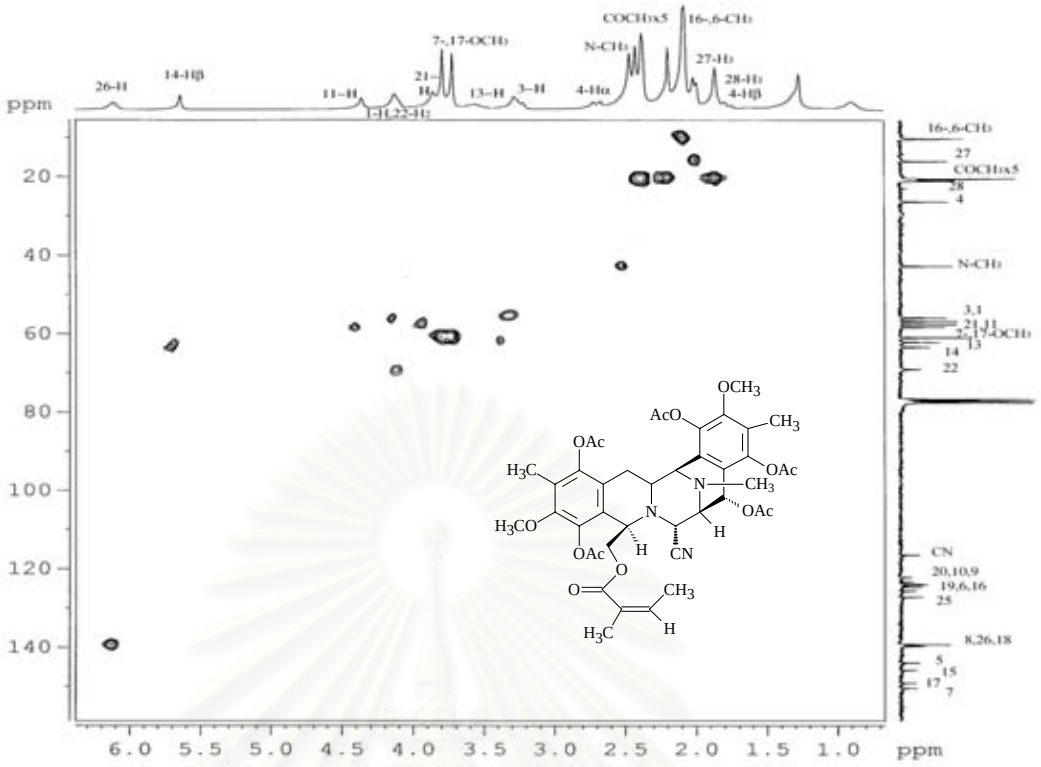

Figure 162 The 300 MHz HMQC spectrum of 5,8,14,15,18-penta-*O*-acetyl bishydroquinone renieramycin M in $CDCl_3$

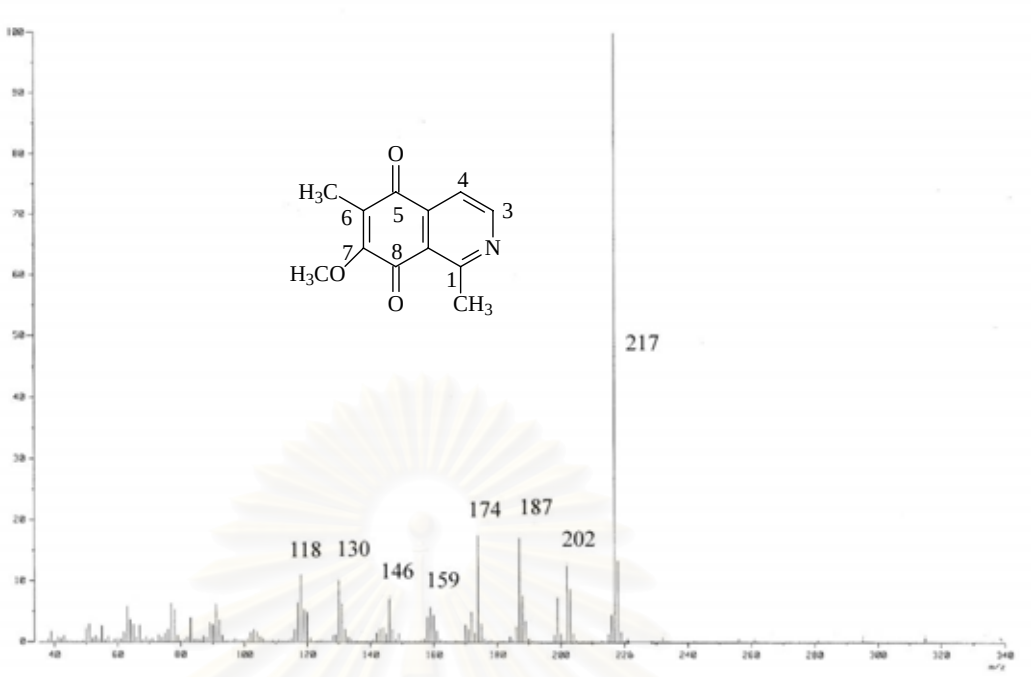

Figure 163 The EI-mass spectrum of of 1,6-dimethyl-5,8-dihydro-5,8 dione

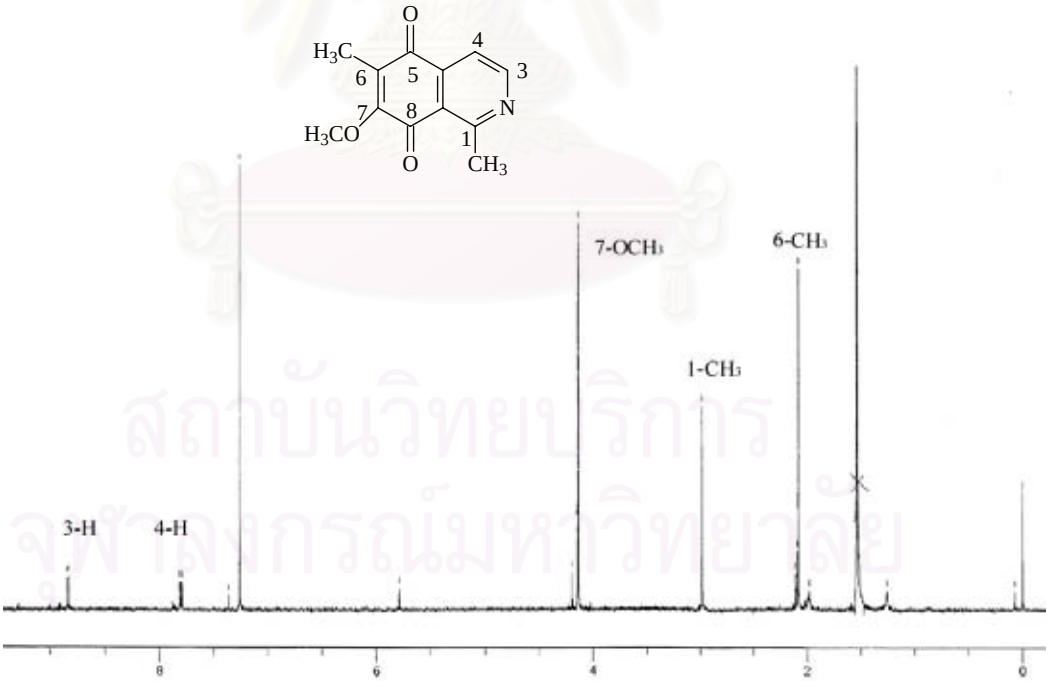

Figure 164 The 270 MHz ^{1}H-NMR spectrum of 1,6-dimethyl-5,8-dihydro-5,8 dione in $CDCl_3$

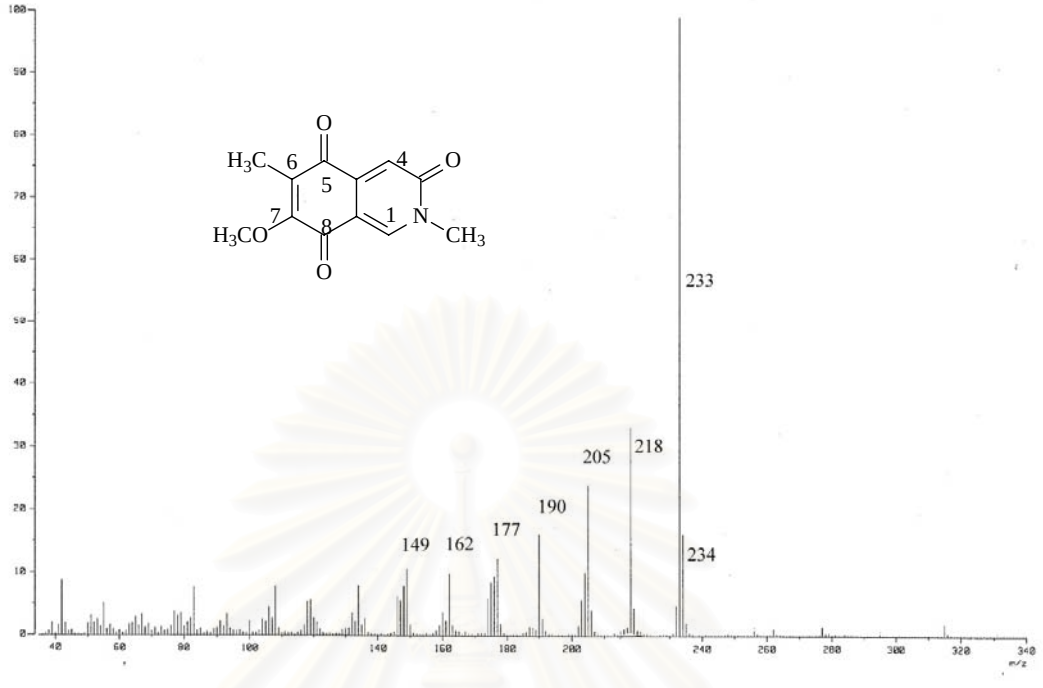

Figure 165 The EI-mass spectrum of mimosamycin

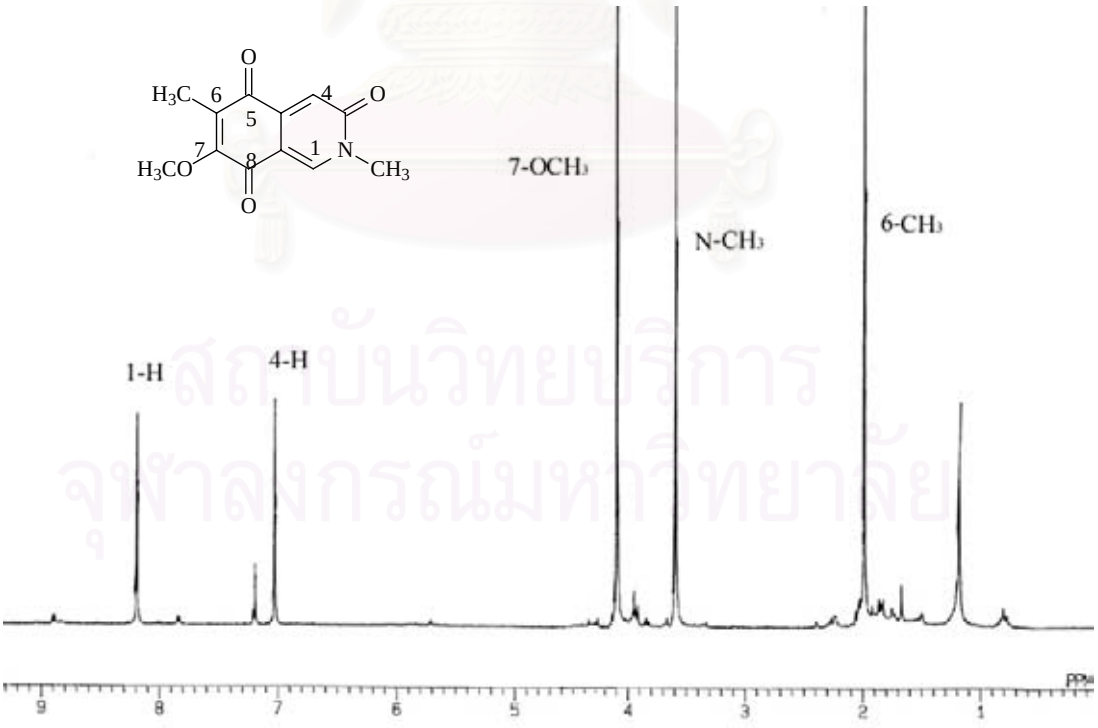

Figure 166 The 270 MHz ^{1}H-NMR spectrum of mimosamycin in $CDCl_3$

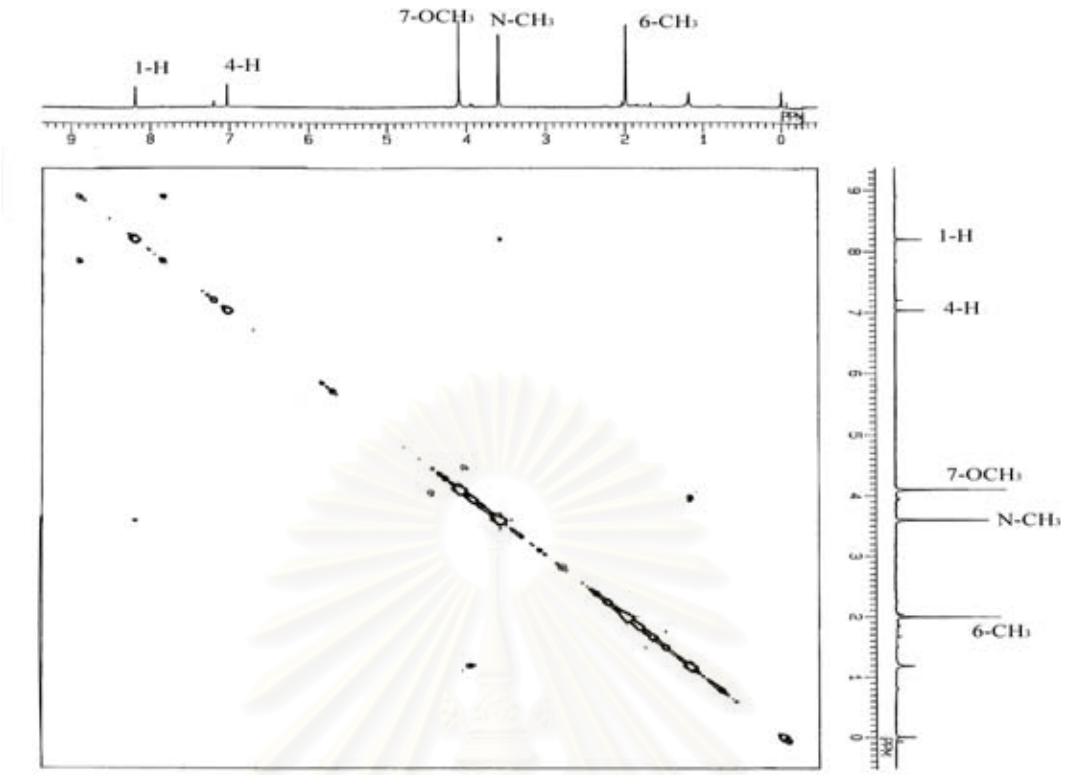

Figure 167 The 270 MHz ^{1}H, ^{1}H-COSY spectrum of mimosamycin in $CDCl_3$

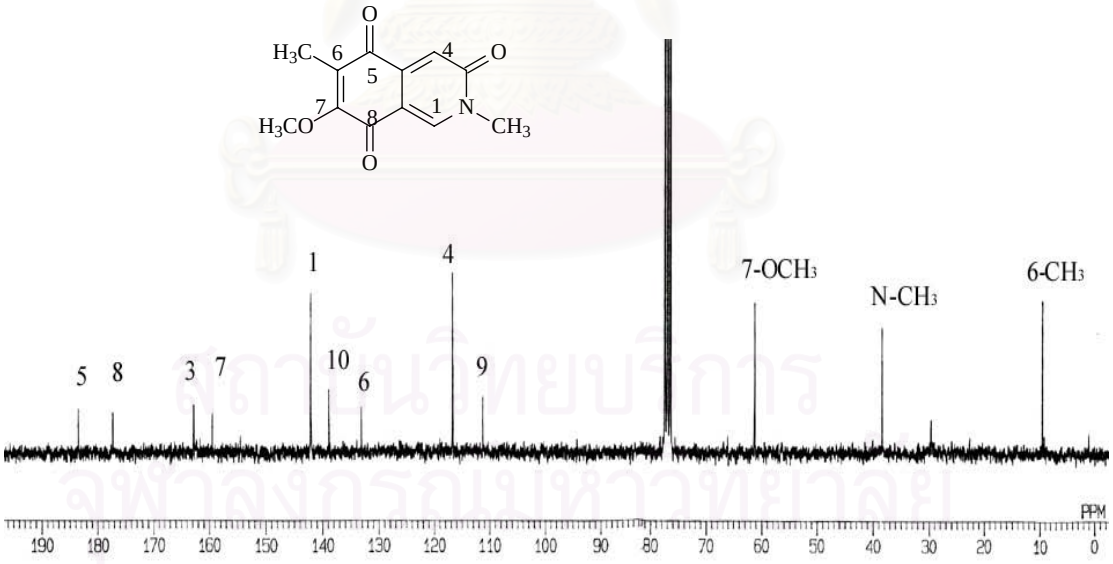

Figure 168 The 67.5 MHz ^{13}C-NMR spectrum of mimosamycin in $CDCl_3$

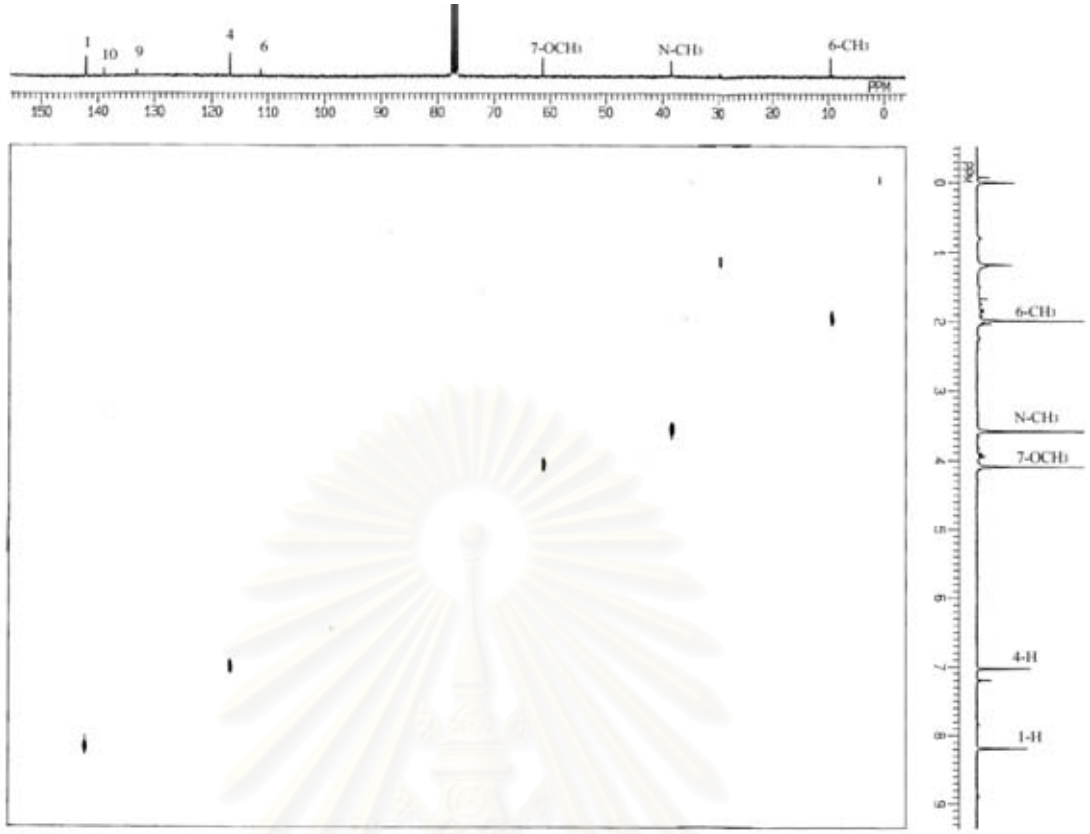

Figure 169 The 270 MHz HMQC spectrum of mimosamycin in $CDCl_3$

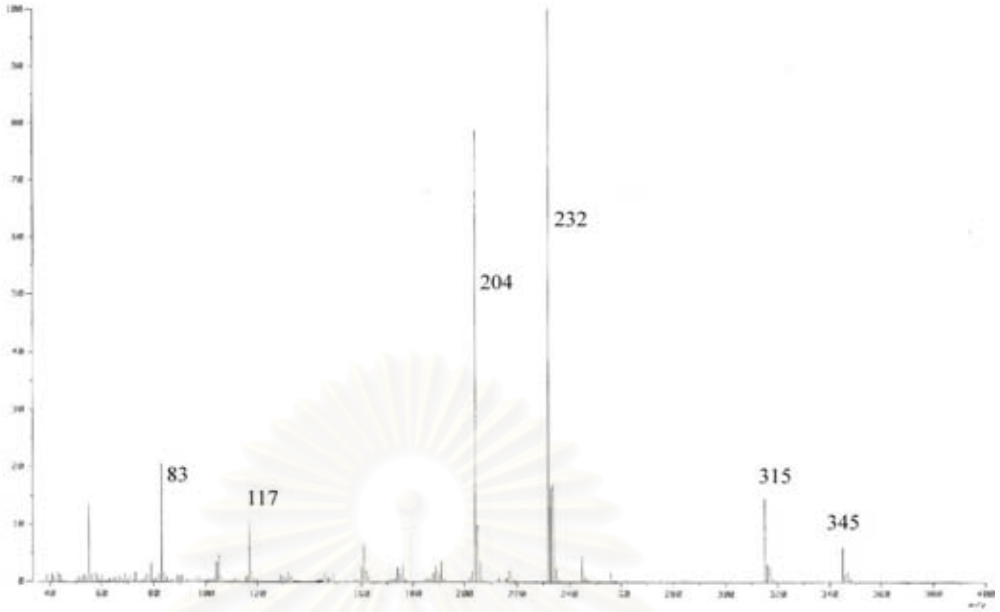

Figure 170 The EI-mass spectrum of N-formyl-1,2-dihydrorenierone

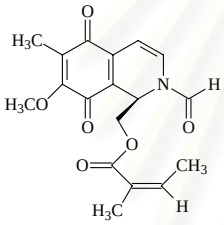

major isomer

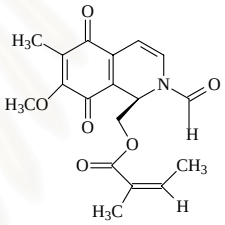

minor isomer

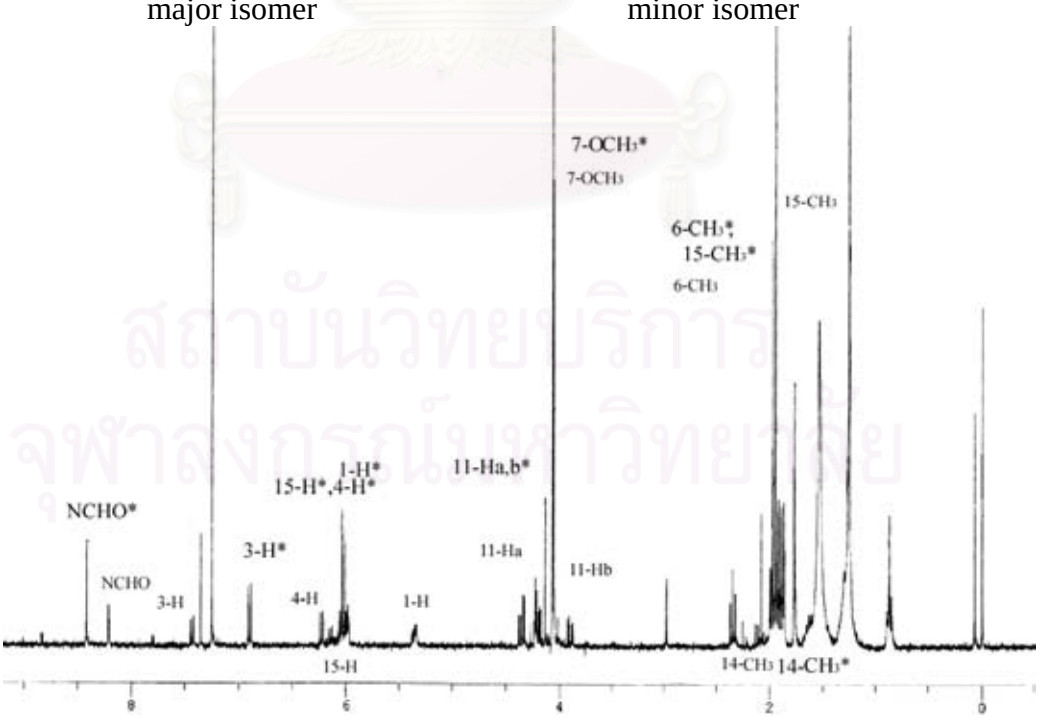

Figure 171 The 270 MHz ^{1}H-NMR spectrum of N-formyl-1,2-dihydrorenierone in $CDCl_3$

* = major isomer

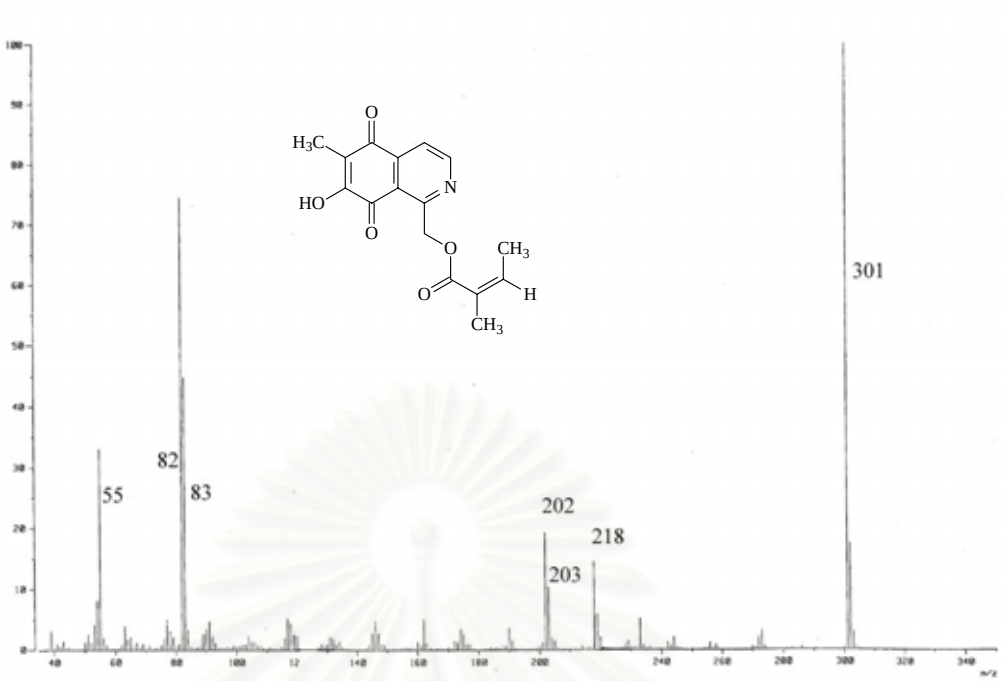

Figure 172 The EI-mass spectrum of *O*-demethyl -renierone

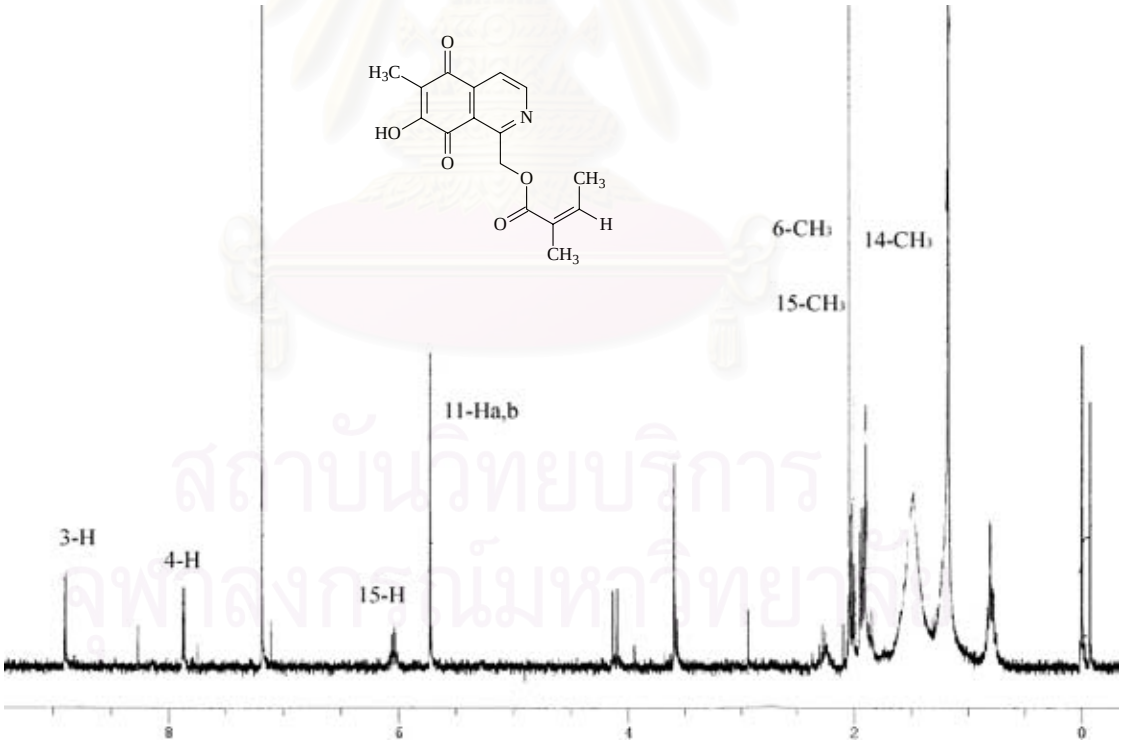

Figure 173 The 270 MHz ^{1}H-NMR spectrum of *O*-demethyl-renierone in $CDCl_3$

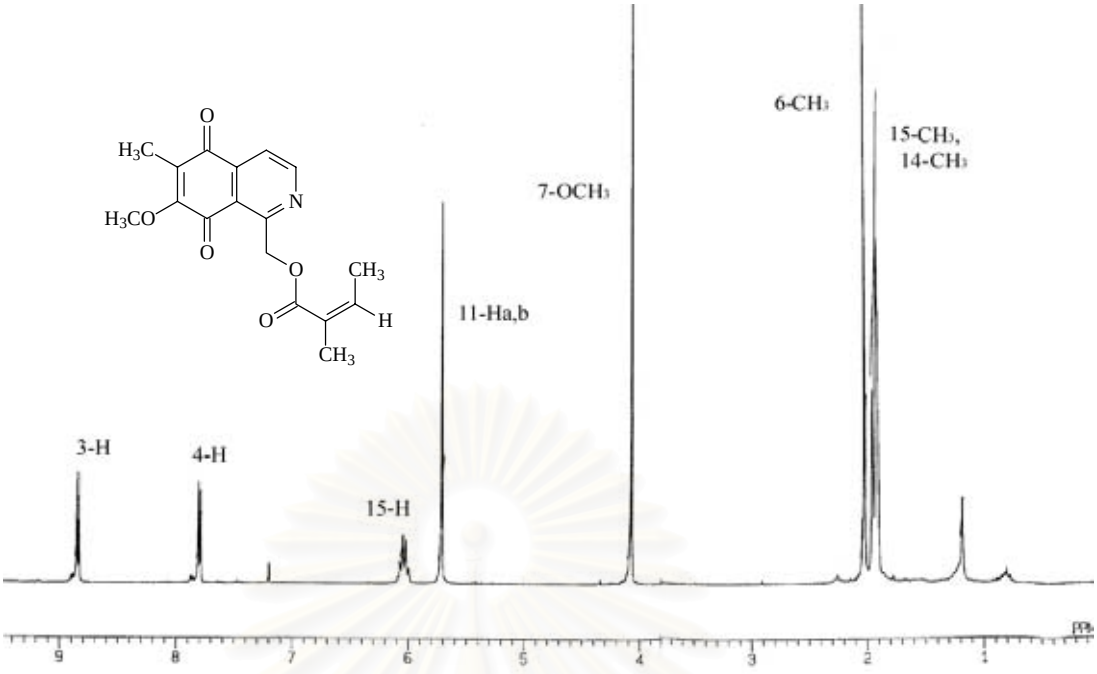

Figure 174 The 270 MHz ^{1}H-NMR spectrum of renierone in $CDCl_3$

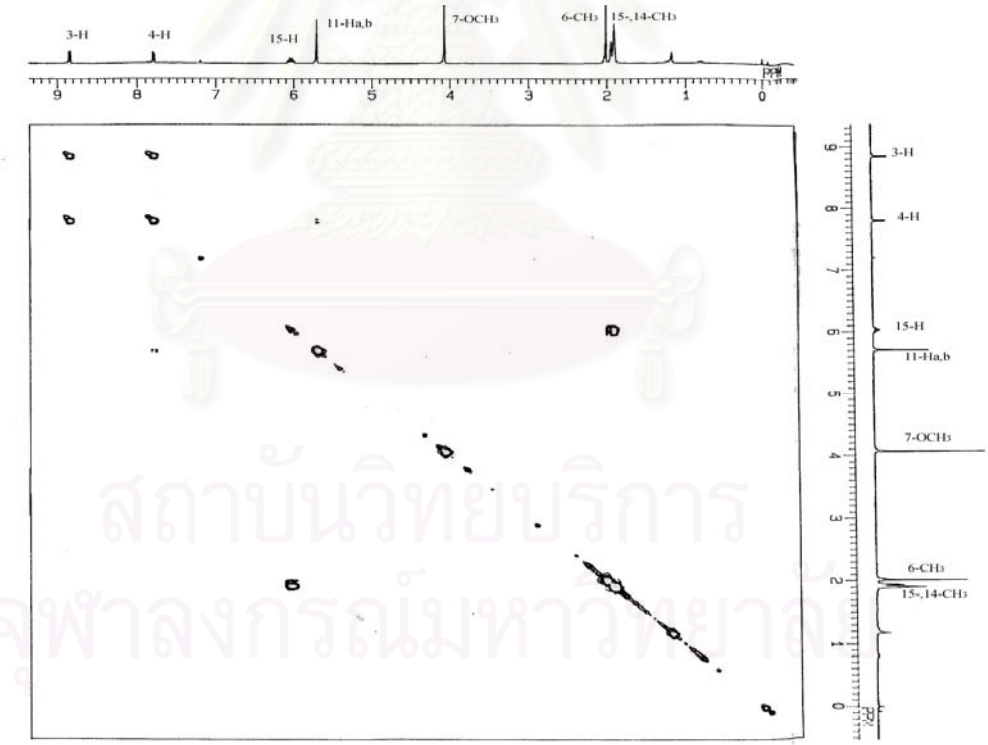

Figure 175 The 270 MHz ^{1}H, ^{1}H-COSY spectrum of renierone in $CDCl_3$

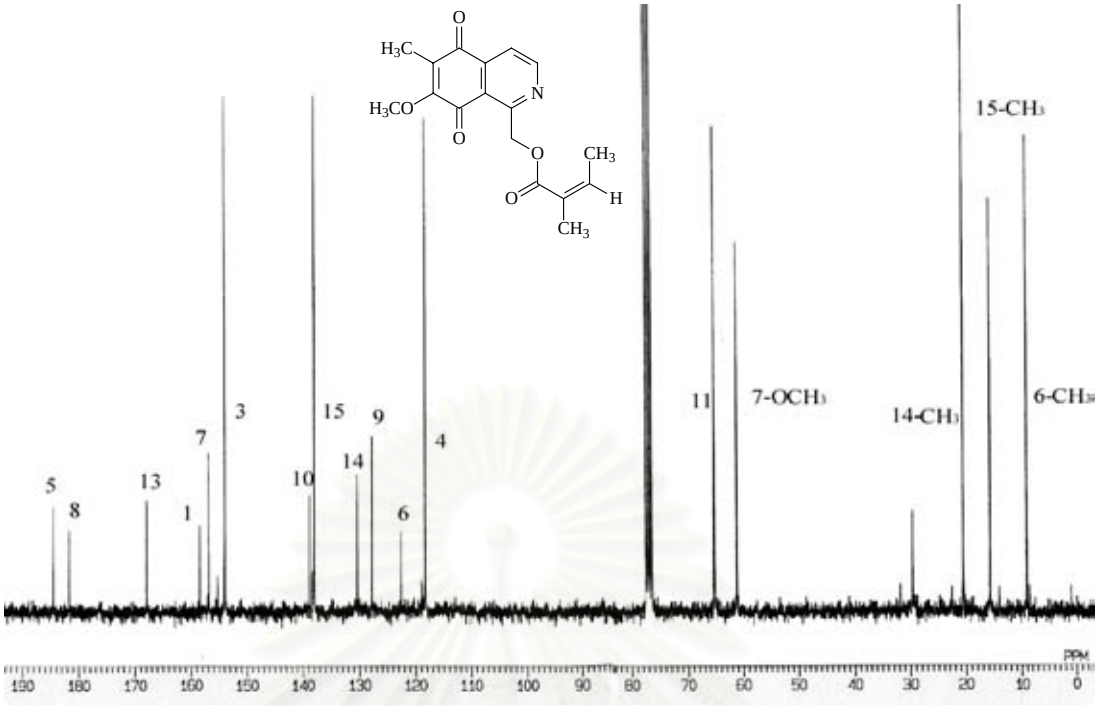

Figure 176 The 67.5 MHz ^{13}C-NMR spectrum of renierone in $CDCl_3$

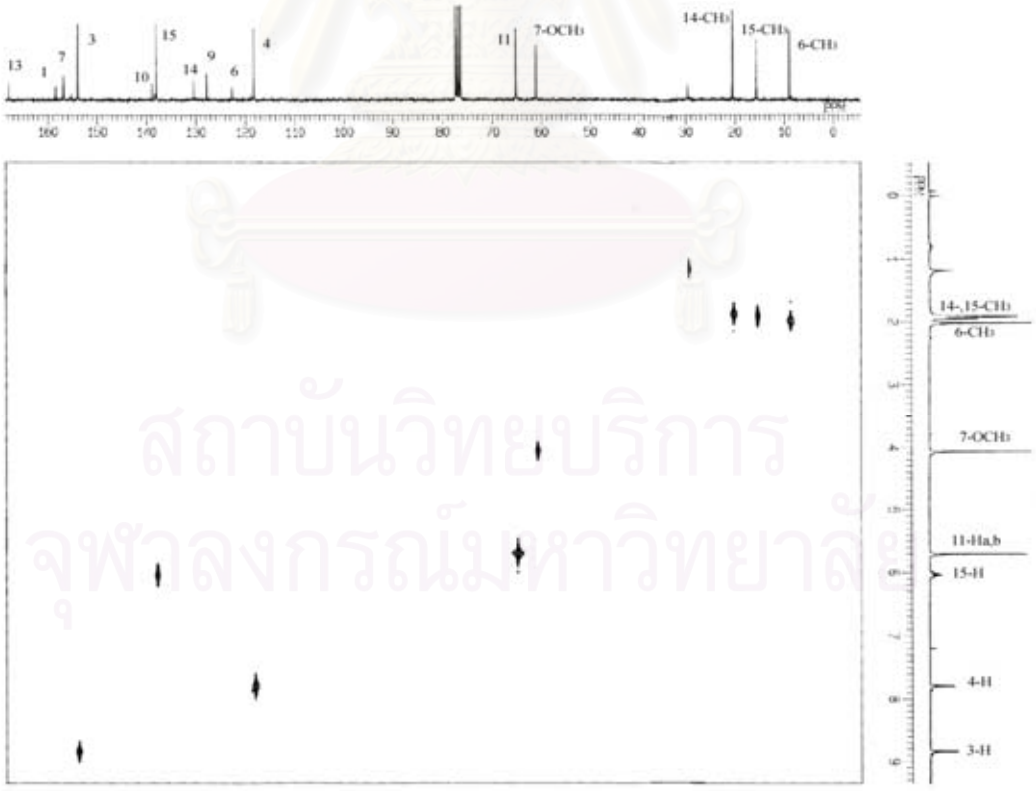

Figure 177 The 270 MHz HMQC spectrum of renierone in $CDCl_3$

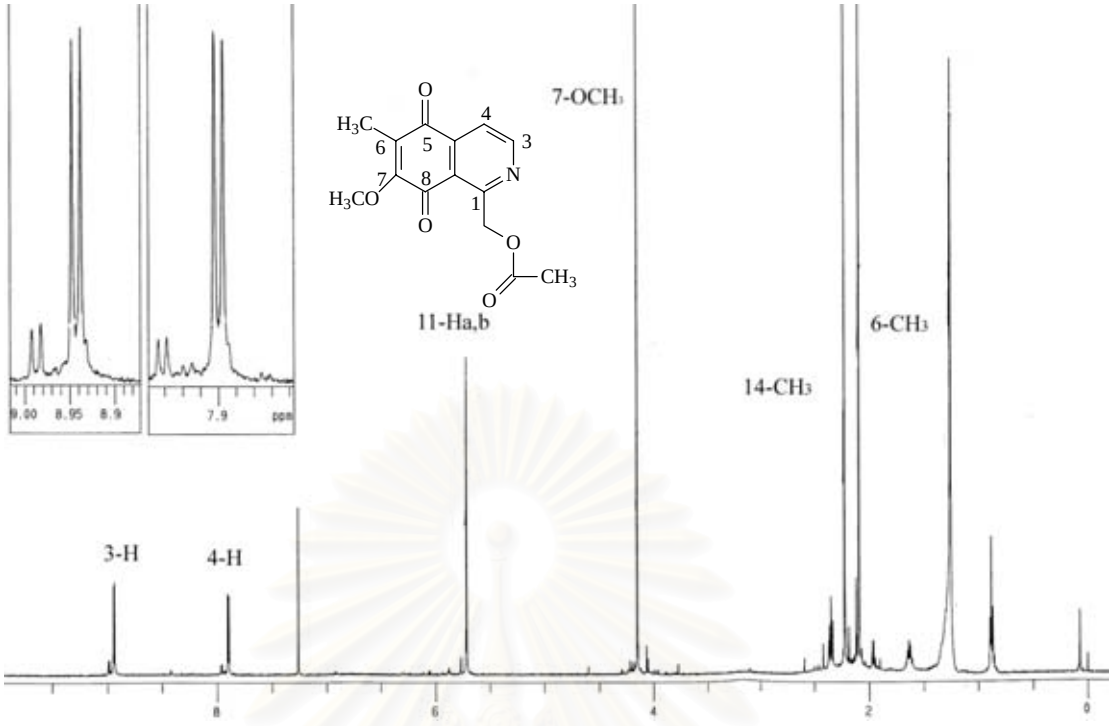

Figure 178 The 500 MHz ^{1}H-NMR spectrum of renierol acetate in $CDCl_3$

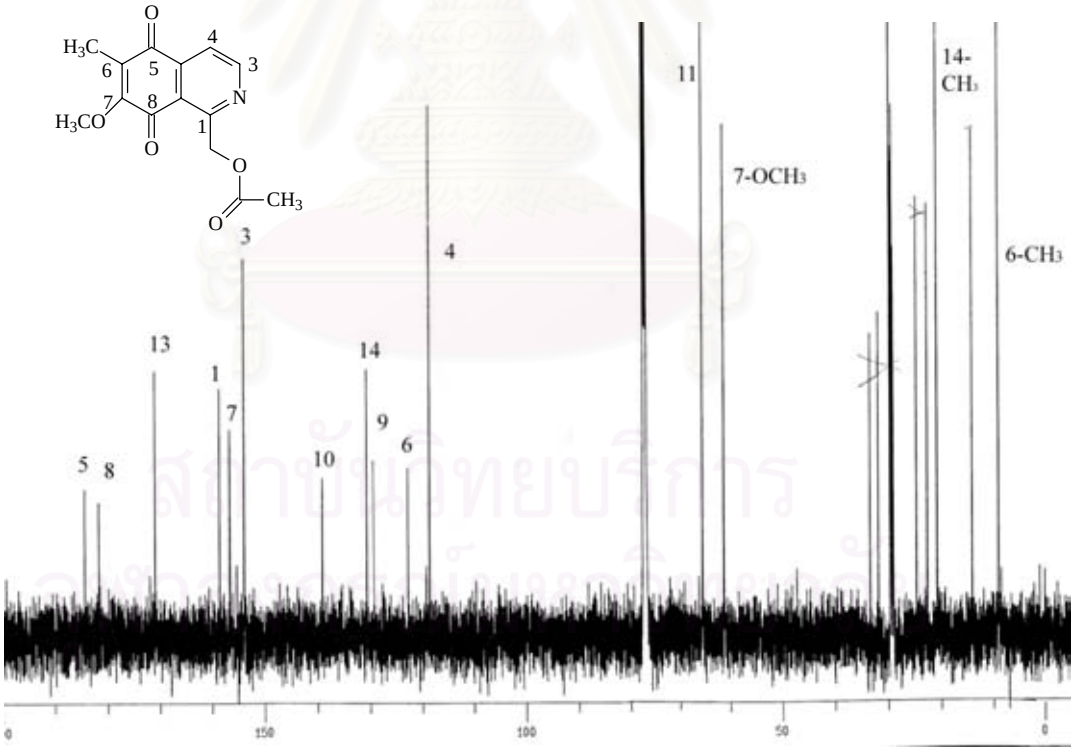

Figure 179 The 125 MHz ^{13}C-NMR spectrum of renierol acetate in $CDCl_3$

VITA

Mrs. Surattana Amnuoypol was born on November 25, 1954 in Bangkok, Thailand. She received her Bachelor of Science in Pharmacy in 1978 and Master of Science in Pharmacy (Pharmacognosy) in 1981 from the Faculty of Pharmaceutical Sciences, Chulalongkorn University, Thailand. Since 1978 she has been a staff at the Department of Pharmacognosy, Faculty of Pharmaceutical Sciences, Chulalongkorn University, Thailand. She was promoted as Assistant Professor and Associate Professor in 1983 and in 1988, respectively.

Publications:

1. Suwanborirux, K., Amnuoypol, S., Plubrukarn, A., Pummangura, S., Kubo, A., Tanaka, C., and Saito, N. 2003. Chemistry of renieramycins. Part 3. Isolation and structure of stabilized renieramycin type derivatives possessing antitumor activity from Thai sponge *Xestospongia* species, pretreated with potassium cyanide. J. Nat. Prod. 66: 1441-1446.

2. Amnuoypol, S., Suwanborirux, K., Pummangura, S., Kubo, A., Tanaka, C., and Saito, N. 2004. Chemistry of renieramycins. Part 5. Structure elucidation of minor components of renieramycins O and Q-S, from Thai marine sponge, *Xestospongia* species, pretreated with potassium cyanide. J. Nat. Prod. 67: 1023-1028.

3. Saito, N., Tanaka, C., Koizumi, Y., Suwanborirux, K., Amnuoypol, S., Pummangura, S., and Kubo, A. 2004. Chemistry of renieramycins. Part 6. Transformation of renieramycin M into jorumycin and renieramycin J including oxidative degradation products, mimosamycin, renierone, and renierol acetate. Tetrahedron 60: 3873-3881.